

**Functional characterisation of the *TUP5* gene in
*Arabidopsis thaliana***

Dissertation

zur Erlangung des akademischen Grades des
Doktors der Naturwissenschaften (Dr. rer. nat.)

Eingereicht im
Fachbereich Biologie, Chemie, Pharmazie
der Freien Universität Berlin

vorgelegt von

Nathalie Frémont
aus Berlin

Februar 2011

1. Gutachter: Prof. Dr. Thomas Schmülling
2. Gutachter: Prof. Dr. Wolfgang Schuster

Disputation am 5. Mai 2011

TABLE OF CONTENT

1	SUMMARY	1
2	ZUSAMMENFASSUNG	3
3	INTRODUCTION	5
3.1	The root of <i>Arabidopsis thaliana</i>	6
3.1.1	Root growth and morphology.....	6
3.1.2	Natural abiotic factors influencing root development.....	8
3.2	Light signalling in plants.....	9
3.2.1	Plant photoreceptors.....	10
3.2.2	Light signalling and root development.....	13
3.3	Amino acid biosynthesis.....	14
3.3.1	Overview of amino acid synthesis pathways.....	15
3.3.2	Mutants of amino acid metabolism.....	20
3.3.3	Arginine function and biosynthesis.....	23
3.4	The mutant <i>tup5-1</i>	27
3.5	Aim of the work.....	28
4	MATERIAL AND METHODS	30
4.1	<i>Arabidopsis thaliana</i> lines.....	30
4.1.1	Ecotypes.....	30
4.1.2	T-DNA insertion lines.....	30
4.1.3	Marker lines.....	30
4.1.4	Mutant lines.....	31
4.2	Growth conditions for <i>Arabidopsis thaliana</i>	31
4.2.1	Growth temperature and day length (photoperiod).....	31
4.2.2	Growth on soil.....	31
4.2.3	In vitro culture.....	32
4.2.4	Age of the plants.....	32
4.3	Localisation of the perception site of root growth inhibition by light.....	32
4.4	Histology.....	33
4.4.1	Viability test.....	33
4.4.2	GUS staining.....	33
4.4.3	Tissue clearing.....	34
4.4.4	Fast protoplast isolation for GFP analysis.....	35
4.5	Plant DNA extraction.....	35
4.6	Gene mapping.....	36
4.7	Sequencing.....	38
4.8	Generation of transgenic <i>A. thaliana</i>	40
4.8.1	Cloning of a DNA fragment into a vector with restriction enzymes.....	40
4.8.2	Cloning of a DNA fragment into a vector with Gateway.....	43
4.8.3	Transformation of <i>E. coli</i>	44
4.8.4	Transformation of <i>A. tumefaciens</i>	47
4.8.5	Floral dip transformation of <i>A. thaliana</i>	48
4.9	Yeast transformation with a modified lithium acetate method.....	49
4.10	Analysis of free amino acid content in <i>A. thaliana</i>	50
4.11	Real-time PCR.....	52
4.11.1	RNA extraction and purification.....	52
4.11.2	RNA quantification and quality check.....	53
4.11.3	cDNA synthesis.....	53
4.11.4	Real-time PCR reaction.....	54
4.12	Primers.....	54
4.13	Databases and Softwares.....	55
4.14	Microbial strains, vectors and gene constructs.....	56
4.14.1	Microbial strains.....	56
4.14.2	Vectors and gene constructs.....	57
4.15	Solutions.....	57

4.15.1	Stock solutions.....	57
4.15.2	Buffers.....	58
4.15.3	Growth media.....	59
4.16	Chemicals.....	60
4.17	Abbreviations.....	60
5	RESULTS.....	61
5.1	Studies on root meristem structure and viability in <i>tup5-1</i>	61
5.1.1	Where is the root growth-inhibiting light perceived in the <i>tup5-1</i> mutant?.....	61
5.1.2	Light signalling pathway of root growth inhibition.....	62
5.1.3	Hormonal status and cell cycle activity according to <i>GUS</i> -markers in the <i>tup5-1</i> root meristem.....	64
5.1.4	Viability of the root meristem.....	67
5.2	Identification of the gene <i>TUP5</i>	69
5.2.1	Mapping.....	70
5.2.2	Screening of <i>T-DNA</i> insertion lines for <i>TUP5</i> alleles.....	72
5.2.3	Sequencing of candidate genes.....	72
5.2.4	A false candidate: cinnamoyl CoA reductase.....	73
5.2.5	Pooled complementation with BAC subclones.....	74
5.2.6	The <i>tup5-1</i> mutation is located in <i>At1g80600</i> , a putative acetylornithine aminotransferase gene.....	78
5.2.7	Complementation of the mutant with the overexpressed <i>At1g80600</i>	79
5.2.8	Structure and predicted function of <i>TUP5</i>	81
5.3	Proof of the predicted function of <i>TUP5</i>	85
5.3.1	Supplementation of <i>tup5-1</i> with different amino acids.....	85
5.3.2	Heterologous complementation of a yeast ACOAT mutant.....	88
5.4	Impact of the <i>tup5-1</i> mutation on the amino acid content.....	89
5.4.1	Free arginine content in WT and <i>tup5-1</i>	90
5.4.2	The concentrations of serine and glycine was increased in <i>tup5-1</i> in a light-dependent manner.....	91
5.4.3	The level of many amino acids was altered in <i>tup5-1</i>	92
5.5	Subcellular localisation of <i>TUP5</i>	97
5.5.1	Database prediction and previous studies on the subcellular localisation of ACOAT.....	97
5.5.2	Localisation of <i>TUP5</i> by GFP fusion marker.....	98
5.6	Temporal and spatial expression pattern of <i>TUP5</i> in <i>A. thaliana</i>	99
5.6.1	Database information on <i>TUP5</i> expression.....	100
5.6.2	Testing <i>TUP5</i> -reporter gene fusions.....	103
5.6.3	Quantitative real-time PCR.....	103
5.7	Characterisation of T-DNA insertion alleles of the <i>TUP5</i> gene.....	106
5.7.1	Homozygous <i>tup5-2</i> and <i>tup5-3</i> insertion alleles are embryo lethal.....	108
5.7.2	Phenotypic analysis of transheterozygous plants.....	111
5.8	Analysis of plants overexpressing <i>TUP5</i>	113
5.8.1	Root phenotype of <i>TUP5</i> overexpressing plants.....	114
5.8.2	Leaf and silique phenotype.....	115
5.8.3	Free amino acid content of <i>TUP5</i> overexpression plants.....	118
6	DISCUSSION.....	121
6.1	Determination of the <i>TUP5</i> gene function.....	121
6.2	<i>TUP5</i> loss-of-function affects gametogenesis and embryogenesis.....	123
6.3	Effect of overexpression of <i>TUP5</i> on <i>Arabidopsis</i> development and metabolism.....	126
6.4	Developmental expression pattern of <i>TUP5</i> and exogenous stimuli influencing <i>TUP5</i> expression.....	130
6.5	<i>TUP5</i> has a chloroplastic localisation.....	132
6.6	The <i>tup5-1</i> mutation has an impact on overall amino acid metabolism.....	133
6.7	The root phenotype of the <i>tup5-1</i> mutant.....	136
6.8	Conclusions and perspectives.....	141
7	REFERENCES.....	143
8	ACKNOWLEDGMENTS / DANKSAGUNGEN.....	159

9	SUPPLEMENTAL DATA	161
9.1	Gene search.....	161
9.2	Vectors and gene constructs	166
9.3	Primers.....	168
9.4	<i>TUP5::GUS</i> reporter gene constructs	171
9.5	Free amino acid content of WT and <i>tup5-1</i>	171
9.6	T-DNA insertion lines of <i>TUP5</i>	173
9.7	Amino acid content of overexpression lines.....	174

1 Summary

Arginine is one of 20 standard amino acids necessary for the formation of peptides and proteins. It is also used as a nitrogen storage compound in seeds. Furthermore, arginine is the precursor of polyamines and nitric oxide which play an important role in many developmental processes and the response to various environmental stresses. Plant amino acid pathways have for a long time been mainly deduced from studies in bacteria and fungi. In this work the first conclusive study on an arginine biosynthetic *Arabidopsis* mutant is described. The EMS mutant *tup5-1* (*tumor prone 5-1*) was found in a screen for *Arabidopsis* mutants of which hypocotyl and root explants were cultivated on medium containing low auxin and cytokinin concentrations. The phytohormone concentrations were under the threshold of callus induction in the wild type, while the *tumor prone* mutants produced calli (Riefler, 2001). Furthermore, *tup5-1* also has a unique blue light-dependent short root phenotype: The root meristem is lost under blue light irradiation, resulting in root growth stop in the mutant (Frémont, 2004). In the following work, it was shown that the inhibiting light is perceived by the root. The cells constituting this short, growth arrested root have a strongly reduced metabolic activity, but are still viable. The gene encoding *TUP5* was identified as an acetylornithine aminotransferase (ACOAT), catalysing the fourth step of arginine biosynthesis. The *tup5-1* mutation is located in the third exon of At1g80600 causing an amino acid substitution (G424R). The amino acid targeted by this substitution is conserved in the homologous genes of bacteria, fungi and plants. Consistently, the free arginine content was reduced in *tup5-1* compared to the wild type and root growth was restored in the mutant by exogenous supplementation of arginine. As an additional functional proof, a yeast mutant lacking ACOAT which was auxotrophic for arginine could restore its arginine autotrophy after transformation with the *Arabidopsis TUP5* cDNA. Microarray data and real-time PCR showed that *TUP5* is expressed in rosette leaves, stems, flowers, siliques and roots. Furthermore, *TUP5* expression is positively regulated by light. A *TUP5*-GFP fusion showed that *TUP5* is most likely localised in chloroplasts. A knock-out of *TUP5* is lethal, as was shown for T-DNA insertion alleles. This confirms the crucial role of *TUP5* as a single copy gene. The loss of root meristem in *tup5-1* might be directly caused by the lack of arginine or by accumulation of other metabolites in toxic amounts, as the amino acid metabolism is more generally deregulated in *tup5-1*. The mechanisms linking the short root phenotype to arginine deficiency and blue light signalling still have

1. SUMMARY

to be elucidated. The mutant *tup5-1* provides a link between primary metabolism, plant development and blue light signalling.

2 Zusammenfassung

Arginin ist eine von 20 proteinogenen Aminosäuren, die für die Bildung von Peptiden und Proteinen benötigt werden. Zusätzlich wird Arginin zur Stickstoffspeicherung in Samen eingelagert und ist außerdem eine Vorstufe von Polyaminen und Stickoxid, die eine wichtige Rolle in Entwicklungsprozessen und bei der Streßantwort auf Umwelteinflüsse spielen. Die Synthesewege von Aminosäuren in Pflanzen wurden lange Zeit vorwiegend von bekannten Stoffwechselwegen aus Bakterien und Pilzen abgeleitet. In der vorliegenden Arbeit wird die erste umfassende Charakterisierung einer Argininbiosynthese-Mutante in *Arabidopsis* beschrieben. Die EMS-Mutante *tup5-1* (*tumor prone 5-1*) wurde in einem genetischen Hormonsensitivitätsscreen gefunden. Wurzel- und Hypokotylexplantate dieser Mutante bildeten *in vitro* vermehrt Kalli auf Medium mit geringen Auxin- und Cytokininkonzentrationen (Riefler, 2001). *tup5-1* zeigte außerdem eine bisher nicht beschriebene blaulichtabhängige Ausdifferenzierung des Wurzelmeristems, die zum Stop des Wurzelwachstums führte (Frémont, 2004). In der vorliegenden Arbeit wurde die Mutante weiter charakterisiert und die Funktion des betroffenen Gens untersucht. Es konnte gezeigt werden, daß das inhibierende Licht in der Wurzel perzipiert wird, und daß die Wurzelzellen des ausdifferenzierten Wurzelmeristems in ihrer Stoffwechselaktivität stark eingeschränkt sind. Das Gen, das für *TUP5* kodiert, wurde als Acetylornithin-Aminotransferase (ACOAT) identifiziert. Das Enzym katalysiert den vierten Schritt der Arginin-Biosynthese. Die *tup5-1* Mutation ist im dritten Exon von At1g80600 lokalisiert und bewirkt eine Aminosäuresubstitution (G424R). Die von dieser Substitution betroffene Aminosäure ist in homologen ACOATs von Bakterien, Pilzen und Pflanzen konserviert. Die aufgrund von Sequenzvergleichen postulierte Funktion von TUP5 in der Argininbiosynthese konnte auf verschiedene Weise bestätigt werden: Zum einen war der Arginingehalt in *tup5-1* im Vergleich zu Wildtyp wegen der Störung in der Argininbiosynthese stark reduziert, zum anderen konnte das Wurzelwachstum in der Mutante durch exogene Gabe von Arginin wiederhergestellt werden. Als zusätzlicher funktioneller Nachweis konnte eine Hefe-Mutante, die aufgrund des fehlenden homologen ACOAT-Gens argininauxotroph war, durch Transformation mit der *Arabidopsis TUP5* cDNA komplementiert werden. Microarray-Daten und qRT-PCR-Experimente zeigten, daß *TUP5* in Rosettenblättern, Sproß, Blüten, Schoten und Wurzeln exprimiert und durch Licht positiv reguliert wird. Durch Untersuchung eines TUP5-GFP-Fusionsproteins in transformierten Protoplasten konnte gezeigt werden, daß

TUP5 mit größter Wahrscheinlichkeit in Chloroplasten lokalisiert ist. Die Untersuchung von T-DNA-Insertionslinien ergab, daß sich ein kompletter Verlust der *TUP5* Funktion letal auswirkt. Dies bestätigt die überlebenswichtige Rolle von *TUP5*, von dem nur eine einzige Kopie im *Arabidopsis*-Genom vorliegt. Zusammenfassend kann gesagt werden, daß die Mutante *tup5-1* eine bisher unbekannte Verbindung zwischen Primärmetabolismus, Pflanzenentwicklung und Blaulicht-Perzeption in *Arabidopsis* aufzeigt.

3 Introduction

The aim of developmental biology is to answer the interesting question: which mechanisms make it possible for a single cell, the zygote, to become a multicellular organism with complex organ structures? In contrast to animals, plants need to maintain a lifelong morphological plasticity due to their sessile way of life. While animals usually cannot regrow lost organs and limbs, plants are able to regenerate shoots and roots after herbivore attacks or if they need to extend their shoots to less shaded areas and roots to more humid or nutrient rich soils. Formation of plant organs takes place in meristems in which cells divide from initial cells and differentiate under the influence of plant hormones, cell-cell communication signals and environmental cues (Tucker and Laux, 2007; Werner and Schmülling, 2009). Cell division and differentiation needs to be kept under tight control, because uncontrolled cell proliferation leads to tumour growth and unrestrained differentiation causes meristem loss and growth arrest. Skoog and Miller (1957) described an important role of the two plant hormones cytokinin and auxin for cell proliferation and differentiation. They showed that in tobacco cell culture, a high auxin to cytokinin ratio led to root growth in calli, while a high cytokinin to auxin ratio promoted shoot growth (Skoog and Miller, 1957). If auxin and cytokinin are applied in a certain balanced ratio, an undifferentiated cell proliferation takes place, yielding growing calli. Auxin and cytokinin often act antagonistically: Auxin is important for stem cell maintenance and cell division by activating the *PLETHORA* genes, while cytokinin is necessary for the restriction of the meristem and cell differentiation in the root meristems (Dello Ioio *et al.*, 2008). In the shoot meristem it is cytokinin which promotes cell division, while auxin induces organogenesis (Sablowski, 2007).

M. Riefler made a screen in EMS-mutagenised *Arabidopsis* plants in order to find cytokinin- and auxin-dependent genes involved in cell cycle and differentiation control (Riefler, 2001). For this purpose explants of the EMS-treated plants were cultivated on medium containing low auxin and cytokinin concentrations which normally do not induce callus (or root and shoot) formation in WT explants (Riefler, 2001). Five mutants named *tumor prone (tup1 - tup5)* with the ability to form calli under these conditions were identified (Riefler, 2001). This work is focusing on the study of the mutant *tup5* (renamed *tup5-1*) and the elucidation of the gene's function. Beside the above-mentioned phenotype, *tup5-1* also has a striking blue light-dependent short root phenotype, making it an interesting object for the study of the unusual connection between light signalling and root develop-

ment (Riefler, 2001; Frémont, 2004). Due to the set-up of the mutant screening, regulatory elements connected to hormone signalling were expected as candidates for the *tup5-1* gene. Interestingly, the result of the gene search was much unexpected (see chapter 5.2).

3.1 The root of *Arabidopsis thaliana*

3.1.1 Root growth and morphology

General organisation of the Arabidopsis root

The root of *Arabidopsis* is radially symmetric with four concentric layers of (from outside to inside) epidermis, cortex, endodermis and pericycle with vascular tissue in its center (Figure 3-1, A) (Scheres *et al.*, 2002). Longitudinally, the root is constituted of four different developmental zones (shootward from root tip): root cap, root meristem, elongation zone and differentiation zone (Scheres *et al.*, 2002; Baskin *et al.*, 2010).

The root cap

The root cap is composed of two types of tissue: The columella cells in the inner zone of the root cap, which contain starch granules used for sensing gravity, and the lateral root cap cells which constitute the peripheral zone of the root cap (Figure 3-1, A) (Scheres *et al.*, 2002). These two cell types are formed by different initial cells: the columella initials and the epidermal/lateral root cap initials (Nakajima and Benfey, 2002). The root cap protects the growing root tip against mechanical damages when penetrating the soil (Taiz and Zeiger, 2002, p. 355). During this process root cap cells are peeled off, but they are constantly renewed by cell division (Taiz and Zeiger, 2002, p. 355).

The root meristem

The meristematic zone lies shootward of the root cap. In its center the meristem contains four mitotically (almost) inactive Quiescent Center (QC) cells which are surrounded by a single layer of five types of initials (Nakajima and Benfey, 2002). The columella initials are positioned rootward from the QC (Scheres *et al.*, 2002). They are the origin of the columella cells. These initials do not contain starch granules, because these are only formed during the differentiation process of columella cells (van den Berg *et al.*, 1997). The columella initials are radially surrounded by the epidermal/lateral root cap initials which generate the epidermis and the lateral root cap cells. The cortical/endodermal initials lay radially around the QC cells. They generate the cortex layer and the endodermis (Figure 3-1, A)

(Scheres *et al.*, 2002). The pericycle and the vascular tissue (together forming the stele) are generated by their respective initial cells, which lay shootward from the QC (Figure 3-1, A) (Nakajima and Benfey, 2002).

Differentiation of tissues from initial cells

The initial cells first undergo an anticlinal division, which means perpendicular to the growth axis. The daughter cell in contact with the QC remains an initial cell which does not differentiate. The other one, which is more distant from the QC, can either differentiate, as in the case of columella cells or divide periclinally, which means parallel to the growth axis. Therefore an additional radial cell layer is formed, as for example cortical/endodermal initials do (Figure 3-1, B) (Dolan *et al.*, 1993). In this case the second periclinal division generates the endodermis and the cortex layer (Figure 3-1, A and B).

Due to ongoing divisions of the initials, clonal cell files are formed longitudinally. Older daughter cells are therefore located more shootward from the meristem, except for columella cells. In the elongation zone they divide a few more times periclinally and then start to expand anisotropically (Scheres *et al.*, 2002). The radial expansion takes place in the elongation zone, defining the ultimate root radius (Scheres *et al.*, 2002). In the differentiation zone lying shootward of the elongation zone, the cells receive their tissue-specific properties (Taiz and Zeiger, 2002, p. 355) .

Regulation and signalling controlling root meristem function

It is important for the functionality of the meristem that the initials remain mitotically active and do not differentiate. This maintenance of an embryonic state is controlled by signals from the QC which prevent the surrounding initial cells from differentiating by direct cell to cell contact (van den Berg *et al.*, 1997). The QC identity itself is defined by external signals (van den Berg *et al.*, 1995). The QC is positioned at the overlap of the SCARECROW (SCR)/SHORT ROOT (SHR) signalling pathway on the radial axis and of the *PLETHORA* genes which are activated by the auxin polarly transported into the root tip through vascular cells on the longitudinal axis (Sablowski, 2007; Dinneny and Benfey, 2008). The *RETINOBLASTOMA-RELATED* gene promotes cell differentiation and restricts proliferation within the root meristem (Wildwater *et al.*, 2005).

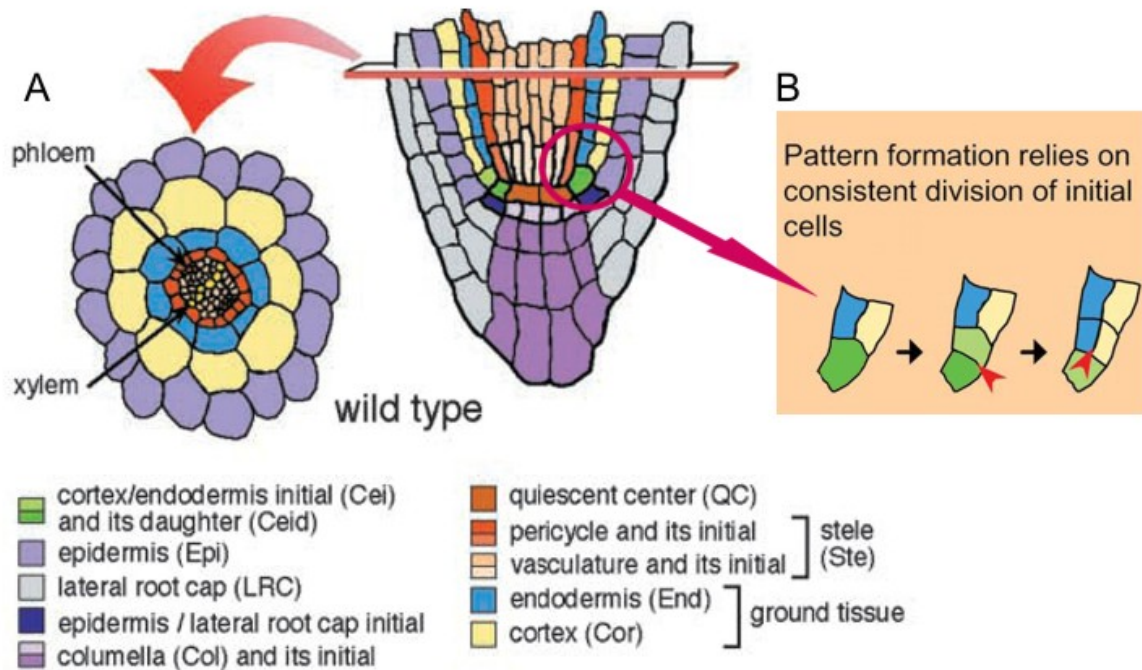


Figure 3-1: Root meristem structure and mechanism of asymmetric cell division.

A: Scheme of transverse (left) and longitudinal (right) section of the *Arabidopsis* root tip (Dolan *et al.*, 1993; Nakajima and Benfey, 2002); B: Mechanism of asymmetric cell divisions that the cortex/endodermis initial cell and its daughter undergo (adapted from: Scheres *et al.*, 2002).

3.1.2 Natural abiotic factors influencing root development

The roots have to anchor the plant in the soil and ensure the nutrients and water supply. Roots can use several physical and chemical cues to direct their growth into the appropriate direction. A very basic physical cue perceived by the root to grow into the soil is gravity, which is sensed through the position of starch granule-filled amyloplasts in columella cells, leading to positive gravitropic growth (Rosen *et al.*, 1999). To avoid mechanical obstacles in the soil, as for example rocks, plant roots can sense mechanical stimuli (Monshausen and Gilroy, 2009). As a reaction to these stimuli, a transient cytosolic Ca^{2+} increase followed by transient changes in pH and increased production of extracellular ROS (reactive oxygen species) occur in roots (Monshausen *et al.*, 2009). If the root cannot force its way through the obstacle it will bend and moreover can induce lateral root development (Monshausen *et al.*, 2009). Roots can also sense soil moisture by yet unknown molecular mechanisms and direct their growth into the direction of better water supply, this reaction is called hydrotropism (Monshausen and Gilroy, 2009). To react to possible nutrient-deprivation, plants have evolved signalling pathways indicating the internal and external nutrient status, which can lead to changes in root architecture (López-Bucio *et al.*, 2003). Especially nitrogen, phosphorus, iron and sulphur deprivation can alter root development

(López-Bucio *et al.*, 2003). Plants do not only react by changes in root growth, but also by enhancing the formation and elongation of root hairs to increase the absorptive surface as for example in the case of low iron and phosphorus availability (López-Bucio *et al.*, 2003). Interestingly, root meristems can undergo a determinate developmental program which causes the loss of the meristem possibly due to phosphate starvation (Sánchez-Calderón *et al.*, 2005). Though it is being discussed whether the ultimate reason for this root growth inhibition is higher and therefore toxic iron availability due to the phosphate reduction (Ward *et al.*, 2008).

The soil can contain amino acids from decomposing animals and plants which might be used as nitrogen sources (Forde and Lea, 2007). It might therefore be beneficial for plants to sense soil areas of higher amino acid concentrations (Forde and Lea, 2007). The amino acid L-glutamate has a specific primary root growth-inhibiting effect which is perceived at the root tip and which reduces mitotic activity in the primary root apical meristem when applied exogenously (Walch-Liu *et al.*, 2006; Forde and Lea, 2007). Besides this, lateral root formation is induced near the root apex. The newly formed lateral roots also become glutamate-sensitive when they have reached a length of 5-10 mm (Walch-Liu *et al.*, 2006; Forde and Lea, 2007). This leads to a dense root system where glutamate concentration is high (Forde and Lea, 2007). In the study of Walch-Liu *et al.* (2006) the primary root growth recovery after glutamate treatment was assessed. The primary root meristem was lost if a critical duration of glutamate exposure was exceeded (Walch-Liu *et al.*, 2006).

The amino acid L-tryptophan also has an effect on root growth when applied exogenously, but it might be an auxin effect, as tryptophan is a precursor of indole-3-acetic acid (IAA) (Müller *et al.*, 1998; Walch-Liu *et al.*, 2006).

The effect of light on root development will be discussed in chapter 3.2.2.

3.2 Light signalling in plants

Light is an energy source and an important environmental signal for plants (Liscum *et al.*, 2003). For example, the day length gives information on the season and helps the plant to anticipate the environmental conditions and adapt its development to them (Sullivan and Deng, 2003). Light, together with other factors, controls developmental processes such as germination, photomorphogenesis, shade avoidance, phototropism, chloroplast movement, stomatal opening, circadian clock adjustment and flowering time (Sullivan and Deng, 2003). *Arabidopsis* has different light receptor types: phytochromes, cryptochromes,

phototropins, the Zeitlupe family genes and possibly UVB receptors (Nemhauser and Chory, 2002; Christie, 2007b).

3.2.1 Plant photoreceptors

Phytochrome

Phytochromes are photoreceptors which perceive mainly the red / far red wavelengths (600 – 750 nm) of light spectrum (Sullivan and Deng, 2003). Phytochromes act as homodimers, each monomere being composed of an apoprotein with a molecular weight of approximately 125 kDa and a linear tetrapyrrole (phytochromobilin) as chromophore (Casal *et al.*, 2003; Bae and Choi, 2008). *Arabidopsis* has five phytochrome apoprotein genes (*PHYA - PHYE*). The highest concentrations of phytochromes are found in young undifferentiated tissues, especially in shoot and root apical meristem (Taiz and Zeiger, 2002, p. 381). *phyA* and *phyB* are localised in the cytosol in dark-grown seedlings (Casal *et al.*, 2003). Light induces their translocation to the nucleus (Bae and Choi, 2008). This translocation is critical for their role in the regulation of gene expression (Nagatani, 2004).

Seeds use light signals via phytochrome together with humidity and temperature for the determination of germination time (Nemhauser and Chory, 2002; Bentsink and Koornneef, 2008). Another important role of phytochrome is the light perception for shade avoidance. Overhanging leaves of neighbouring plants selectively absorb red light and let far red light pass through, resulting in light with a low red/far red ratio perceived by phytochromes (Sullivan and Deng, 2003). When the plant perceives these unfavourable photosynthetic conditions, it can react with elongation growth and increased apical dominance to try to overgrow the shading plants (Sullivan and Deng, 2003). Phytochromes are also involved in deetiolation of seedlings, circadian clock adjustment and the transition to flowering together with other photoreceptors (Casal *et al.*, 2003; Sullivan and Deng, 2003).

Cryptochrome

Cryptochromes are blue light and UV-A photoreceptors found in bacteria, fungi, animals and plants (Lin and Shalitin, 2003). Most plant cryptochromes have a molecular weight of 70-80 kDa (Lin and Shalitin, 2003). They are composed of a photolyase-related domain (PHR) at the amino-terminus and a CCT (cryptochrome carboxy-terminal) domain not related to photolyases and which is critical for the function of *Arabidopsis cry1* and *cry2* (Lin and Shalitin, 2003; Liscum *et al.*, 2003). The PHR domain binds flavin adenine dinucleotide (FAD) as catalytic cofactor and Methenyltetrahydrofolate (MTHF) as antenna chromophore (Batschauer *et al.*, 2007). Cryptochromes are phosphorylated in response to

blue light; this is necessary for their biological activity (Batschauer *et al.*, 2007). Three cryptochromes have been found in *Arabidopsis*: cry1, cry2 and a cryDASH protein named cry3 (Batschauer *et al.*, 2007; Zirak *et al.*, 2009). cry1 and cry2 are involved mainly in deetiolation of seedlings, day length perception and circadian clock adjustment; and the transition to flowering together with the phytochromes (Sullivan and Deng, 2003). A function as photolyase was shown *in vitro* for cry3 which is targeted to chloroplasts and mitochondria, but its *in vivo* function is still under discussion (Pokorny *et al.*, 2008; Reisbacher, 2009).

cry1 and cry2 interact with COP1 (Batschauer *et al.*, 2007). COP1 is an E3 ubiquitin ligase which targets the photomorphogenesis inducing transcription factor HY5 for degradation (Batschauer *et al.*, 2007). cry1 is localised to the nucleus in darkness and exported to the cytosol after light treatment (Lee *et al.*, 2008b). After illumination with blue light, the CCT domain of cryptochrome is phosphorylated and it probably undergoes conformational changes to an active state (Batschauer *et al.*, 2007). In the active state CCT represses the COP1 function and cause the export of COP1 from the nucleus (Batschauer *et al.*, 2007). HY5 can therefore accumulate in the nucleus and activate light-induced genes according to that model (Batschauer *et al.*, 2007). cry2 seems not to be shifted between cellular compartments, it is phosphorylated and degraded in the nucleus (Yu *et al.*, 2007).

Phototropin

Phototropins are flavoprotein blue light / UV-A photoreceptors involved in “movements” of plant organs due to light stimuli, such as phototropism, light-induced stomatal opening or chloroplast relocation to improve the photosynthetic rate (Quail, 2002; Christie, 2007a). Additionally, phototropins play a role in cotyledon and leaf expansion and the rapid hypocotyl elongation after shift of dark-grown seedlings to blue light (Christie, 2007a). *Arabidopsis* has two phototropins, phot1 and phot2, localised in the plasma membrane and having an approximate molecular weight of 120 kDa (Sakamoto and Briggs, 2002). Phototropins are composed of a photosensory domain at the amino-terminus and a serine/threonine kinase domain at the carboxy-terminus (Christie, 2007a). The photosensory domain contains two so-called LOV domains, found in members of the light, oxxygen, voltage-regulated protein family (Liscum *et al.*, 2003; Sullivan and Deng, 2003). Each LOV domain binds one molecule of flavin mononucleotide (FMN) as chromophore (Banerjee and Batschauer, 2005). Phototropins undergo blue-light dependent autophosphorylation (Sakamoto and Briggs, 2002). While phot1 mediates reactions to low fluence

rates of blue light, phot2 plays only a role in high fluence rate perception (Sakamoto and Briggs, 2002). The positive phototropism of the hypocotyls is mediated by phot1 at low and by both, phot1 and phot2 at high fluence rates of blue light. The phototropin-mediated directional light perception probably forms a signalling gradient which causes auxin accumulation on the shaded side of the hypocotyl (Sakamoto and Briggs, 2002; Christie, 2007a). This induces an increased growth on the shade side and therefore bending towards the light source (Sakamoto and Briggs, 2002; Christie, 2007a). Phytochromes and cryptochromes are also involved in hypocotyl phototropism, but only phototropin mediates the directional light sensing (Christie, 2007a). Chloroplasts relocate according to light conditions: They move towards the light irradiated surfaces within the cell to increase their photosynthetic rate. This effect is mediated by phot1 and phot2. If irradiation is too high and might cause damages to the photosynthetic system, the chloroplasts are redistributed in a light avoiding manner (Briggs and Christie, 2002). This effect is mediated solely by phot2 (Christie, 2007b). Stomatal opening which is regulated by both phototropins is mediated by swelling of the guard cells (Lin, 2002). As a consequence of blue light signals, ion fluxes and osmotic changes within the guard cell lead to water intake and increased turgor pressure (Kwak *et al.*, 2009).

Zeitlupe family and another LOV containing protein in Arabidopsis

Three proteins constitute a novel blue light receptor family; these are ZLP (Zeitlupe), FKF1 (Flavin-binding Kelch repeat F-box 1) and LPK2 (LOV Kelch Protein 2) (Christie, 2007a; Demarsy and Fankhauser, 2009). All three possess a single LOV domain (see phototropin) at the aminoterminal, an F-box motif and six kelch repeats (Banerjee and Batschauer, 2005; Christie, 2007a). The LOV domain of the ZLP family members shows typical light sensor properties comparable to phototropins, except for dark-reversion found in phototropins but not in the ZLP family (Banerjee and Batschauer, 2005; Christie, 2007a). The F-BOX motif is found in E3 ubiquitin ligases which target proteins for degradation. The function of ZLP family proteins is therefore considered to be the targeting of circadian clock-related proteins for degradation (Banerjee and Batschauer, 2005; Christie, 2007a). The Kelch domain repeats might be important for protein-protein interactions (Banerjee and Batschauer, 2005; Christie, 2007a). The ZLP family plays a role in circadian clock and flowering time control (Banerjee and Batschauer, 2005; Christie, 2007a). ZLP is also involved in photomorphogenesis (Spalding and Folta, 2005).

Another LOV-containing protein was found in *Arabidopsis* (Christie, 2007a). The function of the so-called PAS/LOV protein is not known yet (Christie, 2007a).

UV-B photoreceptors

UV-B is an important environmental signal which influences plant development, metabolism and stress responses such as DNA damage signalling, reactive oxygen species accumulation and signalling; and wound/defense signalling (Jenkins, 2009). UV-B promotes branching and reduces stem and leaf elongation for example and it induces the production of secondary metabolites such as flavonoids for UV protection (Jansen, 2002; Jenkins, 2009). There are different signalling pathways involved in UV-B perception and up to now it is not known how many pathways do exist in plants (Jenkins, 2009). Many molecules, as for example phenolic compounds, nucleic acids and proteins, absorb UV-B (Jenkins, 2009). The existence of specific UV-B photoreceptors has been discussed, but the molecular components have not been found yet (Jenkins, 2009).

3.2.2 Light signalling and root development

Though roots are mainly located in the soil where light plays a minor role as environmental signal, phytochromes, cryptochromes and phototropins were found in root tissue (Tóth *et al.*, 2001; Sakamoto and Briggs, 2002; Canamero *et al.*, 2006). Light might have an impact on root development as it can be transmitted through the upper soil layers (Mandoli *et al.*, 1990). Additionally, light can be conducted axially from the stem to the roots (Sun *et al.*, 2005). Blue and red light have antagonistic effects on *Arabidopsis* root phototropism: blue light induces phototropin-mediated negative phototropism, while red light induces a weak phytochrome-mediated positive phototropism (Ruppel *et al.*, 2001; Sakai *et al.*, 2001). The blue light-mediated negative phototropism might prevent the root from growing toward the stressful upper soil layers (Boccalandro *et al.*, 2008). And indeed, phot1 was found to have an impact on drought tolerance, because phot1-deficient roots grow less efficiently into deeper soil layers (Galen *et al.*, 2007a). PHYTOCHROME KINASE SUBSTRATE 1 (PKS1) is involved in blue light-dependent negative root phototropism and it negatively regulates root gravitropism (Boccalandro *et al.*, 2008). PKS1 interacts with phot1 and the blue light signal that induces *PKS1* expression is perceived by phyA, therefore indicating that PKS1 links both photoreceptor signalling pathways (Lariguet *et al.*, 2003; Lariguet *et al.*, 2006).

Light does not only play a role in root phototropism, but also in root growth. Phytochromes inhibit root elongation in etiolated seedlings treated with red light and additionally influence root gravitropism (Correll and Kiss, 2005). In contrast to Correll and Kiss (2005), Canamero et al. (2006) found that continuous red light promoted root growth. Cryptochromes have antagonistic effects on primary root growth in blue light: cry1 promotes root growth, while cry2 inhibits it (Canamero *et al.*, 2006).

Two recently described *Arabidopsis* mutants are impaired in seedling development and root growth (Tong *et al.*, 2008; Leasure *et al.*, 2009). This developmental arrest is due to UV-B light exposure of the root (Tong *et al.*, 2008). Both, *rus1* (*root UV-B sensitive1*) and *rus2-1* carry a mutation in homologous genes containing a DUF647 domain (domain of unknown function 647) highly conserved in eukaryotes (Tong *et al.*, 2008; Leasure *et al.*, 2009). RUS1 and RUS2 interact and are probably localised in plastids (Leasure *et al.*, 2009).

At last, root hair development is promoted by phytochrome in a light-dependent manner (De Simone *et al.*, 2000).

3.3 Amino acid biosynthesis

Amino acids have a fundamental role in living organisms. Beside their function as building blocks of proteins, they are also important in primary and secondary metabolism. Nitrogen, which is assimilated in the form of amino acids for the plant's metabolism, is a rate-limiting factor in plant growth (Lam *et al.*, 1995). Glutamate, glutamine, aspartate and asparagine are needed for nitrogen transport (Lam *et al.*, 1995). Many amino acids are precursors of various products of secondary metabolism, like plant hormones or molecules used for plant defense (Coruzzi and Last, 2000). Hence, genes involved in amino acid biosynthesis play an important role in plant growth and development. The field of amino acid synthesis was extensively studied in bacteria and fungi. The knowledge gained from these organisms is used for investigating plant amino acid biosynthesis which is not fully explored yet (Coruzzi and Last, 2000).

First, an overview of nitrogen assimilation and the synthesis pathways of the different amino acids will be given, with emphasis on the role of light in regulating these processes (chapter 3.3.1). In a second part, plant mutants of amino acid synthesis genes will be presented with a focus on root developmental phenotypes (chapter 3.3.2). Finally, arginine biosynthesis and regulation will be described in more detail (chapter 3.3.3), because the gene *TUP5* studied in this work is involved in this pathway (see chapter 5.2.8).

3.3.1 Overview of amino acid synthesis pathways

Nitrogen assimilation

All amino acids are synthesised from carbon skeleton backbones produced during photosynthesis, glycolysis, the oxidative pentose phosphate pathway and the citric acid cycle (Coruzzi and Last, 2000). Light and the availability of carbon and nitrogen metabolites are factors regulating the nitrogen assimilation into the nitrogen-transporting amino acids glutamate, glutamine, aspartate and asparagine which represent 70% of the total free amino acids in *Arabidopsis* (Lam *et al.*, 1995; Coruzzi and Last, 2000). As the light-dependent root phenotype of *tup5-1* is probably connected to amino acid metabolism, the light-regulated nitrogen assimilation is described exemplarily in the following part.

The primary nitrogen assimilation in plants takes place by the incorporation of ammonium using glutamate to form glutamine (Figure 3-2) (Rose and Last, 1994). This reaction is performed by glutamine synthetase (GS). Subsequently the amide group is transferred by glutamate synthase (GOGAT) from glutamine to α -ketoglutarate to form two molecules of glutamate (Coruzzi and Last, 2000). These two reactions form the GS/GOGAT cycle.

Two isoforms of glutamine synthetase were found: a cytosolic one (GS1), and a chloroplastic one (GS2) (Coruzzi, 2003). The three GS1 isoenzymes encoded by *GLN1.1-1.3* supposedly work in primary nitrogen assimilation in roots: the assimilated nitrogen is exported as glutamine into other plant organs through the xylem (Coruzzi, 2003). GS2 is light-regulated through the phytochrome signalling pathway and mainly expressed in leaves (Coruzzi, 2003). The leaf GS2 isoenzyme is thought to have a function in primary ammonia assimilation and in reassimilation of ammonia from photorespiration (Coruzzi and Last, 2000; Coruzzi, 2003).

Glutamine, a metabolically reactive amino acid, is accumulated in the light (Coruzzi and Last, 2000). When nitrogen has been assimilated in glutamate and glutamine, it can be transferred as an amino group onto other compounds by aminotransferases. The transfer of the amino group from glutamate to oxalacetate yielding aspartate and regenerating α -ketoglutarate is catalysed by aspartate aminotransferase (Figure 3-2) (Coruzzi and Last, 2000). α -ketoglutarate can again be used for primary nitrogen assimilation while aspartate is used for inter- and intracellular transport of carbon and nitrogen (Coruzzi and Last, 2000). Many plant species use asparagine as inert nitrogen storage and transport compound with a high N / C ratio (Figure 3-2) (Coruzzi, 2003). The level of asparagine raises in dark-adapted plants (Coruzzi, 2003), when carbon backbones become scarce. Asparagine synthetase (AS) catalyses the transfer of an amino group from glutamine to aspartate, yielding

asparagine and glutamate (the hydrolysed former glutamine) (Figure 3-2) (Coruzzi, 2003). *ASN1*, one of the three AS genes of *Arabidopsis* accounts for the main synthesis of free asparagine. Its expression is repressed by light and induced in darkness (Coruzzi, 2003). The *ASN1* expression correlates with free asparagine levels measured in light (low) and darkness (high) (Figure 3-2). *ASN1* expression is inhibited by exogenously applied sucrose (Lam *et al.*, 1994). This effect can be partly rescued by application of glutamate, glutamine or asparagine, suggesting that a high nitrogen to carbon ratio induces *ASN1* expression (Lam *et al.*, 1994).

The assimilated nitrogen can then be used for the synthesis of all other amino acids, of nucleotids and secondary metabolites (such as chlorophyll, flavonoids, lignin, and the phytohormones cytokinin, auxin and ethylene) (Rose and Last, 1994; Coruzzi, 2003).

Alanine

Alanine is produced by the transfer of an amino group from glutamate to pyruvate by alanine aminotransferase (Figure 3-3) or by desulfurisation of cystein when sulfur is used for the production of iron–sulfur (Fe–S) clusters; this is catalysed by cysteine desulfurases (Liepman and Olsen, 2004; Balk and Lobréaux, 2005). High alanine concentrations are accumulated in the roots under hypoxia (Miyashita *et al.*, 2007). Alanine aminotransferase catalyses the degradation of alanine thereby releasing the stored carbon and nitrogen when normal oxygen conditions are restored (Miyashita *et al.*, 2007).

Aromatic amino acid synthesis

The aromatic amino acid pathway is not only used for tryptophan, phenylalanine and tyrosine synthesis as protein building blocks (Figure 3-3); but also for the synthesis of aromatic secondary metabolites in plants (Coruzzi and Last, 2000). The synthesis pathway is as follows: Erythrose-4-phosphate and phosphoenolpyruvate are converted to shikimate in four reactions (Herrmann, 1995). In three more reaction steps, chorismate is formed from shikimate (Herrmann, 1995). Chorismate can then either be converted to anthranilate for tryptophan synthesis or to prephenate for tyrosine and phenylalanine biosynthesis (Figure 3-3) (Radwanski and Last, 1995; Coruzzi and Last, 2000). Feedback inhibition by end products and activation by concurring end products exist at the branching points of the three aromatic amino acid synthesis pathways (Siehl and Conn, 1988; Radwanski and Last, 1995; Mobley *et al.*, 1999; Coruzzi and Last, 2000)

Aromatic amino acid biosynthesis takes place in plastids (Coruzzi and Last, 2000). Tryptophan can be further metabolised to the phytohormone auxin, to indolic alkaloids and indolic glucosinolates (Radwanski and Last, 1995). These compounds play a role in plant development, pathogen defense, pollinator attraction and other processes (Radwanski and Last, 1995). Phenylalanine and tyrosine are used for many secondary metabolites as for example lignins, alkaloids and flavonoids. (Coruzzi and Last, 2000)

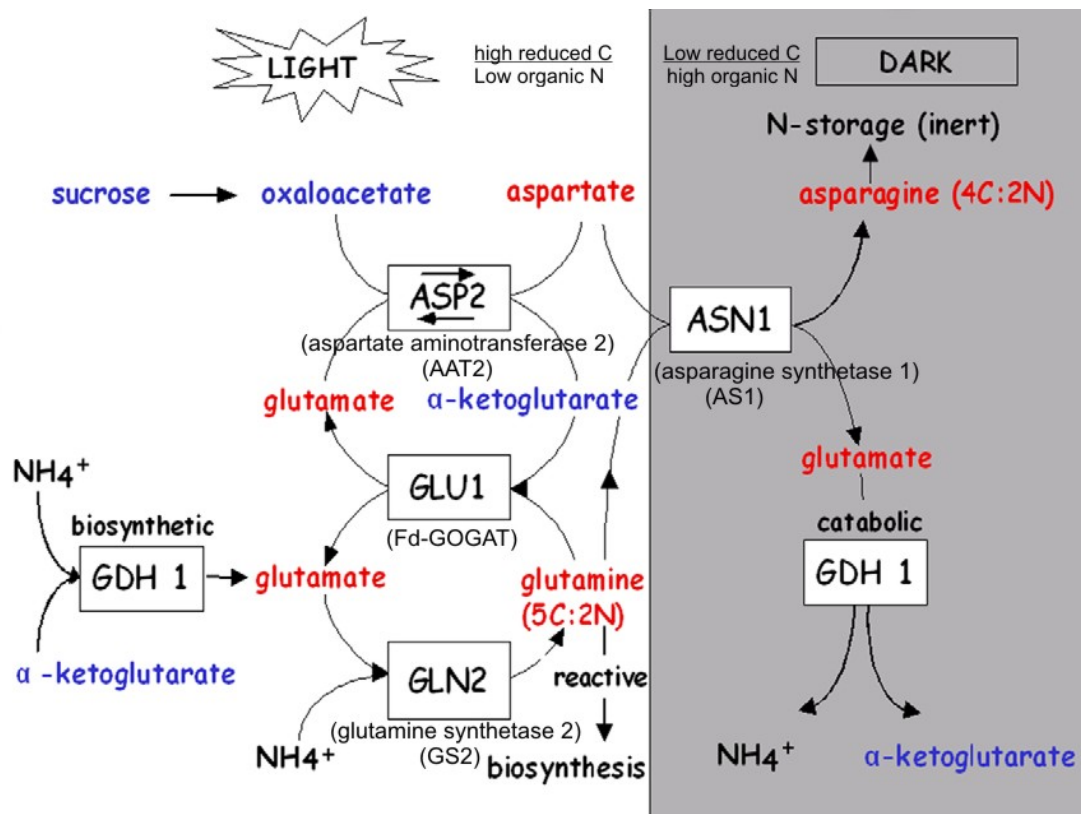


Figure 3-2: A model for the metabolic flow of nitrogen assimilation into the nitrogen-transport amino acids glutamate, glutamine, aspartate, and asparagine in light and darkness.

In the light, inorganic nitrogen is assimilated initially into glutamate and glutamine by the combined actions of the plastid enzymes: chloroplastic glutamine synthetase 2 (*GS2*) encoded by *GLN2*, and ferredoxin-dependent glutamate synthase (Fd-GOGAT) encoded by *GLU1*. The conversion of glutamate into aspartate in the light is controlled by the cytosolic aspartate aminotransferase AAT2 encoded by *ASP2*. In the dark, this pool of aspartate is converted into asparagine by asparagine synthetase (*ASN1*). Gene names are shown in boxes, protein names in brackets below (adapted from Coruzzi and Last (2000) and Coruzzi (2003)).

Aspartate-derived amino acids

Lysine, methionine, threonine are synthesised from aspartate in a common pathway (Figure 3-3) (Coruzzi and Last, 2000; Jander and Joshi, 2009). Isoleucine, a branched-chain amino acid, is derived from threonine (Figure 3-3). All four amino acids are synthesised in plastids (Coruzzi and Last, 2000; Jander and Joshi, 2009). Methionine is a precursor of *S*-adenosylmethionine (SAM), ethylene and polyamines (Coruzzi and Last, 2000). The biosynthesis of aspartate-derived amino acid is controlled by allosteric regulation of

the branch-point enzymes (Jander and Joshi, 2009). *AGD2* is another example of light-regulated gene expression in amino acid biosynthesis: it encodes for L,L-diaminopimelate aminotransferase acting in lysine biosynthesis and it is upregulated by light (Song *et al.*, 2004; Hudson *et al.*, 2006; Jander and Joshi, 2009).

Branched-chain amino acids

Threonine is deaminated to 2-ketobutyrate for the synthesis of isoleucine (Figure 3-3). After this step, valine and isoleucine are synthesised in parallel by four enzymes with dual substrate specificity using 2-ketobutyrate as starting substance for isoleucine and pyruvate as precursor for valine (Singh, 1999; Coruzzi and Last, 2000). The intermediate of the third step in valine synthesis, 2-ketoisovalerate, can be used as substrate for the synthesis of leucine in four more enzymatic steps (Singh, 1999; Coruzzi and Last, 2000). The branched-chain biosynthetic pathway seems to be located in plastids (Singh, 1999). It is regulated by feedback inhibition of different enzymes at committing steps of the pathway (Singh, 1999). Threonine deaminase, which catalyses the first committing step to isoleucine synthesis, is activated by valine (Halgand *et al.*, 2002; Binder *et al.*, 2007).

Glutamate-derived amino acids

Both, glutamate and its derivative ornithine, are precursors in the proline biosynthesis pathway (Verbruggen and Hermans, 2008). Proline accumulates in plants in response to various stresses, especially osmotic stress. Proline has various functions in the plant's adaption to stress: in osmoprotection, ROS scavenging, molecular chaperone action, and others (Verbruggen and Hermans, 2008). Both, glutamate and ornithine are the precursors in young *Arabidopsis* plants for proline accumulation under osmotic stress, while in older plants mainly the glutamate pathway is used (Roosens *et al.*, 1998). Δ^1 -pyrroline-5-carboxylate synthase 1 (*P5CS1*) catalyses the first two reactions of proline biosynthesis via the glutamate pathway (Verbruggen and Hermans, 2008). The transcription of *P5CS1* and proline accumulation is promoted by light and repressed by brassinosteroids in *Arabidopsis* (Ábrahám *et al.*, 2003; Szabados and Saviouré, 2010).

Arginine biosynthesis will be discussed in chapter 3.3.3.

Histidine

Histidine is synthesised in a highly energy consuming process of eleven reaction steps from phosphoribosyl- α -1-diphosphate (PRPP), which is also a starting product for the *de*

novo biosynthesis of purines (Stepansky and Leustek, 2006). It is assumed that the entire histidine biosynthesis pathway is located in chloroplasts (Ward and Ohta, 1999; Stepansky and Leustek, 2006). Feedback regulation takes place at the first enzymatic step of histidine biosynthesis: ATP-phosphoribosyl transferase is inhibited by histidine (Ohta *et al.*, 2000). Beside its role as proteinogenic amino acid, histidine can act as chelator for metal ions and is therefore important for metal ion homeostasis in plants (Stepansky and Leustek, 2006).

Glycine, serine and cysteine

Glycine and serine can be interconverted; therefore their biosynthesis is tightly connected (Bourguignon *et al.*, 1999). There are two synthesis pathways for serine. 3-phosphoglycerate, an intermediate of glycolysis, is used to produce serine in three reaction steps in the so-called “phosphorylated” or “glycolytic” pathway (see in “Plant Metabolic Network”: <http://www.plantcyc.org:1555/ARA/server.html>; Rhee *et al.*, 2006) (Bourguignon *et al.*, 1999). Serine can then be reversibly converted to glycine. This pathway seems to be important in non-photosynthetic tissues and under environmental stress conditions (Ho and Saito, 2001). The other pathway for serine synthesis is derived from photorespiration. Glyoxylate, an intermediate in the photorespiratory pathway, can be transaminated to glycine. Glycine can then be converted to serine (Bourguignon *et al.*, 1999). The photorespiratory pathway is highly active in photosynthetic tissues, though its contribution to net serine and glycine production is not clear, because the latter are mostly redirected into the calvin cycle (Bourguignon *et al.*, 1999). An additional pathway for glycine synthesis is via threonine aldolase (Joshi *et al.*, 2006).

Cysteine can be synthesised from serine in two reaction steps (Saito, 1999). In the second reaction, sulphur is integrated. This is the main integration pathway of sulphur into organic molecules (<http://www.plantcyc.org:1555/ARA/server.html>: “Plant Metabolic Network”; Rhee *et al.*, 2006). The sulphur can be transferred from cysteine to the other sulphur-containing amino acid methionine and other important compounds as glutathione, thiamine, coenzyme A and biotin (<http://www.plantcyc.org:1555/ARA/server.html>) (Saito, 1999).

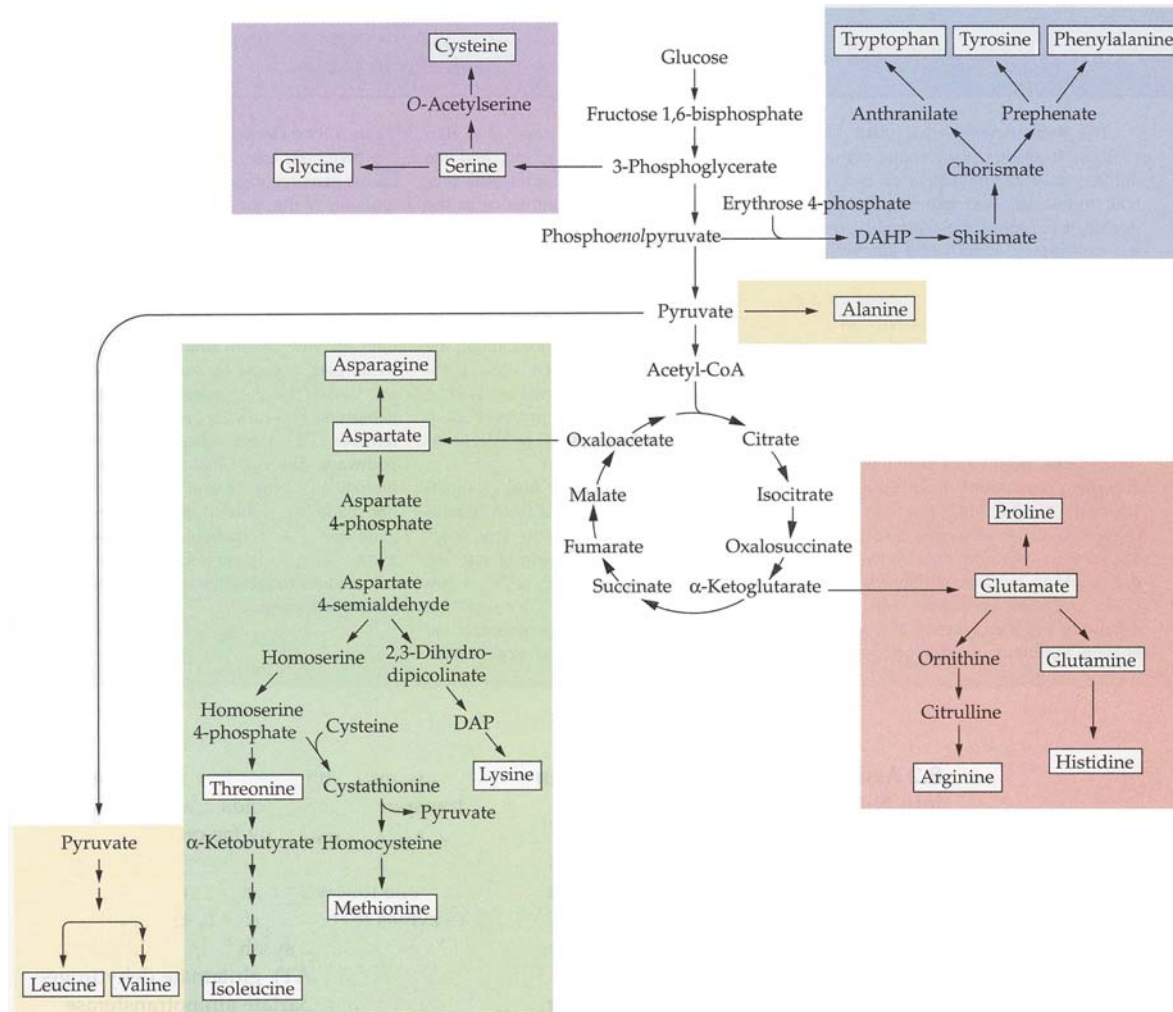


Figure 3-3: Amino acid biosynthesis pathways in plants (Coruzzi and Last, 2000).

3.3.2 Mutants of amino acid metabolism

A large collection of auxotrophic bacteria and fungi has been used for the study of biosynthetic pathways. Screens were performed to find auxotrophic plants, but compared to microorganisms there are only a few plant mutants available up to now (Muralla *et al.*, 2007). Some of them will be described here with a special focus on root developmental phenotypes.

Aspartate

Arabidopsis contains different aspartate aminotransferase isoenzymes having distinct functions and located in different subcellular locations (Coruzzi, 2003). From the five analysed mutant alleles of aspartate aminotransferase 2 (AspAT2) several showed changes in amino acid content (Miesak and Coruzzi, 2002). The AspAT2 mutant alleles *aat2-2* and *aat2-T* had a reduced root growth phenotype (Schultz *et al.*, 1998; Miesak and Coruzzi, 2002). In the case of *aat2-2* this effect was enhanced when aspartate was applied exoge-

nously, implying a dual role of the enzyme in aspartate catabolism beside its function in biosynthesis (Coruzzi, 2003).

Histidine

There are two histidinol-phosphate aminotransferases (HPA) in *Arabidopsis* required for histidine biosynthesis (Mo *et al.*, 2006). A mutation in one of them, *AtHPA1*, causes a defect in primary root growth and root meristem maintenance (Mo *et al.*, 2006). The mutant had a reduced content in free, but not in protein-bound histidine. The root phenotype could be rescued by exogenous application of histidine. The histidine-dependence of root development was higher in young seedlings than in older plants (Mo *et al.*, 2006). A complete knockout of the gene was embryo lethal (Mo *et al.*, 2006).

apg10 (*albino and pale green 10*) carries a mutation in BBMII (N'-[(5'-phosphoribosyl)-formimino]-5-aminoimidazole-4-carboxamide ribonucleotide) isomerase which performs the fourth step in histidine biosynthesis (Noutoshi *et al.*, 2005). The mutant had pale green leaves and a global increase in free amino acids in young seedlings, although the plants recovered later and the phenotype disappeared (Noutoshi *et al.*, 2005). A knockout allele of the gene was embryo lethal (Noutoshi *et al.*, 2005). This embryo lethality was also found for several insertion alleles of different histidine biosynthesis genes (*HISN2-4*, *HISN 6* and *HISN 8*) (Muralla *et al.*, 2007).

Tryptophan

Arabidopsis has two tryptophan synthase β subunit (*TSB*) genes, *TSB1* and *TSB2*, needed for the last step of tryptophan biosynthesis. *trp2-1* which carries a mutation in *TSB1* failed to produce true leaves and roots on medium without tryptophan when grown under standard illumination. Interestingly, the plants could develop without tryptophan treatment when grown under low light (Last *et al.*, 1991). *TSB1* accounts for >90% of the mRNA in leaves. The authors therefore argued that the weakly expressed *TSB2* gene can fulfil the requirements of the slowly growing mutant under low light, while this is not possible at higher metabolic rates occurring under high light (Last *et al.*, 1991). Alternatively, they suggested that the mutation might alter the regulation of *TSB1* or that residual activity of the mutated enzyme might contribute to the tryptophan synthase β enzyme activity in low light intensity (Last *et al.*, 1991).

This conditional light phenotype was also observed in mutants of the *TRP1* gene coding for anthranilate phosphoribosyl-transferase, catalysing the second step in tryptophan synthesis,

and of the *TRP3* gene which codes for tryptophan synthase α (TSA) subunit, which catalyses the penultimate step in tryptophan biosynthesis (Last *et al.*, 1991; Radwanski *et al.*, 1996).

Lysine

agd2-1 (*aberrant growth and death2*) has a mutation in L,L-diaminopimelate aminotransferase which acts in lysine biosynthesis (Song *et al.*, 2004; Hudson *et al.*, 2006; Jander and Joshi, 2009). The mutant was smaller than the wild type, it had enlarged leaf cells and showed some spontaneous cell death and embryo lethality (Song *et al.*, 2004). *agd2-1* also displayed a salicylic acid-dependent resistance to the pathogen *Pseudomonas syringae*, because the wild-type *AGD2* probably represses disease resistance (Rate and Greenberg, 2001). The expression of *AGD2* was light-regulated (Song *et al.*, 2004).

A mutation affecting a dihydrodipicolinate synthase gene (*DHDPS*) which is also involved in the lysine biosynthesis pathway led to reduced plant growth and strong accumulation of threonine and reduction of lysine content in the mutant Rm 57 (Sarrobot *et al.*, 2000). Other amino acid levels were also affected in the mutant (Sarrobot *et al.*, 2000). The growth phenotype of Rm57 might be due to a combined effect: lysine deficiency, toxic concentrations of threonine and changes in other amino acids. The root phenotype was only partly complemented by external application of lysine. A toxic effect of threonine could be mimicked in WT by application of threonine, leading to a reduced root growth comparable to the mutant (Sarrobot *et al.*, 2000).

Threonine

mto2-1, a mutant in threonine synthase, showed reduced plant growth, reduced levels of threonine and over-accumulation of soluble methionine in young rosettes (Bartlem *et al.*, 2000).

Photorespiration, serine and glycine

The photorespiratory *sat* mutants deficient in serine-glyoxylate aminotransferase had reduced photosynthesis rates and accumulated serine and glycine when exposed to photorespiratory conditions. The mutants were only viable in nonphotorespiratory conditions and showed chlorosis and stunted growth when shifted into ambient atmospheric conditions (Somerville and Ogren, 1980).

aoat1-1 is mutated in an photorespiratory glutamate:glyoxylate aminotransferase (GGAT) which also showed activity as alanine:2-oxoglutarate aminotransferase (AOAT), alanine:glyoxylate aminotransferase (AGAT) and glutamate:pyruvate aminotransferase (GPAT) (Igarashi *et al.*, 2003). The mutant was stunted and had chlorotic leaves, elevated glutamate and decreased serine levels when grown under normal air conditions (Igarashi *et al.*, 2003). The mutant could develop almost wildtype-like under low light conditions or on medium containing 3% sucrose (Igarashi *et al.*, 2003).

3.3.3 Arginine function and biosynthesis

A The role of arginine in plants

Arginine is one of the 20 standard amino acids necessary for the assembly of peptides and proteins. It is therefore vital for the functioning of the cell. Arginine is a basic amino acid with the linear formula: $\text{H}_2\text{NC}(=\text{NH})\text{NH}(\text{CH}_2)_3\text{CH}(\text{NH}_2)\text{COOH}$ and a very high N:C ratio (4:6) which makes it ideal for nitrogen storage (Llácer *et al.*, 2008). And indeed, arginine can represent a significant part of nitrogen store in protein or as free amino acid in seeds, bulbs or other parts of plants (VanEtten *et al.*, 1963; Lea and Mifflin, 1980; Boutin, 1982; Micallef and Shelp, 1989). Arginine can account for 11% of the nitrogen pool in *Arabidopsis* seeds (VanEtten *et al.*, 1963; Zonia *et al.*, 1995). Besides this, ornithine (a precursor of arginine) and arginine are necessary for the production of polyamines (Slocum, 2005). However, it seems that in *Arabidopsis* only arginine, but not ornithine, can be used as precursor for the biosynthesis of polyamines (Hanfrey *et al.*, 2001). These small positively charged organic molecules play an important role in plant stress response, senescence, cell growth and division, root growth, fruit development and ripening, and other processes (Kaur-Sawhney *et al.*, 2003). Furthermore, arginine is a source for nitric oxide (NO) which plays an important role in germination, defense responses, hormonal signalling, root growth, and flowering in plants (Crawford, 2006; Grün *et al.*, 2006).

B Synthesis pathway

The synthesis of arginine can be divided into two distinct parts: First the so-called “ornithine pathway” (in bacteria, plants and fungi, but not in animals) in which ornithine is synthesised from glutamate and second, the “arginine pathway” in which arginine is formed from ornithine with the enzymes of the urea cycle, also existing in animals (Slocum, 2005).

In the first step of arginine synthesis, glutamate is acetylated by the N-acetylglutamate synthase (NAGS) (EC 2.3.1.1) (Figure 3-4, step 1). In *Arabidopsis* At2g22910 and At4g37670 might encode this enzyme according to Slocum (2005). NAGS of soybean (*Glycine max* L. var. Mandarin) was localised in the cytoplasm (Jain *et al.*, 1987). In contrast, the database Aramemnon gave a prediction for chloroplastic localisation for both putative *Arabidopsis* NAGS proteins (October 28, 2009) (Schwacke *et al.*, 2003).

In the second step, N-acetylglutamate is phosphorylated by N-acetylglutamate kinase (NAGK) (EC 2.7.2.8), yielding N-acetylglutamate-5-phosphate (Figure 3-4, step 2) (Jain *et al.*, 1987; Slocum, 2005). NAGK activity was shown for At3g57560 (Chen *et al.*, 2006); other candidates are At4g37670, At2g19940 and At2g22910, according to the database AraCyc (Plant Metabolic Network (PMN), October 26, 2009). NAGK of soybean was localised in plastids (Chen *et al.*, 2006).

The third step consists of the removal of the phosphate residue from N-acetylglutamate-5-phosphate by N-acetylglutamate-5-phosphate reductase (NAGPR) (EC 1.2.1.38), yielding N-acetylglutamate-5-semialdehyde (Figure 3-4, step 3) (Slocum, 2005). *NAGPR* is encoded by At2g19940 according to Slocum (2005), though At4g37670 and At2g22910 might also have this function according to AraCyc (October 26, 2009). The database Aramemnon gave a prediction for chloroplastic localisation for At2g19940 (October 28, 2009) (Schwacke *et al.*, 2003).

In the fourth step of ornithine synthesis an amino group is transferred to N-acetylglutamate-5-semialdehyde (from glutamate) by N²-acetylornithine aminotransferase (EC 2.6.1.11), yielding N²-acetylornithine (Figure 3-4, step 4) (Jauniaux *et al.*, 1978; Slocum, 2005). Slocum (2005) gave the enzyme the abbreviation “NAOAT”, while in this work it will be named “ACOAT” following the nomenclature of Heimberg *et al.* (1990). In *Arabidopsis* a single gene, At1g80600, is predicted to encode ACOAT (Slocum, 2005). ACOAT of soybean was localised in plastids (Jain *et al.*, 1987). The gene At1g80600 will be analysed more profoundly in this work.

In the next step of ornithine synthesis, the acetyl residue of N²-acetylornithine should be removed to obtain ornithine. This can be accomplished in two ways: the first possibility is to transfer the acetyl residue back onto a glutamate molecule with N²-acetylornithine:glutamate acetyltransferase (NAOGAcT) (EC 2.3.1.35), resulting in a cyclic pathway (Figure 3-4, step 5) (Shargool *et al.*, 1988; Slocum, 2005). This pathway is used in non-enteric bacteria, fungi and plants (Shargool *et al.*, 1988). At2g37500 might encode this

enzyme in *Arabidopsis* according to Slocum (2005). It is targeted to chloroplasts according to the predictions of the database Aramemnon (October 30, 2009) (Schwacke *et al.*, 2003). The second way of removing the acetyl residue might be accomplished by a putative N²-acetylornithine deacetylase (NAOD) (EC 3.5.1.16). This enzyme fulfils the deacetylation step in enteric bacteria in a linear pathway (Shargool *et al.*, 1988). In this case the acetyl-residue is cleaved from the ornithine in a hydrolysis reaction: H₂O is split in OH⁻ and H⁺ and the hydroxyl group is used to form acetate with the acetyl-residue (Figure 3-4, step 6) (AraCyc database, October 30, 2009). It is not clear whether the linear pathway exists in plants, though a possible candidate coding for this enzyme might be At4g17830 (Slocum, 2005).

The next steps are part of the “arginine pathway”:

Ornithine transcarbamylase (OTC) (EC 2.1.3.3), catalyses the transfer of a carbamoyl residue to ornithine, yielding citrulline (Figure 3-4, step 7) (Slocum, 2005). It is probably encoded by At1g75330 in *Arabidopsis*, as it shares high sequence similarities with OTCs from other organisms (Slocum, 2005). OTC activity in *Arabidopsis* was studied by Slocum *et al.* (2000). OTC activity of pea (*Pisum sativum*) was localised in chloroplasts (Taylor and Stewart, 1981).

Argininosuccinate is formed from citrulline and aspartate by argininosuccinate synthase (AS) (EC 6.3.4.5) (Figure 3-4, step 8) (Thompson, 1980; Slocum, 2005). AS is probably encoded by At4g24830 and localised in chloroplasts in *Arabidopsis* (Slocum, 2005). The chloroplastic localisation is supported by the predictions of the database Aramemnon (November 3rd, 2009) (Schwacke *et al.*, 2003).

Fumarate is cleaved from argininosuccinate by argininosuccinate lyase (AL) (EC 4.3.2.1), yielding arginine (Figure 3-4, step 9) (Thompson, 1980; Slocum, 2005). The gene At5g10920 is predicted to encode for AL in *Arabidopsis* (Slocum, 2005). The putative enzyme might be localised in chloroplasts according to different database predictions (Slocum, 2005). The subcellular localisation is supported by the predictions of the database Aramemnon (November 3rd, 2009) (Schwacke *et al.*, 2003).

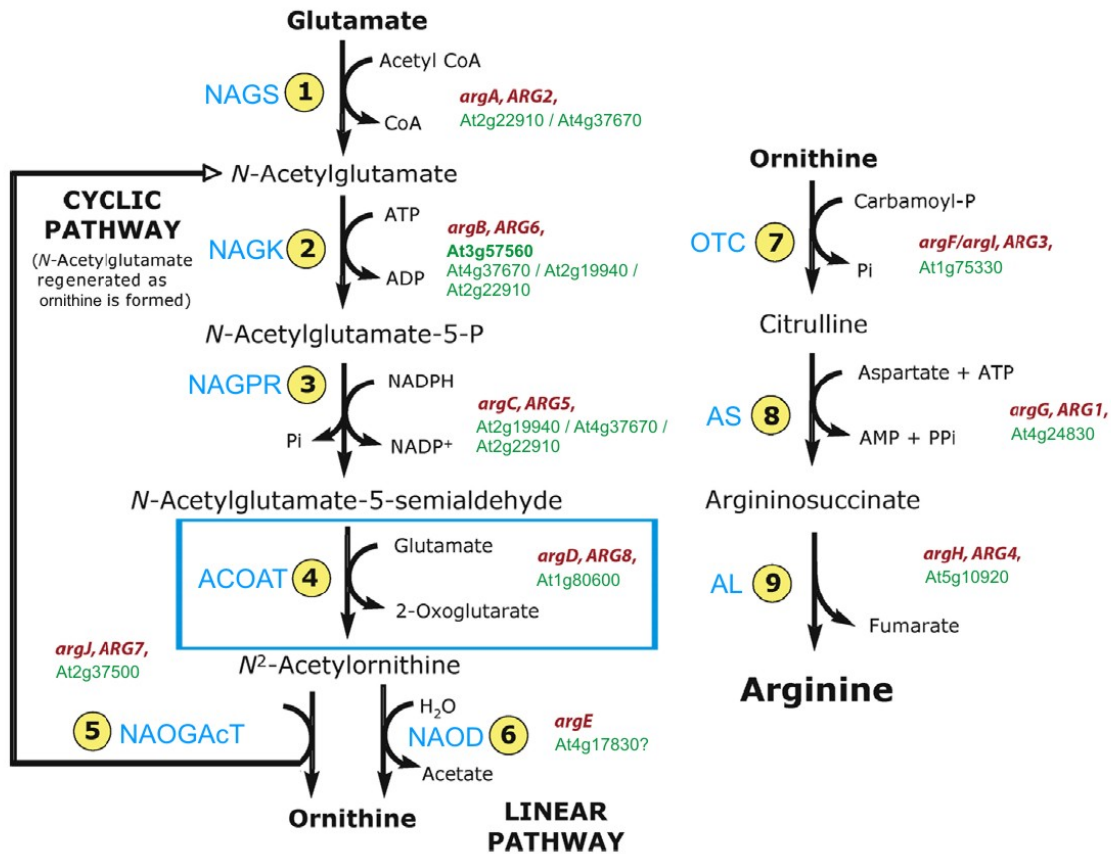


Figure 3-4: Arginine biosynthesis pathway in plants.

Enzymes catalysing the different synthesis steps: 1) N-acetylglutamate synthase (NAGS); 2) N-acetylglutamate kinase (NAGK); 3) N-acetylglutamate-5-P reductase (NAGPR); 4) N²-acetylornithine aminotransferase (ACOAT); 5) N²-acetylornithine:glutamate acetyltransferase (NAOGAcT); 6) N²-acetylornithine deacetylase (NAOD); 7) ornithine transcarbamylase (OTC); 8) argininosuccinate synthase (AS); 9) argininosuccinate lyase (AL). Enzyme abbreviations are shown in blue characters, gene names of bacterial and yeast orthologs in red characters and *Arabidopsis* genes in green characters (bold characters if the gene function was proven). The gene which is the subject of this work is shown in a blue box (modified from Slocum (2005) and Aracyc database).

C Regulation of arginine biosynthesis

A classical feedback regulation controls the first two steps of arginine synthesis in non-enteric bacteria, fungi and plants: The enzymes NAGS and NAGK are inhibited by arginine (Shargool *et al.*, 1988; Pauwels *et al.*, 2003; Slocum, 2005). NAGK is activated by NAG (McKay and Shargool, 1981). The activity of NAGK is also modulated by the PII protein (Chen *et al.*, 2006). PII is a highly conserved protein playing a role in energy status and nitrogen/carbon balance (C/N) sensing in bacteria, eukaryotic algae and higher plants (Feria Bourrellier *et al.*, 2009). The PII protein of *Arabidopsis* is localised in chloroplasts (Chen *et al.*, 2006). When PII binds to NAGK it slightly increases its activity, but it mainly relieves the feedback inhibition by arginine (Chen *et al.*, 2006).

ACOAT which catalyses the fourth step in arginine biosynthesis is arginine repressible in *E. coli* and yeast (Albrecht and Vogel, 1964; Heimberg *et al.*, 1990).

In bacteria and plants carbamoyl-P is used as a common substrate for arginine and pyrimidine biosynthesis (Slocum, 2005). A coordination of both pathways is therefore necessary. According to a model, regulation takes place in the following way: Carbamoyl-phosphate synthase (CPS) and aspartate transcarbamoylase (ATC), which catalyses the committing step to pyrimidine synthesis, are feedback-inhibited by uridine monophosphate (UMP), the molecule from which all other pyrimidines are derived (Slocum, 2005; Zrenner *et al.*, 2006). Carbamoyl-P is preferentially used for UMP biosynthesis. When carbamoyl-P is depleted due to the CPS inhibition by UMP, its availability is also reduced for arginine biosynthesis, therefore ornithine is accumulated. When the ornithine content reaches a certain threshold, it can relieve the CPS inhibition, but not the ATC inhibition, so that new carbamoyl-P is formed and used for arginine biosynthesis. If UMP is depleted, ATC inhibition is relieved and UMP is formed again, depleting the carbamoyl-P stocks until ornithine accumulates again (Slocum, 2005).

3.4 The mutant *tup5-1*

The recessive EMS mutant *tup5-1* forms, in contrast to WT explants, calli on hypocotyl and root explants when grown on medium containing low concentrations of the phytohormones auxin and cytokinin (Riefler, 2001). The mutant *tup5-1* was therefore called *tup5* (*tumor prone 5*) (Riefler, 2001). It was renamed *tup5-1* because additional alleles were used during this work. The mutant has a very short root when grown *in vitro* in light (Figure 3-5, A). The primary root does not grow longer than 1-2 mm under these growth conditions (Riefler, 2001). Also adventitious roots stop growing if not shaded by leaves (data not shown). These growth arrested root primordia at the hypocotyl/root junction formed callus-like structures (Riefler, 2001). Root growth of *tup5-1* has been shown to be inhibited only when exposed to light, while roots developed normally in soil or in darkness (Riefler, 2001; Frémont, 2004). Apparently, the light dose regulates the degree of inhibition, as *tup5-1* roots grown in short day (SD) grow longer than *tup5-1* roots grown under long day (LD) conditions (Frémont, 2004).

The root development of *tup5-1* was analysed histologically. The roots of the mutant seedlings growing in light did not develop an elongation zone and a meristematic zone: the root development of *tup5-1* was disturbed at an early stage (Frémont, 2004). The meristematic

cells of *tup5-1* roots grown in light differentiate, while those grown in darkness or in soil maintained their meristematic identity (Figure 3-5, C) (Frémont, 2004). Roots cultivated in darkness immediately stopped growth when shifted into light (Frémont, 2004). Growth experiments with different monochromatic light qualities showed that the inhibition of root growth in *tup5-1* is induced by blue light, but not by red or far red light, suggesting a possible involvement of a blue light receptor in the signalling pathway of *tup5-1* (Figure 3-5, B) (Frémont, 2004). Furthermore *tup5-1* had a higher germination rate than WT in darkness without previous light treatment (Frémont, 2004). Germination of *tup5-1* was not inhibited by far red light as was WT (Frémont, 2004). These data suggest impairment of blue and red light signalling in *tup5-1*. Therefore *TUP5* is likely to have a function in negative control of blue and far red light dependent processes. At the beginning of this work the mutation was located in an interval of 88 kb on the lower arm of chromosome I, near the telomere (Frémont, 2004).

3.5 Aim of the work

This work should provide a deeper understanding of the role of *TUP5* in *Arabidopsis*. The mutant *tup5-1* was found in a screen for increased ability to form calli on medium containing low auxin and cytokinin concentrations (Riefler, 2001). Additional studies had shown that *tup5-1* has a blue light-dependent short root phenotype (Riefler, 2001; Frémont, 2004). To understand the role of *TUP5*, several questions needed to be answered.

In a first step the gene had to be identified. Different approaches were used to identify *TUP5*, because the gene is located at a cold spot of recombination. Classical mapping alone did not allow the identification of the gene due to this circumstance.

The blue light dependence of the root phenotype raised the question about a possible involvement of known light signalling pathways. Therefore, several light receptor mutants were used to clarify the light signalling pathway of *tup5-1* by epistasis analysis.

Due to the mutant screening conditions and because of the observation of root meristem loss in *tup5-1*, a possible change in cell cycle regulation in *tup5-1* with an impact of the auxin and cytokinin status was expected. The GUS expression pattern of marker lines visualising the hormonal status, cell cycle activity and quiescent center identity in the root of *tup5-1* was analysed to examine the physiological situation of *tup5-1*.

Information about the expression pattern of *TUP5* during different developmental stages, its organs and tissue distribution and the effect of external cues on the expression was col-

lected to characterise the function of *TUP5*. For this purpose, the activity pattern of promoter-GUS and *TUP5*-GFP constructs was examined, real-time PCRs were made and data base information was analysed.

Additional alleles containing T-DNA insertions in *TUP5* and *TUP5*-overexpressing transgenic plants were characterised to gain additional information on the functions of the gene. Finally, the identification of *TUP5* revealed its role in amino acid metabolism. Therefore the amino acid composition of *tup5-1* mutant plants and *TUP5*-overexpressing transgenic plants was analysed.

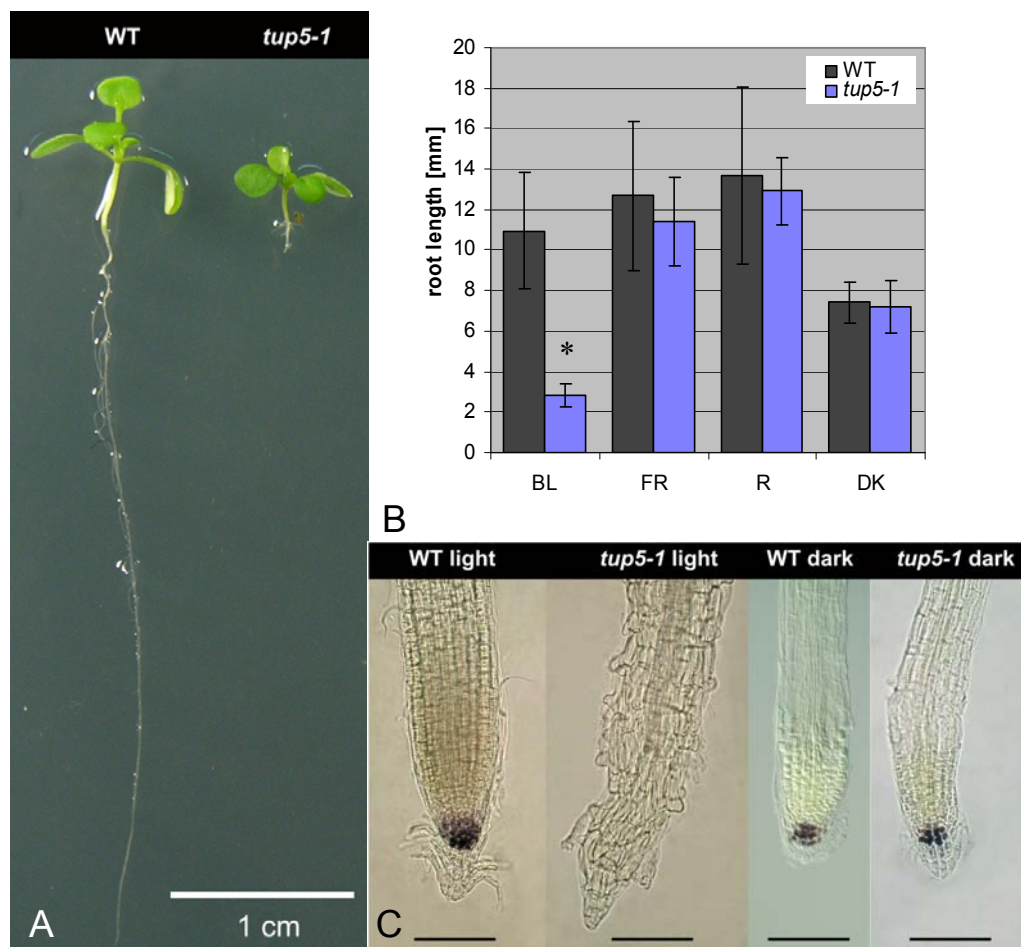


Figure 3-5: Phenotype of the *tup5-1* mutant.

A: Root length of 12-d-old WT and *tup5-1*. B: Root length of 6-d-old WT and *tup5-1* seedlings under different light conditions. (n= 18-26 plants, except far red light: for WT n = 5 plants). All plants were treated with white light for 16 h at the beginning of the experiment to induce germination. BL, Blue light (445 nm) approx. 2 μ E; FR, Far red light (approx. 724 nm) approx. 3,5 μ E; R, Red light (approx. 660 nm) 3,5 μ E; DK: Dark control. Significance: * P < 0,001, Student's *t* test comparing WT and *tup5-1* grown under the same light conditions. C: Root meristem of WT and *tup5-1* grown in light and darkness. Plants grown in light were 5 days old, those grown in darkness were 6 days old. Roots were cleared according to Malamy und Benfey (1997) and starch granules were stained with Lugol solution. Scale bar: 100 μ m. B and C modified from Frémont (2004).

4 Material and methods

4.1 *Arabidopsis thaliana* lines

4.1.1 Ecotypes

The mutant line *tup5-1* had been generated by EMS mutagenesis in *Arabidopsis thaliana* (L.) Heynh. (Riefler, 2001). Col-0 *gl* wild type plants were used as control in this work.

The ecotype Landsberg *erecta* (*Ler*) was used to generate an F₂ generation between Col-0 *gl* (*tup5 / tup5*) × *Ler* (*TUP5 / TUP5*) for the mapping of *tup5-1*.

4.1.2 T-DNA insertion lines

T-DNA insertion lines used for the search of the *TUP5* locus by root phenotype similarities were ordered from Nottingham *Arabidopsis* Stock Center (NASC) and *Arabidopsis* Biological Resource Center (ABRC) (<http://signal.salk.edu/cgi-bin/tdnaexpress>) (Table 9-1).

After the *TUP5* locus was identified, various available T-DNA insertion alleles of the *TUP5* gene were screened for phenotypes and analysed on the molecular level to confirm a T-DNA insertion at the predict locus (Table 5-6). The mutant lines again came from NASC and ABRC.

4.1.3 Marker lines

The marker lines used for analysis of various gene functions and activities in *tup5-1* are listed in Table 4-1.

Table 4-1: Marker lines used for studies on *tup5-1*.

Marker line	Description and reference
<i>DR5::GUS</i>	An auxin-induced marker with a synthetic promoter containing seven repeats of an auxin-responsive element (Sabatini <i>et al.</i> , 1999).
<i>ARR5::GUS</i>	A marker line in which GUS activity is visible in cells responding to cytokinin (D'Agostino <i>et al.</i> , 2000).
<i>FA4C</i>	Recent cell divisions can be visualised with this line. It contains the promoter of <i>CycB1;1</i> and an N-terminal part of the protein encoding a mitotic destruction box fused to GUS (Colón-Carmona <i>et al.</i> , 1999).
<i>QC25</i>	This line shows specific GUS activity in the Quiescent Center (QC) cells (Sabatini <i>et al.</i> , 1999).

4.1.4 Mutant lines

The light receptor and light signalling mutants used for epistasis analysis are listed in Table 4-2.

Table 4-2: *Arabidopsis* mutants used for epistasis analysis.

Mutant allele	NASC code or other source	Description and reference
<i>phyB-1</i> (<i>hy3-Bo64</i>)	N69	Phytochrome apoprotein mutant of phytochrome B (<i>PHYB</i>) gene (Reed <i>et al.</i> , 1993; Rockwell <i>et al.</i> , 2006).
<i>hy2-1</i>	N68	Phytochrome chromophore (phytochromobilin) biosynthesis mutant (Kohchi <i>et al.</i> , 2001).
<i>cry1</i> (<i>hy4-1</i>)	N70	Cryptochrome apoprotein mutant of cryptochrome 1 (<i>CRY1</i>) gene (Ahmad and Cashmore, 1993).
<i>phot1-5</i> (<i>nph1-5</i>)	Winslow Briggs, Stanford University, USA	Phototropine 1 apoprotein null mutant (Huala <i>et al.</i> , 1997; Briggs <i>et al.</i> , 2001).
<i>hy5-1</i>	N71	Mutant of the <i>HY5</i> gene, encoding a bZIP transcription factor that activates light induced genes (Oyama <i>et al.</i> , 1997; Chen <i>et al.</i> , 2004).

4.2 Growth conditions for *Arabidopsis thaliana*

4.2.1 Growth temperature and day length (photoperiod)

The standard growth temperature for *Arabidopsis* was 22°C and the photoperiod comprised 16 h of light and 8 h of darkness unless otherwise stated.

4.2.2 Growth on soil

Arabidopsis seeds were sown on humid sowing soil (Table 4-3), stratified at 4°C for 4 days and then transferred to the greenhouse or a growth chamber. The seeds and the soil were protected from desiccation by a clear plastic dome until the seedlings had reached the size of 5 mm. When plantlets were pricked out, they were transferred to a more nutrient rich soil mixture (“prick out soil”, Table 4-3)

Table 4-3: Soil composition for *Arabidopsis* cultivation.

Soil type	Soil Type P (Einheitserde [®] , Terreau professionnel Gepac) [litre]	Soil Type T (Einheitserde [®] , Terreau professionnel Gepac) [litre]	Sand [kg]	Perligran G (Knauf Perlite GmbH) [litre]
Sowing soil	140	140	25	-
Prick out soil	140	140	-	60

4.2.3 *In vitro* culture

Sodium hypochlorite solution

- 1,2% sodium hypochlorite (from 12% stock)
- 1:10 000 Triton[®] X-100

The seeds were shaken with sodium hypochlorite solution for 15 min (or 20 min when the solution was older than two months) on a vortex or an Eppendorf Thermomixer compact at 1400 rpm. The next steps were performed under a clean bench. For rinsing the seeds the sterilisation solution was replaced by sterile *aqua bidest.* The washing step was repeated four to five times. The seeds were then pipetted onto a sterile filter paper in a Petri dish and dried for 1 h. The dried seeds were then transferred onto medium with sterile toothpicks.

Alternatively the water of the last washing step was replaced by 0,1% sterile agarose and seeds were pipetted onto medium with a 1 ml pipette.

After the seeds were sown on medium, the Petri dishes were loosely sealed with plastic wrap (allowing gas exchange) and stratified at 4°C for 4 days, they were then transferred to the culture room (for culture conditions see chapter 4.2.1).

4.2.4 Age of the plants

The age of the plants (given in days (d), weeks or months) refers to date of transfer into the culture room after stratification, because the exact time point of germination could not always be monitored.

4.3 ***Localisation of the perception site of root growth inhibition by light***

Glass tubes (Schott Duran, \varnothing 2,4 cm, 19 cm high) were filled half with MS medium (with 7 g/l agar). The sterilised seedlings were picked with extra long sterile wooden skewers and transferred onto the medium in the tubes (4-6 seeds of WT and *tup5-1* per tube each). The tubes were closed with plastic lids (Magenta Corp. Chicago). The seeds were then stratified at 4°C for 4 days and shifted to 22°C and light for 16 h to induce germination. After the light treatment, the upper, medium-free part of the tube or the lower, medium filled part (with 0,5 cm above medium level) was wrapped to prevent light to shine into this segment. Some tubes were completely wrapped for dark control and no wraps were used for light control tubes. In this experimental setup the light source was fixed in a 90° angle to the tube axis. As wrapping material aluminium foil with a black non-reflecting surface facing

the glass tube was used. After 28 days the tubes were unwrapped and the root length of the plants was analysed.

The use of a layer of black, not light-transparent medium (by adding 8 g charcoal (activated) to the MS medium) on top of the normal MS medium did not yield good results, because *tup5-1* roots grew horizontally within this black layer. Therefore only normal medium was used, though it can't be excluded that the growing roots were exposed to a small quantity of light.

4.4 Histology

4.4.1 Viability test

Fluorescein diacetate (FDA) is a nonpolar ester which can be transported into intact plant cells where it is hydrolysed by cellular esterases yielding fluorescein, which is a fluorescent compound. As the fluorescence signal is a result of metabolic activity in the cell, it is used as viability marker (Rotman and Papermaster, 1966).

Propidium iodide (PI) cannot pass intact membranes. If the red staining of PI can be found accumulating within cells, these are considered as dead, because the membranes are damaged (Jones and Senft, 1985).

The samples were incubated in FDA (5 µg/ml) for 30 sec, shortly rinsed in water and then transferred into propidium iodide (3 µg/ml) for 1 min. The samples were again rinsed and directly analysed under the microscope (Zeiss Axioskop 2 plus with AxioCam ICc3) using UV light and red filter (excitation: 565/30 nm, emission: 620/60 nm) and eGFP filter (excitation: 470/40 nm, emission: 525/50 nm) filter for PI and FDA respectively.

4.4.2 GUS staining

500 mM sodium phosphate buffer pH7

For 20 ml:

5,77 ml 1 M Na₂HPO₄

4,23 ml 1 M NaH₂PO₄

The volume was filled to 20 ml with *aqua bidest.*

Potassium ferricyanide buffer

- 20 mM Potassium ferricyanide

- 50 mM sodium phosphate pH7 (from 500 mM stock)

- 0,2% Triton[®] X-100 (from 20% stock)

The buffer was stored at 4°C (in darkness) for up to 3 months.

Potassium ferrocyanide buffer

- 20 mM Potassium ferrocyanide
 - 50 mM sodium phosphate pH7 (from 500 mM stock)
 - 0,2% Triton[®] X-100 (from 20% stock)
- The buffer was stored at 4°C (in darkness) for up to 3 months.

GUS buffer

Equal volume of potassium ferricyanide buffer and potassium ferrocyanide buffer were mixed and 0,5 mg/ml X-Gluc was added. To dilute the X-Gluc, the mixture was stirred and slightly warmed. The solution was freshly prepared before the GUS staining experiment. In some cases it was frozen as aliquots for later use.

The plant material was incubated in ice-cold 90% acetone for 1h at -20°C. The acetone was then replaced by 50 mM sodium phosphate buffer (pH7) at RT. This washing step was repeated a second time. The samples were then incubated in GUS staining solution at 37°C for 1 h or longer (up to 24 h). The plant material was destained with 70% EtOH at RT for 3 to 5 h. The samples were stored at 4°C in 70% EtOH (modified from Weigel and Glazebrook (2002)). The plant material was often cleared (for method see chapter 4.4.3) to increase translucency of the tissue, improving the quality of the fotos taken with the microscope or the binocular.

4.4.3 Tissue clearing

A Clearing method for root histology and GUS staining

Seedlings were incubated in 0.24 N HCl / 20% methanol on a 57°C heat block for 15 minutes. The solution was replaced with 7% NaOH / 60% ethanol for 15 minutes at RT. Seedlings were then rehydrated for 5 minutes each in 50%, 40%, 30%, 20% and 10% ethanol, and infiltrated for 15 minutes in 5% ethanol / 25% glycerol. Roots or whole seedlings were mounted in 50% glycerol on glass microscope slides (modified from Malamy and Benfey (1997)).

B Chloral hydrate clearing method for siliques

All steps were performed at RT. The tissue was first fixed in a solution of EtOH and acetic acid (Vol. 9:1) overnight. It was transferred to 90% EtOH for 45 min. Finally the tissue was transferred to 70% EtOH where it was stored until the day of (or the day before) examination. A few siliques (only as many as should be examined directly), were transferred into a chloral hydrate: glycerol: water solution (8:1:2, w:v:v) for 1 h or longer if necessary (up to 24 h), until the siliques became translucent. They were then transferred to 25% gly-

erol until use. The siliques were mounted with 50% glycerol for analysis under the binocular or microscope using bright field (modified from Yadegari *et al.*).

4.4.4 Fast protoplast isolation for GFP analysis

Enzyme mixture

- 400 mM mannitol
 - 8 mM CaCl₂ (from autoclaved 80 mM CaCl₂ stock solution)
 - 1% cellulase
 - 0,25% Macerozym[®]R-10 (Yakult Honsha Co, Ltd., Tokyo, Japan)
- The pH of the solution should be about 5,5. The solution was prepared freshly, without sterile filtration.

1 to 3 *Arabidopsis* leaves were cut into strips with a razor blade in a drop of 500 mM mannitol solution (prepared freshly, without autoclaving). The plant tissue was incubated in 500 mM mannitol solution for 1 h at RT for plasmolysis. The solution was replaced by enzyme mixture (see above) and the samples were shaken at 20 rpm in darkness at RT overnight (~16 h) (Damm and Willmitzer, 1988, modified by Wolfgang Schuster, personal commun.). The protoplasts were then analysed with a Leica TCS SP2 confocal laser scanning microscope. An excitation wavelength of 488 nm and a filter of 510-550 nm were used for the analysis of GFP fluorescence signal and an excitation wavelength of 488 nm and a filter of 610-680 nm for the autofluorescence signal of chloroplasts.

4.5 Plant DNA extraction

CTAB buffer

- 2% CTAB (w/v)
- 100 mM Tris pH 8
- 20 mM EDTA pH 8.0
- 1.4 M NaCl,
- 1% PVP (Polyvinylpyrrolidone)

A small quantity of plant tissue (e.g. a young leaf or small seedling) was frozen in a 1,5 ml microcentrifuge tube in liquid nitrogen. The tissue was then ground with a small pestle and 200 µl CTAB buffer were added to the plant powder. The mixture was briefly vortexed and then incubated on a heating block at 65°C for 10-30 min. 200 µl chloroform:isoamyl alcohol 24:1 (v/v) were added and the solution was shortly vortexed. The sample was centrifuged in a microcentrifuge for 3 min at 13 000 rpm and the supernatant was transferred to a fresh 1,5 ml microcentrifuge tube. 600 µl (3 volumes) ice-cold 96% EtOH were added to the sample. The sample was gently mixed. The mixture was incubated at -20°C for

15 min to let the DNA precipitate. The sample was centrifuged at 13 000 rpm for 15 min at 4°C. The supernatant was decanted. 200 µl 70% EtOH were added to the sample. The sample was gently mixed to wash the pellet. The DNA was again collected at the bottom of the microcentrifuge tube by centrifuging the sample at 13 000 rpm for 10 min at 4°C. The supernatant was decanted. The DNA pellet was dried on a heating block at 40°C until the EtOH was evaporated. The DNA was redissolved in 100 µl TE buffer. The sample was kept at 4°C for short term storage (about a month) or at -20°C for long term storage.

Modifications for high-throughput DNA extraction

The plant samples were collected into Collection Microtubes (Qiagen) and stored at -20°C until extraction. The frozen plant samples were ground to coarse powder with a sterile glass stirring rod of Ø 4 mm, height 150 mm (one per sample). After the addition of CTAB buffer with a multichannel “Eppendorf Research pro” pipette, the stirring rods were removed and a sterile stainless steel bead of Ø 3 mm was added to each sample. After the tubes were sealed with lids, the samples were ground in a Mixer Mill (MM30, Retsch) at a frequency of 30 shakes/sec for 2 min. The samples were then centrifuged in a Heraeus Megafuge 1.0R (with carriers for microplates) at 2800 rcf to collect the solution on the bottom of the tubes (to prevent cross-contaminations when opening the cap strips). All following steps were performed as described above (chapter 4.5), except for the use of Qiagen *Collection Microtubes*, the Heraeus Megafuge 1.0R (with carriers for microplates), multichannel pipettes, a waterbath for incubation at 65°C (caution: the lids may open; Putting something heavy on top could prevent this) and an oven (Memmert, Schwabach, Germany) for drying the DNA pellets at 55°C overnight. This high-throughput method allowed extraction of up to 192 samples in parallel.

4.6 Gene mapping

During meiosis a recombination of the chromosomes takes place. After a homologous pairing of sister chromosomes, DNA fragments are exchanged between them during crossing over. At the end of meiosis the sister chromosome pairs are separated and equally distributed into the newly formed gametes. It is more probable that a crossing over, and therefore a recombination event, takes place if the distance between two loci on a chromosome is high than if the loci are in close vicinity. Loci lying on different chromosomes (non sister chromosomes) segregate independently. These recombination probabilities can be used for mapping a gene: A mutation can be located by calculating the recombination

frequency between the mutated locus (visible by the phenotype) and marker genes or loci for which the position on a chromosome is already known.

For the mapping of *tup5-1*, which is a recessive mutation, a homozygous *tup5-1* (in the ecotype background: Col-0 *gl*) plant was crossed with a plant of the ecotype *Landsberg erecta* (*Ler*). The F₁ generation was uniformly heterozygous. During the formation of sperm cells (in pollen grains) and egg cells (in ovules) in the flowers of F₁ plants, the first meiosis causing recombination events between the two ecotype genomes took place. In the next step the F₂ generation was screened for plants with *tup5-1* phenotype, because this locus is originating from the Col-0 *gl* ecotype. These plants were used for the following mapping analysis.

Differences in the DNA sequence (polymorphisms) between Col-0 *gl* and *Ler* have been characterised and listed in the “Monsanto *Arabidopsis* Polymorphism and *Ler* Sequence Collection” (Jander *et al.*, 2002). Molecular markers can be generated from these polymorphisms (SSLP and CAPS marker were used for the mapping of *tup5-1*; for details see below) to visualise the genotypic constitution of a plant. Specific bands on agarose gel can show whether the analysed plant is homozygous for Col-0 *gl* or *Ler* respectively on this special locus, or whether the plant is heterozygous for this locus. Knowing that the analysed F₂ generation plants with *tup5-1* phenotype carry a Col-0 *gl* fragment at the searched locus (because the mutation was generated in this ecotype), the goal is to find molecular markers which very rarely show *Ler* specific bands in the F₂ mapping population, because *Ler* DNA sequences occur after recombination. If F₂ generation plants only have Col-0 *gl* bands for a certain molecular marker, it is probable that this marker is close to the mutation.

The recombination frequency showing the distance between a marker and the gene locus of interest can be calculated according to the formula:

$$R = \frac{L}{C + L} \times 100 = [\text{cM}]$$

R = Recombination frequency in percent

L = Number of *Ler* -fragments

C = Number of Col-fragments

Unit: cM (centiMorgan)

SSLP marker

Simple Sequence Length Polymorphisms (SSLPs) are microsatellite repeat sequences which vary in lengths for different ecotypes. Primers can be designed to border such a polymorphic region, so that this fragment can be amplified by PCR (Konieczny and Ausubel, 1993; Bell and Ecker, 1994). If Col-0 *gl* for example contains a repeat of 80 bp in the amplified region which does not exist in *Ler*, the PCR product will be 80 bp longer and this product length difference can be visualised on an agarose gel. Heterozygous plants will produce two bands of different lengths corresponding to the two ecotypes Col-0 *gl* and *Ler*.

CAPS marker

CAPS marker (Cleaved Amplified Polymorphic Sequences) use ecotype specific single base exchanges. If an enzymatic restriction site is covering this polymorphic site for one ecotype but not for the other (because the base exchange destroyed the restriction site), this DNA fragment can be amplified via PCR and digested with a suitable restriction enzyme (Konieczny and Ausubel, 1993). The PCR product of the ecotype containing the restriction site will be cleaved into two fragments while the PCR product of the other ecotype will remain uncleaved. The differences in PCR product lengths can be visualised on an agarose gel, showing the ecotype constitution (the genotype) of a plant sample for this locus.

4.7 Sequencing

A Preparations for plasmid sequencing

For sequencing of a gene cloned into a vector, the DNA was extracted by plasmid mini preparation using PeqGold Plasmid Miniprep Kit I (Peqlab, Erlangen, Germany). The extraction was done according to the manufacturer's protocol. The DNA was verified with restriction analysis (chapter 4.8.3, E) and PCR (with *Taq* polymerase, see Table 4-4 and Table 4-5) before further use.

B Preparations for genomic DNA sequencing

If plant genomic DNA was sequenced, the sequence of interest was amplified by PCR with the proofreading DNA polymerase *Pfu* (Table 4-4 and Table 4-5) and the PCR product was purified with MSB Spin PCRapace Kit (Invitek, Berlin, Germany). For this purpose 1 μ l 3 M sodium acetate pH 5,2 was first mixed with the PCR product. The following steps of the

purification were done according to manufacturer's protocol. The elution of the DNA was done with *aqua bidest.* or elution buffer. After centrifugation the eluted DNA solution was loaded onto the column for a second elution round to increase the DNA yield.

Table 4-4: PCR mixture for *Pfu* and *Taq* polymerase reaction

Components	<i>Pfu</i> -Mix Volumes [μ l]	<i>Taq</i> -Mix Volumes [μ l]
Primer f	0,5 (50 μ M)	0,3 (10 μ M)
Primer r	0,5 (50 μ M)	0,3 (10 μ M)
10 \times buffer (<i>Pfu</i> or <i>Taq</i> buffer respectively)	5	2
dNTPs (Mix of 5mM each)	1,6	0,4
MgCl ₂ (100 mM)	- (Mg ²⁺ in <i>Pfu</i> buffer)	0,2
H ₂ O	40,9	15,5
DNA	1	1
Polymerase (<i>Pfu</i> or <i>Taq</i> polym. respectively)	0,5	0,3

Table 4-5: PCR programme for *Pfu* and *Taq* polymerase.

Programme steps	Temperatures for <i>Pfu</i>	<i>Pfu</i> programme	Temperatures for <i>Taq</i>	<i>Taq</i> programme
1. First denaturation	94°C	1 min	94°C	1-4 min
2. Denaturation	94°C	15-20 sec	94°C	20 sec
3. Annealing	60°C	30 sec	55°C	25 sec
4. Polymerisation	72°C	1 min 30 sec to 2 min / kb	72°C	1 min/ kb
5. Final extension step (polymerisation)	72°C	2 min 30 sec to 4 min/ kb	72°C	2 min / kb
6. Pause	16°C	∞	16°C	∞
Number of cycles (step 2-4)		25 \times		25 - 40 \times
Lid temperature	99°C		99°C	

C Determining and adjusting the DNA concentration

After extraction and purification, the DNA concentration of the sample was determined on an agarose gel. Different volumes of purified DNA (for example 2 and 4 μ l) were loaded onto the gel. A 100 bp DNA ladder (100-5000 bp) (P-815 from MBBL) or HyperLadder™ I (Bioline, London, UK) with bands of equimolar mass was also loaded onto the gel in two different (small) volumes. The intensity of the DNA bands of the sample was compared to the reference DNA (Hyperladder). The plasmid concentration was adjusted to the expected value (required by the sequencing companies) by dilution of the DNA, or if the extracted concentration was too low, the DNA sample was concentrated using a Speed Vac.

The samples were sequenced by the following companies:

- Martin Meixner, Institut für Genetik, Chausseestr. 117, 10115 Berlin.

- Seqlab (Sequence Laboratories Göttingen GmbH, Hannah-Vogt-Str. 1, 37085 Göttingen)

- GATC (GATC Biotech AG, Jakob-Stadler-Platz 7, 78467 Konstanz)

The samples were sent to the companies in the required volumes and concentrations with the required primers. For the sequencing of different candidate genes in the *tup5-1* background, Martin Meixner also generated PCR primers and produced the PCR products for sequencing.

The sequences were controlled and (if necessary) edited with the programme Chromas (<http://www.technelysium.com.au/chromas.html>).

The sequences of WT and *tup5-1* were aligned with the programmes ClustalW or Vector NTI[®] to detect mutations (Larkin *et al.*, 2007).

4.8 Generation of transgenic *A. thaliana*

4.8.1 Cloning of a DNA fragment into a vector with restriction enzymes

A PCR product

The DNA fragment that should be cloned into a vector was amplified with the proofreading DNA polymerase *Pfu* (Table 4-4 and Table 4-5). In case of Gateway[®] cloning, the primers contained attachment sites for the BP reaction according to the manufacturer's manual. If amplification was difficult with primers containing attachment sites, the insert was first amplified (10 cycles) with gene-specific primers. The resulting PCR product was then used as template for the PCR with primers containing attachment sites. For classical cloning with restriction site ligation, the PCR product was digested with the appropriate restriction enzymes according to manufacturer's manual. If the restriction enzymes were not compatible with the *Pfu* buffer, the PCR product was first purified with MSB Spin PCRapace Kit (Invitex, Berlin, Germany) (chapter 4.7, B).

B Fragments from BAC clones

Preparation of BAC DNA with QIAGEN[®] Plasmid Midi Kit (with modified protocol for BAC DNA isolation)

A single BAC clone containing *E. coli* colony was picked to inoculate a starter culture of 3 ml LB medium containing the appropriate antibiotic. The culture was cultivated on a shaker at 37°C overnight. From this preculture 1 ml was used to inoculate a 200 ml culture (LB medium containing the appropriate antibiotic). This culture was again incubated over-

night on an incubator shaker at 37°C. The 200 ml of bacterial culture were filled into 4 Falcon tubes of 50 ml and centrifuged at 4000 rcf for 30 min at 4°C. The supernatant was decanted and each pellet was resuspended with 5 ml buffer P1. Two resuspended pellets were pooled respectively. To each of the (10 ml) resuspended samples 10 ml of buffer P2 were added and the tubes were inverted several times. Then 10 ml of cold buffer P3 were added to each tube, the samples were again inverted and incubated on ice for 15 min. The samples were centrifuged at 13000 rpm for 30 min at 4°C. The supernatant was filled into sterile beaker until further use. If white precipitate was still remaining in the supernatant, the centrifugation step was repeated for 15 min. Two Qiagen columns were equilibrated with 4 ml QBT buffer. The supernatant was pipetted onto the columns to bind the DNA on the membrane. The columns were washed twice with 10 ml QC buffer each. The DNA was eluted from each column with 7 ml preheated (65°C) QF buffer and filled into sterile Corex tubes. 4,9 ml isopropanol was added to each sample and the solution was carefully inverted. The tubes were tared and centrifuged in a Beckman® J2-21 centrifuge with the rotor JS13.1 at 9000 rpm for 30 min at 4°C. The supernatant was carefully decanted. 2 ml 70% EtOH were pipetted onto each DNA pellet and the tubes were tared with 70% EtOH. After gentle mixing, the samples were again centrifuged at 9000 rpm for 15 min. The supernatant was decanted and the tubes were turned upside down to let the EtOH drain off. The pellet was dried at RT for one or two hours. After all EtOH was evaporated, each pellet was eluted with 100 µl sterile bidest. The DNA was stored at -20°C. For quality control a restriction analysis was done before further use of the BAC clone DNA. The BAC subcloning strategy was done by two persons: The T21F11 subcloning was performed by Andrea Arbeiter and the F23A5 subcloning was done by N. Frémont.

Restriction analysis

The BAC clones should be used to generate subclones containing a few genes each, which can be used for complementation tests in *tup5-1*. First the sequence of the BAC clone (available from NCBI: <http://www.ncbi.nlm.nih.gov> or TAIR: <http://www.arabidopsis.org>) was analysed with the “Restriction analysis” programme of TAIR (<http://www.arabidopsis.org/cgi-bin/patmatch/RestrictionMapper.pl>). The coordinates of the genes (available from TIGR: http://www.tigr.org/tigr-scripts/euk_manatee/BacAnnotationPage.cgi?db=ath1&asmbl_id=60054&page_size=29&page= for the BAC clone T21F11) located on the BAC clone were compared to the restriction sites of various enzymes. The restriction enzymes which should cleave the BAC DNA were according to the expected gene groups, in which

the genes should possibly included full length, with 2000 bp promoter region and 500 bp 3' region.

Digestion of the BAC clones and agarose gel purification

BAC DNA was digested with the chosen restriction enzymes and the cleaved fragments were separated on an agarose gel. The bands containing the required gene groups were cut out from the gel with a razor blade. The DNA was purified from the gel using QIAEX II Gel Extraction Kit (Qiagen) (for long DNA fragment of 10 to 50 kb) or QIAquick Gel Extraction Kit (Qiagen) (for 70 bp to 10 kb DNA fragments). The DNA was quantified on agarose gel (chapter 4.7, C).

C Preparation of the vector

A single vector-containing *E. coli* colony was picked to inoculate a culture of 10 ml LB medium containing the appropriate antibiotic. The culture was cultivated on a shaker at 37°C overnight. The vector was isolated with the PeqGold Plasmid Miniprep Kit I (Peqlab) according to the manufacturer's manual (one column per 5 ml bacterial culture).

D Restriction of the vector

The vector was then digested with the same restriction enzymes as the DNA fragment that should be inserted into the vector. Restriction of the vector was done according to the restriction enzyme manufacturer's protocol. After restriction it was in some cases necessary to remove the buffer which was not compatible with the CIAP for dephosphorylation of the vector. In this case the DNA was purified by precipitation.

E Purification of DNA by precipitation

Aqua bidest. was added to the DNA sample in a 1,5 ml microcentrifuge tube to reach a volume of 100 µl. The same volume (100 µl) of phenol:chloroform:isoamylalcohol (25:24:1) was added and the sample was mixed. The sample was centrifuged for 3 min at 13000 rpm in a microcentrifuge at RT. Approximately 80 µl of the supernatant were transferred into a fresh 1,5 ml microcentrifuge tube without taking traces of the phenol phase. 0,1 volume of 3 M sodium acetate (pH 5,2) was added to the sample and the solution was mixed. 2,5 volumes of 96% EtOH were added and the the solution was mixed again. The sample was centrifuged at 13000 rpm in a microcentrifuge at 4°C for 15 min. The supernatant was removed and 200 µl of 70% EtOH were added to the sample. The solution was

mixed again. The sample was centrifuged at 13000 rpm in a microcentrifuge at 4°C for 10 min. The supernatant was removed and the DNA pellet was dried on a heating block at 50°C for approximately 30 min until the EtOH was evaporated. The pellet was then eluted in 20 µl (or another appropriate volume) of *aqua bidest.*, 10 mM Tris buffer (pH8) or TE buffer. The sample was stored at -20°C.

F Dephosphorylation of the vector

Dephosphorylation of the vector was done with Calf Intestinal Alkaline Phosphatase (CIAP) (Invitrogen, California, U.S.A.) according to the manufacturer's protocol.

G Ligation

The ligation of vector and DNA fragment was done with T4 DNA ligase (Fermentas GmbH, St. Leon-Rot, Germany) according to manufacturer's protocol in a volume of 20 µl for 1 h at RT. After ligation the ligase was inactivated for 10 min at 65°C. The ligation was then dialysed on a MF-Millipore membrane (filter pore size: 0.025 µm, cat. no.: VSWP02500), because the salts in the ligation mix would disturb the electroporation. The drop of ligation mix was pipetted on the membrane swimming on *aqua bidest.* (shining membrane side facing upwards) and was incubated for 2 h. The desalted ligation mixture was recovered by carefully pipetting the drop from the membrane. The ligation was stored at -20°C until electroporation.

4.8.2 Cloning of a DNA fragment into a vector with Gateway®

The cloning of a DNA fragment into a vector with the Gateway® system was done with the kit "PCR Cloning System with Gateway® Technology (with pDONR™221)" and Gateway® compatible plant destination vectors from Karimi et al. (2005) according to the manufacturer's manual (with a few modifications). The insert (a PCR product bordered by attachment sites, see chapter 4.8.1, A) was first cloned into the donor vector pDONR™221 from Gateway® by BP reaction (Table 4-6). After transformation of *E. coli* (strain DH10B™) (chapter 4.8.3, B) positive clones were selected with the appropriate antibiotics. The plasmid of positive clones was purified by plasmid mini preparation (chapter 4.8.3, D), the insert of the clones was verified by PCR (with *Taq* polymerase, see Table 4-4 and Table 4-5) and restriction (chapter 4.8.3, E). If the identity of the plasmid was confirmed, it

was sequenced (chapter 4.8.3, F). Plasmids with correct insert sequence were used for the LR reaction to clone the insert into the destination vector. Again positive clones were selected and tested as described before (without sequencing). The plasmid of positive LR clones containing the insert of interest in the chosen destination vector was used for transformation of *A. tumefaciens* (chapter 4.8.4) followed by transformation of *A. thaliana* (chapter 4.8.5). The resulting transgenic plants were then analysed.

Table 4-6: BP and LR reaction setup for Gateway® cloning (modified from the manufacturer's manual).

Components of BP reaction	BP reaction (10 µl)	Components of LR reaction	LR reaction (10 µl)
BP buffer	2 µl	LR buffer	2 µl
PCR product (insert)	X µl (up to 6,5 µl)	Entry clone	1 µl (100 ng/µl)
Donor vector pDONR™221	1 µl (150 ng/µl)	Destination vector	1 µl (100 ng/µl)
BP clonase™ enzyme mix	0,5 µl	LR clonase™ enzyme mix	0,5 µl
H ₂ O	X µl (fill to a final reaction vol. of 10 µl)	H ₂ O	5,5 µl
Incubation time	20 h	Incubation time	20 h
Incubation temperature	25°C	Incubation temperature	25°C

4.8.3 Transformation of *E. coli*

A Preparation of competent *E. coli* cells

A single *E. coli* colony (strain used here: DH10B™) was picked to inoculate a starter culture of 50 ml LB medium. All working steps were done under sterile conditions. The culture was cultivated on a shaker at 37°C overnight at 200 rpm. Four flasks containing 250 ml LB medium (prewarmed to 37°C) were inoculated with 12,5 ml starter culture each. The cultures were cultivated until an OD₆₀₀ of 0,8 was reached. Cell density was measured with the photometer at 600 nm (1 ml cell aliquot). When the cells had reached the expected density, the flasks were immediately transferred onto an ice water mixture for up to 20 min and shaken for cooling. The bacterial culture was filled into 4 sterile and cooled 500 ml centrifuge tubes and the tubes were tared. The cells were centrifuged at 3500 rpm for 15 min at 4°C. The supernatant was decanted and each pellet was resuspended with 250 ml cold sterile *aqua bidest.* (always starting with 15 ml for pellet dilution, and always using chilled pipettes with wide openings). The tubes were tared. The cells were again centrifuged at 3500 rpm for 20 min at 4°C. The supernatant was decanted and each pellet was resuspended with 125 ml cold sterile 10% glycerol solution (v/v). Two cell batches were

pooled respectively and again centrifuged at 3500 rpm for 20 min at 4°C. The supernatant was decanted and each pellet was resuspended with 10 ml cold sterile 10% glycerol solution (v/v). The cells were transferred into 50 ml Falcon tubes and centrifuged at 3500 rpm for 20 min at 4°C. The supernatant was carefully decanted and each pellet was resuspended with 1 ml cold sterile 10% glycerol solution (v/v) by careful shaking. The cells were pooled and aliquoted to 50 µl batches in sterile 1,5 ml microcentrifuge tubes and stored at -80°C. The cells were tested for competence prior to use by electroporating them (chapter 4.8.3, B) with the control vector pUC19 with two defined concentrations (10 and 100 µg) and by defining the number of transformed cells (surviving carbenicillin selection) per quantity (in µg) of vector used.

B Electroporation of *E. coli*

A 50 µl aliquot of competent *E. coli* cells was thawed on ice. 1 µl of plasmid or 5 µl of ligated DNA (chapter 4.8.1, G) were pipetted to the cells and carefully mixed by stirring with the pipette tip. The cells were kept on ice during the whole procedure until electroporation to keep the competence of the cells high. The cells were incubated with the DNA on ice for 30 min. The cells were then transferred to a chilled electroporation cuvette and were pulsed in an electroporator (Bio-Rad MicroPulser) with 1,8 kV. After the pulsing, 1 ml of prewarmed LB medium (37°C) was pipetted to the cells and carefully mixed with the pipette. The cells were then transferred into a 1,5 ml tube and were incubated for 1 h at 37°C on a thermomixer (Eppendorf Thermomixer compact) at 180 rpm. The cells were plated out on LB medium containing the appropriate antibiotics for selection and incubated at 37°C overnight.

C Colony PCR

The success of transformation in *E. coli* cells was first tested by colony PCR. This method allows testing of a large number of samples in short time. For this purpose *Taq* polymerase reaction mixes (see Table 4-4) with insert specific primers were filled into PCR tubes (on ice). From each transformant colony, cells were picked with a sterile wooden toothpick and were dipped into one PCR reaction mix each. The toothpick was stirred in the reaction mixture to dilute the cells (caution: This should be done fast to prevent the reaction mixture to be absorbed by the wooden material!). The tubes were sealed and the PCR reaction was performed in a Biometra® T-Gradient PCR cycler. The first denaturation step (94°C)

of the PCR programme was prolonged to 3-4 min to disrupt the cells. Following steps of the PCR programme were as described in Table 4-5. The amplification products of the expected insert DNA sequence were visualised with gel electrophoresis.

D Plasmid preparation (mini prep)

Transformed colonies were picked to inoculate cultures of 5 ml LB medium containing the appropriate antibiotic. The cultures were cultivated on a shaker at 37°C overnight. Transformant cells were collected by centrifuging 1,8 ml in a 2 ml tube at 13000 rpm in a microcentrifuge at RT. The supernatant was decanted. The cells were resuspended in 150 µl cold P1 buffer containing RNase A. 300 µl P2 buffer were added to the sample. The tube was inverted several times. The sample was incubated for 4-5 min (not longer than 5 min!) at RT. 225 µl ice-cold P3 buffer were added to the sample, again the tube was inverted several times. The sample was incubated on ice for 15 min, followed by centrifugation at 13000 rpm at 4°C for 5 min. The colourless supernatant was transferred into a fresh microcentrifuge tube. If the DNA should be very pure, an optional phenol:chloroform purification step was performed. In this case the supernatant was transferred into a 1,5 ml microcentrifuge tube and the same volume of phenol:chloroform was added. The sample was vortexed and centrifuged for 3 min at 13000 rpm at 4°C. The aqueous upper layer was transferred into a fresh 2 ml microcentrifuge tube. The plasmid DNA (with or without phenol:chloroform step) was then precipitated by adding 2 volumes of 96% EtOH. The solution was vortexed and incubated for 2 min at RT. The sample was centrifuged for 5 min at 13000 rpm at 4°C. The supernatant was decanted and 1 ml of 70% EtOH was added to the DNA pellet. The sample was vortexed and again centrifuged for 5 min at 13000 rpm at 4°C. The supernatant was removed and the DNA pellet was dried on a heating block at 50°C for approximately 10 min until the EtOH was evaporated. The pellet was then eluted in 20-40 µl of *aqua bidest.*, 10 mM Tris buffer (pH 8) or TE buffer. The sample was stored at -20°C (protocol modified from Sambrook and Russel, 2001).

E Restriction analysis

First the sequence of the vector and the insert was analysed with the “restriction analysis” programme of TAIR (<http://www.arabidopsis.org/cgi-bin/patmatch/RestrictionMapper.pl>) or Vector NTI® (Invitrogen, California, U.S.A.) to find restriction sites and calculate fragment lengths produced by digestion with the enzyme of interest. The plasmid was then

digested according to the enzyme's manufacturers manual and the DNA fragments were separated with gel electrophoresis. Only clones which had the expected results with PCR and restriction analysis were chosen for further use.

F Sequencing

The DNA of positive clones which were chosen for transformation into *A. tumefaciens* and then *A. thaliana* was purified with PeqGold Plasmid Miniprep Kit I (Peqlab) (chapter 4.8.1, C) and the insert was sequenced to make sure that no mutation had occurred. For this purpose the purified plasmid and insert specific primers were sent to a sequencing company (chapter 4.7, C).

4.8.4 Transformation of *A. tumefaciens*

A Preparation of competent *A. tumefaciens* cells

A starter culture of 5 ml LB medium containing rifampicin and gentamycin was inoculated with *A. tumefaciens* (strain GV3101). The culture was cultivated on a shaker at 28°C overnight (or two days) at 140 rpm. Two flasks containing 250 ml LB medium (with rifampicin and gentamycin) were inoculated with 2,5 ml starter culture respectively. The cultures were cultivated on a shaker at 28°C overnight (~ 16 h) at 140 rpm. The cell density (at OD₆₀₀) was used between 0,8 and 1,2. For measurement of cell density, the photometer was set to a wavelength of 600 nm. A 1 ml cell aliquot was measured. When the cells had reached the expected density, the flasks were immediately transferred onto an ice water mixture for 15 min and were shaken for cooling. The bacterial culture was filled into 2 sterile and cooled 500 ml centrifuge tubes and the tubes were tared. The cells were centrifuged at 7000 rpm for 10 min at 4°C. The supernatant was decanted and each pellet was resuspended with 250 ml cold sterile *aqua bidest.* (always starting with 5 ml for pellet dilution, and always using chilled pipettes with wide openings). The tubes were tared. The cells were again centrifuged at 7000 rpm for 10 min at 4°C. The supernatant was decanted and each pellet was resuspended with 125 ml cold sterile *aqua bidest.* The cells were again centrifuged at 7000 rpm for 10 min at 4°C. The supernatant was decanted and each pellet was resuspended with 25 ml cold sterile *aqua bidest.* The cells were transferred into 50 ml Falcon tubes and centrifuged at 4000 rcf for 10 min at 4°C. The supernatant was carefully decanted and each pellet was resuspended with 1 ml cold sterile 10% glycerol solution

(v/v) by careful shaking. The cells were pooled and filled to 5 ml with cold sterile 10% glycerol solution. The cells were aliquoted to 50 µl batches in sterile 1,5 ml microcentrifuge tubes and stored at -80°C.

B Electroporation of *A. tumefaciens*

The electroporation was done as described for *E. coli*, except that 1 µl of plasmid was used for transformation and that the transformed cells were incubated in liquid LB medium for 2-4 h at 28°C on a thermomixer in the case of *A. tumefaciens*. 2 µl of the transformed cells (diluted in 98 µl LB medium) were plated on LB medium containing the two antibiotics for the strain GV3101 (rifampicin and gentamycin) and the antibiotic for which a resistance was transferred by the plasmid. The transformant colonies were cultivated at 28°C for 2-4 days. The vector transformed into *A. tumefaciens* was already thoroughly tested in *E. coli* (chapter 4.8.3, C-F). The selected *A. tumefaciens* transformants were therefore only tested with colony PCR.

4.8.5 Floral dip transformation of *A. thaliana*

dipping solution

- 5% sucrose
- 0,05% Silwett[®] L-77
- 2,3 g/l MS salts
- 10 µl/l BA (from 1 mg/ml DMSO stock solution)

A. thaliana plants were grown on soil in pots (Ø 9 cm) as a pool of 10 to 20 plants. The plants were used for transformation when the first flower shoots had reached a length of 8 to 12 cm. The *A. tumefaciens* clones containing the plasmid with the transgene which should be inserted into the *A. thaliana* genome were cultivated on a shaker incubator at 28°C in 250 ml LB medium containing the appropriate antibiotics (chapter 4.8.4, B) for 2 to 3 days. The cells were then collected in 500 ml centrifugation tubes for 20 min at 5500 ×g at RT. The supernatant was decanted and the cells were resuspended in dipping solution to a cell density of 0,8 at OD₆₀₀. The cell suspension was filled into a beaker glass and the flower shoots of *A. thaliana* were briefly dipped into the mixture (2-3 sec). The plants were then layed horizontally onto a plastic tray (with a flat lid under the pot to avoid contact of the dipped flower shoots with the tray). The plants were covered with a plastic dome to avoid fast drying of the dipping mixture and were stored in the dark until the following day. On the next day plants were transferred back into the greenhouse. The treated plants

were dipped once more after one week. The seeds produced by these dipped plants were named T₀ generation.

4.9 Yeast transformation with a modified lithium acetate method

Stock solutions:

- A) 10mg/ml carrier DNA (herring sperm)
- B) 1M DTT (always store on ice)
- C) 40% Glucose
- D) 1 g/100ml L-arginine
- E) 0,2 g/100ml uracil
- F) 1 g/100ml L-histidine
- G) 1 g/100ml L-leucine

PLATE mixture (1 ml)

- 900 µl 60% PEG 3350 (use autoclaved stock solution)
- 100 µl 1 M LiAc (use autoclaved stock solution)
- 10 µl 1M Tris-Cl (pH 7,5) (use autoclaved stock solution)
- 2 µl 0,5 M EDTA pH 8 (use autoclaved stock solution)

The cloning of the insert into the yeast vector p423TEF was done with the classical restriction enzyme digestion (*Bam*HI and *Sal*I) and ligation method (see chapter 4.8.1) (Mumberg *et al.*, 1995). The ligated vector was transformed into *E. coli* and the positive clones were checked in the previously described way (chapter 4.8.3, C-F).

S. cerevisiae (mutant strain Y37711) was inoculated in 15 ml YPD medium (with kanamycin) and cultivated at 30°C overnight. 1 ml of cell culture per transformation was centrifuged in a 1,5 ml microcentrifuge tube at 13000 rpm for 30 sec at RT. The supernatant was decanted and the pellet was resuspended with approximately 50-100 µl remaining fluid. 2 µl of 10 mg/ml carrier DNA (Herring sperm, Sigma) which had shortly before been heated at 95°C for 5 min (with vortexing from time to time) and immediately cooled on ice was pipetted to the cells together with 1 µl of miniprep plasmid for transformation. The cells were vortexed and 0,5 ml of freshly prepared PLATE mixture (see buffers, chapter 4.15.2) were added. The cells were vortexed again. 20 µl of 1M DTT was added; the sample was vortexed again and incubated for 24 h at RT. The cells were then incubated at 42 °C for 15 min and centrifuged for 30 sec at 13000 rpm. The pellet was resuspended in 200 µl sterile *aqua bidest.* 100 µl of the cell suspension were plated on SD medium containing the appropriate antibiotics and amino acids (depending on the antibiotic resistance or amino acid autotrophy conferred by the transformed plasmid).

4.10 Analysis of free amino acid content in *A. thaliana*

The free amino acid content in *tup5-1* and WT was analysed by HPLC. All plants were grown *in vitro* under long day conditions (except for dark controls). Seedlings were cultivated in liquid ½ MS medium for seven days. They were grown at standard light intensity (SLI) ($150 \mu\text{mol m}^{-2} \text{sec}^{-1}$), at low light intensity (LLI) ($3 \mu\text{mol m}^{-2} \text{sec}^{-1}$) and in darkness to test the effect of light on amino acid content. To harvest the seedlings, the liquid was removed with a water jet vacuum pump, the seedlings were washed once with 5 ml sterile *aqua bidest.* 100 mg of seedlings per sample were frozen in liquid nitrogen and stored at -80°C until extraction.

Plant samples of shoots and roots were analysed from 11-d-old seedlings grown under long day conditions on vertical plates with MS medium (root material could only be harvested from WT). The seedlings were cut at the border of hypocotyls and root. Shoot and root batches were frozen in liquid nitrogen and stored at -80°C until extraction.

Extraction

The frozen plant material (100 mg) was ground with a frozen mortar and pestle (cooled with liquid nitrogen) to produce a fine plant powder. The powdered sample was transferred into a frozen 2 ml microcentrifuge tube. 400 μl of 80% EtOH / 2.5 mM HEPES (pH 7.5) were added to the frozen powder. The sample was incubated at 80°C for 20 min on an Eppendorf Thermomixer compact and then centrifuged at 13 200 rpm for 10 min at 4°C in a microcentrifuge. The supernatant was transferred into a fresh 2 ml microcentrifuge tube and the pellet was resuspended and incubated with 400 μl 50% EtOH / 2.5 mM HEPES (pH 7.5) for 20 min at 80°C on a thermomixer. The sample was centrifuged at 13 200 rpm for 10 min at 4°C . The supernatant was removed with a pipette and pooled with the first supernatant. The pellet was again resuspended and incubated with 200 μl 80% EtOH for 20 min at 80°C on a thermomixer. The sample was centrifuged at 13 200 rpm for 10 min at 4°C . The supernatant was removed with a pipette and pooled with the other supernatants of the sample. The extraction samples can be stored at -80°C for several weeks. The next steps were performed in the laboratory of Dr. Rainer Höfgen (MPI for Molecular Plant Physiology, Golm).

HPLC analysis

Amino acid stock solution for HPLC standard

No cystein and proline were used, because they could not be analysed in this experimental setup. The concentration of each amino acid in the mixture was 10 mM (diluted in water from 500 μ M stocks): Alanine, arginine, asparagine, aspartic acid, glutamic acid, glutamine, glycine, histidine, isoleucine, leucine, lysine, methionine, phenylalanine, serine, threonine, tryptophan, tyrosine, and valine.

Buffer A

- 22 ml 0,4 M sodium phosphate buffer pH 6,8
 - 2 ml THF
- Filled with *aqua bidest.* to 1 l.

Buffer B

- 25 ml 0,4 M sodium phosphate buffer pH 6,8
- 175 ml methanol
- 110 ml acetonitril
- 225 ml *aqua bidest.*

160 μ l of extracted sample were mixed with 40 μ l of 1 M boric acid (pH 10.7) and incubated for 10 min at RT. The sample was then centrifuged at 13 200 rpm for 10 min at 4°C. 120 μ l of the supernatant were transferred into an HPLC vial. In the HPLC machine 70 μ l of the sample were automatically mixed with 70 μ l of the OPA (ortho-phthaldialdehyde) reagent. The sample was incubated for 90 sec. During this time the amino acids were derivatised with OPA to fluorescent isoindole derivatives. The sample mixture was automatically injected into the HPLC column, where the amino acids were separated. Due to OPA the amino acid could be detected and its quantity running through a column containing octadecyl silica (ODS) (5 μ M particle size) could be measured by detection of the fluorescence signal. The results were visualised as peaks by the programme Chromeleon®. The retention time of a specific amino acid is comparable for each sample. Therefore the peaks of the samples could be compared with those of a standard amino acid mixture which was measured as control. For quantification of the amino acids, 10, 20, 50 and 100 μ M standard mixtures were measured. The area below the peaks was measured for each amino acid by the program Chromeleon® (Dionex, California, U.S.A.). The values were used for a calibration curve. The concentration of each amino acid in the sample could be calculated with the calibration curve of the corresponding amino acid from the standard mixture.

4.11 Real-time PCR

4.11.1 RNA extraction and purification

A RNA extraction with the trizol method

Trizol Reagent

- 38% phenol
 - 800 mM guanidinium thiocyanate
 - 400 mM ammonium thiocyanate
 - 100 mM sodium acetate pH5 (from 3 M stock solution)
 - 5% glycerol
- Always prepare freshly.

RNA salt solution

- 1,2 M sodium chloride
 - 800 mM sodium citrate
- Do not autoclave the solution.

The plant sample was ground with a frozen mortar and pestle (cooled with liquid nitrogen) to produce a fine plant powder. The powdered sample was transferred into a frozen 2 ml microcentrifuge tube (filling up to ½ of the tube volume) and 1 ml of Trizol was added. The sample was vortexed until a homogenous mixture was produced. The sample was incubated at RT for 5 min and then centrifuged at 16 000 ×g for 5 min at 4°C. The supernatant was transferred into a fresh 2 ml microcentrifuge tube and 400 µl Chloroform-Isoamylalcohol (24:1) were added. The sample was vortexed to homogeneity and then incubated at RT for 5 min. It was then centrifuged at 16 000 ×g for 15 min at 4°C. 700 µl of the upper phase of the supernatant were transferred into a fresh 1,5 ml microcentrifuge tube (without taking traces of the interphase into the new tube.). 350 µl isopropanol and then 350 µl RNA salt solution were added. The mixture was inverted until the solution became transparent again. After 10 min of incubation at RT the sample was centrifuged at 12 000 ×g for 10 min at 4°C. The supernatant was completely removed. 900 µl of 75% EtOH were added to the RNA pellet and the mixture was shortly vortexed. The sample was centrifuged at 7500 ×g for 5 min at 4°C. The supernatant was completely removed again. This EtOH washing step was repeated a second time. The RNA pellet was dried on a heating block at 60°C until the EtOH was evaporated. The pellet was then diluted with 30 µl of sterile, RNase-free *aqua bidest.* on a heating block at 60°C for 5 min. The sample was stored at -80°C.

To check if the extraction was successful, 1 µl of the RNA sample was measured with the NanoDrop ND-1000 spectrophotometer at the wavelengths 260, 280 and 230 nm with the predefined RNA-40 programme.

B Purification of RNA with Quiagen RNeasy

This additional purification step was performed on RNA used for real-time PCR. It can be omitted for simple semi-quantitative RT-PCR. The RNA sample was purified with the RNeasy Mini kit (Qiagen) according to manufacturer's protocol ("RNA cleanup"), including on-column DNase digestion to eliminate genomic DNA contamination.

4.11.2 RNA quantification and quality check

1 μ l of the RNA sample was measured with the NanoDrop ND-1000 spectrophotometer at the wavelengths 260, 280 and 230 nm with the predefined RNA-40 programme. To check the quality of the RNA, the RNA samples (1 μ g per sample) were compared on agarose gel to make sure that the concentrations measured before were correct and that no degradation had taken place.

4.11.3 cDNA synthesis

The cDNA synthesis was made with the reverse transcriptase SuperScript™ III (Invitrogen, California, U.S.A.). First mix 1 (see Table 4-7) was incubated for 5 min at 65°C and directly transferred onto ice for 3 min. Mix 2 (see Table 4-7) was added to Mix 1 and the reaction mixture was incubated at 25°C for 5 min, at 50°C for 45 min and at 70°C for 15 min. After cDNA synthesis, the DNA concentration was measured with the NanoDrop ND-1000 spectrophotometer at the wavelengths 260, 280 and 230 nm with the predefined DNA-50 programme. For real-time PCR the cDNA was diluted to a concentration of approximately 200 ng/ μ l.

Table 4-7: Reaction mixture for reverse transcription reaction with SuperScript™ III.

Mix 1		Mix 2	
Components	Volume [μl]	Components	Volume [μl]
Oligo dT (50 μ M)	1	5 \times SuperScript™ III buffer	4
N9 random primer (50 μ M)	1,83	DTT-Mix	1
RNA	X (5 μ g)	RNaseOut™ (Invitrogen)	1
dNTP (10 mM each)	1	SuperScript™ III enzyme (Invitrogen)	1
H ₂ O	X: fill reaction vol.	-	-
Total	13	Total	7

4.11.4 Real-time PCR reaction

The reaction mixture for the real-time PCR was prepared as listed in Table 4-8. To generate three technical replicates per sample, first a master mix containing all components except the primers and the template DNA was prepared. This master mix was portioned and the primers were added. The master mixes containing primers were aliquoted for three samples each (for technical triplicates) and the template DNA was added. Each triplicate mixture was filled in three wells of a microtiter plate for real-time PCR reaction. The PCR reaction was performed in a 7500 Fast Real-Time PCR system (Applied Biosystems, Life Technologies, California, U.S.A.) with the PCR programme as described in Table 4-9. The data were analysed with Applied Biosystems 7500 FAST Software_v2.0.1 (Applied Biosystems, Life Technologies, California, U.S.A.).

Table 4-8: PCR mixture for real-time PCR reaction with Immolase™ DNA polymerase.

Components	Volume [µl]
10 × ImmoBuffer	2
MgCl ₂ (50 mM)	0,8
dNTP (5 mM each)	0,4
10 × SYBR Green I	0,2
ROX (25 µM)	0,04
H ₂ O	13,52
Primer 1 (6 µM)	1
Primer 2 (6 µM)	1
Immolase™ (5 u/µl) (Bioline)	0,04
Template (approxim. 200 ng)	1

Table 4-9: Real-time PCR programme for Immolase™ DNA polymerase.

Programme steps	Temperatures	Duration
1. First denaturation	95°C	15 min
2. Denaturation	95°C	10 sec
3. Annealing	55°C	15 sec
4. Polymerisation	72°C	10 sec
5. Pause	16°C	∞
Number of cycles (step 2-4)		50×

4.12 Primers

The primers used for mapping *TUP5*, for cloning different fragments, for real-time PCR and other purposes are listed in Table 9-8. Primers used for sequencing genes in the mapping interval of *TUP5* and for gene identification during BAC subcloning are listed in Table 9-3.

4.13 Databases and Software

The databases and softwares used for the analysis of *TUP5* are listed in Table 4-10 and Table 4-11.

Table 4-10: Databases used for the analysis of *TUP5*.

Description of use	Name of the database	Reference or internet link
<i>Arabidopsis</i> gene information search	TAIR	The Arabidopsis Information Resource (http://www.arabidopsis.org)
<i>Arabidopsis</i> gene information search	MIPS	Munich Information Centre for Protein Sequences (http://mips.gsf.de)
<i>Arabidopsis</i> gene information search	TIGR	The Institute for Genomic Research (http://www.tigr.org)
Enzymatic reactions and metabolic pathways	KEGG	Kyoto Encyclopedia of Genes and Genomes (http://www.genome.jp/kegg/pathway.html#amino)
Ordering of <i>Arabidopsis</i> seeds and DNA stocks	NASC	Nottingham <i>Arabidopsis</i> Stock Center (http://arabidopsis.info/)
Ordering of <i>Arabidopsis</i> seeds and DNA stocks	ABRC	<i>Arabidopsis</i> Biological Resource Center (http://www.biosci.ohio-state.edu/pcmb/Facilities/abrc/abrchome.htm)
Search for <i>Arabidopsis</i> mutant lines containing T-DNA insertions	SIGnAL	The Salk Institute Genomic Analysis Laboratory (http://signal.salk.edu/cgi-bin/tdnaexpress) (Alonso <i>et al.</i> , 2003)
Metabolic pathways in <i>Arabidopsis</i>	AraCyc	Plant Metabolic Network (PMN) (http://www.plantcyc.org:1555/ARA/server.html) (Rhee <i>et al.</i> , 2006)
Analysis of protein sequences and structures	ExPASy	Expert Protein Analysis System (http://www.expasy.org) (Gasteiger <i>et al.</i> , 2003)
Ordering of yeast mutants	EUROSCARF	EUROpean Saccharomyces Cerevisiae ARchive for Functional Analysis (Frankfurt, Germany) (http://web.uni-frankfurt.de/fb15/mikro/euroscarf/index.html)
Information on <i>S. cerevisiae</i> genes	SGD	<i>Saccharomyces</i> Genome Database (http://www.yeastgenome.org/)
Literature, sequence analysis and others	NCBI	The National Center for Biotechnology Information (http://www.ncbi.nlm.nih.gov)
Gene expression database (microarray data)	Genevestigator	https://www.genevestigator.ethz.ch/gv/user/serveApplet.jsp
Skeletal formula of chemical compounds	Human Metabolome Database	http://www.hmdb.ca (Wishart <i>et al.</i> , 2009)
Colour-coded <i>Arabidopsis</i> organ images of gene expression patterns	electronic Fluorescent Pictograph (eFP)	http://www.bar.utoronto.ca/efp/cgi-bin/efpWeb.cgi (Winter <i>et al.</i> , 2007)

Table 4-11: Software used for the analysis of *TUP5*.

Description of use	Name of the software	Company, reference or internet link
Calculations	Excel	Microsoft Office
Analysis and editing of DNA sequences	Chromas	(http://www.technelysium.com.au/chromas.html)
Alignment of DNA or AA sequences	ClustalW	(Larkin <i>et al.</i> , 2007)
	Clustal W (1.83)	http://www.ch.embnet.org/software/ClustalW.html
	ClustalW2	http://www.ebi.ac.uk/Tools/es/cgi-bin/clustalw2
	Vector NTI®	Invitrogen, California, U.S.A. (http://www.invitrogen.com/site/us/en/home.html)
Shading of conserved amino acids in AA alignment	Boxshade	http://www.ch.embnet.org/software/BOX_form.html
Analysis of HPLC data	Chromeleon®	Dionex (http://www.dionex.com/en-us/software/chromeleon/lp70618.html)
Prediction of subcellular protein targeting	TargetP	(http://www.cbs.dtu.dk/services/TargetP/) (Emanuelsson <i>et al.</i> , 2007)
	Aramemnon	(http://aramemnon.botanik.uni-koeln.de/) (Schwacke <i>et al.</i> , 2003)
	PSORT	(http://psort.ims.u-tokyo.ac.jp/form.html) (Nakai and Horton, 1999)
Analysis of real-time PCR data	Applied Biosystems 7500 FAST Software_v2.0.1	Applied Biosystems
Image analysis	ImageJ	(Abramoff <i>et al.</i> , 2004)

4.14 Microbial strains, vectors and gene constructs

4.14.1 Microbial strains

The microbial strains used for cloning and for the analysis of *TUP5* function are listed in Table 4-12.

Table 4-12: Microbial strains used for the analysis of *TUP5*.

Name	Description	Source
DH10B™	<i>E. coli</i> strain used for transformation	Invitrogen, California, U.S.A.
GV3101:pMP90	<i>A. tumefaciens</i> strain used for transformation, rifampicin and gentamycin resistant.	(Koncz and Schell, 1986)
Y37711	<i>S. cerevisiae</i> homozygous, diploid strain in which the <i>acetylornithine aminotransferase</i> gene <i>YOL140w</i> on chromosome XV is deleted. Kanamycin resistant, arginine, histidine, leucine, urea auxotrophic.	Euroscarf, Frankfurt, Germany

4.14.2 Vectors and gene constructs

The vectors which were used for cloning are listed in Table 9-5. Gene constructs received from other sources used for the analysis of *TUP5* are listed in Table 9-6. Gene constructs which were produced during this work for the analysis of *TUP5* are shown in Table 9-7, except for BAC subclones (see Table 5-1 and Table 5-2).

4.15 Solutions

4.15.1 Stock solutions

Only those stock solutions are described, which are not listed within the buffer protocols in chapter 4.15.2 and 4.15.3.

DNA handling

The components of TBE, TAE and EDTA stock solutions are listed in Table 4-13.

Table 4-13: Protocol for TBE, TAE and EDTA stock solutions.

10x TBE (Tris/borate/EDTA) buffer (for 1 l)	50x TAE (Tris/acetate/EDTA) buffer	0,5 M EDTA(1 l)
108 g Tris base 55 g boric acid 40 ml 0,5M EDTA (pH 8) Fill to 1 l with <i>aqua bidest.</i>	242 g Tris base 57,1 ml glacial acetic acid 100 ml 0,5M EDTA (pH 8) Fill to 1 l with <i>aqua bidest.</i>	Dilute 186,1 g EDTA with approximately 800 ml <i>aqua bidest.</i> , titrate to pH 8 with approximately 20 g of NaOH pellets, fill to 1 l, autoclave.

Antibiotics

The antibiotics used in this work are listed in Table 4-14.

Table 4-14: Antibiotics stock solutions

Antibiotic	Concentration in growth medium [mg/l]
Ampicillin	100
Carbenicillin	50
Chloramphenicol	34
Gentamycin	25
Kanamycin	50
Phosphinothricin (for plants)	12
Rifampicin	50
Spectinomycin	50

Amino acids and other organic compounds

Stock solutions of chemicals used for complementation tests of *tup5-1*. The concentration was always 250 mM (diluted in water): acetylmornithine, arginine, citrulline, DNQX, fumaric acid, glutamic acid, α -ketoglutaric acid (2-oxoglutaric acid), lysine, ornithine, proline, putrescine, spermidine, spermine, urea, except glutathione which had 100 mM.

4.15.2 Buffers

TE buffer pH 8

- 10 mM Tris / HCl pH 8 (from 1 M Tris / HCl pH 8 stock solution)
- 1 mM EDTA pH 8.0 (from 500 mM EDTA pH 8.0 stock solution)

Bacterial plasmid isolation

The composition of bacterial plasmid isolation buffers are listed in Table 4-15.

Table 4-15: Components of bacterial plasmid isolation buffers.

P1 (+RNase A)	P2	P3 (for 100 ml)
- 25 mM Tris-Cl - 10 mM EDTA pH 8 with 25% HCl The solution was autoclaved. A 100 ml batch was aliquoted to which 100 mg/l RNase A (from stock solution) was added before use. The RNase-containing buffer was stored at 4°C.	- 0,2 N NaOH (from 10 N stock) - 1% (w/v) SDS (from 10% stock) The solution was freshly prepared before each plasmid preparation.	- 60 ml of 5 M potassium acetate - 11,5 ml glacial acetic acid - 28,5 ml <i>aqua bidest.</i>

DNA purification by precipitation

Phenol: chloroform: isoamyl alcohol (25:24:1)

PCR buffers

The composition of 10 × *Taq* and *Pfu* polymerase buffer is listed in Table 4-16.

Table 4-16: Components of 10 × *Taq* and *Pfu* polymerase buffer.

10× <i>Taq</i> buffer	10× <i>Pfu</i> buffer
500 mM KCl 100 mM Tris (pH 9) 1% Triton® X-100	200 mM Tris-HCL (pH 8 at 25°C) 100 mM KCl 100 mM (NH ₄) ₂ SO ₄ 20 mM Mg SO ₄ 1 mg/ml nuclease-free BSA 1% Triton® X-100

Gel loading buffer

The composition of blue and orange gel loading buffer is listed in Table 4-17.

4. MATERIAL AND METHODS

Table 4-17: Components of blue and orange gel loading buffer.

Blue gel loading buffer	Orange G gel loading buffer (50 ml)
0,25% (w/v) bromophenol blue 0,25% (w/v) xylenecyanol FF 40% (w/v) sucrose in H ₂ O (Sambrook and Russel, 2001)	33,5 g sucrose 200 mg orange G 5 ml EDTA 500 mM (pH 8) Fill to 50 ml with <i>aqua bidest.</i> , warm the mixture to solubilise. (caution: only very little water is necessary!)

4.15.3 Growth media

The composition of MS media for *in vitro* culture of *A. thaliana* are listed in Table 4-18 and the growth media for *E. coli*, *A. tumefaciens* and *S. cerevisiae* are listed in Table 4-19.

Table 4-18: Components of MS medium for *A. thaliana*

Components	Solid medium		½ MS liquid medium
	Concentration	Stock solutions used	Concentration
MS salts	4,6 g/l	-	2,3 g/l
Myo-inositol	0,1 g/l	-	-
MES	0,5 g/l	-	0,5 g/l
Sucrose	10-30 g/l	-	1 g/l
Thiamine	20 mg/l	From 1000× mixed stock	-
Nicotinic acid	1 mg/l		-
Pyridoxine	1 mg/l		-
Biotin	1 mg/l	From 1000× stock (in DMSO)	-
Agar (extra pure)	7-9 g/l	-	-
pH		5,7	6

Table 4-19: Components of growth media for *E. coli*, *A. tumefaciens* and *S. cerevisiae*.

Growth medium for <i>E. coli</i> and <i>A. tumefaciens</i>	Growth medium for <i>S. cerevisiae</i>	
LB medium	YPD medium	SD medium
- Tryptone: 10 g/l - Yeast extract: 5 g/l - NaCl: 10 g/l - (Agar: 15 g/l) pH 7	- 1% Yeast extract - 2% Peptone - 2% Glucose (add glucose after autoclaving from a sterile 40% stock solution) - (1% Agar (Merck) for solid medium) For 500 ml YPD medium: Dilute 5 g yeast extract and 10 g peptone in 400 ml <i>aqua bidest.</i> , titrate to pH 6,5 with 1M HCl, fill to 475 ml with <i>aqua bidest.</i> and autoclave. Add 25 ml of glucose from a sterile 40% stock solution.	- 0,67% Yeast nitrogen base without amino acids - 2% Glucose (add glucose after autoclaving from a sterile 40% stock solution) - (1% Agar (Merck) for solid medium) For 1 l SD medium: Dilute 6,7 g yeast nitrogen base without amino acids in 800 ml <i>aqua bidest.</i> , titrate to pH 5,8 with 1M KOH, fill to 900 ml with <i>aqua bidest.</i> , add 10 g agar and autoclave. When the medium has cooled to 55°C, add 50 ml of glucose from a sterile 40% stock solution and 50 ml of sterile <i>aqua bidest.</i> or amino acid solutions for supplementation of auxotroph yeast mutants (to reach a total volume of 1 l).

4.16 Chemicals

The chemicals were mainly provided by the companies Merck (Darmstadt, Germany), Sigma-Aldrich (U.S.A.), Roth (Karlsruhe, Germany), Serva (Heidelberg, Germany) and Boehringer Mannheim GmbH (Mannheim, Germany).

4.17 Abbreviations

<i>Aqua bidest.</i>	Aqua bidestillata	MetOH	Methanol
Arg	Arginine	MgCl	Magnesium chloride
<i>A. thaliana</i>	<i>Arabidopsis thaliana</i>	µm	Micrometre
BA	Benzyladenine	µM	Micromolar
bp	base pair	mm	Millimetre
°C	degree Celsius	mM	Millimolar
CAPS	Cleaved Amplified Polymorphic Sequence	min	Minute
CIAP	Calf Intestinal Alkaline Phosphatase	mRNA	<i>messenger</i> RNA
cm	Centimetre	MS medium	Murashige & Skoog medium
Col <i>gl</i>	Columbia <i>glabra</i>	NaOH	Sodium hydroxide
CTAB	cetyltrimethylammonium bromide	nM	nanomolar
d	day	OPA	ortho-phthaldialdehyde
DMSO	Dimethyl sulfoxide	PCR	Polymerase chain reaction
DNA	Desoxyribonucleic acid	PI	Propidium iodide
dNTPs	Deoxynucleoside triphosphates	PPT	Phosphinothricin
DNQX	6,7-dinitroquinoxaline-2,3- dione	PVP	Polyvinylpyrrolidone
DTT	Dithiothreitol	rcf	relative centrifugal force
EDTA acid	Ethylenediamine tetraacetic acid	Rif.	Rifampicin
EMS	Ethyl methanesulfonate	RNA	Ribonucleic acid
EtBr	Ethidium bromide	rpm	revolutions per minute
EtOH	Ethanol	RT	room temperature
FDA	Fluorescein diacetate	s or sec	second
g	Gramme	SD	standard deviation
<i>g</i>	Gravitational acceleration	SDS	Sodium dodecyl sulfate
Gent.	Gentamycin	SSLP	Simple Sequence Length Polymorphism
h	hour	<i>Taq</i>	<i>Thermophilus aquaticus</i>
HCl	Hydrochloric acid	TBE	Tris/Borat/EDTA buffer
HEPES	N-(2-Hydroxyethyl)piperazine -N'-(2-ethanesulfonic acid)	T-DNA	Transfer DNA
l	Litre	TE	Tris EDTA
Ler	Landsberg <i>erecta</i>	THF	Tetrahydrofuran
LD	Long day	Tris	Tris(hydroxymethyl)- aminomethane
Lithium acetate	LiAc	U	enzyme unit
M	molar	v/v	volume / volume
MES	2-(N-morpholino) ethanesulfonic acid	WT	wild type
		w/v	weight / volume
		X-Gluc	5-bromo-4-chloro-3-indolyl-β- D-glucoronide

5 Results

5.1 Studies on root meristem structure and viability in *tup5-1*

The primary root of *tup5-1* undergoes a growth arrest almost immediately after germination at a length of approximately 1,5 mm when exposed to white light (e.g. *in vitro* culture) (Riefler, 2001). The reason for this growth arrest might be the loss of structure in the RAM by differentiation of the meristematic cells (chapter 3.4).

To clarify the mechanisms of light perception in this context, the following questions were addressed: Which organ perceives the root growth-inhibiting light in *tup5-1* (chapter 5.1.1)? And which light signalling pathway is being used for this (chapter 5.1.2)?

Phytohormones - like auxin and cytokinin - play an important role in root growth control. *tup5-1* was found in a screen for the ability of callus formation under culture conditions of reduced phytohormone concentrations (chapter 3.4). Therefore the mutant might have an altered response to these phytohormones. Experiments addressing this question are reported in chapter 5.1.3, A and B.

A reduced mitotic activity in the root might be a reason for the growth arrest. To clarify if divisions take place in the *tup5-1* primary root at all, a cell cycle marker was studied in the *tup5-1* background (chapter 5.1.3, C).

As stated above, the meristem is suspected to lose its embryonic identity in the *tup5-1* root. To track the fate of the QC, a QC marker was analysed in *tup5-1* (chapter 5.1.3, D).

The analysis of marker lines showed a general decrease in GUS activity. To judge whether these were specifically reduced responses or a general loss of viability in the root cells, the state of viability in the root was analysed (chapter 5.1.4, A).

The root meristem loss of *tup5-1* can be avoided by supplementing the seedling with arginine (chapter 5.3.1). Can the meristem which has already undergone the process of differentiation still be rescued by adding arginine at a later stage of development? Which means: Is the process reversible (chapter 5.1.4, B)?

These different aspects are elucidated in the following chapters.

5.1.1 Where is the root growth-inhibiting light perceived in the *tup5-1* mutant?

Previous experiments showed that the root growth inhibition of *tup5-1* seedlings is light-dependent (Frémont, 2004). To find out whether the perception of the inhibiting light takes place in the shoot or in the root, WT and *tup5-1* plants were grown *in vitro* in glass tubes

with selective illumination of different parts of the plants: Illumination of the whole plant, illumination of the shoot but not the root, or the whole plant in the dark. When grown in light *tup5-1* showed a severe root growth defect with a root length of $1,28 \pm 0,25$ mm, whereas WT had a maximum root length of $22,5 \pm 5$ mm (Figure 5-1). When the roots were kept in darkness with the shoot illuminated, the maximum root length of *tup5-1* increased about 11 times ($14,6 \pm 3,45$ mm) compared to light-grown *tup5-1* plants. Nevertheless the *tup5-1* plants growing with the shoots in the light and roots in the dark did not reach the root length of WT under the same conditions ($28,8 \pm 3,8$ mm). This could be due to the imperfect darkening of the root part. A small quantity of light was still penetrating the medium from above.

From these results it can be concluded that the root is the organ which perceives the inhibiting light signal in the *tup5-1* phenotype.

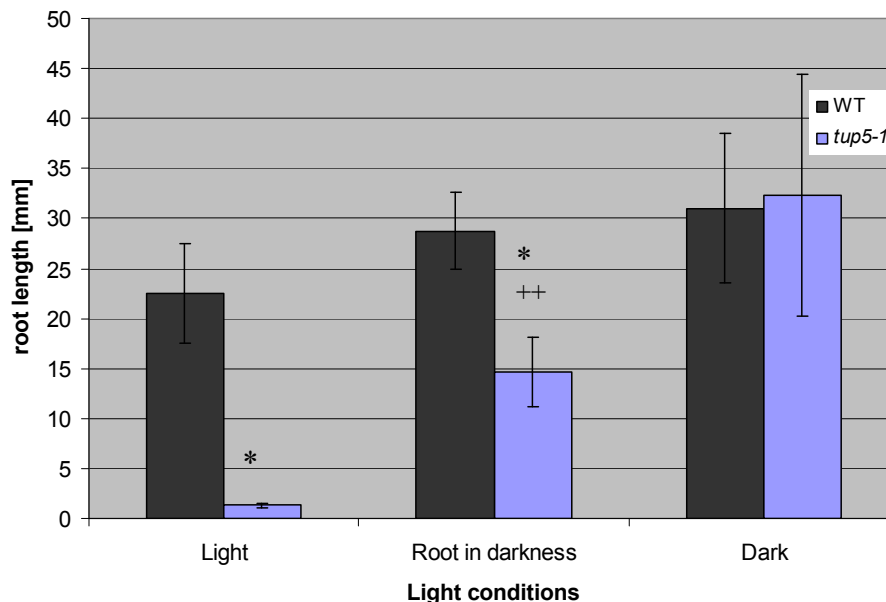


Figure 5-1: Effect of organ specific light application on *tup5-1* root growth.

Root length of WT and *tup5-1* plants: grown in light (left); with shoot in light and root in the dark (middle); grown in the dark (right). All plants were 28 d old and grown *in vitro*. Mean \pm SD of 4 to 7 plants. Significance: * or + $P < 0,01$; ** or ++ $P < 0,001$, Student's *t* test comparing WT and *tup5-1* samples: *; when comparing "light" with "root in darkness" for WT or *tup5-1*, respectively: +.

5.1.2 Light signalling pathway of root growth inhibition

The root growth arrest in *tup5-1* is caused by blue light (Frémont, 2004). To elucidate the light signalling pathway involved in this mechanism, epistasis analyses were performed with *tup5-1* crossed with light signalling mutants. If a double mutant phenotype is found, the signalling pathways of the two genes involved are considered to be independent (no epistasis).

The following light receptor mutants were crossed into *tup5-1*: the phytochrome apoprotein mutants *phyA-201* and *phyB-1(hy3-Bo64)* (phytochrome A and B genes) (Nagatani *et al.*, 1993; Reed *et al.*, 1993; Reed *et al.*, 1994; Rockwell *et al.*, 2006), the phytochrome chromophore biosynthesis mutant *hy2-1* (Kohchi *et al.*, 2001), the cryptochrome apoprotein mutant *cry1 (hy4-1)* and *cry2-1* and *phot1-5 (nph1-5)* (Ahmad and Cashmore, 1993; Hoffman *et al.*, 1996; Lin *et al.*, 1996; Huala *et al.*, 1997). Mutants of light signalling factors were also crossed into *tup5-1*: the negative regulator of phyA signalling *spal*, the bZIP transcription factor mutant *hy5-1*, the E3 ubiquitin ligase mutant *cop1* (COP1 is required for degradation of several transcription factors involved in light-regulated transcription) and *det1* (Deng *et al.*, 1992; Pepper *et al.*, 1994; Oyama *et al.*, 1997; Hoecker *et al.*, 1999).

In this work the analysis of the double mutants was focused on those mutants which have a clear and recessive phenotype in white light. These were *hy2-1*, *hy5-1*, *cry1* and *phyB-1*. In the F₂ generation of *tup5-1* × *hy2-1*, *tup5-1* × *hy5-1*, *tup5-1* × *cry1* and *tup5-1* × *phyB-1* double mutants with short roots were found (see an example in Figure 5-2). In the F₂ generation of the double mutant *tup5-1* × *hy2-1*, as an example, six *tup5-1 hy2-1* double mutants were found in a population of 88 plants. This frequency of 1:14,6 is in accordance with the expected value of 1:15 according to Mendel's Laws. In the case of *tup5-1* × *hy5-1* eight *tup5-1 hy5-1* double mutants were found in a population of 128 plants in the F₂ generation (a frequency of 1:15 as expected).

From these findings it can be deduced that the analysed light receptors or light signalling factors are not epistatic to *tup5-1*.



Figure 5-2: Phenotype of the double mutant *tup5-1* × *hy2-1*.
From left to right: WT, *hy2-1*, *tup5-1* and two *tup5-1 hy2-1* double mutant plants (F₂ generation).

5.1.3 Hormonal status and cell cycle activity according to GUS-markers in the *tup5-1* root meristem

A *Auxin status*

DR5::GUS is an auxin-induced marker gene with a synthetic promoter containing seven repeats of an auxin-responsive element (Sabatini *et al.*, 1999). The blue staining visualises auxin-induced GUS activity in the cell. The pattern of GUS activity in the WT root covers the QC, the columella initials, mature columella root cap cells and the vasculature of the differentiation and elongation zone (Figure 5-3, A). In the root meristem of *tup5-1* the auxin-induced activity was strongly reduced in 5-d-old seedlings (Figure 5-3, B). No activity was visible in the vasculature of the differentiation and elongation zone. In the differentiating meristem the activity was restricted to a few cells and the intensity of blue staining was reduced (Figure 5-3, B). This could be due to a reduction of auxin level or of auxin-induced response in the meristem of the mutant. Another explanation could be a more general loss of viability in the differentiated root meristem of *tup5-1*.

Auxin-induced *DR5::GUS* expression is also found in pericycle cells during the initiation of lateral roots formation in WT (Figure 5-4, A and B) (Benková *et al.*, 2003). This *DR5::GUS* activity was also observed in the short *tup5-1* primary root which had arrested its growth and of which the meristem had undergone major differentiation (Figure 5-4, C).

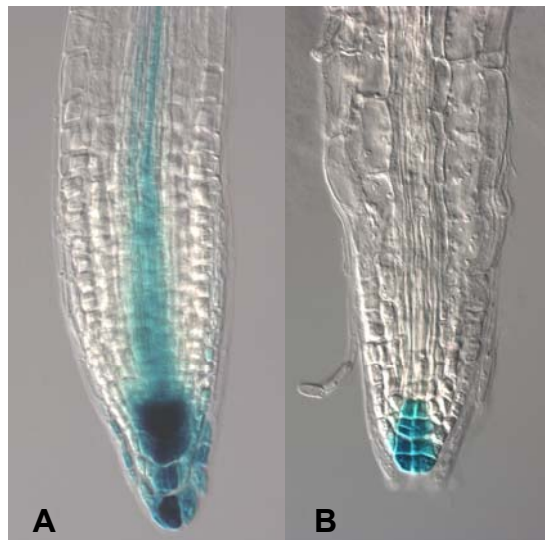


Figure 5-3: Auxin-induced *DR5::GUS* expression in the primary root tip of *Arabidopsis* seedlings. A: WT; B: *tup5-1* (5 d old, *in vitro*) (magnification: 200-fold).

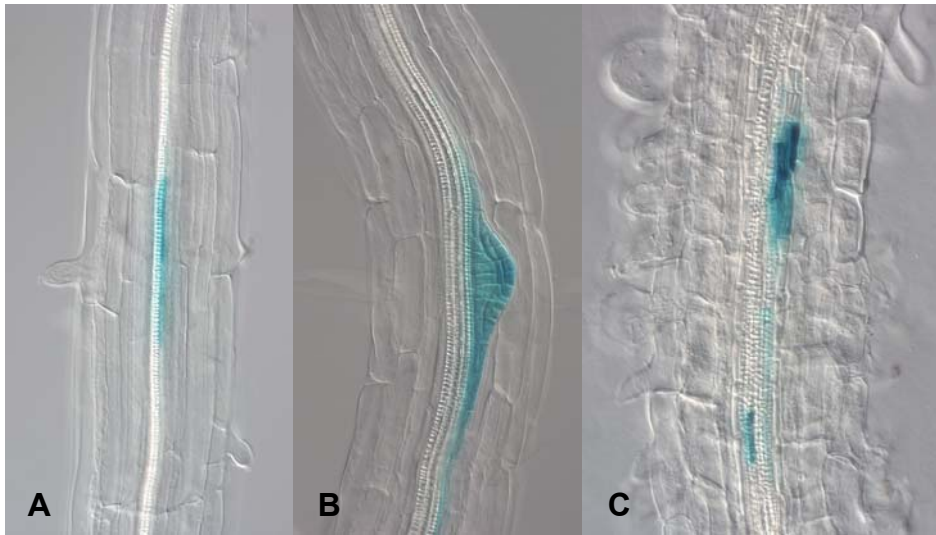


Figure 5-4: Auxin-induced *DR5::GUS* expression in the pericycle of the primary root of *Arabidopsis* seedlings during lateral root formation. A and B: WT; C: *tup5-1* (5 d old, *in vitro*) (magnification: 200-fold).

B Cytokinin status

In the cytokinin sensitive *ARR5::GUS* marker line GUS activity is visible in cells responding to cytokinin (D'Agostino *et al.*, 2000). In WT a strong activity can be observed in the root tip and the vasculature of the root (Figure 5-5, A). In *tup5-1* this response was extremely weak or completely vanished (Figure 5-5, B). In some cases a faint blue staining occurred in a few cells of the columella and in the vasculature of the elongation zone (data not shown). The intensity of GUS seemed to correlate with the differentiation state of the meristem.

Again the question is: Is it a direct effect of a cytokinin response decrease (or a lack of cytokinin), or is it a secondary effect of a loss of cell viability in the root meristem of *tup5-1*?



Figure 5-5: GUS staining with the marker *ARR5::GUS* in the primary root tip of seedlings. A: WT; B: *tup5-1* (5 d old, *in vitro*) (magnification: 200-fold).

C Cell cycle-induced response

The marker FA4C contains the promoter of *CycB1;1* and an N-terminal part of the protein encoding a mitotic destruction box fused to GUS. The destruction box restricts the accumulation of the cyclin (or in this case the GUS protein) to the late G2- and M-phase of the cell cycle (Colón-Carmona *et al.*, 1999). Thus the GUS activity pattern shows recent cell divisions. The latter occur mainly in the “elongation zone” of the RAM (Figure 5-6, A) as defined by Scheres *et al.* (2002) (chapter 3.1.1).

tup5-1 roots grown *in vitro* had a strongly reduced cell cycle depending GUS activity. Only in a few cells a weak signal was visible (Figure 5-6, B). This indicates an arrest of cell cycle activity in the mutant root meristem. These findings would confirm previous results: The differentiating root meristem of *tup5-1* seemed to be constituted of a reduced number of larger cells than WT (Frémont, 2004). The observation of reduced cell cycle-dependent GUS activity seems very likely to be a direct result of the actual cell cycle state in the *tup5-1* RAM. But as a general reduction of GUS activity was observed in all analysed marker lines, it cannot be excluded that this is a secondary effect of a general viability loss.

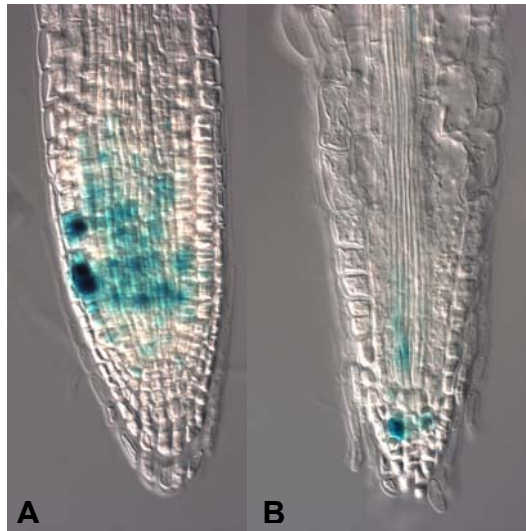


Figure 5-6: Cell cycle-dependent GUS staining with the marker FA4C in the primary root tip of seedlings.

A: WT; B: *tup5-1* (5 d old, *in vitro*) (magnification: 200-fold).

D Quiescent center identity

The QC is composed of four cells in the RAM which do not divide and which keep the surrounding initial cells in an undifferentiated state. Thus the QC is important for the root meristem maintenance (van den Berg *et al.*, 1997). The marker QC25 shows specific GUS activity in the QC cells (Figure 5-7, A). In the *tup5-1* background the signal was weakening in light-grown roots according to the degree of meristem loss. When the meristematic

structure was not completely lost, a light blue colour showed a decreased GUS activity in the QC cells (Figure 5-7, B). The shape of the QC cells was also changed: while the cells were flattened in the WT meristem, they stretched parallel to the root axis in *tup5-1* RAM (Figure 5-7, A and B).

When the loss of meristematic structure had progressed, the GUS activity in the QC of *tup5-1* roots had almost vanished (Figure 5-7, C).

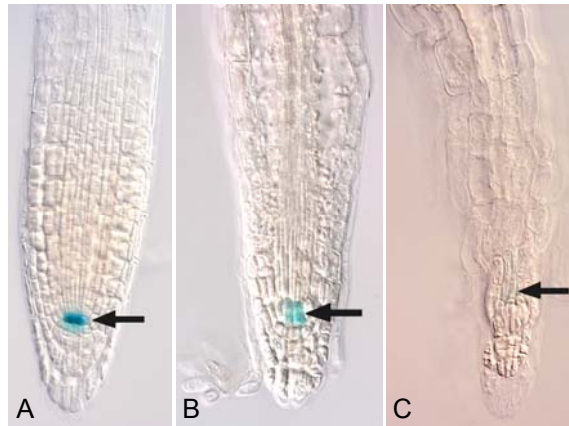


Figure 5-7: GUS activity of the marker QC25 in the QC of the RAM in primary roots. A: WT, B and C: *tup5-1*. Arrows: GUS staining in the QC (5 d old, *in vitro*).

5.1.4 Viability of the root meristem

A Viability

The *tup5-1* root had reduced GUS activity in the above shown marker lines (chapter 5.1.3). To find out whether these are direct effects (e.g. changed hormonal status) or a general viability loss of the RAM cells, a viability test was done. To determine the viability of the RAM cells, the tissue was stained with FDA which gives a fluorescent signal in living cells (shown in green) and PI which accumulates in dying or dead cells (shown in red) (Jones and Senft, 1985). In the WT root a strong green fluorescent FDA signal was observed with the eGFP filter as a sign for metabolic (esterase) activity and viability of the cells (Figure 5-8, B, F and J), whereas only a faint red signal from PI appeared with the red filter (Figure 5-8, C, G and K). In the *tup5-1* root grown under LD conditions the FDA signal was weak (Figure 5-8, B), indicating reduced metabolic activity. The PI signal was slightly stronger in the *tup5-1* root, but the red fluorescence signal was mainly restricted to the cell wall and did not accumulate in the cells, showing that cell membranes are intact (Figure 5-8, C and D) (Jones and Senft, 1985; Moreno *et al.*, 2006). Only in some cases a strong PI accumulation was found in the RAM in *tup5-1*, in cells that might correspond to what had been the quiescent center and the columella cells (Figure 5-8, K and N, root at the right).

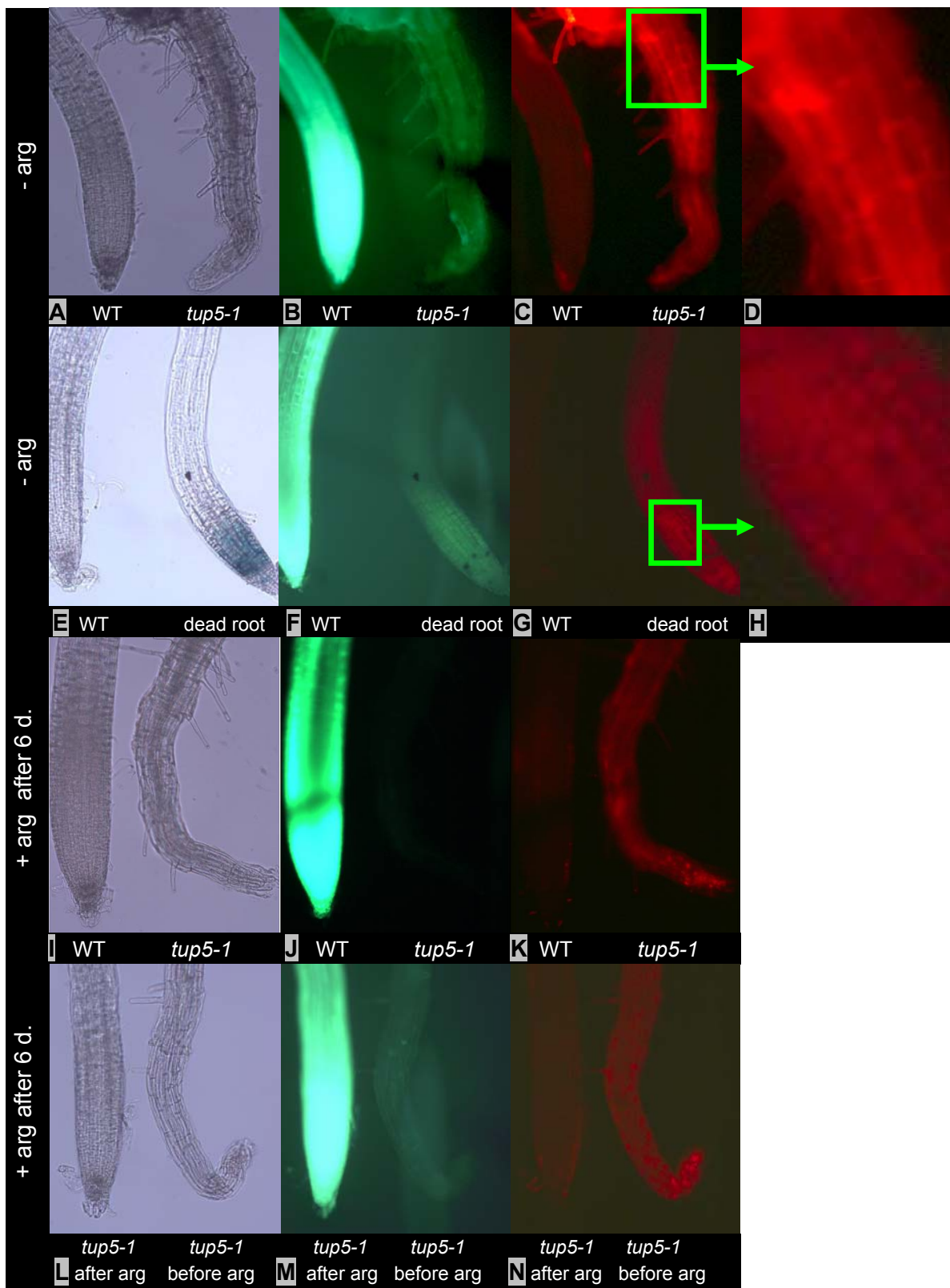


Figure 5-8 : Viability of the RAM in *tup5-1* compared to WT.

A-D: WT (left) and *tup5-1* (right) primary root grown under standard conditions; E-H: “Dead control test” comparing the signal of a fresh WT root (left) and a dead root (of 5-d-old plant cleared according to chapter 4.4.3) (right); I-K: Inability of 6-d-old *tup5-1* primary root meristem grown on MS without arg to become reactivated after transfer to MS +100 μ M arg for 8 d.; L-N: Newly developed *tup5-1* adventitious root formed after transfer to MS + 100 μ M arg (left) had a functional meristem in contrast to *tup5-1* primary root (right) where the meristem differentiated during the 6 d before arg treatment. Left column (A, E, I and L): bright field; central column (B, F, J and M): eGFP filter for FDA signal; right column (C, G, K and N): red filter for PI signal. D and H: Magnified detail of C and G respectively. Seedlings were grown under LD conditions (14 d old).

B Is the process of root meristem loss and root growth arrest reversible?

The mutant root meristem loses its structure and the root arrests its growth (chapter 3.4). This phenotype can be complemented by the addition of arginine (chapter 5.3.1). To find out whether the differentiated meristem can be reactivated, 6-d-old seedlings were transferred to medium containing arginine. After eight days of treatment the primary root development and the meristem structure were assessed. The RAM of these 14-d-old *tup5-1* primary roots treated with arginine could not restructure their meristems and the primary roots did not start growing again (Figure 5-8, I-K). Adventitious roots of *tup5-1* seedlings which developed after the transfer to arginine-supplemented medium had a normal meristematic structure (Figure 5-8, L-N), this would not have been the case without arginine (chapter 5.3.1) (Frémont, 2004, Figure 3.21 and p. 55).

5.2 Identification of the gene *TUP5*

After the description of the *tup5-1* phenotype in Frémont (2004) and in chapter 5.1, the interesting question now was: Which gene is causing this developmental defect?

The state of the gene search from previous works was as follows (Frémont, 2004): First the gene was mapped to an interval of 87,7 kb on the lower arm of chromosome I. Then, 56 T-DNA-insertion lines with insertion loci in 27 of 29 annotated genes in the *tup5-1* interval were screened for corresponding root phenotypes. One candidate gene (*AtZFP1*) which was found to be light-regulated (Chrispeels *et al.*, 2000) was sequenced but no mutation was found.

In this thesis, the gene search was continued as follows: The mapping was continued (chapter 5.2.1). As the mutation lays on a cold spot of recombination (near the telomere), no more recombinants could be found to narrow down the mapping interval of 87,7 kb. For this reason, various parallel approaches were followed: The screen of T-DNA-insertion lines was continued (chapter 5.2.2). Then candidate genes were sequenced (chapter 5.2.3). A complementation assay was done on *tup5-1* with a candidate gene (chapter 5.2.4). This complementation assay being unsuccessful, a pooled complementation with BAC subclones was done (chapter 5.2.5). The gene found in complementing lines of the BAC subclone complementation was sequenced for mutations in the *tup5-1* background (chapter 5.2.6). The complementing gene of the BAC subclone complementation was overexpressed in *tup5-1* as an independent proof of complementation (chapter 5.2.7). The predicted function of the gene is presented in chapter 5.2.8.

5.2.1 Mapping

As stated above, in previous work the mapping interval was narrowed down to 87,7 kb on the lower arm of chromosome I (from 30 353 397 bp to 30 441 123 bp, coordinates according to TAIR in 2004) (Frémont, 2004) (Figure 5-9). The interval contains 29 predicted genes (from At1g80550 to At1g80830) according to the database „TIGR“ (www.tigr.org, 19.12.2003). In this work, 354 more plants of the mapping population were tested. No more recombinants were found for markers laying within the interval borders (data not shown). In total the mapping population contained 2354 plants. At this point, the classical mapping was stopped and the gene search was continued with other methods (see below).

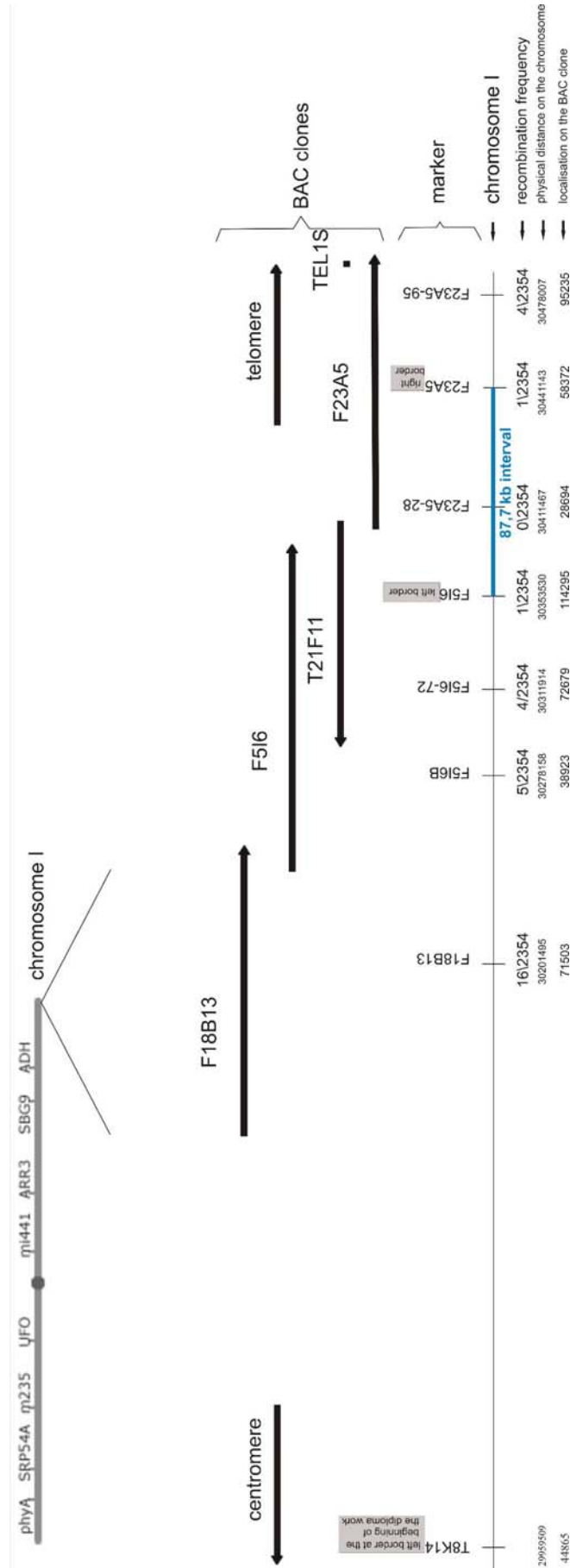


Figure 5-9: Map of the telomeric region at the lower arm of chromosome I indicating the mapping interval of *tup5-1*. Upper left corner: Scheme of chromosome I (modified from www.arabidopsis.org). Below: A magnification of the telomeric region containing the mapping interval of *tup5-1* with the position of BAC clones and the recombination frequency for different mapping markers (modified from Frémont (2004)).

5.2.2 Screening of T-DNA insertion lines for *TUP5* alleles

T-DNA insertions can lead to a knockout of the gene into which they were inserted (Krysan *et al.*, 1999). T-DNA insertion lines for 27 of the 29 predicted genes of the *tup5-1* interval were available to order from Nottingham *Arabidopsis* Stock Center (NASC) or *Arabidopsis* Biological Resource Center (ABRC) (Frémont, 2004) (Alonso *et al.*, 2003).

To identify the mutated gene in *tup5-1* and to find other alleles of the gene, 56 T-DNA insertion lines which had annotated insertions in 27 of 29 predicted genes in the *tup5-1* interval, were screened for root phenotypes in previous works (Frémont, 2004). This strategy was continued in this work: 48 more T-DNA insertion lines were analysed (Supplemental data, Table 9-1). Seedlings were grown *in vitro* and were examined at the age of two to four weeks. The T-DNA insertions were not verified on a molecular level. No root phenotypes were found in these lines. Thus, overall 104 T-DNA insertion lines for these 27 genes were screened for a root phenotype similar to the point mutation line *tup5-1*. However, since *tup5-1* is not a null allele, a T-DNA mutation could result in a different phenotype.

5.2.3 Sequencing of candidate genes

Because the classical mapping and the screening for root phenotypes in T-DNA insertion lines did not lead to any additional results, genes in the mapping interval were sequenced. The candidates were chosen according to criteria as light-dependent or root-specific gene expression. One gene (At1g80730) had been sequenced in previous work (Frémont, 2004). No sequence difference was found in this gene.

In this work 17 additional candidate genes were sequenced in the *tup5-1* mutant (at HU Berlin) and compared to WT (Supplemental data, Table 9-4). Ten genes did not contain any mutation. Sequencing data of four genes contained small gaps, but did not have mutations in the sequenced parts. Two genes had a few ambiguous bases in the sequence data. These were likely to result from technical artefacts. In the gene At1g80820 (cinnamoyl CoA reductase) a mutation was found (a C→T transition) which caused an amino acid exchange (P97S) in the predicted second exon. According to database predictions this mutation leads to a change in the secondary structure of the enzyme (data not shown). The gene is five times upregulated after blue light treatment (according to Genevestigator response viewer (Hruz *et al.*, 2008)). It was therefore considered to be a candidate for the mutated

gene causing the phenotype in *tup5-1*. To test this hypothesis, further analyses were done (chapter 5.2.4).

5.2.4 A false candidate: cinnamoyl CoA reductase

The gene At1g80820 (cinnamoyl CoA reductase) which is involved in lignin synthesis had a mutation changing the amino acid sequence of the enzyme (chapter 5.2.3). It was therefore considered to be a candidate for the *tup5-1* mutation. Thus, further analyses were done to prove this hypothesis: The transgenic line SAIL_207_G05 (N809694) was predicted to carry a T-DNA insertion in the second exon of At1g80820. This was confirmed via PCR (data not shown). The line was studied for aberrant root development.

No differences in root length compared to WT could be found (Figure 5-10, A). However, it could not be excluded that the putative allele of *tup5-1* caused a different phenotype. To find out whether the point mutation found in the cinnamoyl CoA reductase gene in the *tup5-1* background is the origin of the *tup5-1* phenotype, an allelism test was done between the T-DNA insertion line N809694 and *tup5-1*. For this purpose homozygous plants of both lines were crossed reciprocally. It was expected that the F₁ generation would present the *tup5-1* root phenotype if the same gene is affected in both lines (with the T-DNA insertion line being a knockout). The roots of the F₁ plants had a WT phenotype (Figure 5-10, A). There are two possible explanations for this fact: The lines are not allelic or the T-DNA insertion line is not a complete knockout allele. To check whether cinnamoyl CoA reductase transcript can be detected in the T-DNA insertion line, an RT-PCR was done. A low level of transcript was found in the knockout line (Figure 5-10, B). Therefore, a sufficient amount of cinnamoyl CoA reductase enzyme might be produced in the plant to allow a normal development and metabolism. This could explain the WT root phenotype in the F₁ generation of the allelism test. Thus, it could still not be excluded that At1g80820 was the mutated gene causing the phenotype in *tup5-1*. For this reason a complementation test was done. First, the WT gene cinnamoyl CoA reductase was cloned with its own promoter (1989 bp upstream of the gene) into a binary vector and transformed into the *tup5-1* background by the floral dip method (Clough and Bent, 1998). None of the transformants had a WT-like root (data not shown). In case that the native promoter would not be sufficient to restore the WT level of expression (for example because an enhancer element is missing), the cinnamoyl CoA reductase was cloned downstream of a constitutive 35S promoter. The overexpression construct was transformed into a *tup5-1* homozygous line by the floral dip

method (Clough and Bent, 1998) and by hypocotyl transformation (Inoue *et al.*, 2001; Akama and Beier, 2003). This overexpression gene construct did also not complement *tup5-1* (data not shown).

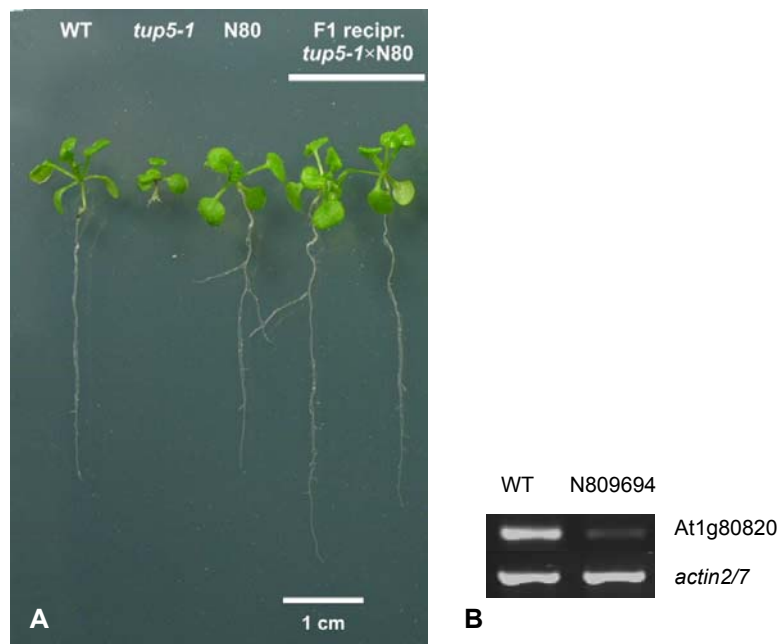


Figure 5-10: Allelism test and transcript level analysis of the T-DNA-insertion allele of cinnamoyl CoA reductase.

A: Allelism test between *tup5-1* and the T-DNA-insertion line of cinnamoyl CoA reductase “N80” (N809694). B: Semi-quantitative RT-PCR of the cinnamoyl CoA reductase transcript in WT and the T-DNA-insertion line (N809694) (duplex PCR with *actin2/7* as control).

5.2.5 Pooled complementation with BAC subclones

The complementation assay with the candidate gene cinnamoyl CoA reductase did not restore a WT root phenotype in *tup5-1* (chapter 5.2.4). Therefore the gene search had to be continued. This was done with the following strategy. The smallest *tup5-1* mapping interval of 87,7 kb is covered by two BAC clones: T21F11 and F23A5 (Figure 5-9). To be sure that the sought-after gene would not be excluded because of a single false positive recombination result, the interval was extended to 138 kb, where two independent recombination events had been found at each mapping border. The BAC clones were fragmented with appropriate restriction enzymes to produce overlapping pieces containing a few genes at a time, if possible covering the whole mapping interval (Table 5-1 and Table 5-2). The presence of the genes was verified by PCR and restriction analysis. Because of the laborious nature of this strategy, the BAC subcloning work was divided: The T21F11 subcloning was performed by Andrea Arbeiter. The resulting fragments were cloned into a binary vector (pCB302) and transformed into *tup5-1* homozygous plants by the floral dip method (Clough and Bent, 1998; Xiang *et al.*, 1999). The transformants containing the subclones

5. RESULTS

were screened for restored root growth *in vitro*. Three subclone lines from BAC T21F11, i.e. Sfo4, Drd71 and Eco1.2, complemented *tup5-1* (Sfo4 and Drd71 transformants shown in Figure 5-11). Sfo4 contains only one full length gene: At1g80600, a predicted acetylornithine aminotransferase. This gene is also present in Drd71 and Eco1.2 (Figure 5-12). The gene is also present in Spe1.21, but the root phenotype was not complemented in the transformants. The promoter might be too short (Table 5-3).

Table 5-1: Subclones of the BAC clone T21F11.

Lavender: subclones used for complementation of *tup5-1*. **F:** The gene was present in full length in the clone, **I:** The gene was incomplete in the clone ("incomplete" also comprises genes of which 2000 bp promoter or 500 bp 3' untranslated region are incomplete, but the coding sequence is in full length). **S:** Gene was sequenced / **PS.:** Gene was partly sequenced (see 5.2.3). The 3 letters in the clone name indicate the restriction enzyme used for fragmenting the BAC clone. Blue marked gene: *TUP5*.

Gene number →	small interval (87,7 kb)											extended interval			
	At1g80650	At1g80640	At1g80630	At1g80620	At1g80610	At1g80600	At1g80590	At1g80580	At1g80570	At1g80560	At1g80550	At1g80540	At1g80530	At1g80520	At1g80510
Clone name ↓															
Sequencing state →	PS	S	S				S	S	S		PS				
Pst1.64	F	F	F	F	I										
Pst2.11								F							
Pst3.4								I							
Pst2.12											I				
Pst1.56													F	F	I
Sac2.1							I	F							
Spe1.24	F														
Spe1.21						I	F	F	F						
Spe3.6											I	I			
Spe2.15														F	F
Sfo59	F	F	F	I											
Sfo4						F									
Sfo3							I	F							
Drd71				I	F	F									
Eco1.16	I	F	F												
Eco1.2					I	F	F	F							
Eco2.4										I					
Eco3.10											I				
Eco2.16														F	I

5. RESULTS



Figure 5-11: Phenotype of complemented primary transformants of *tup5-1*, transformed with the subclones Sfo4 and Drd71. From left to right: WT, *tup5-1*, PPT-resistant control line (PRC) (14-d-old plants); T₀ of *tup5-1* transformed with Sfo4, T₀ of *tup5-1* with Drd71 (24-d-old plants) (*in vitro*, transgenic plants on medium containing PPT, non-transgenic plants on medium without PPT).

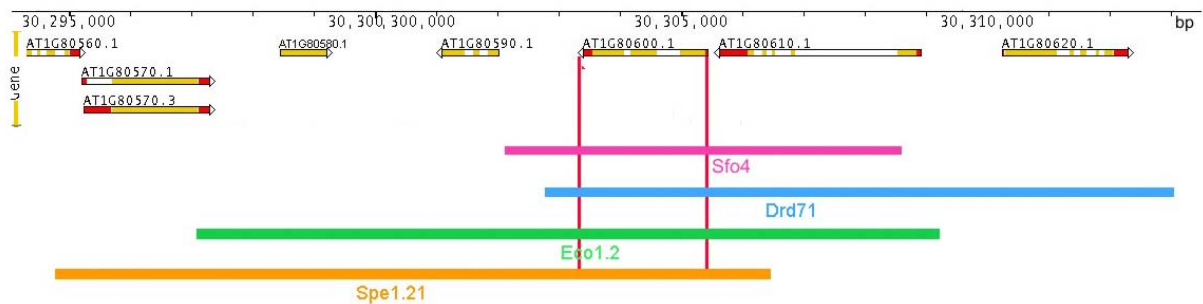


Figure 5-12: Overlapping BAC subclones within the *tup5-1* mapping interval containing At1g80600. The BAC subclones Sfo4, Drd71, Eco1.2 and Spe1.21, all containing At1g80600, are shown as pink, blue, green and orange boxes. Arrows: ORFs (colour code within the arrows: red for UTRs, yellow for exon, white for introns), with their ATG number above. Black line: chromosome I with physical coordinates (bp) (modified from TAIR).

Table 5-3: Coordinates of complementing BAC subclones and phenotype of primary transformants. The coordinates were calculated from restriction enzyme cutting site predictions, in the case of Drd71 the borders do not correspond to cutting sites, the length is given approximately based on PCR and restriction analysis.

Complementing clone	Length of 5' region	Length of 3' region	Number of transformants	Number of transformants with short roots	Number of transformants with long roots
Sfo4	3091bp	1251 bp	24	0	24
Drd71	> 6,8 kb	1178 bp	16	3	13
Eco1.2	3648 bp	6748 bp	1	0	1
Spe1.21	1228 bp	8884 bp	6	6	0

5.2.6 The *tup5-1* mutation is located in At1g80600, a putative acetylornithine aminotransferase gene

The BAC subclone Sfo4, which complemented the root phenotype of the mutant contained only one complete predicted gene (At1g80600) (Figure 5-12). It was therefore very likely that this gene is mutated in *tup5-1*. To prove this, the gene was sequenced in the *tup5-1* background. A mutation was found in the third exon (base n° 1735 of the unspliced sequence: a transition from G to A) (Figure 9-1 in supplemental data). This base exchange leads to an alteration in amino acid sequence (G424R) (Figure 5-13). According to the secondary structure prediction tool APSSP2 (Raghava, 2002) a slight shift in secondary structure might be caused by the mutation in *tup5-1*, but this was not confirmed by the prediction programme PSIPRED 3.0 (Jones, 1999). Nevertheless, it might be possible that the predictions were not accurate and that unpredicted structural changes are produced in *tup5-1* protein. It is also possible that the tertiary structure is altered due to the mutation, causing changes in regulatory or catalytic properties of the protein.

```

TUP5-WT      MASLSQITLPRAPSSEIGLLRRRLERPIIRTRIGFNGRIASVLTNAGDQAVSVKASVSQK 60
tup5-1-mut  MASLSQITLPRAPSSEIGLLRRRLERPIIRTRIGFNGRIASVLTNAGDQAVSVKASVSQK 60
*****

TUP5-WT      VIEEEAKVIVGTYARAPVVLSSGKGCKLFDPEGKEYLDCASGIAVNALGHGDPDWLRAVT 120
tup5-1-mut  VIEEEAKVIVGTYARAPVVLSSGKGCKLFDPEGKEYLDCASGIAVNALGHGDPDWLRAVT 120
*****

TUP5-WT      EQAGVLAHVSNVYYTIPQIELAKRLVASSFADRVFFCNSGTEANEAAIKFSRKFQRFTHP 180
tup5-1-mut  EQAGVLAHVSNVYYTIPQIELAKRLVASSFADRVFFCNSGTEANEAAIKFSRKFQRFTHP 180
*****

TUP5-WT      EDKEVATGFIAFTNSFHGRTL GALALTSKEQYRTPFEPIMPGVTFLEYGNIQAATDLIRS 240
tup5-1-mut  EDKEVATGFIAFTNSFHGRTL GALALTSKEQYRTPFEPIMPGVTFLEYGNIQAATDLIRS 240
*****

TUP5-WT      GKIAAVFVEPIQEGGGIYSATKEFLQSLRSACDAAGSLLVDFDEVQCGLGRTGLMWAYEAF 300
tup5-1-mut  GKIAAVFVEPIQEGGGIYSATKEFLQSLRSACDAAGSLLVDFDEVQCGLGRTGLMWAYEAF 300
*****

TUP5-WT      GVTPDIMTVAKPLAGGLPIGAVLVTEKVAETINYGDHGSTFAGSPLVCSAAIAVMDKVSK 360
tup5-1-mut  GVTPDIMTVAKPLAGGLPIGAVLVTEKVAETINYGDHGSTFAGSPLVCSAAIAVMDKVSK 360
*****

TUP5-WT      PSFLSSVSNKGRYFRDLLVKKLGGNSHVKEVRGEGLIIGVELDVPASSLVDACRDSGLLI 420
tup5-1-mut  PSFLSSVSNKGRYFRDLLVKKLGGNSHVKEVRGEGLIIGVELDVPASSLVDACRDSGLLI 420
*****

TUP5-WT      LTAGKGNVVRIVPPLVISEEEIERAVEIMSQNLTALD- 457
tup5-1-mut  LTA█KGNVVRIVPPLVISEEEIERAVEIMSQNLTALD- 457
***

```

Figure 5-13: Amino acid alignment of *tup5-1* (*tup5-1-mut*) and the wild-type sequence TUP5 (TUP5-WT).

The amino acid exchange in *tup5-1* (of the amino acid number 424) is marked in red. The analysis was carried out with Clustal W.

5.2.7 Complementation of the mutant with the overexpressed At1g80600

The subclone Sfo4, which complemented *tup5-1*, contains 6,3 kb of plant DNA insert (Table 5-3). According to database predictions this sequence contains only one putative ORF (At1g80600). To prove that this ORF is the complementing element in Sfo4, an over-expression construct of At1g80600 was used for an additional complementation assay. For this purpose the cDNA of At1g80600 (provided in the clone U15579 by the Arabidopsis Biological Resource Center) was cloned downstream of the constitutive CaMV 35S promoter (Figure 5-14, A). The transgene was transformed into *tup5-1* homozygous plants by the floral dip method (Clough and Bent, 1998). The *tup5-1* root phenotype was complemented with this construct because T₀ plants formed a long root in light (Figure 5-14, B). Additionally, this result shows that the cDNA sequence of the clone U15579 is functional and the predicted splicing sites are correct (Figure 5-37 and Figure 9-1 in supplemental data).

The transcript level of *TUP5* was tested by semi-quantitative RT-PCRs in the *35S::TUP5* lines. The RT-PCRs were set up as duplex PCRs with two primer pairs: The primer for *TUP5* and those for *actin2/7* as internal control (Figure 5-15, A). The transcript quantity of *TUP5* was increased in all transgenic lines compared to WT and *tup5-1* (Figure 5-15, A). More independent lines and *35S::TUP5* lines in *tup5-1* background were tested, all showing an increase in *TUP5* transcript level (data not shown). The quantity of actin PCR product was reduced in the transgenic lines, probably due to the strong competition for nucleotides with the At1g80600 amplification reaction (Figure 5-15, A). The *35S::TUP5* lines were used for further phenotypical analyses (chapter 5.8.1 to 5.8.3). Additionally, real-time PCR was done with one overexpressing line to verify the increased expression level with an independent method. An approximately 4,65-fold increase of *TUP5* expression was measured in the homozygous transgenic line OE4 compared to WT (Figure 5-15, B).

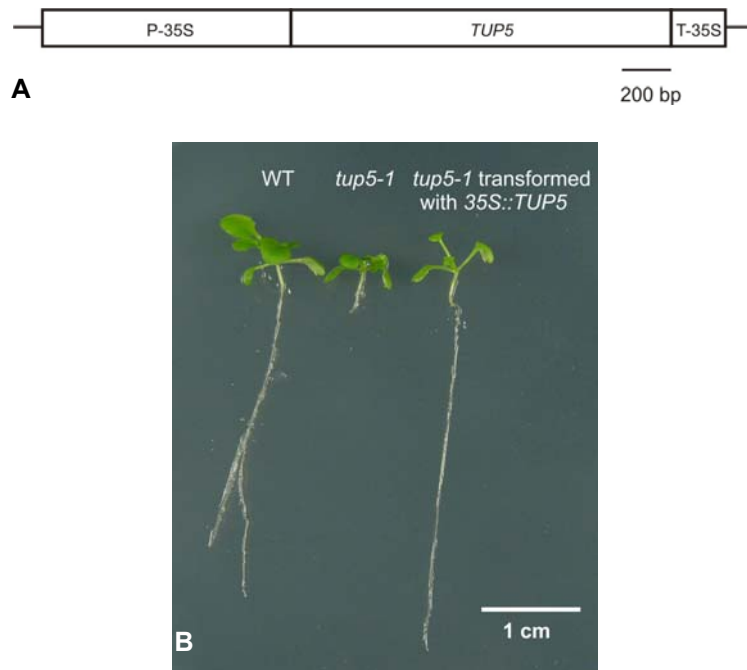


Figure 5-14: Complementation of *tup5-1* with 35S::TUP5.

A: Vector construct used for the overexpression of At1g80600. The cDNA of At1g80600 was cloned between the 35S promoter (P-35S) and the 35S transcriptional terminator sequence (T-35S) in the vector pB2GW7 (Karimi *et al.*, 2005). **B:** Root phenotype of a complementing primary trans-formant of *p35S::TUP5* in the *tup5-1* background (15 d old, *in vitro*). From left to right: WT; *tup5-1*; T₀ of *p35S::TUP5* in *tup5-1* back-ground.

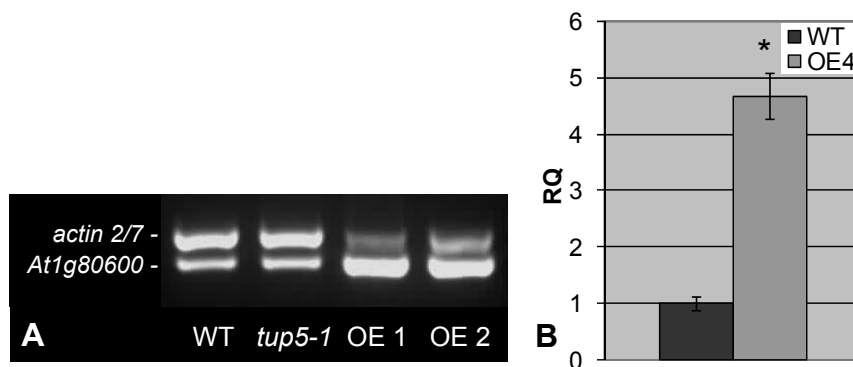


Figure 5-15: *TUP5* transcript level of *TUP5* overexpressing lines.

A: The transcript level of WT, *tup5-1* and two 35S::TUP5 lines tested by semi-quantitative RT-PCR. The primers of the control gene *actin 2/7* (At5g09810) and *TUP5* were used in a duplex PCR. OE1 and 2 are independent overexpression lines of *TUP5* (T₁ generation) in WT background. The reactions were done with the Qiagen One Step RT-PCR Kit. **B:** Real-time PCR of WT and a 35S::TUP5 line. WT: Wild type; OE4: homozygous *TUP5* overexpression line (T₃ generation). RQ: relative quantity. WT was set 1. In each case one biological sample was used for three PCR reactions originating from one master mix. The real-time PCR was performed with Applied Biosystems 7500FAST. Plants (48 d old) were grown on soil at standard conditions. Error bars: minimal and maximal RQ. n = 3. Significance: * P < 0,01, Student's *t* test comparing WT and OE4.

5.2.8 Structure and predicted function of TUP5

The gene At1g80600 is predicted to code for an acetylornithine aminotransferase (ACOAT) (EC 2.6.1.11.) (by the databases TAIR: www.arabidopsis.org and MIPS: <http://mips.gsf.de>). The function of this enzyme has been studied for its homologues in bacteria, yeast and some plant species (Vogel, 1953; Dougall and Fulton, 1967; Jauniaux *et al.*, 1978). The protein is predicted to have a molecular weight of 48,8 kDa and a length of 457 amino acids (by the database TAIR: www.arabidopsis.org). The programme TargetP predicts a chloroplastic transit peptide with a score of 0,716, while 1 is the highest score. This is in accordance with biochemical experiments on soybean protoplasts where acetylornithine aminotransferase activity was mainly found in the plastid fraction (Jain *et al.*, 1987). The enzyme catalyses the transfer of an amino group from L-glutamate to acetyl-L-glutamate 5-semialdehyde yielding α -ketoglutarate and acetylornithine (www.expasy.org/enzyme/2.6.1.11) (Figure 5-16), using pyridoxal 5-phosphate as a cofactor (Vogel, 1953; Albrecht and Vogel, 1964). This reaction can be catalysed in both directions. The synthesis of acetylornithine is the fourth step (from glutamate) in *de novo* arginine biosynthesis (Slocum, 2005) (Figure 5-17, A). Arginine and its precursors citrulline and ornithine are also used for the biosynthesis of other important metabolic compounds like polyamines for example (Figure 5-17, B) (see KEGG database (Kanehisa *et al.*, 2008)).

Genes having high similarities to TUP5 on the amino acid level can be found in bacteria, fungi and plants (Figure 5-18). Highly similar amino acid sequences of *Populus trichocarpa* (dicots), *Oryza sativa* (monocots), *Physcomitrella patens* (mosses), *Chlamydomonas reinhardtii* (algae), *Saccharomyces cerevisiae* (fungi) and *Escherichia coli* (bacteria) were aligned with TUP5 (Figure 5-18). The genes of *C. reinhardtii*, *S. cerevisiae* and *E. coli* used in this alignment were already confirmed acetylornithine aminotransferases (Heimberg *et al.*, 1990; Remacle *et al.*, 2009). The amino acid mutated in *tup5-1* (G424) was conserved in all seven organisms. This residue might therefore have an important function in the protein TUP5, though up to now no reaction site or protein domain has been predicted for this amino acid (Prosite, data not shown). The phylogenetic relationship of the seven aligned proteins corresponds to the relationship between the source organisms: TUP5 is closely related to the *Populus trichocarpa* protein and farthest related to the bacterial and fungal ACOAT (Figure 5-19).

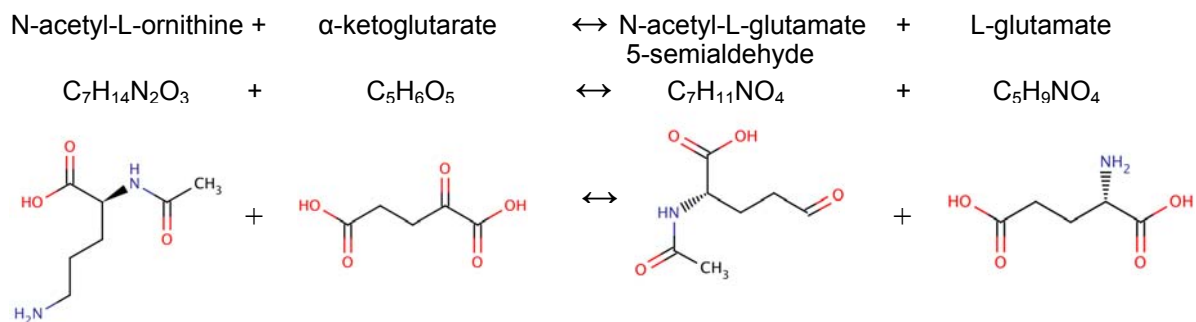


Figure 5-16: Chemical reaction catalysed by ACOAT.

First line: name of the chemical compounds, second line: text formula, third line: skeletal formula. Red: OH-residues, blue: NH₂-residues (from AraCyc: <http://www.plantcyc.org> and Human Metabolome Database: www.hmdb.ca).

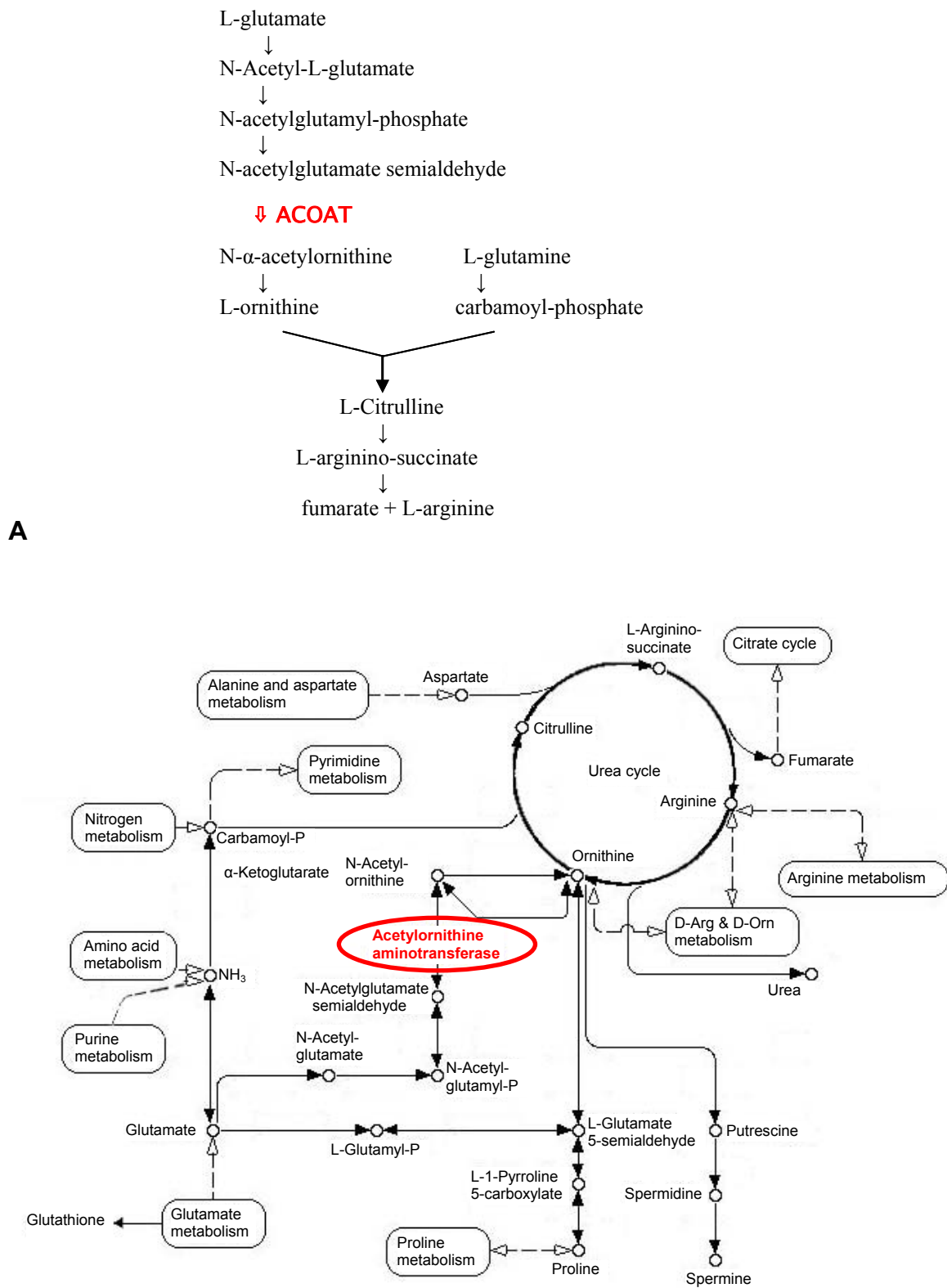


Figure 5-17: Acetylornithine aminotransferase reaction step within arginine biosynthesis. A: Arginine biosynthesis pathway. The red arrow indicates the reaction step of ACOAT (modified from AraCyc: <http://www.plantcyc.org>, date: 02.2009). B: Overview of the urea cycle. The reaction of ACOAT (in red characters) is circled in red (modified from KEGG: [http://www.genome.jp/kegg/pathway/ map](http://www.genome.jp/kegg/pathway/map), date: 05.2006).

5. RESULTS

At1g80600	1	-----MASLSQITLPRAPSSEIQLRRRLER-PIIRTRIGF
Pt	1	-----MGSLQHFLNSPISVPPFSP-NLNHRRSFF
Os05g0129100	1	-----MNSLQSFALNPPAAAAALGGARLRPSRVTA-CLATPPTP
Pp	1	MAAHNQASNLTFGCVAALQVVKARDASARRVKMAAVESGLAGVQLTKVRPGADVLRKRAKR
Cr	1	-----MAQLQQHQGRAAAAQPKRARQLAVAPRAALT
Sc	1	-----
Ec	1	-----
At1g80600	36	NGRIASVLTNAGDQAVSVKASVQKVL EE EAKVIVGTYARAP-VVLSSGKGGCKLFD-PBG
Pt	28	LRACLNLVDVHAPDSVKPKTHLKSREVEMEGKVLVGTYARNP-VV IS SGKGGCKLYD-PBG
Os05g0129100	41	PPPTSAPLAPAAAAARRELSAASRAVVEDEARYIVGTYNRSR-VVLVAGRGCKLYD-ADG
Pp	61	KSVVFQAVFTSEPEVNANDISQEIIGAESQYFVQTYARSP-VV FV SGKGGCKLYD-VEG
Cr	32	FNPASLFKGLTSSKPTPKDAAFKQVLADESKYVLOTYGRAP-VVISHGKGGAKMWD-VEG
Sc	1	-----MFKRYLSSTSSRRFTSLLEEKAFQVTTYSRPEDLCITRGNKAKLYDDVNG
Ec	1	-----MAIEQVLAITRATFDEVILPIYAPAE-FIPVKGGSR I WD-QQG
At1g80600	94	KEYLDCASGIAVNALGHGDDPDLRAVTEQAGVLAHVSNNVYITPEQTE L LAKRLVASS----
Pt	86	REYLDCTSGIAVNALGHGDDPDKAVVBOANL L LTHVSNVYFYSVPEQVELARRLVACS----
Os05g0129100	99	REYLDMAAGIAVNALGHADPDWVAVASQAQATLVHASNVQYITPEQVALAKRLVEAS----
Pp	119	NEYLDMTAGIAVNALGHGDDPTWVKAVTEQAGKLAHVS N L F HTVPEQVLAERLVRSS----
Cr	90	KEYIDMAAGIAVNALGHSDSQWYAALVEQAEKLAHTSNLYHTPEQVELAKRLVENS----
Sc	51	KEYIDFTAGIAVNALGHANPKVAEILHHQANKL L HSSNLYFTKECLDSEKIV E KTKQFG
Ec	42	KEYVDFAGGIAVNALGHCHPALVNALKTQGETLWHISNVFTNBEALRL C RKLEAT----
At1g80600	150	---FADRVFFCNSTGTEANEAALKFSR K QRFTHP-----EDKEVATGTEAFTNSFHGRTL
Pt	142	---FADRVFFTNSGTEANEAALKFARK M QRFTNP-----DEKQVTEFTSFSNSFHGRTM
Os05g0129100	155	---FADRVFFANTGTEANEAALKFARK F QRVARP-----DG-DAPTEFMSFTNGFHGRTM
Pp	175	---FADRVFMVNSTGTEANEAALKFARKM H YALAKSN--GDTAQGATELVAFTNGFHGRTL
Cr	146	---FADRAFFCNTGTEANEAALKFARK M ARVRAGIDPYDGGAVAPYELV S FTSCFHGRTM
Sc	111	QOHDASRVFLCNSGTEANEAALKFARK H GGIMKNP-----SKQGI V AFENSFHGRTM
Ec	98	---FAERVVFMNSGTEANETA F KLARH M ACVRHS-----PFKTKL L AFHNAFHGRSL
At1g80600	202	GALALTSKEQYRTPFEP L MPGVTFLEYGNIQ A ATDLIRSGK---IAAVFVPEP V QEGGGIY
Pt	194	GALALTSKEQYRTPFEP V MMPGVNFLEYGDVQAATEL L KSGR---IAAVFVPEP V QEGGGIY
Os05g0129100	206	GSLALTSKVQYREPFAPVMPGATFAEYGNLEEAKKVIQSGK---IAAVFVPEP V QEGGGIH
Pp	230	GALSLTSKIQYRTPFEP L VP P GSFVNF G DLEATREIVAG-K---TAAV F VPEP V QEGGGIC
Cr	203	GALALTYKEQYKTPFYPMMPGHQLAEYNNLESAAAVIKKGG---TAAV F VPEP V QEGGGVT
Sc	162	GALSVTWNSKYRTPFGDLVPHVSFLNLDNEMTKLQSYIETKKDEIAGL L IVPEP V QEGGGVF
Ec	147	FTWSVGGQPKYSDGFG P KPADIIHVP E NDLH A VKAVMD-DH---TC A VVPEP V QEGGGVT
At1g80600	259	SATKEFLQSLRSACDAAGSLLV F DEVQCG L GRGTGLMWAYEAYG--VTPD I MTLAKPLAGG
Pt	251	SATKEFLQSLRSACDDAGSLLV F DEVQCG L GRGTGYLWAYEAYG--VVPD I MTLAKPLAGG
Os05g0129100	263	SATKEFLQGLRDACDEAGALLV F DEVQCG L GRGTGYLWAYEAYG--VLPD I MTLAKPLAGG
Pp	286	PATASFRLRLRELCD E TGTL L V F DEIQCG L GRGTGLWAYHETVD--VRPD I MTLAKPLAGG
Cr	260	PSTQAF L KGLRQLCDEAGALLV F DEVQCG L GRGTGLWCHQLFG--VEPD M MTLAKPLAGG
Sc	222	PVEVEK L TGLKIKCQ N NDVIV H DEIQCG L GRSGK L WAYAYLPSEAH P DIFTSAKALCNG
Ec	203	AATPEFLQGLRELCDQHQALLV F DEVQCG M GRGTGLFAMHYG--VTPD I LTSAKALGGG
At1g80600	317	LPICAVLMT E KVAETIN Y CDHGSTFAGSPLVCSAAIAVMDK V SKP S FLSSVSNKGRYFRD
Pt	309	LPIGAALVSEKVA A AIKYGDHGSTFAGSPLV C NAIAVLDK I SKPGFLASVSEKQYFK
Os05g0129100	321	LPIGVVLMT E KVASAINFGDHGSTFAGSPLV C QAALTTLDK I QKPGFLAEVAKGENFKQ
Pp	344	LPICAVLMTDRVASSIAAGDHGSTFAGSPLV C HAALAVLDRIQAPGFLE S VAEK G AYLKS
Cr	318	LPIGTVLLKQHVADVMKPGDHGSTFAGNPLV C HVACSVFDIINSEAF L AAVEAKGERLRA
Sc	282	FPIAATLVN E KVN N ALRVGDHGSTTYG N PLACSVSNYVLD T LAD E T V LQVSKKSDI L QK
Ec	261	FPIISAM L TTAETIASAFH G SGHSTYGCNPLACAVAGA A FDIINTE V EL E GIQAKRQRFVD
At1g80600	377	LVVKKLGGNS-HVKEV R GEGLIIGV E LDVPAS----SLV D ACR E SGLLIITAGKGNV V RI
Pt	369	LIHKLGGNS-HVREVRGLGLIIGV E LDVSAS----PLV D ACR E SSLLIITAGKGNV V RL
Os05g0129100	381	LVSTKLSGNA-HVKEIRGIIGLV G IELDVPAG----PLV D ACR E LRGVIVLITAGKGNV V RL
Pp	404	QINERLKGNS-HVKEV R GEGLLVG I QLDVPAS----PLV A SALKEKLLIITAGKGDV V RL
Cr	378	GRRTMAGNP-HVQEV R GVGLLVGV Q LDMMAG----PVV D AAR E MGV M ITAGKGDV V RL
Sc	342	RREIQAKYPNQK T TRGKGLIGAEFVEPPT----EVIK K ARELGLLITAGK S -TVRF
Ec	321	HLQKIDQQYD-VFSDIRGMGLLIGAE L KPQYKGRARDFIYAGAEAGV M VLNAC - PDV M RF
At1g80600	432	VPPLVISEEIERAVEIMSQNLTALD----
Pt	424	VPPLIITSEQELERAAEIIIECLPALDKTS-
Os05g0129100	436	VPPLIITSEKELQAAEVIRDCPALDASTS
Pp	459	APPLIITSKQEI D QAVDILVKCMPSLK----
Cr	433	VPPLVITDAEIDTACEVLAAALNKVAPK--
Sc	397	VPALTI E DELIEGMDAFEKALEAVYA---
Ec	379	APSLVVEDADIDEGMQRFAHAAKVVGA--

Figure 5-18: Amino acid sequence alignment of TUP5 with ACOAT from other organisms or highly similar protein sequences with yet unknown function.

Identical AAs are marked in black. The aminotransferases class-III pyridoxal-phosphate attachment site is marked with a blue line above the AAs. Red: AA mutated in *tup5-1* conserved in all 7 aligned organisms. At1g80600, *Arabidopsis thaliana* TUP5; Pt, *Populus trichocarpa* unknown gene ABK95025.1. Os05g0129100: *Oryza sativa* (japonica cultivar-group) GI:115461885, putative ACOAT; Pp, *Physcomitrella patens subsp. patens* GI:162664563 predicted protein ACOAT family; Cr, *Chlamydomonas reinhardtii* ACOAT GI:159480034; Sc, *Saccharomyces cerevisiae* ACOAT GI:151945496; Ec, *Escherichia coli* ACOAT GI:242378886. The analysis was carried out with Clustal W (1.83) and Boxshade (Larkin *et al.*, 2007).

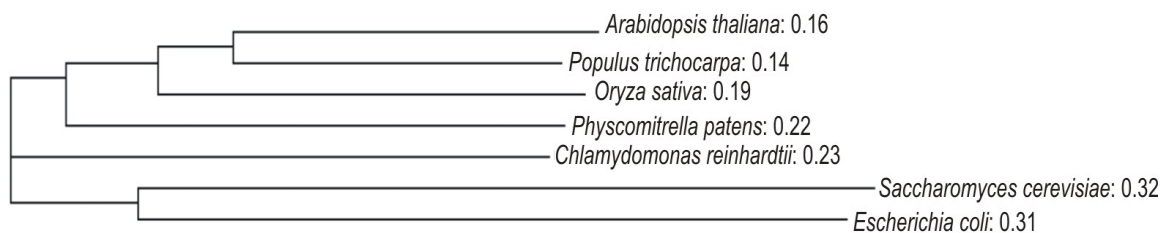


Figure 5-19: Phylogram of ACOAT from different organisms or highly similar protein sequences with yet unknown function.

The abbreviations are identical to those in Figure 5-18. The genetic distances are indicated beside the organism names. The analysis was carried out with ClustalW2 (Larkin *et al.*, 2007).

5.3 Proof of the predicted function of TUP5

Acetylornithine aminotransferase (EC 2.6.1.11.) has been studied in *E. coli*, *S. cerevisiae* and some plant species (Vogel, 1953; Dougall and Fulton, 1967; Jauniaux *et al.*, 1978). For *Arabidopsis thaliana*, only database predictions were available. If this gene is necessary for the synthesis of acetylornithine, feeding *tup5-1* with this presumably lacking amino acid or its downstream product arginine is expected to complement the root phenotype (chapter 5.3.1). This complementation would give strong support for the correctness of the prediction. A final proof of the gene function can be obtained by heterologous complementation of a yeast mutant lacking the homologous acetylornithine aminotransferase gene (chapter 5.3.2). Protocols for an enzymatic assay with *Arabidopsis* ACOAT are lacking. An enzymatic activity assay was tested with different methods modified from Hervieu *et al.* (1993) and Kim *et al.* (1994), but failed (data not shown).

5.3.1 Supplementation of *tup5-1* with different amino acids

The putative acetylornithine aminotransferase (At1g80600) is predicted to be involved in the production of acetylornithine, which is necessary for arginine synthesis (Figure 5-17, A). Due to the mutation, *tup5-1* should not be able to synthesize the amino acids which are produced downstream of the ACOAT enzymatic reaction. These amino acids are: N- α -acetylornithine, L-ornithine, L-citrulline and L-arginine (Figure 5-17, A) (chapter 3.3.3, B and Figure 5-17) (Slocum, 2005). Therefore, if the prediction is correct, supplementation of the mutant with these amino acids should complement the root phenotype. Figure 5-20 to Figure 5-22 show that this is indeed the case: At a concentration of 10 mM acetylornithine in the medium the root length of *tup5-1* nearly reached WT length (Figure 5-20). In the

case of arginine the optimal concentration for complementation was between 100 μ M and 1mM (data not shown). At 1 mM arginine the concentration was slightly toxic for *Arabidopsis* seedlings, but the root development of *tup5-1* was comparable to WT (Figure 5-21). Ornithine and citrulline also complemented the *tup5-1* root phenotype. This seems coherent, because these amino acids are downstream of acetylornithine in the metabolic pathway of arginine synthesis (chapter 3.3.3, B).

A number of other metabolites linked to the arginine synthesis pathway were tested for their effect on *tup5-1* root development (Figure 5-22). Concentration ranged from 1 mM to 10 mM, except for DNQX (6,7-dinitroquinoxaline-2,3-dione) which was tested at a concentration of 0,4 mM. Some of these metabolites have known functions in plant growth regulation: Polyamines (putrescine, spermidine, spermine) are synthesised from arginine and play a role in diverse developmental processes, including root growth (Kaur-Sawhney *et al.*, 2003). Glutamate, which is supposed to have a function in root development (Walch-Liu *et al.*, 2006), is involved in the enzymatic reaction of ACOAT (chapter 5.2.8 and Figure 5-16). The effect of glutamate on *tup5-1* was tested because it was hypothesised that the glutamate content might be altered in the *tup5-1* mutant. The glutamate-receptor antagonist DNQX was tested because a rice glutamate receptor-like gene may play a role in cell division and differentiation in the root (Li *et al.*, 2006). *Arabidopsis* has some predicted glutamate receptor-like genes (Lam *et al.*, 1998; Brenner *et al.*, 2000). Neither polyamines nor glutamate or DNQX complemented the *tup5-1* root phenotype (Figure 5-22).

Glutathione, which is synthesised from glutamate and cysteine, is important for root meristem maintenance: the glutathione synthesis mutant *rlm1* (*root meristemless1*) had a short-root phenotype which was rescued by supplementation of the mutant with glutathione (Vernoux *et al.*, 2000). In the case of *tup5-1* no complementation of the root phenotype was observed (Figure 5-22).

Proline was tested, because it can be synthesised from ornithine (Adams and Frank, 1980; Kishor *et al.*, 2005); but this amino acid did not complement *tup5-1* (Figure 5-22).

Arginine can be a source of nitric oxide (NO), which plays a role in root growth and many other developmental processes in plants (Crawford, 2006; Grün *et al.*, 2006). For this reason NO was tested for complementation of the *tup5-1* root phenotype with sodium nitroprusside as NO donor. Also in this experiment, no complementation of the *tup5-1* phenotype was observed (data not shown).

5. RESULTS

The *argD* gene of *E. coli* encoding for ACOAT has a dual catalytic function in arginine and lysine biosynthesis (Ledwidge and Blanchard, 1999). This was not expected to be the case in *Arabidopsis*, but nonetheless the effect of lysine on the *tup5-1* root was tested to exclude a possible involvement of this pathway in root growth inhibition of the mutant.

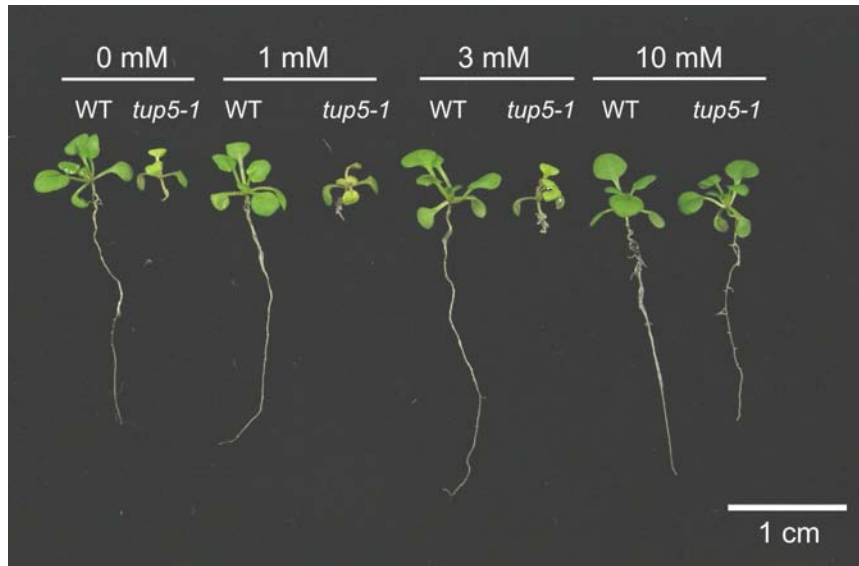


Figure 5-20: Root development of WT and *tup5-1* on acetylornithine supplemented media. From left to right: WT and *tup5-1* seedlings (18 d old) grown on MS medium containing 0 mM, 1 mM, 3 mM or 10 mM acetylornithine.



Figure 5-21: Root development of WT and *tup5-1* on arginine supplemented media. From left to right: WT and *tup5-1* seedlings (18 d old) grown on MS medium containing 0 mM, 1 mM, 3 mM or 10 mM arginine.

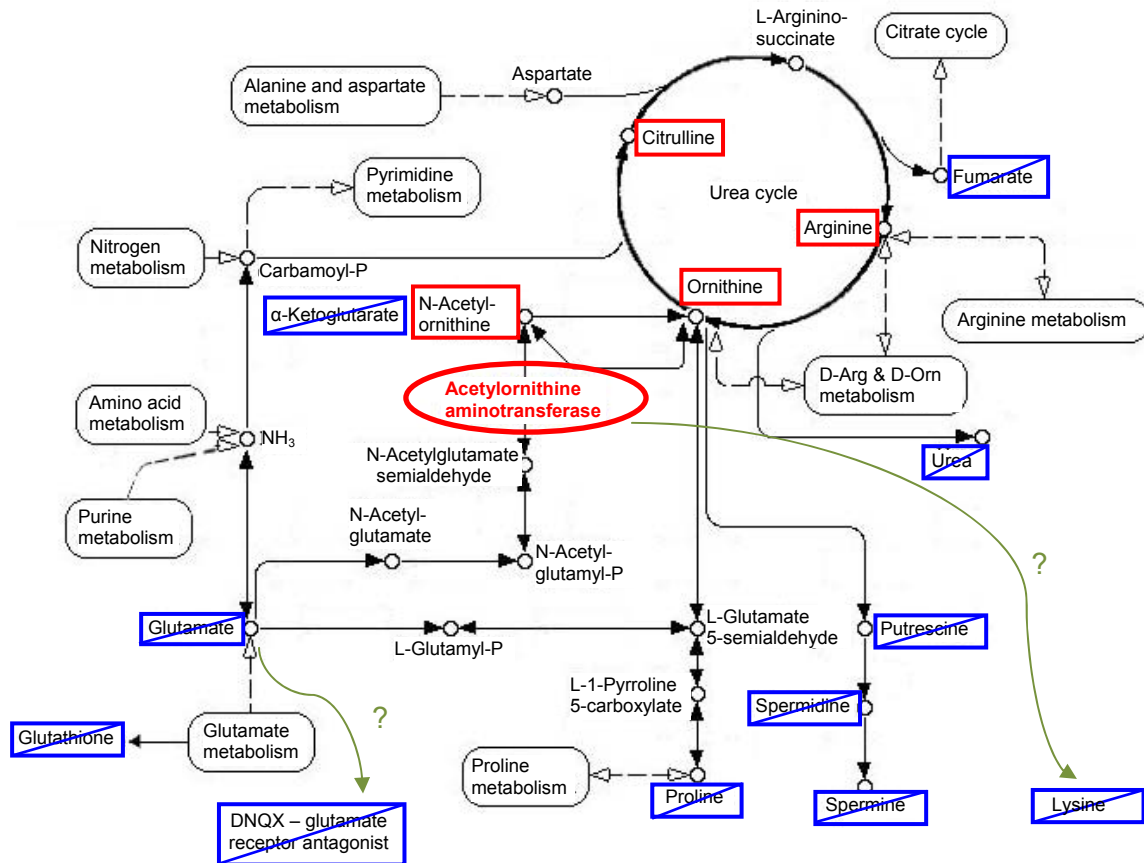


Figure 5-22: Metabolites tested for a complementing effect on the *tup5-1* root phenotype. Red boxes: complementing substances; blue boxes: substances which did not complement the root phenotype; α -ketoglutarate and lysine: preliminary results which have to be confirmed. Green arrows: speculative physiological or metabolic connections, for details see text. The concentrations used were: 1, 3 and 10 mM, except for DNQX (0,4 mM). The enzyme ACOAT (in red characters) is circled in red (modified from KEGG, <http://www.genome.jp/kegg/pathway/map/map00220.html> from 05.2006).

5.3.2 Heterologous complementation of a yeast *ACOAT* mutant

The yeast acetylornithine aminotransferase gene YOL140w on chromosome XV is deleted in the yeast strain Y37711 (homozygous, diploid) (Euroscarf; Saccharomyces Genome Database). Growth tests showed that the strain was as expected arginine auxotrophic. To prove that At1g80600 has the same function as the known yeast gene, the plant gene was transformed into the yeast mutant to test whether yeast strain Y37711 would become arginine autotrophic. For this purpose the genomic *Arabidopsis* WT sequence, the genomic *tup5-1* sequence and the *Arabidopsis* WT cDNA sequence, respectively, were cloned into the yeast vector p423TEF, which contains the strong constitutive promoter of *translation elongation factor 1 α* (TEF) for the expression of the gene of interest (Mumberg *et al.*, 1995). The yeast mutant transformed with the empty vector p423TEF, (as negative con-

trol), with the genomic WT sequence and the genomic *tup5-1* sequence was not able to grow on medium lacking arginine (Figure 5-23, B1,2,4). In contrast, the yeast mutant transformed with the WT cDNA sequence of At1g80600 became arginine autotrophic (Figure 5-23, B3).

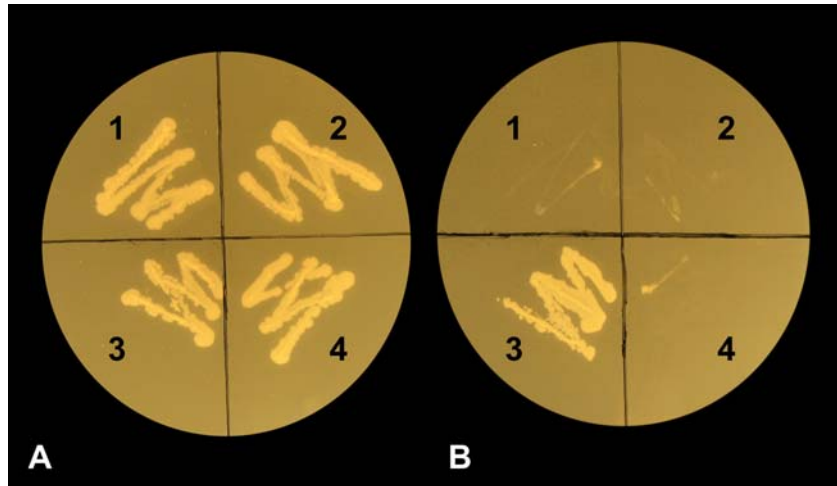


Figure 5-23: Heterologous complementation of the yeast mutant Y37711 with At1g80600. A: Transformed yeast on medium containing arginine; B: Transformed yeast on medium lacking arginine. Y37711 transformed with 1: the empty vector p423TEF; 2: vector containing the genomic *Arabidopsis* WT sequence; 3: vector containing the *Arabidopsis* WT cDNA sequence; 4: vector containing the genomic *tup5-1* sequence.

5.4 Impact of the *tup5-1* mutation on the amino acid content

The gene *TUP5* (At1g80600) is coding for an *ACOAT* which catalyses the fourth step in arginine synthesis (chapter 5.2.8). In agreement with this the root phenotype of *tup5-1* can be complemented with arginine and its non-proteinogenic precursor amino acids of the urea cycle (chapter 5.3.1). This indicates that the arginine content might be reduced in *tup5-1*. The overall amino acid metabolism of the mutant might also be impaired because of the metabolic linkage between the different amino acids (see for example Igarashi *et al.*, 2003; Voll *et al.*, 2004; Mo *et al.*, 2006). HPLC analyses were made to monitor changes in the level of free amino acids in *tup5-1* compared to WT. The amino acid content of 7-d-old seedlings grown under different light conditions was measured. These measurements were done twice in independent experiments. The results of these two experiments varied quantitatively, therefore they are presented separately. The free amino acid content of 17-d-old seedlings was also measured. Finally, the distribution of amino acids between shoot and root was analysed in 11-d-old seedlings because the root phenotype of *tup5-1* suggests

some organ-specific differences. Root material was only harvested from WT plants, due to the minimal root material available from *tup5-1* mutants.

5.4.1 Free arginine content in WT and *tup5-1*

A The free arginine concentration is reduced in *tup5-1* seedlings

As expected, the concentration of free arginine in *tup5-1* was significantly reduced (61 to 85%) in four different sample sets from seedlings of different ages: In 7-d-old seedlings grown at standard light (SL), the arginine concentration was 69% to 85% lower in *tup5-1* than in WT (Figure 5-24, A; Table 9-9 and Table 9-10 in supplemental data). Again in 11-d-old seedlings a reduction in arginine concentration of 61% was observed in *tup5-1* shoots compared to WT shoots (WT contained 3084 ± 673 nmol/g FW and *tup5-1* 1214 ± 252 nmol/g FW) (Figure 5-24, B and Table 9-11). In 17-d-old plantlets the reduction reached 76% in *tup5-1* compared to WT (WT contained 2099 ± 655 nmol/g FW and *tup5-1* 509 ± 40 nmol/g FW) (Figure 5-28, Table 9-12).

B The free arginine content is reduced to a comparable level in WT and *tup5-1* in darkness

While *tup5-1* had a low arginine content compared to WT in SL, no difference in arginine concentration was found in WT and *tup5-1* in darkness. The arginine concentration was decreased for seedlings grown in dark compared to seedlings grown in SL: In WT the decrease was about 89% and in *tup5-1* approximately 67% compared to the arginine concentrations measured at SL (322 ± 130 and 295 ± 102 nmol/g FW, respectively) (Figure 5-24, A).

The effect of low light on arginine content was also studied (data not shown). There were hints that the arginine content increased in *tup5-1* under low light conditions and that it decreased in WT, so that the difference in arginine content was decreased between WT and *tup5-1*. More detailed studies investigating the effect of light quality and quantity on arginine content are needed to confirm these results.

C The free arginine concentration in WT root is extremely low compared to WT shoot

The distribution of free arginine between root and shoot was very unequal. WT roots contained 50 times less arginine than WT shoots (61 ± 11 compared to 3084 ± 673 nmol/g FW) (Figure 5-24, B). *tup5-1* shoots contained approximately 39% less arginine than WT

shoots (1214 ± 252 compared to 3084 ± 673 nmol/g FW), but about 95% more than WT roots (1214 ± 252 compared to 61 ± 11 nmol/g FW) (Figure 5-24, B). This is the most extreme difference in shoot / root distribution of all amino acids analysed in this experiment (Figure 5-27). The two amino acids with the lowest concentration in the root compared to shoot after arginine were tryptophan (26% of shoot concentration) and lysine (42% of shoot concentration) (Table 9-11).

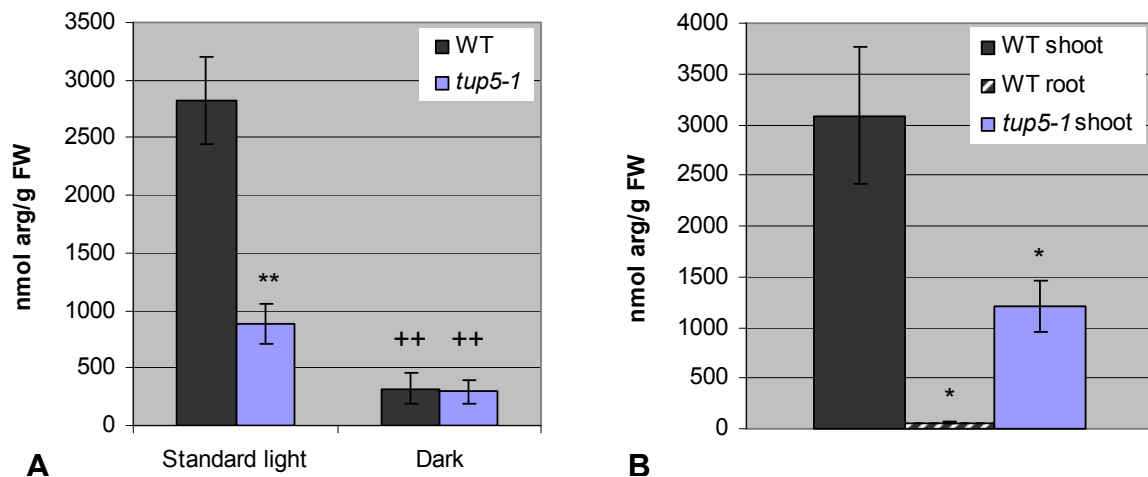


Figure 5-24: Free arginine content in WT and *tup5* seedlings.

A: Arginine content of WT and *tup5-1* at standard light intensity (LD) and in darkness. Seedlings were 7 d old and grown in $\frac{1}{2}$ MS liquid culture. Mean \pm SD of three samples, except WT and *tup5-1* at standard light in B: n = 6. Significance: ** or ++ P < 0,001, Student's *t* test comparing WT and *tup5-1* samples: *; when comparing standard light with other light conditions for WT or *tup5-1*, respectively: +. B: Free arginine content in WT shoot, WT root and *tup5-1* shoot. Seedlings were 11 d old and grown on vertical plates of MS medium at standard light intensity (LD). WT shoot n=4; WT root n=3; *tup5-1* shoot n=4. Significance: * P < 0,01, Student's *t* test comparing WT root and shoot or WT and *tup5-1* shoot samples.

5.4.2 The concentrations of serine and glycine was increased in *tup5-1* in a light-dependent manner

Serine and glycine are two amino acids produced during photorespiration (Foyer *et al.*, 2009). Interestingly, both are increased in *tup5-1* compared to WT under standard conditions, while these differences were strongly reduced under low light conditions or in darkness: In 7-d-old *tup5-1* seedlings grown at standard light the concentration of free serine (ser) was increased by 93% and the glycine (gly) concentration by 382% compared to WT seedlings (Figure 5-25, Table 9-10). This strong accumulation especially of glycine in *tup5-1* under standard light was found in different experiments (supplemental data: Table 9-9 and Table 9-11). In low light the serine and glycine concentration decreased in both

WT and *tup5-1* (Figure 5-25). Under LL the serine concentration decreased to 22% in WT and 27% in *tup5-1* compared to WT in SL, the difference is not significant according to Student's *t* test (data not shown). The glycine concentration in LL was decreased to 29% in WT and 47% in *tup5-1* compared to WT in SL (Figure 5-25, Table 9-10). The difference between WT and *tup5-1* in LL is still significant but strongly reduced compared to standard light: In standard light *tup5-1* contained almost 5 times more glycine than WT, while in low light the difference was only 1,6-fold.

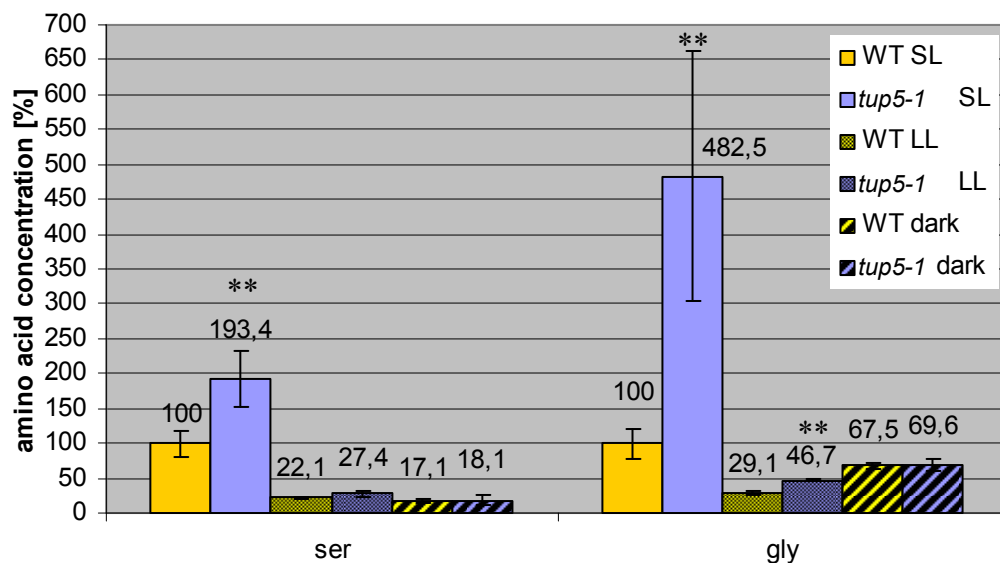


Figure 5-25: Free glycine and serine content of WT and *tup5-1* under different light conditions. Seedlings were 7 d old and grown in ½ MS liquid culture at standard light (SL), low light (LL) and in darkness (dark). The results of the second experiment are shown (see Table 9-10). The concentration of each amino acid in *tup5-1* is shown in percent referring to the values measured in WT at SL set as 100% respectively. Mean ± SD of three samples, except WT and *tup5-1* at standard light n = 6. Significance: ** P < 0,01, Student's *t* test comparing WT and *tup5-1* samples grown under the same light condition.

5.4.3 The level of many amino acids was altered in *tup5-1*

The free amino acid content of WT and *tup5-1* was measured in 7-, 11- and 17-d-old seedlings. An overview of all results is shown in Table 5-4. In 7- and 11-d-old seedlings several amino acid concentrations were increased in *tup5-1* compared to WT. These were: Aspartate (asp), asparagine (asn), (glycine – see above), Threonine (thr), alanine (ala), valine (val), and phenylalanine (phe) (Figure 5-26 and Figure 5-27, Table 9-9 to Table 9-11 and Table 5-4). Interestingly, in 17-d-old seedlings only asparagine and glutamine (gln) were increased in *tup5-1* compared to WT (Figure 5-28, Table 9-12).

Glutamate (glu) and histidine (his) were not significantly changed at any of the three analysed plant stages (7, 11, 17 days old) (Figure 5-26 to Figure 5-28, Table 9-9 to Table 9-12)

and Table 5-4). The concentration of free leucine (leu) and lysine (lys) was reduced in *tup5-1* compared to WT in some measurements, but the results did not show clear tendencies (Figure 5-26 to Figure 5-28, Table 9-9 to Table 9-12 and Table 5-4). Among all amino acids only the arginine concentration was decreased in *tup5-1* compared to WT in all measurements, an overview is shown in Table 5-4.

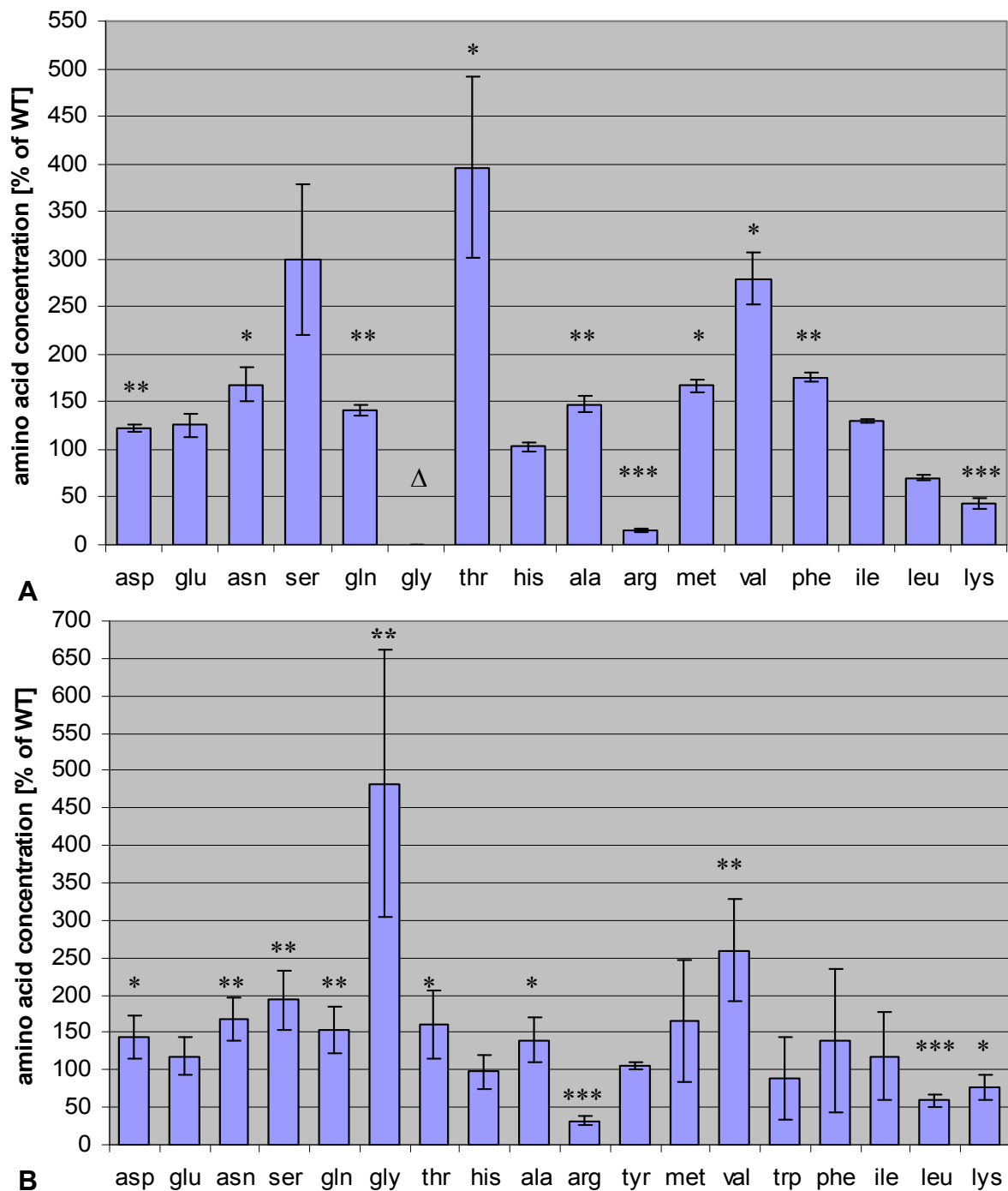


Figure 5-26: Free amino acid content of 7-d-old seedlings of *tup5-1* compared to WT grown under standard conditions.

A: First experiment. B: Second independent experiment. Seedlings were grown in $\frac{1}{2}$ MS liquid culture. The concentration of each amino acid in *tup5-1* is shown in percent referring to the values measured in WT set as 100% (see supplemental data: Table 9-9 for A and Table 9-10 for B). Mean \pm SD of three samples in A, mean \pm SD of six samples in B. Significance: * $P < 0,05$; ** $P < 0,01$; *** $P < 0,001$, Student's *t* test comparing WT and *tup5-1* samples. Δ (in A): Gly was not detected in WT, thus 100% could not be defined in this case.

5. RESULTS

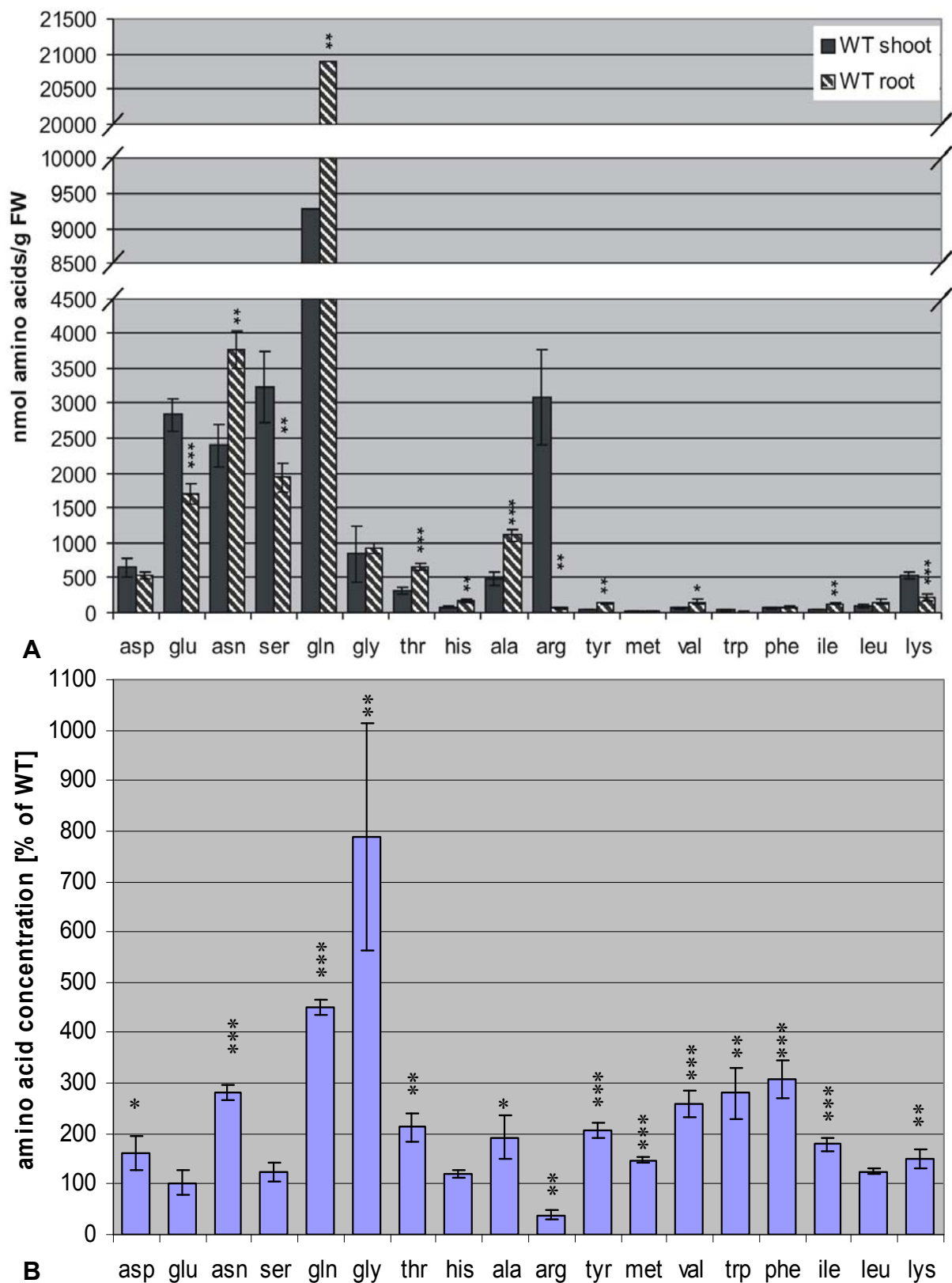


Figure 5-27: Free amino acid content of 11-d-old WT and *tup5-1* seedlings grown under standard conditions.

A: Comparison between WT shoot and root (values in nmol/g FW). B: Comparison between WT and *tup5-1* shoot (the concentration of each amino acid in *tup5* shoot is shown in percent referring to the values measured in WT shoot set as 100%). Seedlings were grown on vertical plates of MS medium at standard light intensity. The mean values are listed in Table 9-11. WT shoot n=4; WT root n=3; *tup5-1* shoot n=4. Significance: * P < 0,05; ** P < 0,01; *** P < 0,001, Student's *t* test comparing WT root and shoot or WT and *tup5-1* shoot samples.

5. RESULTS

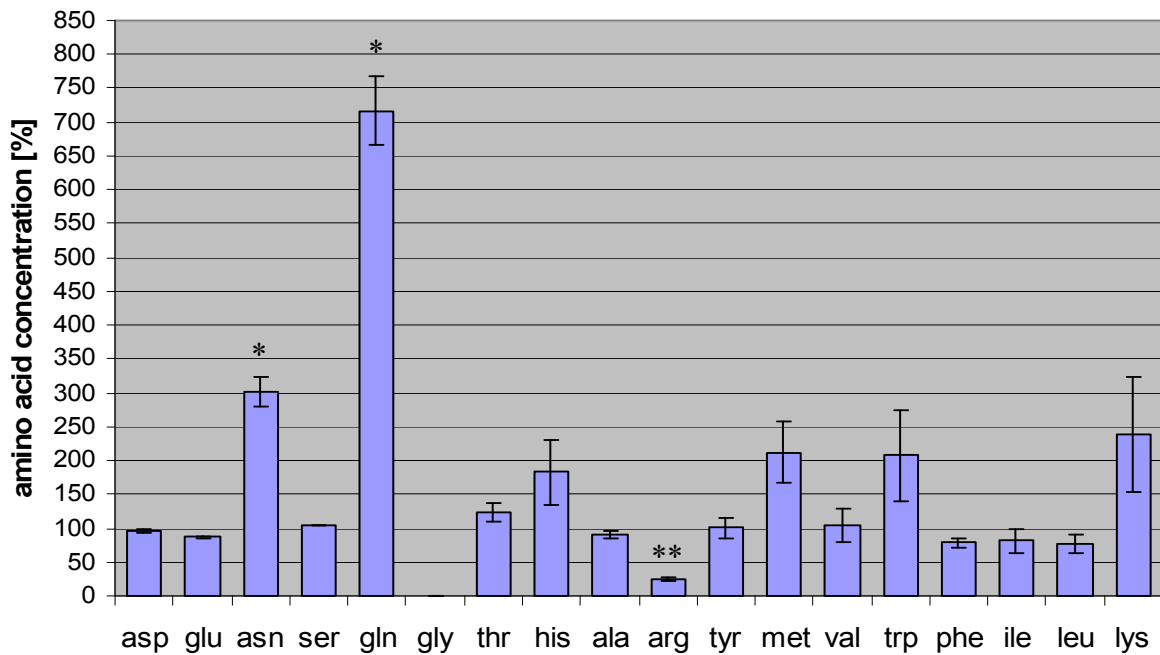


Figure 5-28: Free amino acid content of 17-d-old seedlings of *tup5-1* compared to WT grown under standard conditions.

Seedlings were grown on vertical plates of MS medium at standard light intensity. The concentration of each amino acid in *tup5-1* is shown in percent referring to the values measured in WT set as 100% respectively (see Table 9-12). Mean \pm SD of five samples for WT and two samples for *tup5-1*. Significance: * $P < 0,05$; ** $P < 0,01$, Student's *t* test comparing WT and *tup5-1* samples.

Table 5-4: Comparison of different amino acid measurements in WT and *tup5-1* plants grown at standard light.

Red boxes: Amino acid (AA) level is reduced in *tup5-1* in all experiments ($\downarrow\downarrow$); blue boxes: AA level is increased in *tup5-1* in all experiments ($\uparrow\uparrow$); yellow boxes: AA level is increased in *tup5-1* in 7-d-old seedlings and 11-d-old shoots (\uparrow); green boxes: AA in which no significant difference was measured between WT and *tup5-1* in any measurement. n.s.: difference not significant; significance: * $P < 0,05$; ** $P < 0,01$, Student's *t* test comparing WT and *tup5-1* samples.

Amino acid	1. experiment 7-d-old seedlings	2. experiment 7-d-old seedlings	shoot 11 d old	17-d-old seedlings
asp	** \uparrow	* \uparrow	* \uparrow	n.s.
glu	n.s.	n.s.	n.s.	n.s.
asn	* $\uparrow\uparrow$	** $\uparrow\uparrow$	*** $\uparrow\uparrow$	* $\uparrow\uparrow$
ser	n.s.	**	n.s.	n.s.
gln	** $\uparrow\uparrow$	** $\uparrow\uparrow$	*** $\uparrow\uparrow$	* $\uparrow\uparrow$
gly	-	** \uparrow	** \uparrow	
thr	* \uparrow	* \uparrow	** \uparrow	n.s.
his	n.s.	n.s.	n.s.	n.s.
ala	** \uparrow	* \uparrow	* \uparrow	n.s.
arg	*** $\downarrow\downarrow$	*** $\downarrow\downarrow$	** $\downarrow\downarrow$	** $\downarrow\downarrow$
tyr	-	n.s.	***	n.s.
met	*	n.s.	***	n.s.
val	* \uparrow	** \uparrow	*** \uparrow	n.s.
trp	-	n.s.	**	n.s.
phe	** \uparrow	n.s.	*** \uparrow	n.s.
ile	n.s.	n.s.	***	n.s.
leu	n.s.	***	n.s.	n.s.
lys	***	*	*	n.s.

5.5 Subcellular localisation of TUP5

The subcellular localisation of a studied protein gives information about its biochemical surrounding and the available substrates and interaction partners. Predictions of the subcellular localisation peptides can be calculated with programmes like TargetP, PSORT, Aramemnon and others (Nakai and Horton, 1999; Schwacke *et al.*, 2003; Emanuelsson *et al.*, 2007). The prediction results can widely differ and have to be confirmed experimentally (see for example the comparison of database predictions in Slocum (2005)). Classical biochemical approaches for localisation consist in isolating different organelles and in testing for enzymatic activity (of the enzyme of interest) in these different fractions (for example Taylor and Stewart (1981) or Jain *et al.* (1987)). The reliability of the results depends on the purity of the isolated fractions. Furthermore, if different genes encode for proteins with the same enzymatic activity, their activity cannot be distinguished in these tests. Another, more recent approach, is the fusion of the gene of interest with a marker gene like GFP to track an *in vivo* fluorescence signal in the cell (Chalfie *et al.*, 1994).

The database predictions of *TUP5* and previous biochemical studies on the subcellular localisation of ACOAT are presented in chapter 5.5.1. In this work the localisation was experimentally tested using the marker gene *GFP*. The results are presented in chapter 5.5.2.

5.5.1 Database prediction and previous studies on the subcellular localisation of ACOAT

In this work the prediction for the localisation of *TUP5* was calculated with the programme TargetP (Table 5-5) (Emanuelsson *et al.*, 2007). It predicted a chloroplastic transit peptide with a score of 0,716 (the highest possible score is 1) (Date: March 2009). This score belongs to the prediction reliability class four (RC = 4), which indicates a low reliability for this prediction (five is the lowest reliability class). The database Aramemnon also gave a prediction for chloroplastic localisation (Date: March 2009) (Schwacke *et al.*, 2003). Other database predictions given at the time of the study were contradictory. The databases TAIR and TIGR gave the following annotation for At1g80600: “Acetylornithine aminotransferase, mitochondrial, putative”. In the study of Slocum (2005), where different database predictions were compared for the localisation of *TUP5*, TargetP gave a prediction for chloroplastic, Predotar for mitochondrial, PSORT for cytosolic and ProtComp for mitochondrial localisation. Beside these database predictions, data of previous biochemical

studies were available for the localisation of the enzyme ACOAT in soybean. These experiments were done mainly in cell cultures and showed a plastidic localisation of ACOAT (Jain *et al.*, 1987).

Table 5-5: Prediction results for the subcellular localisation of TUP5 by the programme TargetP. The highest score in this prediction was calculated for a chloroplastic transit peptide with a value of 0,716 (with 1 as highest possible score value). Len = Amino acid length of the protein; cTP = chloroplastic transit peptide; mTP = mitochondrial targeting peptide; SP = secretory pathway signal peptide; other = other signal peptide; Loc: localisation (C = chloroplast); RC = reliability class (1 to 5, with 1 = highest reliability); TPlen = transit peptide length (Emanuelsson *et al.*, 2007).

Name	Len	cTP	mTP	SP	other	Loc	RC	TPlen
Sequence	457	0.716	0.370	0.019	0.053	C	4	43
cutoff		0.000	0.000	0.000	0.000			

5.5.2 Localisation of TUP5 by GFP fusion marker

The cDNA of *TUP5* (amplified without stop codon from the clone U15579) was cloned with the Gateway[®] system into the vector pB7FWG2 (Yamada *et al.*, 2003; Karimi *et al.*, 2005). In this construct At1g80600 was fused at the carboxyl-terminal end to an enhanced *green fluorescent protein* (Egfp) as a marker and cloned downstream of the constitutive CaMV 35S promoter (Figure 5-29) (Karimi *et al.*, 2005). The transgene was transformed into *tup5-1* homozygous plants and WT plants by the floral dip method (Clough and Bent, 1998). The *tup5-1* root phenotype was complemented with the GFP construct, because T₀ plants formed a long root in light, indicating that the fusion protein restored *TUP5* function (data not shown). The subcellular localisation was analysed in the tissue of stably transformed lines in WT background. In the leaf tissue of seedlings the autofluorescence signal of chlorophyll was so strong that no GFP signal could be seen (data not shown). In the root tissue, where chlorophyll is absent, a signal could be detected in globular structures (Figure 5-30). To test the prediction for chloroplastic localisation (chapter 5.5.1), protoplasts of leaf tissue from *TUP5-GFP* transgenic lines (in WT background) were isolated with a fast method of enzymatic digestion of the cell wall (chapter 4.4.4) and analysed with a confocal laser scanning microscope. The GFP signal was visible in globular structures within the protoplasts (Figure 5-31, A). These globular organelles could be defined as chloroplasts because of their autofluorescence signal (Figure 5-31, B). Both signals came from the same

organelles, as seen in the overlay (Figure 5-31, A and B). The predicted chloroplastic localisation of TUP5 was confirmed by this experiment.

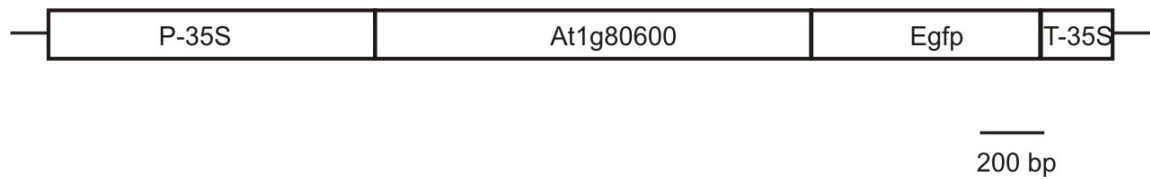


Figure 5-29: Vector construct used for the subcellular localisation of TUP5.

The cDNA of At1g80600 (without stop codon) was cloned between the 35S promoter (P-35S) and enhanced *green fluorescent protein* (Egfp), followed by the 35S transcriptional terminator sequence (T-35S) in the vector pB7FWG2 (Karimi *et al.*, 2005).

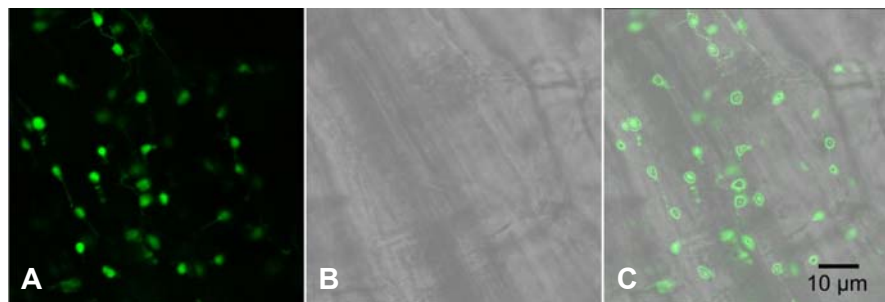


Figure 5-30: TUP5-GFP signal in root tissue.

A: Fluorescence signal of GFP, B: Root tissue of A in bright field, C: Overlay of A and B. Images were taken with the confocal laser scanning microscope Leica TCS SP2.

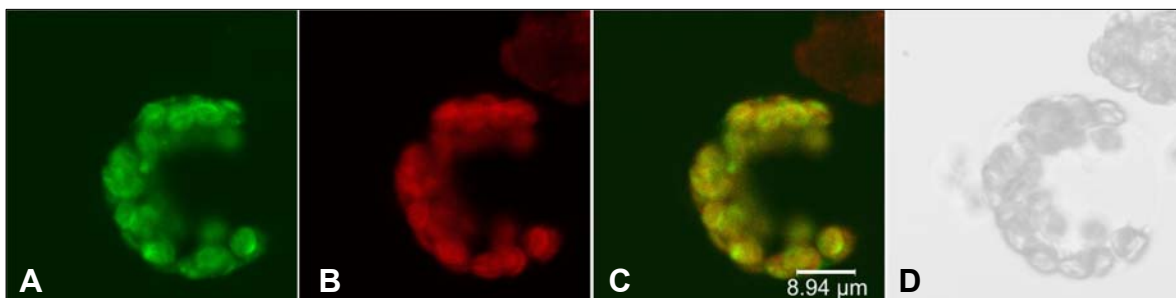


Figure 5-31: TUP5-GFP signal in leaf protoplasts.

A: Fluorescence signal of GFP; B: Autofluorescence signal of the chloroplasts; C: Overlay of A and B, D: Protoplast of A and B in bright field. Images were taken with the confocal laser scanning microscope Leica TCS SP2.

5.6 Temporal and spatial expression pattern of TUP5 in *A. thaliana*

The anatomical and temporal expression pattern of a gene can give valuable hints about the gene's function in plant development and metabolism. Microarray expression data for *TUP5* gene expression are available from databases such as eFP Browser or Genevestigator (Winter *et al.*, 2007; Hruz *et al.*, 2008). Microarray data have to be confirmed

experimentally by reporter gene analysis (chapter 5.6.2) or quantitative real-time PCR (chapter 5.6.3).

5.6.1 Database information on *TUP5* expression

According to the developmental map of the eFP Browser (electronic Fluorescent Pictograph - <http://www.bar.utoronto.ca/efp/cgi-bin/efpWeb.cgi>) *TUP5* is expressed in all analysed tissues (Figure 5-32). The maximum expression level (expression potential) of the probe set was 2043 absolute signal value (a.s.v.). Rosette leaves, sepals, pedicels and cotyledons reached the highest expression levels in the developmental map with about 550 to 650 a.s.v. (Figure 5-32). The expression level in roots was about 300 a.s.v. (Figure 5-32). The *TUP5* expression was about 380 a.s.v. in an early stage of seed development and decreased during maturation to a level of approximately 209 a.s.v. in dry seeds. The lowest expression (virtually null) was found in mature pollen (7 ± 7 a.s.v.), (Figure 5-32).

At tissue resolution, the highest expression was found in ovaries (840 ± 103 a.s.v.) and the lowest in the later stages of pollen development (14 to 20 a.s.v.), while in early stages of pollen development, namely the uninucleate microspore and the bicellular pollen, the expression was still at a level of approximately 130 a.s.v. (Figure 5-33). Within the root the highest level of *TUP5* expression was found in epidermal atrichoblast cells (456 a.s.v.) (Figure 5-33).

According to Genevestigator *TUP5* is expressed in all developmental stages of the plant (<https://www.genevestigator.ethz.ch/gv/user/serveApplet.jsp>) (data not shown). In earlier stages of development the expression increased from 3689 average signal intensity value (a.s.i.v.) in germinated seeds to the peak of 4652 a.s.i.v. in bolting plants and decreased again after that stage towards later developmental stages (data not shown). In the anatomical overview the highest expression was found in juvenile leaves, stamen abscission zone, pedicels, sepals and root tips (from 5121 to 6640 a.s.i.v.) (data not shown). The lowest expression was found in pollen and sperm cell (from 55 to 156 a.s.i.v.) (data not shown). According to Genevestigator the expression of *TUP5* was low in ovary (2123 a.s.i.v.) compared to the other tissues (data not shown), though this tissue had a high *TUP5* expression according to the data of eFP Browser (Figure 5-33).

After treatment with cycloheximide *TUP5* was downregulated to about half the level of untreated plants, indicating that *de novo* protein synthesis is necessary for *TUP5* expression. In contrast, it was upregulated to a ratio of 2,3 after treatment with isoxaben and 4,15

5. RESULTS

fold after infection with nematodes (data not shown). Changes in *TUP5* expression were also found in mutants: *TUP5* was downregulated in *agl65/66* to a ratio of 0,39 compared to WT, *agl65* (ratio 0,42), *agl66* (ratio 0,5), and upregulated 2,9-fold in *agl65/66/104* compared to WT (data not shown). *TUP5* is not light-regulated according to most experiments shown in Genevestigator, except for “dark 4” (comparing 7-day-old seedlings grown in dark or light) where *TUP5* was downregulated 1,9-fold compared to light-grown control plants and “Night extension late” (gene expression in rosette leaves grown in a 14 h photoperiod at the end of the night and after a 6 h extension of the dark period) where it was downregulated 1,7 fold compared to control plants (data not shown).

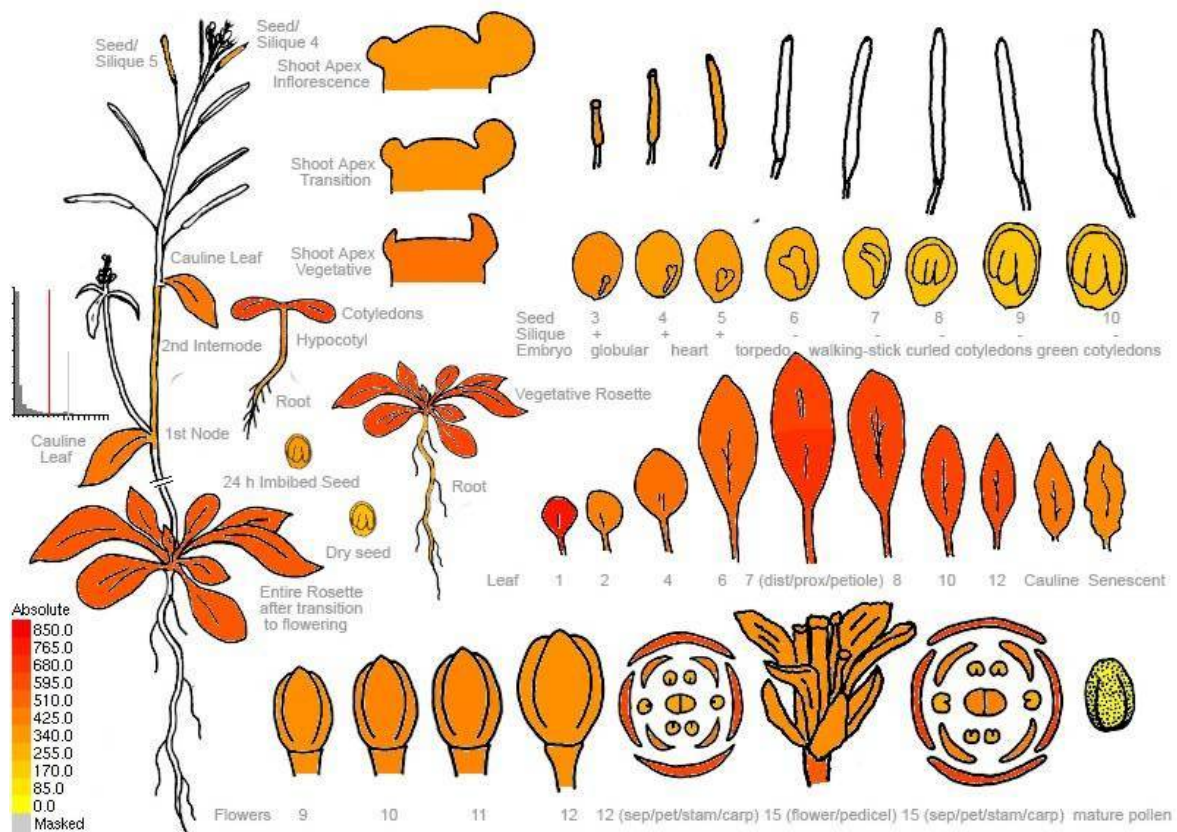


Figure 5-32: Expression pattern of *TUP5* according to the developmental map of the eFP Browser (Winter *et al.*, 2007).

The colour legend displays absolute transcript level of *TUP5*, yellow indicating low level to red showing high level of gene expression (<http://www.bar.utoronto.ca/efp/cgi-bin/efpWeb.cgi>, date: January 2009).

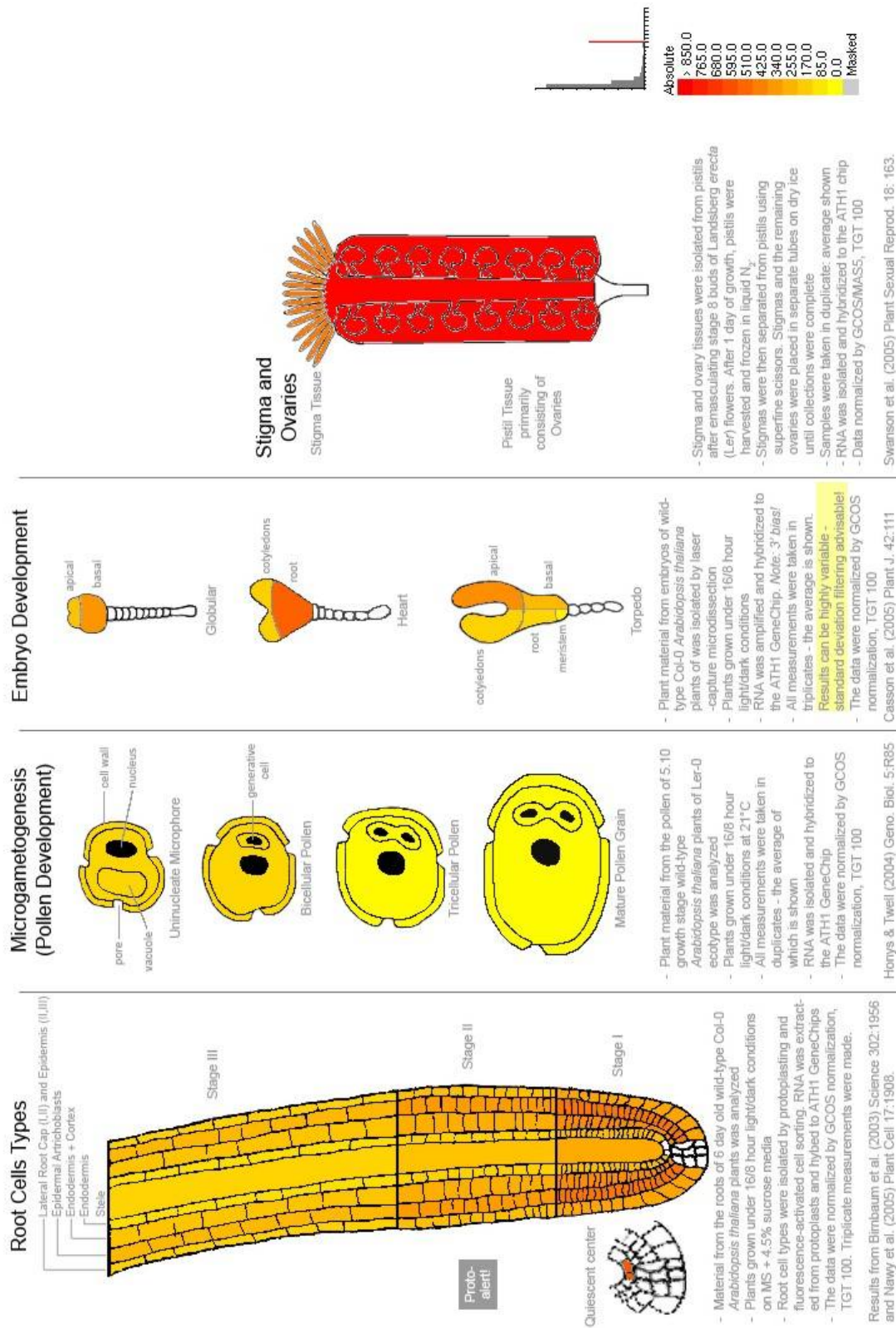


Figure 5-33: Expression pattern of *TUP5* on the cellular level according to the eFP Browser (Winter et al., 2007). The colour legend displays absolute transcript level of *TUP5*, yellow indicating low level to red showing high level of gene expression (<http://www.bar.utoronto.ca/efo/cai-bin/efoWeb.cai>, date: January 2009).

5.6.2 Testing *TUP5*-reporter gene fusions

To confirm the expression pattern of *TUP5* experimentally, the promoter of *TUP5* was cloned upstream of the *GUS* gene (β -glucuronidase) into the vector pCB308 (Xiang *et al.*, 1999) (for details of the cloning strategy see chapter 4.8). In a first approach, 2 kb upstream of *TUP5* were used (Table 9-7 and Figure 9-3, A). No blue staining was found in transgenic plants (data not shown). Therefore longer promoter sequences were cloned, but no GUS staining was found for constructs containing 2,5 kb, 3 kb or 3,2 kb upstream of *TUP5* (Table 9-7 and Figure 9-3, B-D). Further regulatory elements might be positioned within the coding sequence; therefore parts of the *TUP5* ORF were fused with GUS (Table 9-7 and Figure 9-3, E-G). But again, no blue staining was found in the tissues of transgenic plants (data not shown). Interestingly, the transgene containing the whole *TUP5* gene fused to *GUS* (Figure 9-3, G) partially complemented the *tup5-1* root phenotype when transformed into *tup5-1* homozygous plants, indicating that there has to be at least a low level of expression and functional TUP5 protein.

5.6.3 Quantitative real-time PCR

Expression of TUP5 in different plant organs

The expression of *TUP5* was tested with real-time PCR (qPCR) to verify the microarray data from eFP Browser and Genevestigator. Plant material from different organs was harvested from adult WT and *tup5-1* plants (32 and 35 d) grown on soil in the greenhouse under long day conditions. The lowest expression was found in the roots with no significant difference between WT and *tup5-1* (Figure 5-34). Highest expression was found in rosette leaves. The expression was approximately 4 times higher for WT and approximately 7 times higher for *tup5-1* compared to expression in roots (Figure 5-34). The difference in expression level between WT and *tup5-1* in rosette leaves was statistically not significant, this result should be verified. Compared to the expression level of roots, the expression was about twice as high in the stem, about three times higher in flowers and about 3,5 times higher in siliques (Figure 5-34).

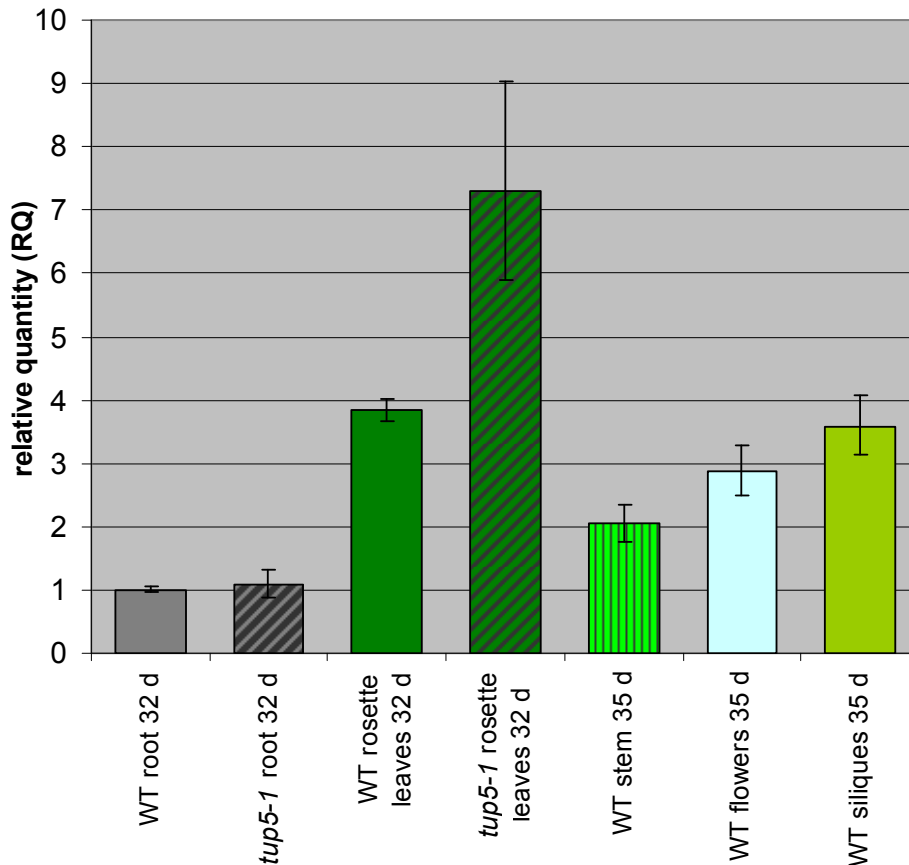


Figure 5-34: *TUP5* and *tup5-1* expression in different plant organs of *A. thaliana* in WT and *tup5-1* mutant plants.

Roots and rosette leaves were used from 32-d-old WT and *tup5-1* plants. For stem, flower and silique tissue only WT was analysed (35 d old). Plants were grown on soil under standard conditions. One biological sample respectively was used for three PCR reactions originating from one master mix. The real time PCR was performed with Applied Biosystems 7500FAST. Error bars: minimal and maximal RQ. $n = 3$. WT and *tup5-1* root or rosette leaves respectively were compared: The differences were not significant with Student's *t* test.

Influence of arginine treatment on TUP5 expression

Arginine treatment represses ACOAT in *E. coli* and yeast (Albrecht and Vogel, 1964; Heimberg *et al.*, 1990). An influence not only on enzymatic activity but also on expression level might be possible. Therefore the influence of arginine treatment on *Arabidopsis TUP5* expression was tested. Seedlings grown under standard conditions were treated for 14 h with 100 μ M arginine (which is a concentration sufficient to complement the *tup5-1* root phenotype: see chapter 5.3.1). The *TUP5* expression was not significantly changed in arginine treated seedlings compared to untreated WT and *tup5-1* seedlings (Figure 5-35).

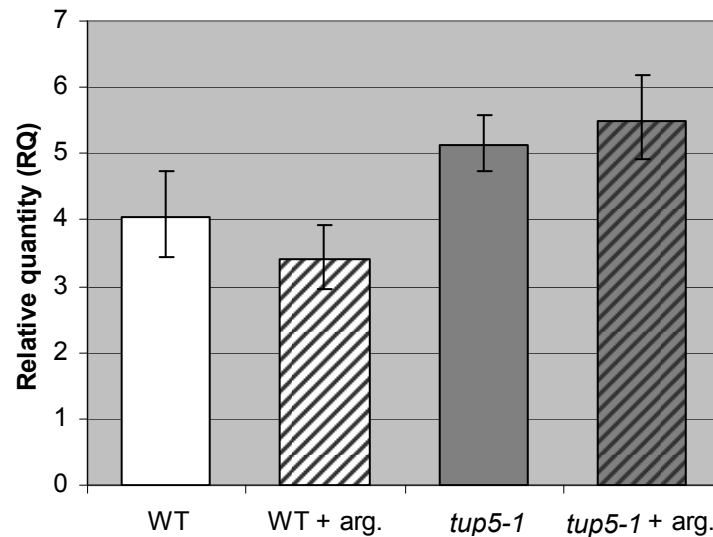


Figure 5-35: Arginine treatment has no influence on *TUP5* expression in *Arabidopsis* seedlings. Seedlings (6 d) were grown in liquid culture at 22°C under long day conditions. They were treated with 100 μ M arginine at day 5 for 14 h before harvest. One biological sample was used for three PCR reactions originating from one master mix. The real time PCR was performed with Applied Biosystems 7500FAST. Error bars: minimal and maximal RQ. $n = 3$. WT and *tup5-1* with and without arginine respectively were compared: The differences were not significant with Student's *t* test.

Light-dependent TUP5 expression in seedlings

Information from eFP Browser and Genevestigator gave only weak hints to a light-dependent regulation of *TUP5* expression (data not shown). The influence of white light on *TUP5* expression was nevertheless studied, because *tup5-1* shows a light-dependent root phenotype. Seedlings were cultivated in liquid MS medium in constant darkness or under long day conditions. In light-grown seedlings the expression level of *TUP5* was four times higher in WT and five times higher in *tup5-1* compared to dark-grown WT seedlings (Figure 5-36, A).

Since the seedlings used for dark-grown control were etiolated in the experiment described above and had therefore a presumably strongly changed overall metabolism, a second experiment was done. In this case the seedlings were first grown under long day conditions and were then subjected to an adaptation phase of 24 h in dark or light (see scheme above Figure 5-36, B). After this adaptation phase they were shifted to light or darkness respectively for 8 h. Control samples which were not subjected to the 8 h shift, were collected at the beginning and the end of the shift phase (after 24 h and 32 h respectively). Again in this experiment a light-dependent increase in *TUP5* expression was observed: 24 h and 32 h light-adapted seedlings had a 3- to 4-fold higher expression level than 24 h and 32 h dark-adapted seedlings (Figure 5-36, B, only 32 h control samples shown). The *TUP5* expression was significantly decreased in light-adapted seedlings that were shifted into darkness compared to light-adapted control plants (Figure 5-36, B). Correspondingly,

TUP5 expression was significantly increased in dark-adapted seedlings shifted into light compared to the dark-adapted controls (Figure 5-36, B). These results need to be verified and studied in more detail.

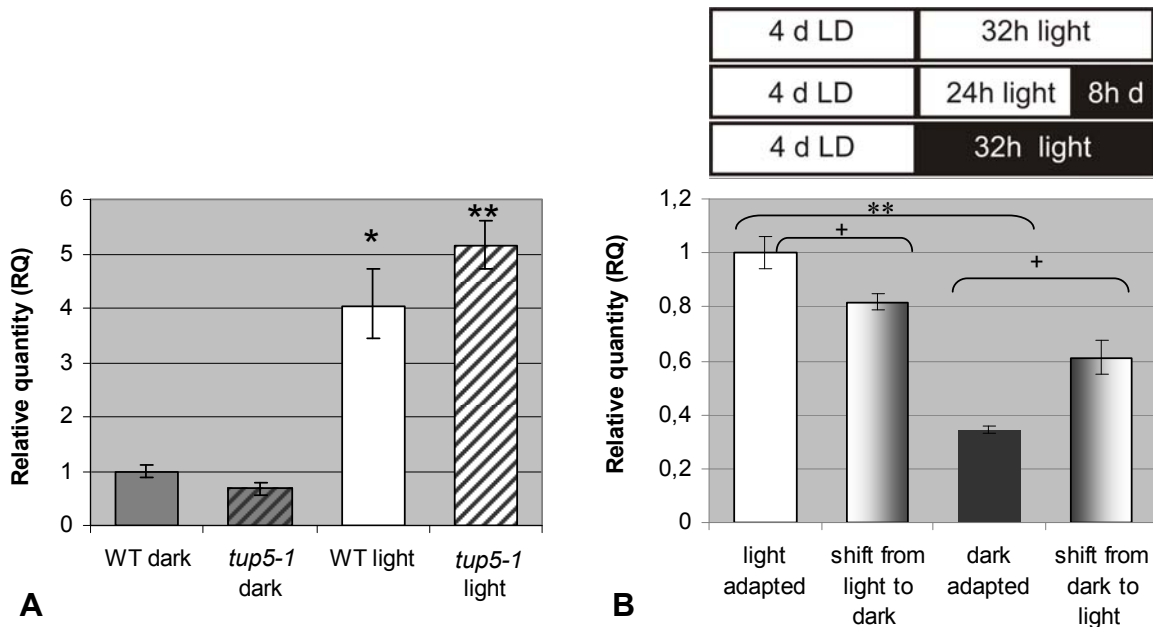


Figure 5-36: Effect of light on *TUP5* expression in *Arabidopsis* seedlings.

All seedlings (6 d) were grown in liquid culture at 22°C. One biological sample respectively was used for three PCR reactions originating from one master mix. RQ: Relative quantity. Error bars: minimal and maximal RQ. The real time PCR was performed with Applied Biosystems 7500FAST.

A: *TUP5* expression in light and darkness. Seedlings were grown under long day conditions or in darkness respectively (dark-grown plants were treated with light for 18 h at day 1 to induce germination). $n = 3$. Significance: * $P < 0,05$; ** $P < 0,01$, Student's *t* test comparing WT and *tup5-1* grown in darkness with their respective light-grown controls.

B: Changes in *TUP5* expression in *Arabidopsis* seedlings after 8 h of shift into light or darkness. Seedlings were grown at long day (LD) conditions for four days and subsequently light or dark-adapted for 24 h. After this treatment seedlings were shifted for 8 h into dark (d) or light (l) respectively and then harvested (see scheme above B). Control plants were collected after 32h of light- or dark-adaptation. All seedlings were harvested at day 6. $n = 3$. Significance: * or + $P < 0,05$; ** or ++ $P < 0,01$, Student's *t* test comparing light-adapted samples with those shifted from light to dark and dark-adapted samples with samples shifted from dark to light: +, when comparing light-adapted and dark-adapted seedlings respectively.*.

5.7 Characterisation of T-DNA insertion alleles of the *TUP5* gene

In the *tup5-1* mutant carrying a point mutation the *TUP5* gene function is altered or reduced (chapter 5.2.6). The *TUP5* transcript level in *tup5-1* is not influenced by the mutation (Figure 5-15, A). To gain a better understanding of the role of *TUP5*, additional T-DNA insertion alleles were analysed. T-DNA insertion lines often lead to a complete knockout of the gene in contrast to point mutations (Krysan *et al.*, 1999). Eight T-DNA insertion lines which were predicted to have an insertion in At1g80600 or its close vicinity

were analysed. The insertion of the T-DNAs was predicted to be in exon regions of the gene for three lines, four lines were predicted to have an insertion less than 1000 bp upstream of At1g80600 and one line was predicted to have an insertion less than 300 bp downstream of the 3' region (Table 5-6). Before genotyping, the insertion lines were screened for obvious phenotypes with special attention to the root. No visible phenotypical alterations were found in the examined lines (data not shown).

PCR analyses were done on genomic DNA to verify the T-DNA insertions of the lines. For SAIL_1171_B12 (*tup5-2*) and SAIL_672_D10 (*tup5-3*) a hybrid sequence of T-DNA and At1g80600 bordering the insertion site was amplified, proving the insertion in the gene (data not shown). The same primer pair was used for both lines, but the resulting PCR products were different in size, proving that these lines originate from independent insertion events. The PCR products were sequenced to verify the insertion sites. The sequencing reaction was done with a T-DNA border primer. The exact insertion sites could not be determined because the beginning of the sequences could not be read, but the prediction of the insertion for the third exon of At1g80600 was confirmed. In all the other T-DNA insertion lines no hybrid sequence of T-DNA border and At1g80600 could be amplified.

The two verified lines *tup5-2* and *tup5-3* were used for further phenotypical analyses. The insertion loci predicted by Alonso et al. (2003) and <http://signal.salk.edu/cgi-bin/tdnaexpress> are shown in Figure 5-37.

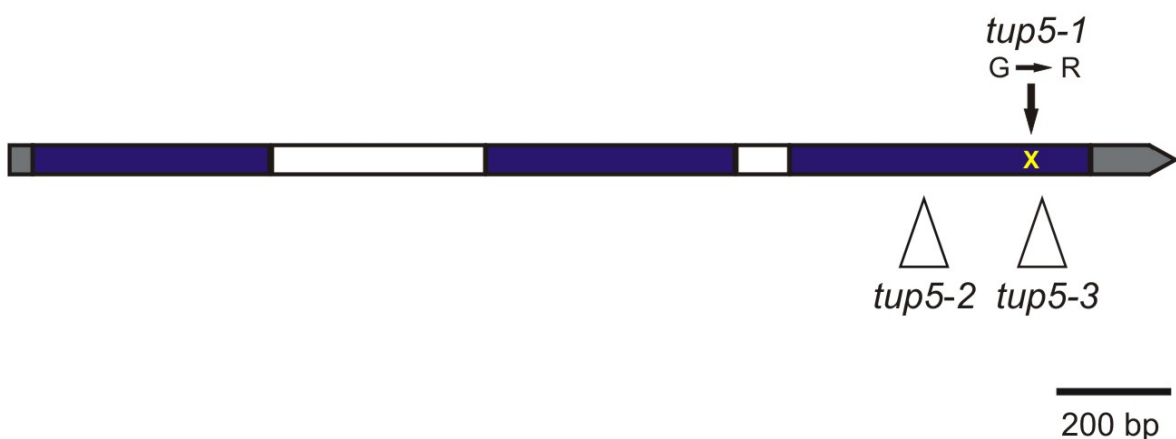


Figure 5-37: Schematic representation of the gene At1g80600 with the mutation sites of different alleles. Blue bars: exons; white bars: introns; grey bar and arrow: UTRs; black arrow: point mutation of *tup5-1* in base n° 1735 (a transition from the nucleotide G to A, which causes an amino acid exchange G→R); white arrow heads: predicted T-DNA insertion loci of *tup5-2* and *tup5-3*. (modified from MIPS).

Table 5-6: Putative T-DNA insertion lines in At1g80600 screened for root phenotype and tested via PCR.

1000-Promoter: insertion within 1000 bp of promoter region. 300-UTR5 / -3: insertion within 300 bp of 5' or 3' untranslated region of the gene (Alonso et al. (2003) and <http://signal.salk.edu/cgi-bin/tdnaexpress>).

Working name	New official name	NASC code	SALK / SAIL number	T-DNA insertion locus (according to database)	Experimental result
<i>TUP5</i> - IS1	-	N504776	SALK_004776	1. Exon	Insertion could not be confirmed by PCR
<i>TUP5</i> - IT1	<i>tup5-3</i>	N875828	SAIL_672_D10	3. Exon	Yes. PCR product on genomic DNA
<i>TUP5</i> - IT2	<i>tup5-2</i>	N878354	SAIL_1171_B12	3. Exon	Yes. PCR product on genomic DNA
<i>TUP5</i> - IS2	-	N622547	SALK_122547	1000-Promoter	Insertion could not be confirmed by PCR
<i>TUP5</i> - IT3	-	N800360	SAIL_7_D11	1000-Promoter	Insertion could not be confirmed by PCR
<i>TUP5</i> - IS3	-	N601072	SALK_101072	300-UTR5	Insertion could not be confirmed by PCR
<i>TUP5</i> - IT4	-	N831132	SAIL_705_A07	300-UTR3	Insertion could not be confirmed by PCR
<i>TUP5</i> - IS4	-	N648692	SALK_148692	300-UTR5	Did not germinate

5.7.1 Homozygous *tup5-2* and *tup5-3* insertion alleles are embryo lethal

Both confirmed T-DNA insertion lines *tup5-2* and *tup5-3* were screened for homozygous plants. F₁ populations of heterozygous self-fertilised parents of both lines were tested by PCR on genomic DNA. Among 118 plants tested in *tup5-2* and 62 plants tested in *tup5-3* no homozygous line was found. This indicates that the homozygous state might be lethal for both alleles. Siliques of heterozygous *tup5-2* and *tup5-3* plants were cleared and examined for malformed or missing embryos. Indeed, empty spaces in the siliques of both lines were visible (Figure 5-38). Microscopical examinations showed that these spaces in the siliques contained very small, aborted ovules or embryos (Figure 5-39). The percentage of aborted embryos was about $42 \pm 4\%$ in *tup5-2* and $35 \pm 7\%$ in *tup5-3* while in WT and *tup5-1* only 1 to 2% of aborted embryos were found (Table 5-7).



Figure 5-38: Siliques of heterozygous *tup5-2* and *tup5-3* plants with WT and *tup5-1* as control. Siliques were cleared by the chloralhydrate method (Yadegari *et al.*, 1994).

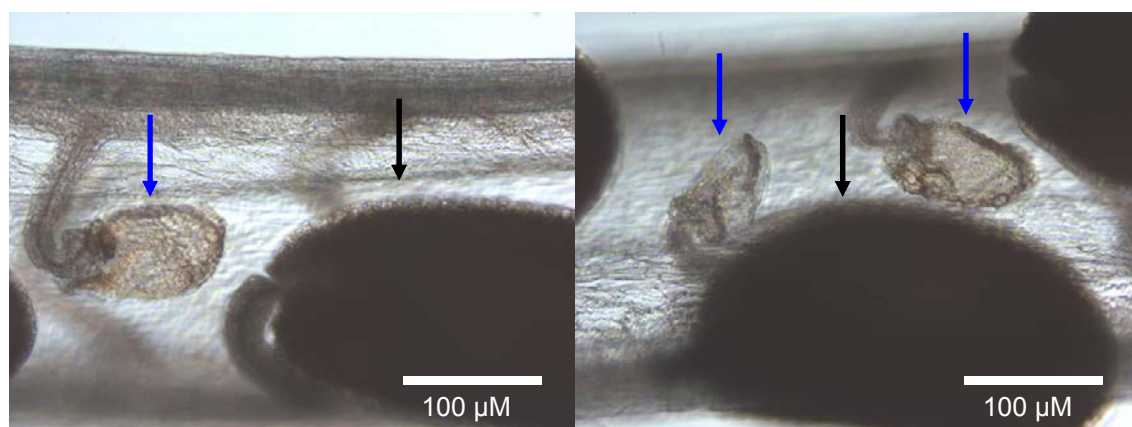


Figure 5-39: Aborted embryos in siliques of heterozygous *tup5-2* plants. Black arrows: normally developed seeds, blue arrows: seeds which arrested development. Siliques were cleared by the chloralhydrate method and dissected (Yadegari *et al.*, 1994).

Table 5-7: Seed filling of silique in WT, *tup5-1* and heterozygous *tup5-2* and *tup5-3* plants.

Seeds and aborted embryos were counted under the binocular. Mean values of $n = 5$ siliques for WT and *tup5-1* each and $n = 10$ for *tup5-2* and *tup5-3* each. Significance: *** $P < 0,001$, Student's *t* test comparing WT with the other lines respectively.

Line	Percentage of aborted embryos per silique [%]
WT	$0,6 \pm 0,8$
<i>tup5-1</i>	$2,3 \pm 2,2$
<i>tup5-2</i> (IT 2-8)	$41,9 \pm 4,3$ ***
<i>tup5-3</i> (IT 1-13)	$34,9 \pm 6,7$ ***

Another interesting aspect was the meiotic drift found in the F_1 generation of heterozygous self-fertilised *tup5-2* and *tup5-3* lines. In *tup5-2* only $36 \pm 10\%$ of the plants and in *tup5-3* $43 \pm 11\%$ were heterozygous for the T-DNA insertion allele in At1g80600 (Table 5-8). All

other plants contained the *TUP5/TUP5* allele combination. According to Mendel's Laws, the ratio between WT and heterozygous (het) plants should be 1:2. For *tup5-2* the ratio was 1,7:1 and for *tup5-3* 1,3:1. Thus, the T-DNA insertion alleles were heavily under-represented in the segregating populations. Curiously, when using the number of *TUP5/TUP5* individuals to calculate the number of heterozygous and *tup5-2* or *tup5-3* homozygous plants that should have been produced in a silique of a heterozygous plant, the number of aborted ovules seems too low to represent these individuals. In the case of heterozygous *tup5-2* plants, the number of "missing plants" was calculated to be $60 \pm 6\%$ and in the case of heterozygous *tup5-3* plants as $55 \pm 10\%$ (raw data not shown), while the percentage of counted aborted embryos was $42 \pm 4\%$ and $35 \pm 7\%$ respectively (Table 5-7).

Reciprocal crosses of *tup5-2* and *tup5-3* heterozygous plants with WT were done to find out whether the embryo development was affected (leading to the lethality), or whether pollen and/or ovule fertility was impaired. PCR analysis showed that the T-DNA insertion allele was transmitted into the F_1 generation of the crossings by both, pollen and ovule. Though, in both cases the transmission frequency was reduced: Only 20 to 40% of the F_1 generation carried the T-DNA insertion allele (data not shown), instead of 50% which would have been expected for non-lethal gametes according to Mendel's Law.

The low T-DNA allele frequency in the self-fertilised *tup5-2* and *tup5-3* lines and in the reciprocal crosses indicates an impairment of embryo development even in a heterozygous state. It seems that *TUP5* null alleles reduce gametophytic fitness and therefore cause meiotic drift. A clear origin of the lethality could not be identified in these analyses. A combination of pollen, ovule and embryo lethality might be responsible for the inexistence of homozygous plants and the reduced number of heterozygous plants.

Table 5-8: Segregation of the T-DNA insertion allele in the F_1 populations of heterozygous self-fertilised *tup5-2* and *tup5-3* lines.

T-DNA insertion line	Percentage of plants <i>TUP5/TUP5</i>	Percentage of plants <i>TUP5/tup5-2</i> or <i>TUP5/tup5-3</i>	Total number of analysed plants per line	Observed ratio	Expected ratio
<i>tup5-2</i>	$64 \pm 10\%$	$36 \pm 10\%$	118	1,7:1	1:2
<i>tup5-3</i>	$57 \pm 11\%$	$43 \pm 11\%$	62	1,3:1	1:2

5.7.2 Phenotypic analysis of transheterozygous plants

To study the phenotype of transheterozygous *tup5* plants, crosses of heterozygous *tup5-2* and *tup5-3* plants with *tup5-1* were done. In F₁ progeny of both crossing combinations, *tup5-2* × *tup5-1* and *tup5-3* × *tup5-1*, WT-like plants and plants with a *tup5-1*-like phenotype were found (Figure 5-40, A). From the plants with a *tup5-1*-like phenotype, 16 were genotyped. All plants contained the T-DNA insertion and the *tup5-1* allele. WT-like plants of these populations did not contain the T-DNA-insertion allele (41 plants genotyped). Therefore, it seems that the allele combination *tup5-1/tup5-2* or *tup5-1/tup5-3* leads to a *tup5-1*-like phenotype, while *tup5-1/TUP5* is known to have WT phenotype because the mutation is recessive (chapter 3.4). On average $17 \pm 6\%$ of the F₁ generation had a *tup5-1* phenotype in the different crossing combinations (data not shown). This is much lower than the expected 50%, when supposing that the phenotype appears in the transheterozygous allele combination. The transheterozygous plants, which are supposed to have an even more reduced At1g80600 activity than *tup5-1* were phenotypically analysed.

The *tup5*-transheterozygous plants produced a range of phenotypes, one class consisting of “*tup5-1*-like” phenotype, another class with a more severe phenotype than *tup5-1*, which did not produce true leaves when grown under standard *in vitro* conditions, and an extremely impaired phenotype: bleached plants with very small cotyledons (Figure 5-40, B). The transheterozygous seedlings were transferred to medium containing 250 μM arginine for 18 days to produce roots and were then transferred to soil for cultivation in the greenhouse in summer. The general development and life cycle was slower in the transheterozygous plants than in WT. The rosette and the root of soil-grown plants developed normally. In contrast, the flower development was impaired in the transheterozygous plants (data not shown). The flower organs were malformed. The sepals and petals were thinner and more pointed than in the WT and the sepals were longer compared to the WT. The stamens did not produce pollen and the gynoecia remained small and undeveloped (data not shown). Transheterozygous plants were watered with 200 μM arginine and sprayed with 1 mM, later 2 mM arginine solution as soon as they were transferred from arginine containing medium to soil, to test whether the sterility phenotype can be complemented by external application of arginine. The seed production could not be restored. A few single seeds were found per plant (not more than ten per plant) (data not shown).

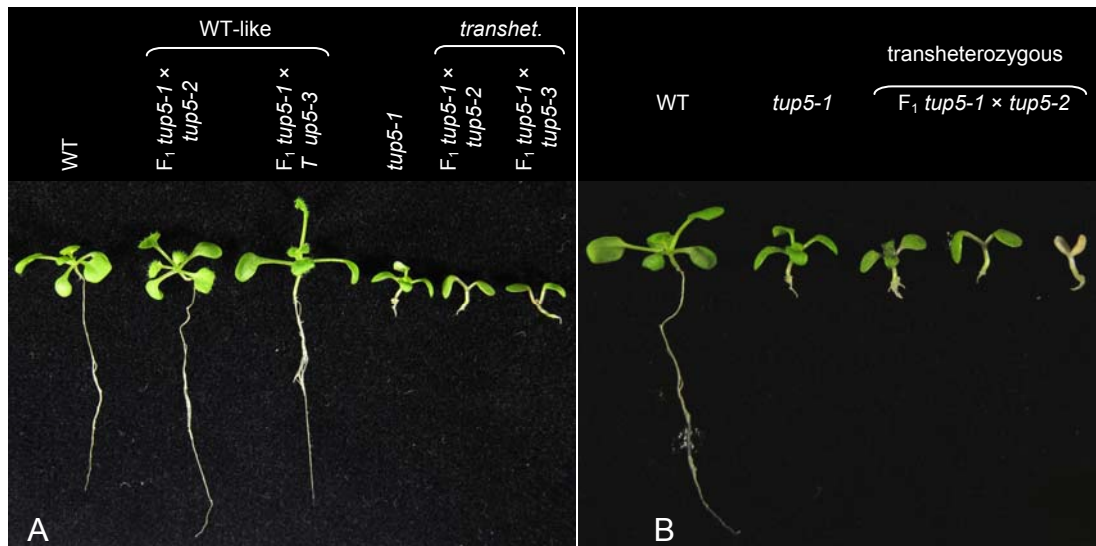


Figure 5-40: Phenotype of *tup5*-transheterozygous seedlings.

A: Phenotype of the F_1 progeny of crosses between *tup5-1* and *TUP5/tup5-2* or *TUP5/tup5-3* respectively. From left to right: WT, WT-like plants in the F_1 generation of *tup5-1* \times *TUP5/tup5-2* and *tup5-1* \times *TUP5/tup5-3* respectively, *tup5-1*, transheterozygous (transhet.) *tup5-1*-like plants in the F_1 generation of *tup5-1* \times *TUP5/tup5-2* and *tup5-1* \times *TUP5/tup5-3*. B: Range of transheterozygous phenotypes in the F_1 generation of *tup5-1* \times *TUP5/tup5-2*. From left to right: WT, *tup5-1*, three transheterozygous plants (which had been transferred to arginine containing medium for seedling rescue since three days, therefore starting to produce small secondary/adventitious roots, because arginine supplementation restored root growth.). All plants were 15 d old.

Seasons and resulting abiotic factors might alter the phenotype of transheterozygous plants

As stated above, the transheterozygous plants had a phenotype comparable or more severe than *tup5-1* when grown *in vitro* (Figure 5-40, A and B). As *tup5-1* develops a normal root system when germinated and grown on soil, the root development of transheterozygous plants was tested under these conditions. In transheterozygous plants grown directly on soil in summer the root grew longer than *in vitro* (compare Figure 5-40 to Figure 5-41, A), but not as long as WT, as in the case of *tup5-1* (chapter 3.4) (Frémont, 2004). The shoot development of the transheterozygous plants grown on soil was again heavily impaired, comparable to *in vitro* culture. The shoot actually stopped developing at the cotyledon stage, while the first pair of true leaves remained tiny (Figure 5-41, A). In rare cases *tup5-1* was also severely impaired when grown in the greenhouse in summer (data not shown). The development of transheterozygous plants on soil was again monitored in the greenhouse in winter. In this experiment, the developmental impairment was less severe (Figure 5-41, B and C). The transheterozygous plants developed in a range from small, slowly growing plants to almost normal sized plants (but with retarded growth) with small siliques containing a few seeds (Figure 5-41, B and C). Culture conditions and seasonal light changes might play a role in the severity of the transheterozygous phenotype.

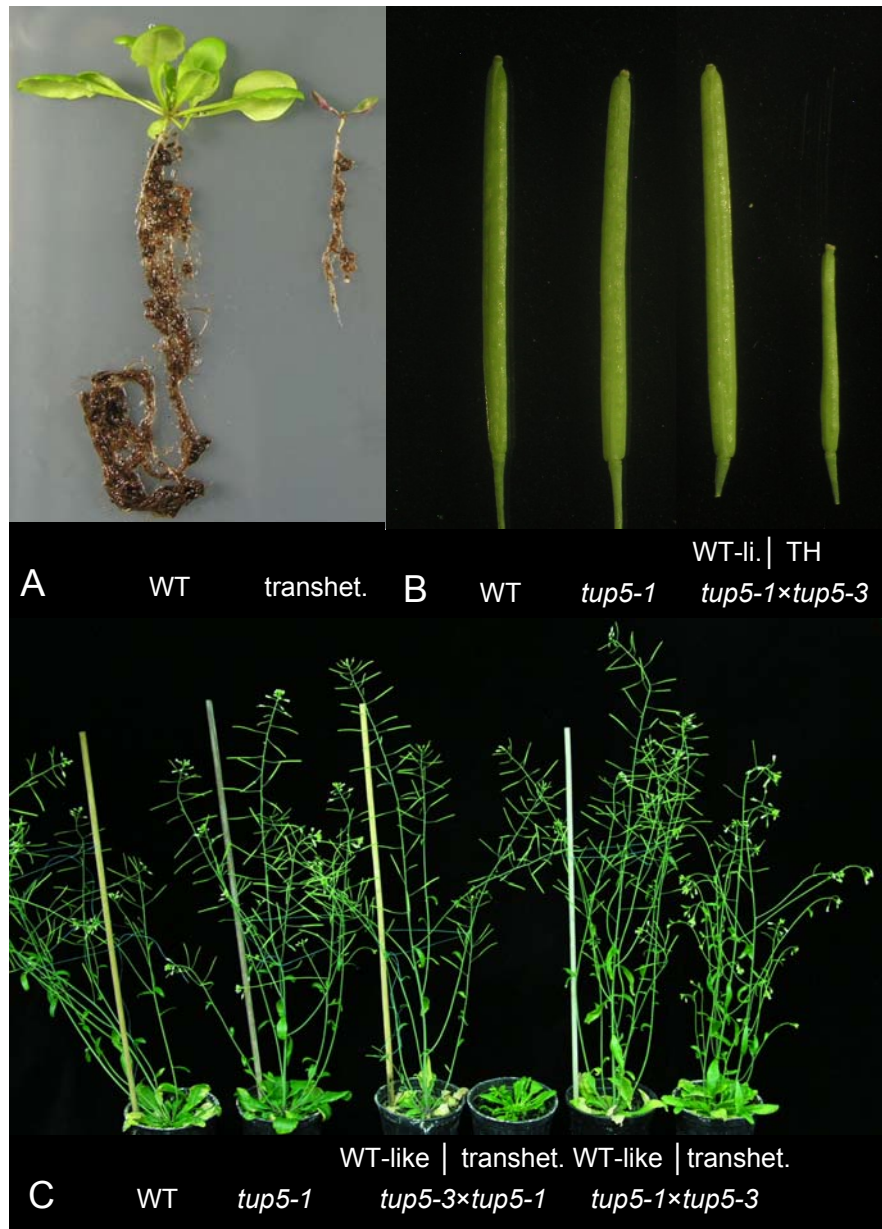


Figure 5-41: Phenotype of the transheterozygous plants grown on soil in summer and winter in the greenhouse.

A: Plants in summer (24 d old). The transheterozygous plants stopped growing at this stage. B and C: Plants in winter (38 d old). B: Siliqua phenotype. C: Shoot phenotype. Note the improved development of transheterozygous plants in winter. In all cases seeds were directly germinated on soil, as growth on medium would probably lead to developmental problems due to light exposure of the roots. Plants marked as “*tup5-3*×*tup5-1*” or “*tup5-1*×*tup5-3*”: Plants from F₁ generation of crosses between homozygous *tup5-1* and heterozygous *tup5-3* plants. WT-like (WTI-li.): Plants which received the WT *TUP5* allele from the *tup5-3* parent; transheterozygous (TH): Plants which received the T-DNA insertion allele from the *tup5-3* parent.

5.8 Analysis of plants overexpressing TUP5

The function of a gene during plant development can be investigated through loss-of function or gain-of-function mutations, overexpression (OE) of the gene of interest is an example of the latter. The cloning and transformation of *35S::TUP5* into WT and *tup5-1* back-

ground and the confirmation of the functionality of the construct were described in chapter 5.2.7. The effect of an increased expression of *TUP5* on plant development is reported in the following chapter.

5.8.1 Root phenotype of *TUP5* overexpressing plants

The root elongation of *TUP5* overexpressing lines (in WT background) was measured *in vitro*. Eight non-segregating lines (T₂ generation) originating from four primary transformants (OE1, OE2, OE4 and OE5) were analysed. The T₂ lines originating from a primary transformant were considered as one line (for example: OE2-1 and OE2-2 are both from line OE2). One line originating from each independent transformant is shown exemplarily in Figure 5-42. The plants were grown on vertical plates of MS medium at standard conditions. The root length of each seedling was marked as a starting point after three days of growth. The root length was then marked again in 6-, 10- and 13-days-old plants. Three growth phases (GP) were defined: Growth phase 1 comprises day 3 to 6, growth phase 2 spans day 6 to 10 and growth phase 3 comprises day 10 to 13. The root length of the seedlings in each phase was measured with the programme ImageJ (Abramoff *et al.*, 2004). A daily growth rate was calculated for each line in each growth phase (GP). The results are presented separately for the different growth phases in Figure 5-42. In growth phase 1 all overexpressing lines except OE4-2 had growth rates comparable to WT (WT: $0,47 \pm 0,06$ cm /day) (Figure 5-42, A, not all data shown). In the second growth phase the root growth in the overexpression line OE4 (consisting of OE4-1, OE4-2 and OE4-3) was strongly reduced (1,6 to 10% of WT) (Figure 5-42, B, not all data shown). A less strong (but significant) reduction of root growth was found in line OE2 ($0,41 \pm 0,09$ and $0,46 \pm 0,04$ cm /day in OE2-1 and OE2-2 respectively, compared to WT: $0,60 \pm 0,07$ cm /day). The other two overexpression lines OE1 and OE5 had root growth rates comparable to WT in GP2 (Figure 5-42, B). In the third growth phase line OE4 and line OE2 roots completely stopped to grow (Figure 5-42, C). In OE1 the growth rate was significantly reduced compared to WT (with a significance of $P < 0,001$ in a Student's *t* test) (data not shown). The root growth in OE5 remained comparable to WT (Figure 5-42, C).

Interestingly, the root growth arrest seemed to correlate with the frequency of the phenotype occurring in cauline leaves of the *TUP5* overexpressing lines (chapter 5.8.2 and Figure 5-43, D). In the T₂ generation of OE2 and OE4 the cauline leaf phenotype was fre-

quently found, while it was rare in the T₂ generation of OE1 and not seen in the T₂ generation of OE5 (data not shown).

The root growth was also examined when the *TUP5* overexpressing lines were cultivated on soil. The root ball was assessed in mature plants (37 d) of 4 independent lines (seven T₂ lines originating from the four independent *TUP5* overexpressing T₁ lines: OE1, OE2, OE4 and OE5). The soil-grown root system of all *TUP5* overexpressing lines was comparable to that of WT (Figure 5-43, A and B).

5.8.2 Leaf and silique phenotype

The rosette leaves of the *TUP5* overexpressing lines were analysed phenotypically. For this purpose 16 independent transgenic lines, together with WT and *tup5-1* as controls, were grown on soil (in single pots) in a growth chamber under standard conditions. From all 16 lines none showed a recurring rosette leaf phenotype (Figure 5-43, C). In contrast, the cauline leaves in 7 of 14 independent transgenic lines formed chlorotic leaf areas in the intervascular tissue, while the leaf vasculature remained darker green (Figure 5-43, D). This was also observed in cauline leaves that appeared at the bottom of the floral shoot, close to the rosette leaves (data not shown). In Figure 5-43, D, plants were from the T₁ generation. This phenotype recurred in the T₂ generation (data not shown).

The siliques of transgenic plants overexpressing *TUP5* were compared to WT siliques. Their surface appeared to be wrinkled in comparison to the smooth surface of WT siliques. The forming seeds were more visible beneath the valves in the transgenic plants than in WT (Figure 5-43, E).

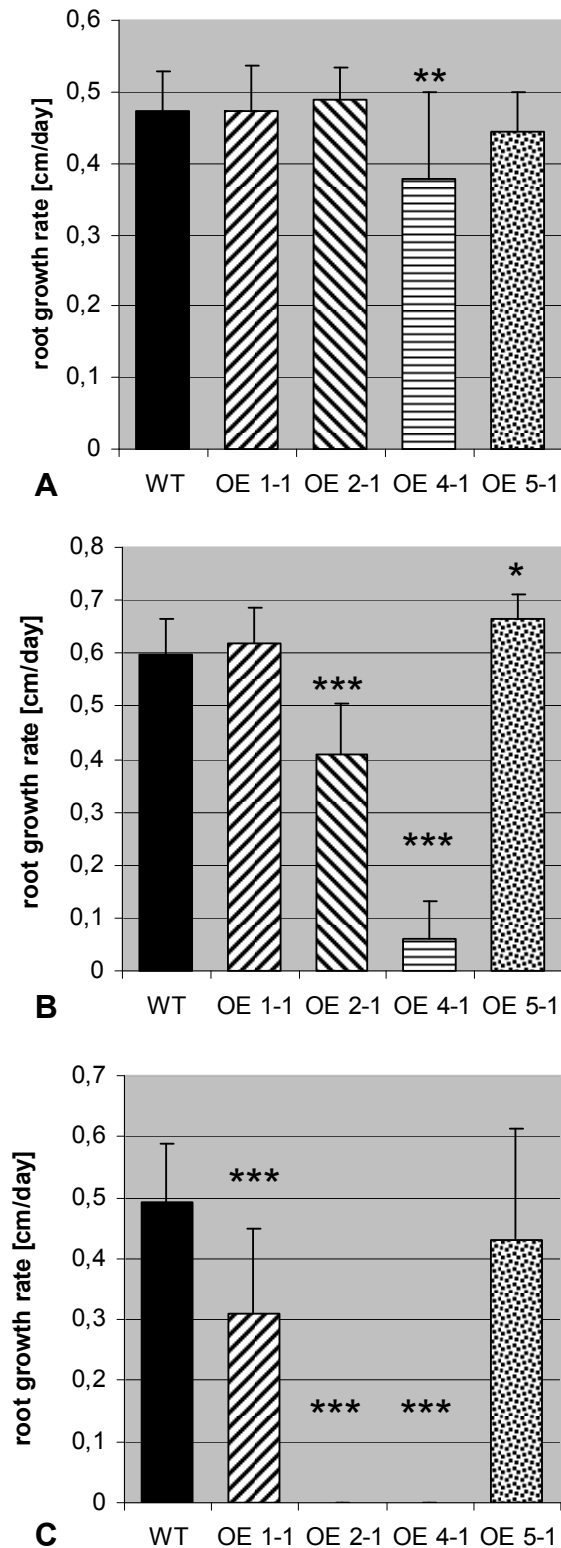


Figure 5-42: Root growth rates of *TUP5* overexpression lines during different growth phases. From left to right: WT as control and the overexpression lines (non-segregating T_2 generation). A: Growth phase 1 from day 3 to 6, B: Growth phase 2 from day 6 to 10; C: Growth phase 3 from day 10 to 13. Plants were grown at standard conditions on vertical plates of MS medium. The primary root tip was marked at the indicated time points and root length was measured with the programme ImageJ (Abramoff *et al.*, 2004). Mean \pm SD of 6 to 30 plants. Significance: * $P < 0,05$; ** $P < 0,01$; *** $P < 0,001$, Student's *t* test comparing WT and OE lines.

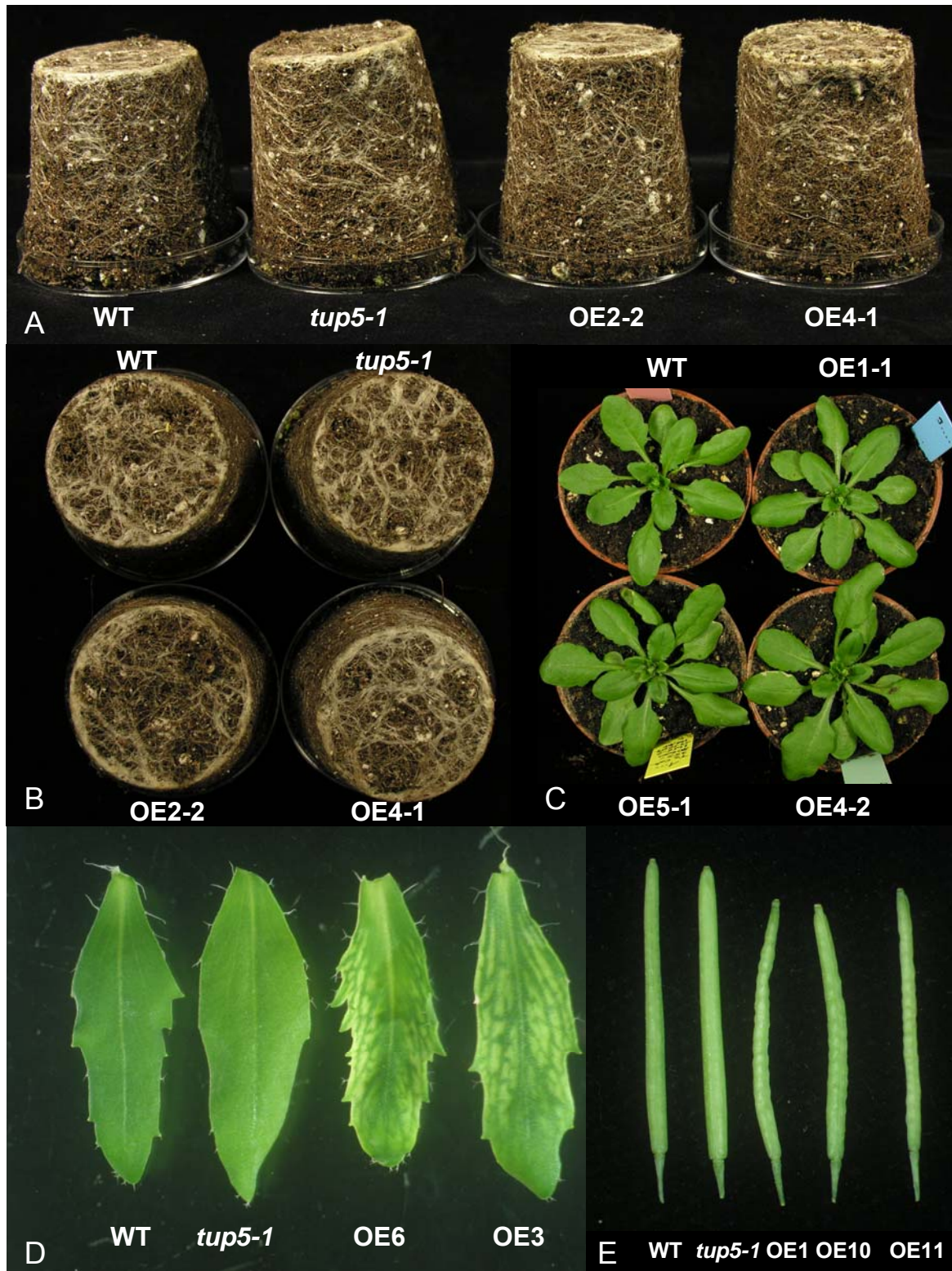


Figure 5-43: Phenotype of soil-grown *TUP5* overexpression lines.

A and B: Root system of WT, *tup5-1* and *TUP5* overexpressing lines (the two independent T_2 overexpressing lines OE2-2 and OE4-1). Typical examples of roots from 37-d-old plants are shown after removal of the pots. A: Side view of the root ball. B: Root ball seen from below. C: Rosette leaf phenotype of 24-d-old plants. D: Cauline leaf phenotype (T_1 generation) of 30-d-old plants. E: Silique phenotype of 44-d-old plants. The plants were all cultivated in a growth chamber under long day conditions.

5.8.3 Free amino acid content of *TUP5* overexpression plants

The *tup5-1* mutation affects the amino acid metabolism (chapter 5.4, A). The affected gene, *ACOAT*, is involved in arginine synthesis (chapter 5.2.8 and 5.3). In accordance with this, the free arginine content is strongly decreased in *tup5-1* (chapter 5.4, A). The overexpression of *TUP5* led to a complementation of the *tup5-1* root phenotype (chapter 5.2.7). If the root phenotype in *tup5-1* is caused by the lack of arginine, the free arginine content in *tup5-1* overexpressing *TUP5* must be re-established to WT level, if not be increased. To test this hypothesis and to monitor general changes in amino acid metabolism in *TUP5* overexpressing plants, HPLC analysis were done with several transgenic lines in *tup5-1* and WT background. The transgenic plants had to be used in the T₁ generation, which still segregates. Therefore the plants were grown on PPT containing MS medium. To detect possible effects of PPT on amino acid metabolism, a PPT-resistant *Arabidopsis* line (*pCKX1::GUS*) was grown in parallel on MS medium with and without PPT.

A Arginine content: increased to normal level, but not higher than WT

The WT control plants contained 2099 ± 655 nmol arg /g FW, while *tup5-1* contained 509 ± 40 nmol arg /g FW (Figure 5-44, A, Figure 9-4 and Table 9-13). Between *pCKX1::GUS* plants grown on medium with or without PPT no significant differences in arginine concentration were found (Table 9-13). PPT seems therefore not to have an effect on arginine level in *Arabidopsis*. In the overexpression lines with *tup5-1* background (OE I - OE IV) arginine concentration was in the range from 1599 to 3054 nmol arg /g FW (Table 9-13) with an average value of 1910 ± 474 nmol arg /g FW (data not shown). This average is in the range of WT. Also the *TUP5* overexpression lines with WT background had arginine concentrations comparable to WT, except for one line (OE 5), which had a lower arginine concentration than WT (Figure 9-4 and Table 9-13). The arginine concentration of OE 1, OE 2, OE 3, OE 7, OE 8, OE 9 and OE 10 was between 1475 and 2506 nmol arg /g FW (Table 9-13). A dramatic increase in arginine concentration might have been expected in the *TUP5* overexpression lines, but was not observed (Figure 5-44, A, Figure 9-4 and Table 9-13).

B Other changes in amino acid content in *TUP5* overexpression lines

Asparagine (asn) was increased by a factor of three in *tup5-1* compared to WT (11100 ± 791 compared to 3677 ± 667 nmol asn /g FW respectively) (Figure 5-44, B, Table 9-14). In *tup5-1* lines transformed with the *TUP5* overexpression construct, the level decreased to a

range from 3431 to 4819 nmol asn /g FW, which is comparable to WT (Figure 5-44, B and Table 9-14). Also the *TUP5* overexpression lines with WT background had asparagine levels comparable to WT (Figure 5-44, B and Table 9-14).

Glutamine (gln) was increased by a factor of seven in *tup5-1* compared to WT (*tup5-1*: 67476 ± 4741 compared to WT: 9419 ± 704 nmol gln /g FW) (Figure 5-44, C and Table 9-15). The concentration of glutamine was dramatically decreased in At1g80600 overexpression lines with *tup5-1* background, though the level was still elevated compared to WT: The concentration of gln was in a range of 13163 to 18848 nmol gln /g FW (Table 9-15). A possible influence of PPT might explain this fact: *pCKX1::GUS* plants grown on PPT contained approximately the double amount compared to plants of the same line grown on medium without PPT (19603 ± 1711 compared to 10338 ± 1335 nmol gln /g FW) (Table 9-15).

The tryptophan (trp) concentration of WT and *tup5-1* was 153 ± 35 and 317 ± 103 nmol trp /g FW respectively (Figure 5-44, D and Table 9-16). In the *TUP5* overexpression lines the concentration varied from 31 to 120 nmol trp /g FW. Tryptophan was significantly decreased in *TUP5* overexpression lines compared to WT, when comparing all WT samples to all overexpression lines in a Student's *t* test ($P \approx 0,005$, considered as significant when $P < 0,05$) (data not shown).

The same was the case for lysine (lys): It was significantly decreased in *TUP5* overexpression lines compared to WT. The lysine concentration in WT was 712 ± 296 and in *tup5-1* 1698 ± 598 nmol lys /g FW (Figure 5-44, E and Table 9-17). In *TUP5* overexpression lines the lowest concentration was 77 and the highest 681 nmol lys /g FW (Table 9-17). The decrease in lysine concentration was significant when comparing all WT samples to all overexpression lines in a Student's *t* test ($P \approx 0,025$).

Also threonine, serine and phenylalanine were significantly reduced in *TUP5* overexpression lines compared to WT (on average 21% reduction of thr, 19,5% of ser and 31% reduction phe in overexpression lines) (data not shown).

Glycine could not be detected in 17-d-old light-grown *tup5-1* plants (Figure 5-44, F and Table 9-18), while in 7- or 11-d-old light-grown *tup5-1* seedlings the concentration of free glycine was increased compared to WT in all three measurements (Figure 5-25 to Figure 5-27). In *TUP5* overexpression lines the glycine level was significantly increased compared to WT ($P \approx 0,0001$ in a Student's *t* test, data not shown) (Figure 5-44, F and Table 9-18).

5. RESULTS

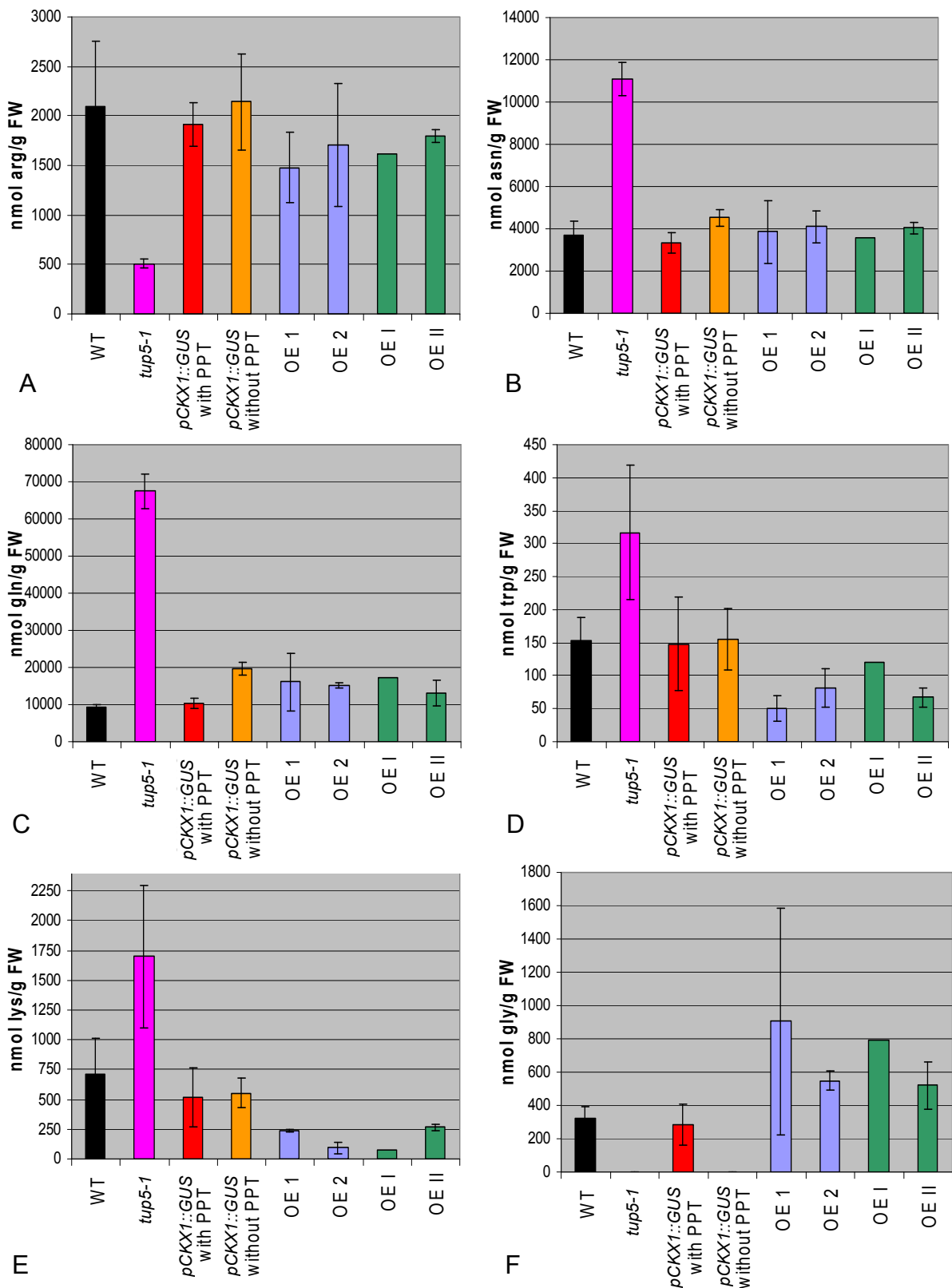


Figure 5-44: Free amino acid content in *TUP5* overexpressing lines.

A: Arginine (arg). B: Asparagine (asn). C: Glutamine (gln). D: Tryptophan (trp). E: Lysine (lys). F: Glycine (gly). Plants (17 d old) were grown *in vitro*: WT, *tup5-1* and *pCKX1::GUS* as controls were grown on MS medium without PPT, transgenic plants: *TUP5* overexpressing lines and *pCKX1::GUS* were grown on MS medium containing PPT. Examples of overexpression lines (OE) of *TUP5* (T_1 generation). OE 1 and 2: WT background; OE I and II: *tup5-1* background. The tested lines were independent overexpression lines in WT or *tup5-1* background respectively. (WT: n = 5; *tup5-1*: n = 2; *pCKX1::GUS* with PPT: n = 4; *pCKX1::GUS* without PPT: n = 3; *TUP5* overexpressing lines: n = 2, except for OE I: n = 1.)

6 Discussion

At the beginning of this work it was known that in the mutant *tup5-1* the blue part of the light spectrum was responsible for the loss of root meristem (Frémont, 2004). But it was not yet clear which organ or part of the plant perceives the inhibiting light signal. It was also not known whether the cells of the primary root, which become mitotically inactive and differentiate in light, are still viable or metabolically active. The identity of the *TUP5* gene was unknown, though the mapping interval had been narrowed down to 88 kb on the lower arm of chromosome I (Frémont, 2004). In this work the *tup5-1* mutation was identified and the predicted gene function needed to be verified. Other questions addressed in this work were: Where and when is *TUP5* expressed during plant life? Is the gene light-regulated? How does overexpression or loss of function of *TUP5* affect plant development? These questions have been investigated and the results will be discussed in the following chapters.

6.1 Determination of the *TUP5* gene function

A point mutation in At1g80600 causes the root phenotype in tup5-1

The mapping of the *tup5-1* mutation led to an interval of 88 kb (chapter 5.2.1). The size of the interval could not be reduced because of the low recombination frequency in this genomic region: Only one recombination event was found at each border of the 88 kb interval in a mapping population of 2354 plants. Various strategies were pursued to find the mutated gene, but with none of them *TUP5* could be identified (chapter 5.2). Therefore, the method of complementing *tup5-1* plants with BAC subclones was finally chosen (chapter 5.2.5). From 27 BAC subclones, three subclones of different sizes which all contained one predicted gene named At1g80600 complemented the *tup5-1* root phenotype. The smallest subclone Sfo4 contained only At1g80600 as complete ORF. At1g80600 was therefore the most likely candidate gene for *TUP5*. One clone, Spe1.21, also containing At1g80600 did not complement the root phenotype in *tup5-1*. In this clone only 1228 bp upstream of At1g80600 were included. This is probably not the complete promoter sequence necessary for a correct expression of At1g80600. As an independent proof, *tup5-1* was transformed with the cDNA of At1g80600 under the control of the constitutive CaMV 35S promoter. Again, the root phenotype of *tup5-1* was complemented, confirming that *TUP5* corresponds to At1g80600. A point mutation was found in the third predicted exon of

At1g80600 in *tup5-1* (chapter 5.2.6). A base transition leads to an amino acid exchange from glycine to arginine in the amino acid residue n° 424 (TUP5^{G424R}). This mutation is not predicted to cause changes in secondary structure, though this would need confirmation through X-ray crystallography. The mutation does not lie in a known functional domain of the protein, but the affected amino acid is conserved throughout bacterial, fungal and plant kingdom (see chapter 5.2.8) and might therefore be crucial for the protein function. The mutation might alter the catalytic and regulatory properties of TUP5.

To map the function of different protein domains and amino acid residues in TUP5, several new alleles could be created. For this purpose mutated *TUP5* transgenes might be tested in a heterologous system, for example in the arginine auxotrophic yeast ACOAT mutant (see chapter 5.3.2). The growth rate of the transformed yeast mutant can be used as an indicator of the catalytic efficiency of the mutated TUP5 protein. Subsequently, interesting *TUP5* mutations could be introduced into an *Arabidopsis* knockout background. Plants homozygous for a T-DNA-insertion in *TUP5* are not viable (chapter 5.7.1). Therefore, heterozygous *TUP5* loss-of-function mutants (*tup5-2* or *tup5-3*) would have to be transformed and the next generations could be screened for plants homozygous for the T-DNA-insertions, surviving due to the mutated transgene. It might be necessary to grow the primary transformants on medium containing arginine to enable the seedlings to survive. The phenotype of seedlings expressing the transgene could be assessed and enzymatic activity assays could be performed with these mutated proteins to determine the changes in catalytic efficiency for the different mutations.

TUP5's function as an acetylornithine aminotransferase

The function of At1g80600 was predicted as “putative acetylornithine aminotransferase” (EC 2.6.1.11.) in databases such as TAIR or MIPS. From studies in *E. coli* and other bacteria and fungi, it is known that ACOAT catalyses the biosynthesis of acetylornithine (chapter 5.2.8). Acetylornithine is a non-proteinogenic precursor amino acid in the pathway of arginine biosynthesis (Vogel, 1953; Albrecht and Vogel, 1964; Cunin *et al.*, 1986; Davis, 1986). If ACOAT activity is impaired, a lack of acetylornithine and arginine can be expected in mutant plants. Indeed, the concentration of free arginine was significantly reduced in *tup5-1* plants compared to WT (chapter 5.4). Moreover, the root phenotype of *tup5-1* was complemented by supplementation of the mutant seedlings with acetylornithine, ornithine, citrulline and arginine (chapter 5.3.1). These findings were not sufficient to prove that TUP5 is an acetylornithine aminotransferase, but it showed that it has a func-

tion in arginine biosynthesis. To verify the predicted gene function, a heterologous complementation test was done with a yeast mutant lacking its acetylornithine aminotransferase (chapter 5.3.2) (Heimberg *et al.*, 1990). The yeast mutant, which is dependent on arginine supplementation, became autotrophic when transformed with the cDNA of At1g80600 under the control of a constitutive yeast promoter. This result gives strong evidence for At1g80600 to encode the predicted *Arabidopsis* acetylornithine aminotransferase. The high sequence homology of *TUP5* to *ACOATs* of several different species (see Figure 5-18) makes its function as acetylornithine aminotransferase activity most likely. Though, an enzymatic assay showing a reduced ACOAT activity in *tup5-1* compared to WT could give the final proof.

6.2 TUP5 loss-of-function affects gametogenesis and embryogenesis

After the characterisation of the *tup5-1* mutant, eight putative T-DNA insertion alleles of *TUP5* were analysed to get more information on the gene function (chapter 5.7). A point mutation as in the case of *tup5-1* often only reduces the functionality of a gene. In contrast, T-DNA insertions frequently cause a complete gene knockout if an exon is affected (Krysan *et al.*, 1999). In two independent lines, *tup5-2* and *tup5-3*, an insertion within the third exon of *TUP5* was confirmed by PCR. These lines were used for further studies.

TUP5 loss-of-function causes gametophytic or embryo lethality

Segregating populations of both alleles, *tup5-2* and *tup5-3*, were screened for homozygous plants to analyse them phenotypically, but none were found. The absence of homozygous plants is a strong indication for lethality of gametes or embryos. Very small, underdeveloped ovules or embryos found in the siliques of *tup5-2* and *tup5-3* plants confirmed this supposition (chapter 5.7.1). Moreover, the number of heterozygous plants in segregating populations of *tup5-2* and *tup5-3* was much lower than expected, suggesting that also the heterozygous allele combination leads to a reduced embryo survival rate. The reduced transmission frequency of T-DNA insertion alleles might be due to a dysfunction of ovules or pollen grains carrying this genotype. Reciprocal crosses of *tup5-2* and *tup5-3* with WT showed that the T-DNA insertion alleles could be transmitted by both gametes, but at a lower frequency than expected. This proves that pollen and ovules carrying a disrupted *TUP5* gene can be functional, but produce viable embryos only in a reduced frequency. The reduced transmission and viability might be a combination of a reduced fit-

ness of gametes carrying a *TUP5* null allele and a reduced survival rate of embryos carrying only one functional *TUP5* allele. The exact origin of the embryo lethality was not identified. Further studies would be needed to understand the underlying mechanisms more profoundly.

Transheterozygous plants show retarded growth and reduction of fertility

Transheterozygous plants of *tup5-1/tup5-2* and *tup5-1/tup5-3* were retarded throughout the whole life cycle (chapter 5.7.2). The root remained very short and the shoot did not develop normally in plants grown in summer. The growth impairment of the seedlings was in a range of comparable to *tup5-1* to more severe than *tup5-1*. Transheterozygous plants did not arrest seedling development and could develop to adult plants without arginine supplementation when grown in winter. Different plant phenotypes were found: plants which did not produce generative shoots and normal, though slowly growing plants with WT-like flowers and reduced seed production (Figure 5-41, B and C). This seasonal difference might be due to changing external conditions, for example light, which is known to inhibit root growth in *tup5-1*. The influence of abiotic factors on the development of transheterozygous plants needs further experimental testing. Their development might possibly improve under low light or short day conditions. As a general observation, transheterozygous plants had more severe developmental defects than *tup5-1* which usually developed normally on soil (though slightly slower) and which was not impaired in seed production. This aggravation of developmental defect is probably due to the reduced amount of acetylornithine aminotransferase needed for arginine biosynthesis. Apparently, a graduation of phenotypes depending on the dose of *TUP5* activity can be observed: homozygous *tup5-2* or *tup5-3* plants are not viable (presumably due to a complete knockout of *TUP5*), while transheterozygous plants still have one mutated *tup5-1* allele which might be sufficient to allow plant development under favourable growth conditions, though growth is slower and seed production is severely impaired (Figure 5-41, B and C). *tup5-1* homozygous plants have the mildest phenotype compared to the other genotypes, as they are practically not impaired in development when grown on soil.

Lack of amino acids as a factor of embryo lethality

Meinke (1991) and Bryant et al. (2011) pointed out that embryonic development is often interrupted in mutants defective in essential housekeeping genes, such as amino acid, vitamin, or nucleotide biosynthesis. As a classical example, Meinke (1991) cited a biotin

auxotrophic embryo lethal *Arabidopsis* mutant. Since then, other examples, such as amino acid synthesis mutants were found, showing comparable embryo lethal phenotypes: Seeds were aborted at the preglobular stage of embryo development in many histidine biosynthesis mutants; and in the case of *hisn8* (encoding histidinol dehydrogenase) ovules were aborted (Muralla *et al.*, 2007). A mutation in the gene encoding LL-diaminopimelate aminotransferase (*agd2*) acting in a lysine biosynthetic pathway also causes embryo lethality (Song *et al.*, 2004; Hudson *et al.*, 2006). A knockout mutation in *Δ -1-pyrroline-5-carboxylate synthetase 2* which encodes an enzyme of proline biosynthesis causes embryo lethality as well (Székely *et al.*, 2008). Similarly, a defect in protein translation can lead embryo developmental defects, as seen in the case of many mutants in aminoacyl-tRNA synthetases (Berg *et al.*, 2005). In all cases vital protein production is disturbed, probably therefore causing an arrest in embryo development. Arginine is the amino acid with the highest nitrogen to carbon ration (4:6) (Coruzzi and Last, 2000; Llácer *et al.*, 2008). It is a nitrogen storage form for many plant seeds, such as *Vicia faba*, Soybean, pumpkin, peach tree and many other dicotyledonous plants (Splittstoesser, 1969; Micallef and Shelp, 1989). In *Arabidopsis* seeds arginine can account for 11% of the nitrogen pool (VanEtten *et al.*, 1963; Zonia *et al.*, 1995). Its biosynthesis might therefore have an additional importance during seed development.

The knowledge about how amino acid supply of developing seeds takes place is still incomplete for *Arabidopsis* (Baud *et al.*, 2008). All amino acids, but mainly glutamine, glutamate, aspartate, asparagines, serine and alanine, are transported from source tissues of the mother plant to the seed via the phloem (Sanders *et al.*, 2009). The arriving amino acids can be converted to other amino acids in the seed coat (maternal tissue) or in the embryo (Baud *et al.*, 2008; Sanders *et al.*, 2009). So far it was not clear if *Arabidopsis* embryos need to be arginine autotrophic or whether their demand can be covered by maternal tissue. The embryo lethal phenotype found in *tup5-2* or *tup5-3* suggests that the need of arginine in the developing ovule or embryo might not be covered by import from the heterozygous mother plant. The heterozygous T-DNA lines do not show obvious growth phenotypes except for embryo lethality. As they are presumably hemizygous for *TUP5*, it might be interesting to test whether the transcript level and the arginine content are reduced in these plants. If the single functional *TUP5* allele can sustain a normal free arginine content in the maternal plant, this would prove that normally no sufficient maternal feeding of arginine can be provided and that *TUP5* enzymatic activity in the embryo is necessary for embryo development. If the arginine content is also reduced in the heterozygous maternal

plant, it cannot be excluded that arginine feeding is usually provided by the mother plant, but that it is reduced due to the maternal deficiency. Spraying or watering of heterozygous knockout mutants in histidine biosynthesis genes reduced the rate of embryo abortion (Muralla *et al.*, 2007; Petersen *et al.*, 2010). Siliques of transheterozygous *tup5-1/tup5-2* and *tup5-1/tup5-3* plants were sprayed and watered with arginine, but this did not restore seed set (chapter 5.7.2). One possible reason could be that arginine might not be transported through the siliques into the embryos, another explanation might be that the deficiency was too severe in transheterozygous plants to be complemented by this method. A preliminary observation that the few seeds produced by transheterozygous plants are often located at the basis of the siliques (data not shown) needs to be confirmed. This characteristic is often connected to a reduced transmission of mutant pollen tubes, so that only pollen tubes carrying the WT allele reach the basis of the silique (Meinke, 1991; Muralla *et al.*, 2007). A small scale preliminary test was done to test whether impaired pollen transmission caused decreased fertility in transheterozygous plants: WT pollen was used to pollinate transheterozygous flowers. Again only a few seeds were produced and they were located at the basis of the siliques (data not shown). The fitness of the plants used for this test might not have been optimal, therefore further experiments need to be done. If the result could be confirmed, it would show that reduced pollen transmission does not cause this phenotype. In this case one could speculate that only the first seeds at the basis can develop normally because they can intercept the small quantity of arginine that the mother plant can provide and which is not sufficient to feed the whole silique. A system to monitor arginine *in vivo* by a FRET-sensor might help to understand arginine fluxes in the transheterozygous siliques and the whole plant (Bogner and Ludewig, 2007).

6.3 Effect of overexpression of TUP5 on Arabidopsis development and metabolism

Transgenic plants overexpressing *TUP5* were generated as described in chapter 5.2.7. The functionality of the construct was confirmed because the T₁ generation of all tested transgenic lines showed an increased *TUP5* transcript level compared to WT and the short root phenotype of *tup5-1* was complemented with the 35S::*TUP5* plasmid. In the T₁ generation of transgenic *tup5-1* plants expressing 35S::*TUP5* the arginine content was restored to WT level, while untransformed *tup5-1* plants were arginine-deficient (chapter 5.8.3; Figure 9-4 and Table 9-13 in supplemental data). Not only the arginine content was restored to a WT-like level, also the asparagine level, which was massively increased in 17-d-old *tup5-1*

plants (chapter 5.8.3) was reduced to WT level in transgenic *tup5-1* plants. If the transgene had no direct effect on the metabolism of 35S::*TUP5* plants with WT background, then the reduction of asparagine in transgenic plants with *tup5-1* background must have been caused by indirect changes in metabolism, namely the (partial) restoration of amino acid homeostasis. Glutamine was also dramatically increased in the *tup5-1* mutant in 17-d-old plants, but in this case the transformation with the 35S::*TUP5* construct led to an incomplete reduction of the glutamine content. Also, the *TUP5* overexpressing plants in WT background contained an increased glutamine concentration comparable to the transgenic *tup5-1* plants, possibly due to other deregulating side effects. Asparagine and glutamine are two amino acids used for nitrogen storage and transport (Lea *et al.*, 2007). Accumulation of surplus amino groups in these storage pools in the *tup5-1* mutant might be caused by a reduced protein biosynthesis capacity due to the lack of arginine as a rate limiting compound (Igarashi *et al.*, 2006). A partial normalisation of metabolism might have taken place after complementation of *tup5-1* with 35S::*TUP5* (chapter 5.8.3 and 9.7). The transgenic plants overexpressing *TUP5* were examined for phenotypical differences to WT (chapter 5.8). Adult plants overexpressing *TUP5* exhibited interveinal chlorosis of cauline leaves and wrinkled siliques (chapter 5.8.2). Interveinal chlorosis has been described as an effect of nutrient deficiency, especially in the case of manganese, magnesium and iron (Taiz and Zeiger, 2002, p. 72-75; Waters *et al.*, 2006). Chlorosis appearing on younger leaves, as it is the case for cauline leaves, indicates the deficiency of a nutrient which is not easily remobilised, because the nutrient is not transported from older to younger leaves (Taiz and Zeiger, 2002, p. 72-73). A nutrient level analysis of *TUP5* overexpressing plants might be useful to test whether the changes in amino acid levels found in these plants can cause changes in nutrient levels or nutrient distribution. Asparagine accumulation (and in one case also arginine accumulation) was found during nutrient deprivation (Lea *et al.*, 2007). A connection between amino acid and nutrient homeostasis control might exist in plants. Interestingly, the *nox1* mutant which contains higher levels of arginine and citrulline and overproduces nitric oxide also has a reticulate leaf pattern (He *et al.*, 2004). In contrast to this, Mollá-Morales *et al.* (2011) found that citrulline deficiency caused a reticulate phenotype in carbamoyl phosphate synthase (CPS) mutants. Carbamoyl phosphate and ornithine are the substrates of ornithine carbamoyltransferase (OTC) producing citrulline. The results of Mollá-Morales *et al.* (2011), though, fit well with the observation that inhibition of OTC by phaseolotoxin results in arginine deficiency and chlorosis (Zhang and Patil, 1997). The effect could be reversed by addition of citrulline or arginine (Patil *et*

al., 1972). However, a reticulate leaf pattern was observed quite often in different mutants, it might therefore be a too unspecific phenotype for more accurate conclusions concerning its causes.

The other observed phenotype, bumpy siliques, has previously been described in cases of misexpression of valve-margin-identity factors in valve tissues or in cases of endocarp layer b lignification loss (Dinneny and Yanofsky, 2005). However, it is not known whether the silique phenotype in *TUP5* overexpressing plants is induced by these factors or by other developmental changes.

Root growth was studied in homozygous overexpression lines in T₂ generation because the *tup5-1* mutation causes primary root growth arrest. No effect or an increase in root growth was expected in the case of *TUP5* overexpression. Instead, the primary root of two independent lines out of four examined lines stopped growing (chapter 5.8.1). The reason for this effect might be gene silencing, which also affects the endogenous *TUP5* expression (Depicker and Van Montagu, 1997). This *TUP5* downregulation could therefore lead to a root growth stop resembling the *tup5-1* root phenotype. However, the fact that interveinal chlorosis of cauline leaves and wrinkled siliques were also observed in the T₂ generation lines with impaired root growth argues against a silencing effect in the whole plant. To test whether such a silencing effect took place and whether it mainly affected the root or also the shoot, RT-PCR could be performed. Additionally, *35S::TUP5-GFP* transgenic plants which also overexpress *TUP5* could be screened for root growth arrest. In the case of silencing, the GFP signal should disappear in these lines. Other reasons for these phenotypes have to be considered as well. It might be possible that other metabolic changes, as for example a reduction in tryptophan or lysine level (Figure 5-44), or other unknown factors are the cause.

The free arginine content was not increased above WT level in overexpression lines with *tup5-1* and WT background (Figure 5-44, A, Figure 9-4 and Table 9-13). A higher free arginine content might not be produced because other enzymatic steps are probably rate limiting. It would be interesting to measure the level of free acetylnithine and ornithine, though an increase of these amino acids might not be expected, because NAGS and NAGK, the two first step in arginine biosynthesis, are feedback-regulated by arginine (Shargool *et al.*, 1988; Slocum, 2005). If these two steps do not fully control the pathway, acetylnithine and ornithine might accumulate at higher levels in the overexpression lines. If this was the case, overexpression lines should be tested for increased germination ability under salt stress conditions and drought and salt tolerance of adult plants. An increase in

ornithine and improved salt and drought tolerance were observed by Kalamaki et al. (2009) in transgenic plants overexpressing tomato *NAGS* (*SINAGSI*) (the first step of arginine synthesis) in *Arabidopsis*. The exact mechanism causing this effect could not be fully explained, though the authors suggested different possible explanations (Kalamaki et al., 2009). Different amino acids, such as ornithine and citrulline, arginine and proline, which can be derived from ornithine, were found to accumulate under drought stress or salinity stress, possibly having a protective role as compatible solutes (Gilbert et al., 1998; Kawasaki et al., 2000; Mansour, 2000; Lea et al., 2007). Also polyamines, which can be derived from ornithine and arginine, play a role in osmoprotection in rice (Yang et al., 2007).

tup5-1 is an arginine biosynthesis mutant which can be used to study the effect of arginine deficiency. Considering the important role of arginine as seed nitrogen storage molecule (VanEtten et al., 1963; Verma and Zhang, 1999) and as a precursor of important molecules such as polyamines and NO (Hanfrey et al., 2001; Slocum, 2005; Crawford, 2006; Grün et al., 2006), it would also be interesting to examine the effect of an increase in arginine level on plant development. As overexpression of *TUP5* did not lead to an increase in arginine level, other approaches, as those described below, would be necessary.

The first committing step of amino acid biosynthetic pathways is often feedback-regulated in plants (Singh and Matthews, 1994; Coruzzi and Last, 2000). In some cases it was possible to increase the amino acid content by overexpressing this committing enzyme or by introducing a feedback-insensitive form into the plant (Galili and Larkins, 1999; Ingle et al., 2005). The two first biosynthetic step enzymes of arginine biosynthesis, *NAGS* and *NAGK*, are inhibited by arginine in plants and therefore play a role as key regulatory steps (Shargool et al., 1988; Slocum, 2005). In the experiment of Kalamaki et al. (2009) overexpression of tomato *NAGS* in *Arabidopsis* plants, only ornithine content was increased but not arginine. It is not mentioned in literature whether the predicted *NAGS* genes of *Arabidopsis* have been tested for overexpression. *NAGK* might play a more important role in regulation of plant arginine biosynthesis than *NAGS* (Slocum, 2005). Its overexpression might therefore lead to an enhancement of arginine production. If this approach is not successful either, it would probably be necessary to introduce the whole set of arginine biosynthetic pathway enzymes as described by Naqvi et al. (2010) to produce transgenic plants with increased arginine content.

6.4 Developmental expression pattern of TUP5 and exogenous stimuli influencing TUP5 expression

The temporal and spatial expression pattern of *TUP5* was studied with different methods because the results were expected to give information about the gene's function in plant development and metabolism. *TUP5* is expressed in all analysed tissues and organs, reaching its highest values in cotyledons, rosette leaves and sepals according to microarray data. Real-time PCR confirmed these results: all analysed tissues (root, rosette leaves, stem, flowers, siliques of adult plants and 6-days-old seedling) showed *TUP5* expression. This is in accordance with its role as a gene of primary metabolism, as *TUP5* is necessary for arginine biosynthesis, arginine being required as protein building block. In tissue-specific analyses the highest expression level was found in ovaries and the lowest in mature pollen (Figure 5-33). The effect of *TUP5* loss-of-function on the functionality of ovule and pollen is discussed in chapter 6.2. The expression level of *TUP5* was four times lower in roots than in rosette leaves according to real-time PCR (Figure 5-34). This is consistent with the much lower free arginine content in roots compared to shoots of light-grown seedling (Figure 5-27). It would be interesting to test the enzymatic activity of TUP5 in shoots and roots in light and darkness to find a possible connection to the root phenotype of *tup5-1* when exposed to light. The protein level and the enzymatic activity of a metabolic enzyme might differ from the mRNA expression level, as the protein stability and enzymatic activity might be influenced at several control levels (Gibon *et al.*, 2004; Gibon *et al.*, 2006; Tian *et al.*, 2006). In a general way, the amount and activity of TUP5 in the different organs of *Arabidopsis* should therefore be confirmed on the protein level by immunodetection and by enzymatic assays.

A positive regulatory protein might influence *TUP5* expression: According to Genevestigator the *TUP5* expression is reduced to about half the level of untreated plants after cycloheximide treatment. This indicates that *TUP5* transcription requires *de novo* protein synthesis, because cycloheximide inhibits this process (Brandstatter and Kieber, 1998; Duval *et al.*, 2005). In the case of *TUP5*, a metabolic feedback regulation might also lead to decreased transcription after cycloheximide treatment. As cycloheximide blocks protein biosynthesis, free amino acids can accumulate and might inhibit their own biosynthesis by feedback-regulation or lead to a more complex cross-pathway regulation of amino acid biosynthesis (Fletcher and Beevers, 1971; Fletcher, 1975; Pratelli and Pilot, 2007). The latter seems to be more likely, as the expression of *TUP5* is not directly inhibited by arginine (Figure 5-35, see below).

Light-dependent TUP5 expression in Arabidopsis seedlings

The inhibiting effect of light on *tup5-1* root development brought the focus onto a possible influence of light on *TUP5* expression. The changes in *TUP5* expression after various light treatments were weak according to publicly available microarray data (chapter 5.6.1). Only in two experiments a reduction of *TUP5* expression to half of the control level was found after dark treatment. To test the effect of light on *TUP5* in an independent experiment, real-time PCR experiments were performed (chapter 5.6.3). The *TUP5* expression was about four times higher in light-grown seedlings compared to seedlings grown in darkness (Figure 5-36, A). In this case the dark-grown seedlings were etiolated, so that the metabolism was strongly altered. To test whether light has a more direct regulating effect, seedlings grown under standard conditions were adapted to light or darkness for 24 h and shifted to darkness or light, respectively, for eight hours. The light-adapted control plants had a threefold higher *TUP5* expression level than the dark-adapted control plants, confirming the light-dependence of *TUP5* expression found in the first experiments (Figure 5-36, B).

Furthermore, already eight hours of light or dark treatment influenced *TUP5* expression: *TUP5* expression was significantly reduced in light-adapted seedlings shifted to darkness and it was significantly increased in dark-adapted seedlings shifted to light (Figure 5-36, B). Thimm et al. (2004) found that many amino acid biosynthesis genes were repressed after longer phases in darkness (“end of the night”) while the transcription of amino acid catabolism genes was activated. They suggested that the carbon becoming scarce after longer periods without photosynthesis leads to these effects because no carbon should be invested in new amino acid molecules. Amino acids should rather be catabolised to release carbon compounds for other purposes (energy supply for example).

These changes in transcript level might still not change the protein level and the enzymatic activity of TUP5, as different examples of metabolic enzymes displayed a strong diurnal expression pattern change, while their enzymatic activity was often attenuated, delayed or did not correlate (Gibon *et al.*, 2004; Gibon *et al.*, 2006; Tian *et al.*, 2006). To get a true picture of the TUP5 function in plant metabolism, it would therefore be necessary to study TUP5 activity on the protein level.

No inhibition of TUP5 expression by arginine

Arginine can inhibit acetylornithine aminotransferase in *E. coli* and yeast (Albrecht and Vogel, 1964; Cunin *et al.*, 1986; Davis, 1986). In *Arabidopsis* the enzymatic activity of

NAGK (N-acetylglutamate kinase), performing the second step in arginine biosynthesis, is inhibited by arginine (Chen *et al.*, 2006). To test whether feedback inhibition regulates the expression of *TUP5*, seedlings were grown in presence or absence of externally supplied arginine. No significant difference in transcript level was found for *TUP5* when grown with arginine supplementation compared to control plants (Figure 5-35). Hence, transcription of *TUP5* is not feedback regulated by arginine in *Arabidopsis*. Even though *TUP5* might not be a major target of arginine biosynthesis control, it cannot be excluded that other feedback regulatory mechanisms, such as amino acid cross-talk regulations, might influence *TUP5* expression.

6.5 *TUP5* has a chloroplastic localisation

The subcellular localisation of a protein provides valuable hints about the biochemical surrounding and the available substrates and interaction partners. For this reason the cDNA of *TUP5* was fused to the marker gene *GFP* and expressed under the constitutive CaMV 35S promoter to visualise its subcellular localisation (chapter 5.5.2). The root phenotype of *tup5-1* plants transformed with *35S::GFP-TUP5* was complemented. This indicates that *TUP5* is functional in this GFP-fusion construct. The fluorescent signal detected in transgenic protoplasts expressing the gene fusion was colocalised with the autofluorescence of chloroplasts, indicating a chloroplastic localisation. This is in good agreement with the database predictions of TargetP and Aramemnon (chapter 5.5.1). Also in previous biochemical experiments with soybean suspension culture cells (originating from roots, not containing chlorophyll) acetylornithine aminotransferase activity was found in the plastid fraction (Jain *et al.*, 1987). The fluorescence signal of TUP5-GFP was also found in globular structures of root cells, which are probably root plastids (Figure 5-30). As the plastids in roots usually do not contain chlorophyll, it is not possible to use its autofluorescence for colocalisation and no marker substances were available for this purpose. *TUP5* was expressed in root tissue according to eFP Browser, Genevestigator and real-time PCR experiments of this work (chapter 5.6). GFP fusion constructs are often expressed with the 35S promoter to increase the signal strength which otherwise would often be too weak for microscopic analysis when using the natural promoter. The analysis of the TUP5-GFP localisation under the *TUP5* promoter would be interesting to study the protein localisation within the chloroplast. *TUP5* might play an important role in the root, because the mutation of *tup5-1* causes a short root phenotype when grown in light. The TUP5 protein might also

be produced in lower amounts in the root than in the shoot, so that a mutation impairing the enzyme's functionality can have a stronger impact in the root. This is supported by the data on *TUP5* expression which is lower in the root than in the shoot (Figure 5-34). A final proof is necessary on the protein level.

6.6 The *tup5-1* mutation has an impact on overall amino acid metabolism

The mutant *tup5-1* carries a mutation in an enzyme of arginine biosynthesis and its root phenotype could be complemented by supplementation with arginine. The mutant was therefore expected to be arginine-deficient. Indeed, the arginine content was reduced in all light-grown *tup5-1* samples tested (chapter 5.4). In darkness the arginine content was reduced in both, WT and *tup5-1*, to a comparable level (chapter 5.4.1). It was also observed that the arginine content increased in *tup5-1* while it decreased in WT when grown in low light, leading to a reduced difference between both. However, these findings need confirmation. This tendency to a more comparable arginine content between WT and *tup5-1* in low light or darkness correlates in an interesting way with the increasing root length of *tup5-1* under these light conditions (chapter 3.4) (Frémont, 2004). In WT, arginine had the most extreme difference in shoot / root distribution of all amino acids analysed, the root containing 50 times less arginine than the shoot (Figure 5-27, A). This might indicate a fine-tuned and sensitive metabolic control system of arginine content in the root, which in case of disturbance leads to an arrest of root development. Also some other *Arabidopsis* mutants impaired in amino acid biosynthesis or metabolism showed defects in root growth, as for example the *hpa1* histidine biosynthesis mutant (Mo *et al.*, 2006), the mutant Rm 57 involved in the lysine biosynthetic pathway (Sarrobot *et al.*, 2000); and two mutants alleles in aspartate aminotransferase AspAT2, *aat2-2* and *aat2-T* (Schultz *et al.*, 1998; Miesak and Coruzzi, 2002). In *tup5-1* it is especially interesting that the short root phenotype caused by arginine deficiency is light-dependent. In other amino acid mutants a similar combination was not explicitly described. The histidine biosynthesis mutant *hpa1* resembles *tup5-1* insofar as it has a short root when grown *in vitro*, but no obvious phenotype in the aerial part and fully fertile plants (Mo *et al.*, 2006). The authors did not mention how the *hpa1* root developed in soil or darkness, but it would be interesting to know whether the mutant has a similar light-dependent root growth phenotype. Other cases of amino acid biosynthetic mutants showing a light-dependent growth phenotype have been described for several tryptophan biosynthetic pathway genes. The mutants are generally

impaired in development under high light, but not under low light conditions (Last *et al.*, 1991; Radwanski *et al.*, 1996). In the case of *trp2-1*, carrying a mutation in *TSB1* which encodes tryptophan synthase β subunit 1, Last *et al.* (1991) suggested that the mutation might alter the regulation of the gene or that residual activity of the mutated enzyme might contribute to low tryptophan synthase β enzyme activity. This residual activity might be able to cover a lower tryptophan demand because of slower growth in low light intensity. The authors therefore suggested that screening for plant amino acid auxotrophs should take place under growth conditions where very active protein synthesis is required. Also in the case of *tup5-1* the mutated ACOAT has probably reduced catalytic activity, as *tup5-1* is viable, but contains lower amounts of arginine. Therefore, when grown in high light intensity, where an increased metabolic rate takes place, the illuminated *tup5-1* root might get into a deficiency situation causing stress and developmental impairment. If this is the reason for the *tup5-1* root phenotype, a transgenic construct containing a relatively strong root-specific promoter fused to the mutated *tup5-1* allele coding sequence should be able to complement the phenotype. On the other hand, the roots of soil-grown *tup5-1* plants grown under standard light develop normally (Frémont, 2004), though high metabolic activity can be expected under these conditions. This argues for specifically light-induced metabolic changes in the root tissue. Another possibility is a light-dependent change in protein stability or catalytic activity of the mutated ACOAT (TUP5^{G424R}). The molecular environment of root plastids is presumably different from that of green tissue chloroplasts, therefore some blue light-regulated proteins might interfere with TUP5 in the illuminated root, or some proteins could also be lacking due to the influence of light. One could also hypothesise that shoot arginine production is sufficient due to higher transcript rates even with the mutated protein; and that the shoot might transport arginine into the root when the latter is grown in dark, but not when grown in light. A more detailed analysis of the influence of light quality and quantity on *TUP5* transcription, ACOAT enzymatic activity and free arginine content and transport in root and shoot might give further information about the underlying mechanisms. An enzymatic activity assay was done, but failed. The protocol would need to be optimised for *Arabidopsis* ACOAT. In addition to an enzymatic assay, a fluorescent arginine biosensor stably transformed or crossed into *tup5-1* background might be an interesting tool for monitoring the arginine-dependent changes of fluorescence after different light treatments of shoot and root *in vivo* (Bogner and Ludewig, 2007). Still, it is not clear yet whether arginine long-distance transport normally plays an important role in *Arabidopsis*, as mainly glutamate, glutamine, aspartate and asparagine were found in

phloem sap and xylem exudates and are therefore supposed to be the major nitrogen transport molecules (Lam *et al.*, 1995; Fischer *et al.*, 2002). Other amino acids are supposed to be mainly synthesised from these transport amino acids at the site of requirement (Lea and Mifflin, 1980).

The concentration of other amino acids was also altered in *tup5-1*. Glycine accumulated at very high levels in *tup5-1* seedlings grown under standard light, in some experiments this was also the case for serine (chapter 5.4.2). In contrast, the glycine and serine content was comparable to WT under low light. Both amino acids are produced during photorespiration (Peterhansel *et al.*, 2010). In photorespiratory mutants in which enzymes metabolising glycine or serine are affected, these two amino acid were also accumulated (Somerville and Ogren, 1980; Somerville and Ogren, 1982). It might therefore be possible that photorespiration is impaired in *tup5-1*. To test this, the concentration of other metabolites related to photorespiration could be analysed in *tup5-1* and the development of the mutant could be studied under non-photorespiratory conditions. There might be a connection between arginine biosynthesis and photorespiration, because there is evidence that excess ammonium produced during photorespiration or supplemented exogenously might be partly assimilated into arginine (Igarashi *et al.*, 2006; Potel *et al.*, 2009).

Glutamine and asparagine are two of the main nitrogen storage and transport amino acids (Coruzzi, 2003). Their level was significantly increased in the *tup5-1* mutant in all samples tested (chapter 5.4.3, Table 5-4). This might be due to the slow growth rate of the mutant and the probably reduced metabolic activity which could eventually lead to accumulation of surplus amino groups in these storage pools (Igarashi *et al.*, 2006).

The level of many amino acids was altered in the *tup5-1* mutant. This sort of general amino acid metabolic deregulation was also found in other amino acid mutants, as for example in *apg10* (*albino and pale green 10*) which carries a mutation in BBMII (N'-[(5'-phosphoribosyl)-formimino]-5-aminoimidazole-4-carboxamide ribonucleotide) isomerase, this enzyme being involved in histidine biosynthesis (Noutoshi *et al.*, 2005). The mutant shows pale green leaves and a global increase in free amino acids. A knockout allele of the gene is embryo lethal (Noutoshi *et al.*, 2005). Some authors discussed the possibility of a cross-pathway regulation of the different amino acid biosynthetic pathways in plants as it is known for yeast (Hinnebusch, 1992). This mechanism might induce a general deregulation of free amino acid content if one amino acid is not sufficiently produced (Guyer *et al.*, 1995; Noutoshi *et al.*, 2005). However, other authors argue that a cross-pathway regulation would not function in plants, as many amino acids are precursors to various secondary

metabolites and are therefore needed in different amounts (Zhao *et al.*, 1998). Alternatively, the increased free amino acid content in *tup5-1* might also be due to protein degradation caused by deleterious effects due to the lack of arginine (Noctor *et al.*, 2002).

6.7 The root phenotype of the *tup5-1* mutant

The growth-inhibiting light is perceived in the root

One intriguing aspect of the *tup5-1* mutant is its blue light-dependent short root phenotype, which is not found in soil-grown *tup5-1* plants. Therefore, it was concluded that the root is probably the site of light perception for this growth arrest. And indeed, when *tup5-1* seedlings were grown on MS medium having the root in darkness and the shoot exposed to light, the roots developed considerably longer than the control *tup5-1* plants fully grown in light (Figure 5-1). This sort of light-specific root meristem arrest phenotype seems to be rare: A comparable phenotype was described only for the *rus1* and *rus2* (*root UVB sensitive*) mutants reacting specifically to UV-B light (Tong *et al.*, 2008; Leasure *et al.*, 2009). *RUS1* and *RUS2* encode two DUF (domain of unknown function) proteins (Tong *et al.*, 2008; Leasure *et al.*, 2009). To the best of my knowledge, for the blue light part of light spectrum only *tup5-1* has been described as yet. And apparently for no other light qualities a comparable root phenotype was shown up to now. Interestingly, the mutant *pdx1.3* might also have a light-dependent short root phenotype. Mutant seedlings were dwarfed and had short roots when grown *in vitro*, but the shoots and roots developed normally when cultivated on soil (except for slight chlorosis of the leaves) (Titiz *et al.*, 2006; Havaux *et al.*, 2009). *pdx1.3* encodes a pyridoxal synthase necessary for the biosynthesis of vitamin B6, an important cofactor in many reactions, especially for amino acid biosynthesis (Percudani and Peracchi, 2003). Pyridoxal phosphate is also the cofactor of plant ACOAT and the amino acid sequence of TUP5 is predicted to contain a pyridoxal phosphate binding site (Figure 5-18) (Dougall and Fulton, 1967). Titiz *et al.* (2006) noted that the *pdx* mutants were indistinguishable from WT under low light conditions. It seems not to have been tested yet whether the root or a specific part of the light spectrum is involved in this growth inhibiting effect. If this was the case, one could argue that a common mechanism might be involved in the *tup5-1* and *pdx1-3* root phenotype. *pdx1-1* had increased peroxidation of membrane lipids after UV light treatment (Chen and Xiong, 2005), possibly showing a link to the UV-sensitive *rus1* and *rus2* mutants.

Developmental defects and dwarfism have been described for many primary metabolite deficiency mutants in *Arabidopsis* (see chapter 6.6). It seems therefore not so surprising that the root of *tup5-1* grown in light is short, considering the deficiency of an important building block. Instead, it seems much more astonishing that the root develops normally in darkness. Thus, one question that should be addressed is: Does a light-grown root need to produce some compounds that are not necessary in dark-grown roots? Roots which are usually protected from light, as they grow in the soil, might need some reparation or protection mechanisms to cope with light stress. Especially the UV-part of light spectrum can damage DNA, membranes and proteins (Suesslin and Frohnmeier, 2003). It would therefore be necessary to test whether the *tup5-1* root phenotype also occurs under UV light. Blue light and UV light might induce stress and give a signal for the production of protective reagents which *tup5-1* cannot produce due to arginine deficiency. Metabolome analyses of roots from seedlings grown under low light and whole seedlings cultivated under standard light conditions might show whether protective compounds are lacking in *tup5-1*.

The light signalling pathway upstream of TUP5 is still elusive

The fact that blue light caused the growth arrest in the *tup5-1* primary root (Frémont, 2004) raised the question whether one of the known light signalling pathways might be involved in this mechanism. To find this out, epistasis analyses were performed between *tup5-1* and the light signalling pathway mutants *hy2-1*, *hy5-1*, *cry1* and *phyB-1*. Double mutants showing the short root phenotype of *tup5-1* and the long hypocotyls phenotype of the light signalling mutants were found in the expected ratio in the F₂ generation. Therefore, the blue light signal inducing the root phenotype of *tup5-1* seems not to be perceived or transmitted by any of the analysed light signalling factors. Some other light receptors were not tested in this work (see chapter 5.1.2), because the experiment would have needed to create multiple allele combinations or because of other technical reasons. However, finding a signalling pathway involved in *tup5-1* phenotype induction might show new connections between amino acid biosynthesis, light perception and root development. Phototropins might be good candidates, as phot1 was found to have a role in blue light perception of the root (Galen *et al.*, 2007b, a). Also cryptochrome 2 might be considered, though cryptochrome effect on root elongation was perceived in the shoot according to a study of Canamero *et al.* (2006). Phytochrome A can absorb blue light and must therefore also be considered as a potential receptor in the *tup5-1* signalling pathway (Lin, 2000). Still, it can not be excluded that an unknown receptor is involved in the signalling pathway of *tup5-1*.

As mentioned above, it would also be interesting to test whether the root phenotype of *tup5-1* is strictly blue light specific or whether it also appears in UV-A and UV-B light. A phenotype in blue light and possibly UV-A would argue for a blue light receptor mediated signalling pathway. If also UV-B causes the root phenotype, also UV-B signalling pathways (which are not yet well understood) or more unspecific mechanisms might be involved. In case of UV-B sensitivity of *tup5-1*, an involvement of the *RUS1* and *RUS2* proteins, which seem to be localised in the plastid as does TUP5 (chapter 5.5.2) (Leasure *et al.*, 2009), might be tested by double mutant analysis.

The cells of the primary root have decreased metabolic activity but are mostly viable

The *tup5-1* root stops growing when cultivated in light. The root meristem loses its characteristic structure under these culture conditions and the root tissue seems to be in a static condition. When different marker lines were tested to assess the state of quiescent center identity, cell cycle activity and response to auxin and cytokinin, it became obvious that all responses were reduced in the *tup5-1* root (chapter 5.1.3). This raised the question, whether these results were specific or whether the cells of the root tissue might not be viable anymore and the reporter genes therefore give a weaker response in general. Staining of *tup5-1* roots with fluorescein diacetate gave a strongly reduced fluorescence signal, showing that the root cells lack the esterase activity that is considered as a sign of cell viability (chapter 5.1.4). On the other hand, propidium iodide, which cannot pass intact membranes and is therefore used for staining dying or dead cells, does not accumulate within most of *tup5-1* root meristem cells. Thus, the membranes must still be intact and the root tissue of the mutant seems to be alive. The root tissue must be in a metabolically inactive state but is still viable. Nonetheless, the loss of root meristem structure is an irreversible process: Root growth activity cannot be restored when the differentiated (consumed) meristem is shifted to arginine-containing medium (Figure 5-8). Interestingly, cells along the vasculature of the short primary *tup5-1* root, probably pericycle cells, show auxin-induced GUS-staining which normally occurs during formation of lateral root primordia (Figure 5-4) (Benková *et al.*, 2003). Besides this, formation of lateral root primordia relatively close to the root tip was observed in *tup5-1* (data not shown). Also the formation of callus-like aggregations of adventitious root primordia shows that a certain activity level is still found in the root and the hypocotyl/root junction of the mutant. The activity of additional reporter gene constructs of factors involved in root meristem maintenance, as for example *SCARECROW*

(*SCR*), *SHORT ROOT (SHR)* and *PLETHORA (PLT)*, might be studied in the *tup5-1* background to find possible residual developmental control activity. It is quite probable that they will all show reduced activity like the reporter constructs previously studied. But if some of these markers would still show activity, this might help to define more precisely the level at which root meristem maintenance is disturbed in *tup5-1*. Furthermore, it might be interesting to observe the modulation of reporter gene activity under various light conditions.

Adventitious and lateral root formation in tup5-1

The *tup5-1* mutant developed callus tissue at the hypocotyl/root junction after 6 weeks of *in vitro* culture in light (Riefler, 2001). These calli were then identified as conglomerates of adventitious root primordia which usually do not elongate when grown in light (data not shown), similarly to the primary root. Also some lateral root primordia form on the short primary root. Only a few cell divisions occur in the primary root meristem and the adventitious or lateral root meristems after their formation (Figure 5-6 for primary root meristem, lateral root meristem: data not shown). The cell division and differentiation events occurring during the formation of the lateral root primordia show that *tup5-1* root tissue is still able to perform mitoses and metabolite consuming developmental programmes. According to the classification by Konishi and Sugiyama (2003), *tup5-1* should be classified as a root growth defective mutant, because not the step of root primordium initiation or formation is impaired, but the growth of the primordium after its formation. The ability to form multiple adventitious root primordia suggests that the mutant can still provide the necessary building blocks and also the required amount of arginine despite a presumable arginine shortage. We can therefore conclude that the mutant is able to invest sufficient arginine for the primordium formation, but that a signal leads to the stop of root growth in a second step. This signal might be triggered by light and presumably by the lack of arginine *de novo* biosynthesis. It would be interesting to understand at which specific developmental stage the developing adventitious root primordia are stopped in *tup5-1* and whether the primordia are fully developed when they start to differentiate.

It would be interesting to monitor the arginine content and possible light-dependent arginine fluxes from the shoot into the root. This might be done by applying labelled arginine to the shoot or by monitoring arginine fluxes, for example with a FRET sensor *in vivo* (Bogner and Ludewig, 2007).

On a hormonal level, the massive adventitious root primordia formation in *tup5-1* might be explained by hormonal deregulation, which might be a consequence of arginine deficiency. According to Kuroha and Satoh (2007), root-borne cytokinin transported to the hypocotyl via xylem sap can inhibit adventitious root formation. *tup5-1* is presumably cytokinin-deficient as GUS staining under the cytokinin-inducible *ARR5* promoter was weak in the stunted primary root (chapter 5.1.3) and because shoot growth (but not root growth) was improved on cytokinin-supplemented medium (Frémont, 2004). Apparently, the shoot growth impairment is, to a certain extent, a secondary effect of poor nutrient and water supply from the dwarfed root and obviously also due to deficiency of root-borne cytokinin. This lack of root-borne cytokinin in *tup5-1* might also relieve the inhibition of adventitious root formation as described by Kuroha and Satoh (2007).

Could TUP5 be a target for plant pathogens?

In addition to the function of *TUP5* in arginine biosynthesis shown in this work, recent findings show that it might also have a role in pathogen interaction. *TUP5/WIN1* was found to interact with the effector protein HopW1.1 of the bacterial plant pathogen *Pseudomonas syringae* and overexpression of *TUP5/WIN1* conferred disease susceptibility to *P. syringae/hopW1-1* (Lee *et al.*, 2008a). Additionally, *TUP5* was upregulated 4-fold upon nematode infection. This was the highest level of upregulation found for *TUP5* after induction with a variety of biotic or abiotic treatments as presented in the database Genevestigator (Winter *et al.*, 2007). Many plant pathogens have evolved mechanisms to influence the nutrient production and nutrient fluxes of their host for their own advantage (Replogle *et al.*, 2011). As an example, plant-pathogenic nematodes can withdraw amino acids from their host by inducing the formation of feeding structures which act as amino acid sinks (Hammes *et al.*, 2006). Interestingly, plant-parasitic nematodes need to secrete CLE-like effector proteins for successful infection and establishment of a feeding site, thereby mimicking plant CLE peptides which are involved in stem cell niche maintenance (Replogle *et al.*, 2011). Peptide signalling was shown to be important for stem cell niche maintenance in the SAM; recent findings suggest that it might also play a role in roots (Wang and Fiers, 2010). Overexpression of various *CLE* genes causes root meristem consumption. The natural function of these peptides is still not clear, as only one *CLE* mutant showed a root phenotype (Wang and Fiers, 2010). As *TUP5* was upregulated after nematode infection, though it is speculative, it cannot be excluded that it acts downstream of the CLE signalling pathway. For this reason, and also because of the aspect of root meristem mainte-

nance, it might be interesting to examine a possible connection between *TUP5* and CLE signaling. The endogenous expression level of root-specific CLE proteins in *tup5-1* or *TUP5* expression in plant CLE peptide overexpression mutants might be studied as well as the phenotype of a *tup5-1* double mutant with *clv2* (*clavata2*) or *crn* (*coryne*), which seem to be both involved in CLE signalling in the root and are required for successful nematode infection (Fiers *et al.*, 2005; Müller *et al.*, 2008; Replogle *et al.*, 2011).

6.8 Conclusions and perspectives

The mutant *tup5-1* was initially found in a screen for EMS mutants with hormone-dependent callus formation on hypocotyl and root explants (Riefler, 2001). Interestingly, while *tup5-1* explants formed calli, the WT control explants had produced roots (Riefler, 2001). It is hypothesised that the calli of the *tup5-1* explants might be aggregations of lateral root primordia similar to those formed at the hypocotyl-root junction of *tup5-1* seedlings. The callus formation of the *tup5-1* explant and seedlings could therefore be interpreted as a repeated attempt to produce a functional root system for nutrient and water supply. This is supported by the observation that no calli were formed in *tup5-1* seedlings grown in darkness or on soil where the root developed normally. It is not surprising that what was initially interpreted as callus formation and reprogramming to an undifferentiated state in the *tup5-1* explants might in fact be the formation of root primordia, as it was recently shown that callus formation actually involves a lateral root development program of pericycle cells forming lateral root meristem-like primordia (Atta *et al.*, 2009; Sugimoto *et al.*, 2010).

The initial goal of the screen for the *tumor prone* mutants was to identify genes involved in cell division and differentiation under the control of auxin and cytokinin (Riefler, 2001). The mutants of the *tup* series were found to be involved in many different processes, showing that plant development is so complex that functional predictions based on phenotypes are difficult. Nevertheless, this sort of screen can give the opportunity to discover previously unknown gene functions as in the case of *TUP5*, encoding ACOAT which catalyses the fourth step of arginine biosynthesis. So far, not many *Arabidopsis* mutants affecting arginine biosynthesis are known. A T-DNA insertion line and two EMS mutants for carbamoylphosphate synthetase (CPS) were described (Potel *et al.*, 2009; Mollá-Morales *et al.*, 2011), though CPS is not exclusively working in the arginine biosynthesis pathway as it also provides a precursor for pyrimidine biosynthesis. Furthermore, a T-DNA insertion

line for ornithine transcarbamylase showing an increased sensitivity to ornithine was reported, though the mutation affected a non-coding region (Quesada *et al.*, 1999). Lee *et al.* (2008a) found *TUP5/WIN1* as a protein interacting with the *P. syringae* HopW1.1 effector protein, but they did not study the role of *TUP5/WIN1* in arginine biosynthesis.

The exceptional link between blue light-dependent root meristem arrest and an impairment in arginine biosynthesis in the *tup5-1* mutant still has to be elucidated. Interestingly, some mutants seem to have a comparable light-dependent short root phenotype. The *rus1* and *rus2* mutants have short roots under UV-B light and the inhibiting light is perceived by the root (Tong *et al.*, 2008; Leasure *et al.*, 2009). *pdx1-3* encoding a pyridoxal synthase necessary for the production of the TUP5 cofactor, might have a light-dependent root growth arrest, though it seems not to have been tested yet whether the root perceives the inhibiting light or whether a specific wavelength is involved (Titiz *et al.*, 2006; Havaux *et al.*, 2009). It would be interesting to study a possible link between these mutants and *tup5-1*, possibly showing a common light-sensitive developmental mechanism.

To get a deeper insight into the processes inducing the *tup5-1* phenotype, various strategies might be followed. A yeast two-hybrid screen might elucidate possible signalling pathways connecting the role of ACOAT to the *tup5-1* blue light root phenotype. Metabolome analysis of light and dark grown roots and shoots could give an idea about metabolic defects caused by arginine-deficiency in the mutant root. Furthermore, an enzymatic assay of TUP5 and the mutated TUP5^{G424R} testing a possible light-dependence of protein activity might be very instructive. Finally the continuation of the double mutant analyses of *tup5-1* with the light signaling mutants which have not been tested yet could possibly reveal the blue light signalling pathway involved in the root growth arrest. Last but not least, the eventually most promising approach to get access to further factors involved in regulating the blue light-dependent root growth inhibition would be a screen for second site suppressor mutations that re-establish root growth under blue light. The mutated gene would be expected to be informative about the pathway involved.

7 References

- Ábrahám, E., Rigó, G., Székely, G., Nagy, R., Koncz, C., and Szabados, L. (2003). Light-dependent induction of proline biosynthesis by abscisic acid and salt stress is inhibited by brassinosteroid in *Arabidopsis*. *Plant Mol. Biol.* **51**, 363-372.
- Abramoff, M.D., Magelhaes, P.J., and Ram, S.J. (2004). Image processing with ImageJ. *Biophotonics International* **11**, 36-42.
- Adams, E., and Frank, L. (1980). Metabolism of proline and the hydroxyprolines. *Annu. Rev. Biochem.* **49**, 1005-1061.
- Ahmad, M., and Cashmore, A.R. (1993). *HY4* gene of *A. thaliana* encodes a protein with characteristics of a blue-light photoreceptor. *Nature* **366**, 162-166.
- Akama, K., and Beier, H. (2003). Translational nonsense codon suppression as indicator for functional pre-tRNA splicing in transformed *Arabidopsis* hypocotyl-derived calli. *Nucleic Acids Res.* **31**, 1197-1207.
- Albrecht, A.M., and Vogel, H.J. (1964). Acetylornithine delta-transaminase. Partial purification and repression behavior. *J. Biol. Chem.* **239**, 1872-1876.
- Alonso, J.M., Stepanova, A.N., Lisse, T.J., Kim, C.J., Chen, H., Shinn, P., Stevenson, D.K., Zimmerman, J., Barajas, P., Cheuk, R., Gadrinab, C., Heller, C., Jeske, A., Koesema, E., Meyers, C.C., Parker, H., Prednis, L., Ansari, Y., Choy, N., Deen, H., Geralt, M., Hazari, N., Hom, E., Karnes, M., Mulholland, C., Ndubaku, R., Schmidt, I., Guzman, P., Aguilar-Henonin, L., Schmid, M., Weigel, D., Carter, D.E., Marchand, T., Risseeuw, E., Brogden, D., Zeko, A., Crosby, W.L., Berry, C.C., and Ecker, J.R. (2003). Genome-wide insertional mutagenesis of *Arabidopsis thaliana*. *Science* **301**, 653-657.
- Atta, R., Laurens, L., Boucheron-Dubuisson, E., Guivarc'h, A., Carnero, E., Giraudat-Pautot, V., Rech, P., and Chriqui, D. (2009). Pluripotency of *Arabidopsis* xylem pericycle underlies shoot regeneration from root and hypocotyl explants grown *in vitro*. *Plant J.* **57**, 626-644.
- Bae, G., and Choi, G. (2008). Decoding of light signals by plant phytochromes and their interacting proteins. *Annu. Rev. Plant Biol.* **59**, 281-311.
- Balk, J., and Lobréaux, S. (2005). Biogenesis of iron-sulfur proteins in plants. *Trends Plant Sci.* **10**, 324-331.
- Banerjee, R., and Batschauer, A. (2005). Plant blue-light receptors. *Planta* **220**, 498-502.
- Bartlem, D., Lambein, I., Okamoto, T., Itaya, A., Uda, Y., Kijima, F., Tamaki, Y., Nambara, E., and Naito, S. (2000). Mutation in the threonine synthase gene results in an over-accumulation of soluble methionine in *Arabidopsis*. *Plant Physiol.* **123**, 101-110.
- Baskin, T.I., Peret, B., Baluska, F., Benfey, P.N., Bennett, M., Forde, B.G., Gilroy, S., Helariutta, Y., Hepler, P.K., Leyser, O., Masson, P.H., Muday, G.K., Murphy, A.S., Poethig, S., Rahman, A., Roberts, K., Scheres, B., Sharp, R.E., and Somerville, C. (2010). Shootward and rootward: peak terminology for plant polarity. *Trends Plant Sci.* **15**, 593-594.
- Batschauer, A., Banerjee, R., and Pokorný, R. (2007). Cryptochromes. In *Light and Plant Development*, G.C. Whitelam and K.J. Halliday, eds (Blackwell Publishing Ltd), pp. 17-48.
- Baud, S., Dubreucq, B., Miquel, M., Rochat, C., and Lepiniec, L. (2008). Storage reserve accumulation in *Arabidopsis*: metabolic and developmental control of seed filling. In *The Arabidopsis Book* (The American Society of Plant Biologists), pp. 1-24.

- Baulcombe, D.C., Saunders, G.R., Bevan, M.W., Mayo, M.A., and Harrison, B.D.** (1986). Expression of biologically active viral satellite RNA from the nuclear genome of transformed plants. *Nature* **321**, 446-449.
- Bell, C.J., and Ecker, J.R.** (1994). Assignment of 30 microsatellite loci to the linkage map of *Arabidopsis*. *Genomics* **19**, 137-144.
- Benková, E., Michniewicz, M., Sauer, M., Teichmann, T., Seifertová, D., Jürgens, G., and Friml, J.** (2003). Local, efflux-dependent auxin gradients as a common module for plant organ formation. *Cell* **115**, 591-602.
- Bentsink, L., and Koornneef, M.** (2008). Seed dormancy and germination. In *The Arabidopsis Book* (The American Society of Plant Biologists), pp. 1-18.
- Berg, M., Rogers, R., Muralla, R., and Meinke, D.** (2005). Requirement of aminoacyl-tRNA synthetases for gametogenesis and embryo development in *Arabidopsis*. *Plant J.* **44**, 866-878.
- Binder, S., Knill, T., and Schuster, J.** (2007). Branched-chain amino acid metabolism in higher plants. *Physiol. Plantarum* **129**, 68-78.
- Boccalandro, H.E., De Simone, S.N., Bergmann-Honsberger, A., Schepens, I., Fankhauser, C., and Casal, J.J.** (2008). *PHYTOCHROME KINASE SUBSTRATE1* regulates root phototropism and gravitropism. *Plant Physiol.* **146**, 108-115.
- Bogner, M., and Ludewig, U.** (2007). Visualization of arginine influx into plant cells using a specific FRET-sensor. *J. Fluoresc.* **17**, 350-360.
- Bourguignon, J., Rébeillé, F., and Douce, R.** (1999). Serine and glycine metabolism in higher plants. In *Plant Amino Acids*, B.K. Singh, ed (New York: Marcel Dekker, Inc.), pp. 111-146.
- Boutin, J.-P.** (1982). Purification, properties and subunit structure of arginase from Iris bulbs. *Eur. J. Biochem.* **127**, 237-243.
- Brandstatter, I., and Kieber, J.J.** (1998). Two genes with similarity to bacterial response regulators are rapidly and specifically induced by cytokinin in *Arabidopsis*. *Plant Cell* **10**, 1009-1020.
- Brenner, E.D., Martinez-Barboza, N., Clark, A.P., Liang, Q.S., Stevenson, D.W., and Coruzzi, G.M.** (2000). *Arabidopsis* mutants resistant to S(+)- β -methyl- α , β -diaminopropionic acid, a cycad-derived glutamate receptor agonist. *Plant Physiol.* **124**, 1615-1624.
- Briggs, W.R., and Christie, J.M.** (2002). Phototropins 1 and 2: versatile plant blue-light receptors. *Trends Plant Sci.* **7**, 204-210.
- Briggs, W.R., Beck, C.F., Cashmore, A.R., Christie, J.M., Hughes, J., Jarillo, J.A., Kagawa, T., Kanegae, H., Liscum, E., Nagatani, A., Okada, K., Salomon, M., Rudiger, W., Sakai, T., Takano, M., Wada, M., and Watson, J.C.** (2001). The phototropin family of photoreceptors. *Plant Cell* **13**, 993-997.
- Bryant, N., Lloyd, J., Sweeney, C., Myouga, F., and Meinke, D.** (2011). Identification of nuclear genes encoding chloroplast-localized proteins required for embryo development in *Arabidopsis thaliana*. *Plant Physiol.* **Preview**, pp.110.168120.
- Canamero, R., Bakrim, N., Bouly, J.-P., Garay, A., Dudkin, E., Habricot, Y., and Ahmad, M.** (2006). Cryptochrome photoreceptors cry1 and cry2 antagonistically regulate primary root elongation in *Arabidopsis thaliana*. *Planta* **224**, 995-1003.
- Casal, J.J., Luccioni, L.G., Oliverio, K.A., and Boccalandro, H.E.** (2003). Light, phytochrome signalling and photomorphogenesis in *Arabidopsis*. *Photochem. Photobiol. Sci.* **2**, 625-636.
- Chalfie, M., Tu, Y., Euskirchen, G., Ward, W.W., and Prasher, D.C.** (1994). Green fluorescent protein as a marker for gene expression. *Science* **263**, 802-805.

- Chen, H., and Xiong, L.** (2005). Pyridoxine is required for post-embryonic root development and tolerance to osmotic and oxidative stresses. *Plant J.* **44**, 396-408.
- Chen, M., Chory, J., and Fankhauser, C.** (2004). Light signal transduction in higher plants. *Ann. Rev. Genet.* **38**, 87-117.
- Chen, Y.M., Ferrar, T.S., Lohmeier-Vogel, E.M., Lohmeier-Vogel, E., Morrice, N., Mizuno, Y., Berenger, B., Ng, K.K.S., Muench, D.G., and Moorhead, G.B.G.** (2006). The PII signal transduction protein of *Arabidopsis thaliana* forms an arginine-regulated complex with plastid N-acetyl glutamate kinase. *J. Biol. Chem.* **281**, 5726-5733.
- Choi, S., Creelman, R.A., Mullet, J.E., and Wing, R.A.** (1995). Construction and characterization of a bacterial artificial chromosome library of *Arabidopsis thaliana*. *Weeds World* **2**, 17-20.
- Chrispeels, H., Oettinger, H., Janvier, N., and Tague, B.** (2000). *AtZFP1*, encoding *Arabidopsis thaliana* C2H2 zinc-finger protein 1, is expressed downstream of photomorphogenic activation. *Plant Mol. Biol.* **42**, 279-290.
- Christie, J.M.** (2007a). Phototropins and other LOV-containing proteins. In *Light and Plant Development*, G.C. Whitelam and K.J. Halliday, eds (Blackwell Publishing Ltd), pp. 49-78.
- Christie, J.M.** (2007b). Phototropin blue-light receptors. *Annu. Rev. Plant Biol.* **58**, 21-45.
- Clough, S., and Bent, A.** (1998). Floral dip: a simplified method for *Agrobacterium*-mediated transformation of *Arabidopsis thaliana*. *Plant Journal* **16?**, 735-743.
- Colón-Carmona, A., You, R., Haimovitch-Gal, T., and Doerner, P.** (1999). Spatio-temporal analysis of mitotic activity with a labile cyclin-GUS fusion protein. *Plant Journal* **20**, 503-508.
- Correll, M.J., and Kiss, J.Z.** (2005). The roles of phytochromes in elongation and gravitropism of roots. *Plant Cell Physiol.* **46**, 317-323.
- Coruzzi, G., and Last, R.** (2000). Amino acids. In *Biochemistry & Molecular Biology of Plants*, B.B. Buchanan, W. Gruissem, and R.J. Jones, eds (Rockville, Maryland: American Society of Plant Physiologists), pp. 358-410.
- Coruzzi, G.M.** (2003). Primary N-assimilation into amino acids in *Arabidopsis*. In *The Arabidopsis Book* (The American Society of Plant Biologists), pp. 1-17.
- Crawford, N.M.** (2006). Mechanisms for nitric oxide synthesis in plants. *J. Exp. Bot.* **57**, 471-478.
- Cunin, R., Glansdorff, N., Pierard, A., and Stalon, V.** (1986). Biosynthesis and metabolism of arginine in bacteria. *Microbiol. Rev.* **50**, 314-352.
- D'Agostino, I.B., Deruere, J., and Kieber, J.J.** (2000). Characterization of the response of the *Arabidopsis* response regulator gene family to cytokinin. *Plant Physiol.* **124**, 1706-1717.
- Damm, B., and Willmitzer, L.** (1988). Regeneration of fertile plants from protoplasts of different *Arabidopsis thaliana* genotypes. *Mol. Gen. Genet.* **213**, 15-20.
- Davis, R.H.** (1986). Compartmental and regulatory mechanisms in the arginine pathways of *Neurospora crassa* and *Saccharomyces cerevisiae*. *Microbiol. Rev.* **50**, 280-313.
- De Simone, S., Oka, Y., and Inoue, Y.** (2000). Effect of light on root hair formation in *Arabidopsis thaliana* phytochrome-deficient mutants. *J. Plant Res.* **113**, 63-69.
- Dello Ioio, R., Linhares, F.S., and Sabatini, S.** (2008). Emerging role of cytokinin as a regulator of cellular differentiation. *Curr. Opin. Plant Biol.* **11**, 23-27.
- Demarsy, E., and Fankhauser, C.** (2009). Higher plants use LOV to perceive blue light. *Curr. Opin. Plant Biol.* **12**, 69-74.
- Deng, X.-W., Matsui, M., Wei, N., Wagner, D., Chu, A.M., Feldmann, K.A., and Quail, P.H.** (1992). *COP1*, an *Arabidopsis* regulatory gene, encodes a protein with both a zinc-binding motif and a G β homologous domain. *Cell* **71**, 791-801.

- Depicker, A., and Van Montagu, M.** (1997). Post-transcriptional gene silencing in plants. *Curr. Opin. Cell Biol.* **9**, 373-382.
- Dinneny, J.R., and Yanofsky, M.F.** (2005). Drawing lines and borders: how the dehiscent fruit of *Arabidopsis* is patterned. *BioEssays* **27**, 42-49.
- Dinneny, J.R., and Benfey, P.N.** (2008). Plant stem cell niches: standing the test of time. *Cell* **132**, 553-557.
- Dolan, L., Janmaat, K., Willemsen, V., Linstead, P., Poethig, S., Roberts, K., and Scheres, B.** (1993). Cellular organisation of the *Arabidopsis thaliana* root. *Development* **119**, 71-84.
- Dougall, D.K., and Fulton, M.M.** (1967). Biosynthesis of protein amino acids in plant tissue culture III. Studies on the biosynthesis of arginine. *Plant Physiol.* **42**, 387-390.
- Duval, I., Brochu, V., Simard, M., Beaulieu, C., and Beaudoin, N.** (2005). Thaxtomin A induces programmed cell death in *Arabidopsis thaliana* suspension-cultured cells. *Planta* **222**, 820-831.
- Emanuelsson, O., Brunak, S., von Heijne, G., and Nielsen, H.** (2007). Locating proteins in the cell using TargetP, SignalP and related tools. *Nat. Protoc.* **2**, 953-971.
- Feria Bourrellier, A.B., Ferrario-Méry, S., Vidal, J., and Hodges, M.** (2009). Metabolite regulation of the interaction between *Arabidopsis thaliana* PII and *N*-acetyl-l-glutamate kinase. *Biochem. Biophys. Res. Co.* **387**, 700-704.
- Fiers, M., Golemic, E., Xu, J., van der Geest, L., Heidstra, R., Stiekema, W., and Liu, C.-M.** (2005). The 14-amino acid CLV3, CLE19, and CLE40 peptides trigger consumption of the root meristem in *Arabidopsis* through a *CLAVATA2*-dependent pathway. *Plant Cell* **17**, 2542-2553.
- Fischer, W.-N., Loo, D.D.F., Koch, W., Ludewig, U., Boorer, K.J., Tegeder, M., Rentsch, D., Wright, E.M., and Frommer, W.B.** (2002). Low and high affinity amino acid H⁺-cotransporters for cellular import of neutral and charged amino acids. *Plant J.* **29**, 717-731.
- Fletcher, J.S.** (1975). Control of amino acid synthesis in tissue culture cells. *Plant Physiol.* **56**, 450-451.
- Fletcher, J.S., and Beevers, H.** (1971). Influence of cycloheximide on the synthesis and utilization of amino acids in suspension cultures. *Plant Physiol.* **48**, 261-264.
- Forde, B.G., and Lea, P.J.** (2007). Glutamate in plants: metabolism, regulation, and signalling. *J. Exp. Bot.* **58**, 2339-2358.
- Foyer, C.H., Bloom, A.J., Queval, G., and Noctor, G.** (2009). Photorespiratory metabolism: genes, mutants, energetics, and redox Signaling. *Annu. Rev. Plant Biol.* **60**, 455-484.
- Frémont, N.** (2004). Molekulare und phänotypische Charakterisierung der lichtabhängigen Wurzelmutante *tup5* in *Arabidopsis thaliana*. Diploma thesis (Freie Universität Berlin).
- Galen, C., Rabenold, J.J., and Liscum, E.** (2007a). Functional ecology of a blue light photoreceptor: effects of phototropin-1 on root growth enhance drought tolerance in *Arabidopsis thaliana*. *New Phytol.* **173**, 91-99.
- Galen, C., Rabenold, J.J., and Liscum, E.** (2007b). Light-sensing in roots. *Plant Signal. Behav.* **2**, 106-108.
- Galili, G., and Larkins, B.A.** (1999). Enhancing the content of the essential amino acids lysine and threonine in plants. In *Plant Amino Acids*, B.K. Singh, ed (New York: Marcel Dekker, Inc.), pp. 487-507.
- Gasteiger, E., Gattiker, A., Hoogland, C., Ivanyi, I., Appel, R.D., and Bairoch, A.** (2003). ExPASy: the proteomics server for in-depth protein knowledge and analysis. *Nucleic Acids Res.* **31**, 3784-3788.

- Gibon, Y., Usadel, B., Blaesing, O., Kamlage, B., Hoehne, M., Trethewey, R., and Stitt, M. (2006). Integration of metabolite with transcript and enzyme activity profiling during diurnal cycles in *Arabidopsis* rosettes. *Genome Biol.* **7**, R76.
- Gibon, Y., Blaesing, O.E., Hannemann, J., Carillo, P., Hohne, M., Hendriks, J.H.M., Palacios, N., Cross, J., Selbig, J., and Stitt, M. (2004). A robot-based platform to measure multiple enzyme activities in *Arabidopsis* using a set of cycling assays: comparison of changes of enzyme activities and transcript levels during diurnal cycles and in prolonged darkness. *Plant Cell* **16**, 3304-3325.
- Gilbert, G., Gadush, M., Wilson, C., and Madore, M. (1998). Amino acid accumulation in sink and source tissues of *Coleus blumei* Benth. during salinity stress. *J. Exp. Bot.* **49**, 107-114.
- Grün, S., Lindermayr, C., Sell, S., and Durner, J. (2006). Nitric oxide and gene regulation in plants. *J. Exp. Bot.* **57**, 507-516.
- Guyer, D., Patton, D., and Ward, E. (1995). Evidence for cross-pathway regulation of metabolic gene expression in plants. *Proc. Natl. Acad. Sci. U.S.A.* **92**, 4997-5000.
- Halgand, F., Wessel, P.M., Laprèvote, O., and Dumas, R. (2002). Biochemical and mass spectrometric evidence for quaternary structure modifications of plant threonine deaminase induced by isoleucine. *Biochemistry* **41**, 13767-13773.
- Hammes, U.Z., Nielsen, E., Honaas, L.A., Taylor, C.G., and Schachtman, D.P. (2006). AtCAT6, a sink-tissue-localized transporter for essential amino acids in *Arabidopsis*. *Plant J.* **48**, 414-426.
- Hanfrey, C., Sommer, S., Mayer, M.J., Burtin, D., and Michael, A.J. (2001). *Arabidopsis* polyamine biosynthesis: absence of ornithine decarboxylase and the mechanism of arginine decarboxylase activity. *Plant J.* **27**, 551-560.
- Havaux, M., Ksas, B., Szewczyk, A., Rumeau, D., Franck, F., Caffarri, S., and Triantaphylidès, C. (2009). Vitamin B6 deficient plants display increased sensitivity to high light and photo-oxidative stress. *BMC Plant Biol.* **9**, 130.
- He, Y., Tang, R.-H., Hao, Y., Stevens, R.D., Cook, C.W., Ahn, S.M., Jing, L., Yang, Z., Chen, L., Guo, F., Fiorani, F., Jackson, R.B., Crawford, N.M., and Pei, Z.-M. (2004). Nitric oxide represses the *Arabidopsis* floral transition. *Science* **305**, 1968-1971.
- Heimberg, H., Boyen, A., Crabeel, M., and Glansdorff, N. (1990). *Escherichia coli* and *Saccharomyces cerevisiae* acetylornithine aminotransferases: evolutionary relationship with ornithine aminotransferases. *Gene* **90**, 69-78.
- Herrmann, K.M. (1995). The shikimate pathway: early steps in the biosynthesis of aromatic compounds. *Plant Cell* **7**, 907-919.
- Hervieu, F., Dily, F.L., Saos, J.L., Billard, J.-P., and Huault, C. (1993). Inhibition of plant ornithine aminotransferase by gabaculine and 4-amino-5-hexynoic acid. *Phytochemistry* **34**, 1231-1234.
- Hinnebusch, A.G. (1992). General and pathway-specific regulatory mechanisms controlling the synthesis of amino acid biosynthetic enzymes in *Saccharomyces cerevisiae*. In *The Molecular and Cellular Biology of the Yeast Saccharomyces: Gene Expression*, E.W. Jones, J.R. Pringle, and J.B. Broach, eds (Cold Spring Harbor, NY: Cold Spring Harbor Laboratory Press), pp. 319-414.
- Ho, C.L., and Saito, K. (2001). Molecular biology of the plastidic phosphorylated serine biosynthetic pathway in *Arabidopsis thaliana*. *Amino acids* **20**, 243-259.
- Hoecker, U., Tepperman, J., and Quail, P. (1999). SPA1, a WD-repeat protein specific to phytochrome A signal transduction. *Science* **284**, 496-499.
- Hoffman, P.D., Batschauer, A., and Hays, J.B. (1996). *PHH1*, a novel gene from *Arabidopsis thaliana* that encodes a protein similar to plant blue light photoreceptors and microbial photolyases. *Mol. Gen. Genet.* **253**, 259-265.

- Hruz, T., Laule, O., Szabo, G., Wessendorp, F., Bleuler, S., Oertle, L., Widmayer, P., Gruissem, W., and Zimmermann, P. (2008). Genevestigator V3: a reference expression database for the meta-analysis of transcriptomes. *Adv. Bioinformatics*.
- Huala, E., Oeller, P.W., Liscum, E., Han, I.-S., Larsen, E., and Briggs, W.R. (1997). *Arabidopsis* NPH1: A Protein Kinase with a Putative Redox-Sensing Domain. *Science* **278**, 2120-2123.
- Hudson, A.O., Singh, B.K., Leustek, T., and Gilvarg, C. (2006). An LL-diaminopimelate aminotransferase defines a novel variant of the lysine biosynthesis pathway in plants. *Plant Physiol.* **140**, 292-301.
- Igarashi, D., Tsuchida, H., Miyao, M., and Ohsumi, C. (2006). Glutamate:glyoxylate aminotransferase modulates amino acid content during photorespiration. *Plant Physiol.* **142**, 901-910.
- Igarashi, D., Miwa, T., Seki, M., Kobayashi, M., Kato, T., Tabata, S., Shinozaki, K., and Ohsumi, C. (2003). Identification of photorespiratory *glutamate:glyoxylate aminotransferase* (*GGAT*) gene in *Arabidopsis*. *Plant J.* **33**, 975-987.
- Ingle, R.A., Mugford, S.T., Rees, J.D., Campbell, M.M., and Smith, J.A.C. (2005). Constitutively high expression of the histidine biosynthetic pathway contributes to nickel tolerance in hyperaccumulator plants. *Plant Cell* **17**, 2089-2106.
- Inoue, T., Higuchi, M., Hashimoto, Y., Seki, M., Kobayashi, M., Kato, T., Tabata, S., Shinozaki, K., and Kakimoto, T. (2001). Identification of CRE1 as a cytokinin receptor from *Arabidopsis*. *Nature* **409**, 1060-1063.
- Jain, J.C., Shargool, P.D., and Chung, S. (1987). Compartmentation studies on enzymes of ornithine biosynthesis in plant cells. *Plant Sci.* **51**, 17-20.
- Jander, G., and Joshi, V. (2009). Aspartate-derived amino acid biosynthesis in *Arabidopsis thaliana*. In *The Arabidopsis Book* (The American Society of Plant Biologists), pp. 1-15.
- Jander, G., Norris, S.R., Rounsley, S.D., Bush, D.F., Levin, I.M., and Last, R.L. (2002). *Arabidopsis* map-based cloning in the post-genome era. *Plant Physiol.* **129**, 440-450.
- Jansen, M.A.K. (2002). Ultraviolet-B radiation effects on plants: induction of morphogenic responses. *Physiol. Plantarum* **116**, 423-429.
- Jauniaux, J.-C., Urrestarazu, L.A., and Wiame, J.-M. (1978). Arginine metabolism in *Saccharomyces cerevisiae*: subcellular localization of the enzymes. *J. Bacteriol.* **133**, 1096-1107.
- Jenkins, G.I. (2009). Signal Transduction in Responses to UV-B Radiation. *Annu. Rev. Plant Biol.* **60**, 407-431.
- Jones, D.T. (1999). Protein secondary structure prediction based on position-specific scoring matrices. *J. Mol. Biol.* **292**, 195-202.
- Jones, K.H., and Senft, J.A. (1985). An improved method to determine cell viability by simultaneous staining with fluorescein diacetate-propidium iodide. *J. Histochem. Cytochem.* **33**, 77-79.
- Joshi, V., Laubengayer, K.M., Schauer, N., Fernie, A.R., and Jander, G. (2006). Two *Arabidopsis* threonine aldolases are nonredundant and compete with threonine deaminase for a common substrate pool. *Plant Cell* **18**, 3564-3575.
- Kalamaki, M.S., Alexandrou, D., Lazari, D., Merkouropoulos, G., Fotopoulos, V., Pateraki, I., Aggelis, A., Carrillo-Lopez, A., Rubio-Cabetas, M.J., and Kanellis, A.K. (2009). Over-expression of a tomato N-acetyl-L-glutamate synthase gene (*SINAGSI*) in *Arabidopsis thaliana* results in high ornithine levels and increased tolerance in salt and drought stresses. *J. Exp. Bot.* **60**, 1859-1871.
- Kanehisa, M., Araki, M., Goto, S., Hattori, M., Hirakawa, M., Itoh, M., Katayama, T., Kawashima, S., Okuda, S., Tokimatsu, T., and Yamanishi, Y. (2008).

- KEGG for linking genomes to life and the environment. *Nucleic Acids Res.* **36**, D480-484.
- Karimi, M., De Meyer, B., and Hilson, P.** (2005). Modular cloning in plant cells. *Trends Plant Sci.* **10**, 103-105.
- Kaur-Sawhney, R., Tiburcio, A.F., Altabella, T., and Galston, A.W.** (2003). Polyamines in plants: An overview. *J. Cell Mol. Biol.* **2**, 1-12.
- Kawasaki, S., Miyake, C., Kohchi, T., Fujii, S., Uchida, M., and Yokota, A.** (2000). Responses of wild watermelon to drought stress: accumulation of an ArgE homologue and citrulline in leaves during water deficits. *Plant Cell Physiol.* **41**, 864-873.
- Kim, H.-R., Rho, H.-W., Park, J.-W., Park, B.-H., Kim, J.-S., and Lee, M.-W.** (1994). Assay of ornithine aminotransferase with ninhydrin. *Anal. Biochem.* **223**, 205-207.
- Kishor, P.B.K., Sangam, S., Amrutha, R.N., Laxmi, P.S., Naidu, K.R., Rao, K.R.S.S., Rao, S., Reddy, K.J., Theriappan, P., and Sreenivasulu, N.** (2005). Regulation of proline biosynthesis, degradation, uptake and transport in higher plants: Its implications in plant growth and abiotic stress tolerance. *Curr. Sci. India* **88**, 424-438.
- Kohchi, T., Mukougawa, K., Frankenberg, N., Masuda, M., Yokota, A., and Lagarias, J.C.** (2001). The *Arabidopsis* *HY2* gene encodes phytochromobilin synthase, a ferredoxin-dependent biliverdin reductase. *Plant Cell* **13**, 425-436.
- Koncz, C., and Schell, J.** (1986). The promoter of T_L-DNA gene 5 controls the tissue-specific expression of chimaeric genes carried by a novel type of *Agrobacterium* binary vector. *Mol. Gen. Genet.* **204**, 383-396.
- Konieczny, A., and Ausubel, F.M.** (1993). A procedure for mapping *Arabidopsis* mutations using co-dominant ecotype-specific PCR-based markers. *Plant J.* **4**, 403-410.
- Konishi, M., and Sugiyama, M.** (2003). Genetic analysis of adventitious root formation with a novel series of temperature-sensitive mutants of *Arabidopsis thaliana*. *Development* **130**, 5637-5647.
- Krysan, P.J., Young, J.C., and Sussman, M.R.** (1999). T-DNA as an insertional mutagen in *Arabidopsis*. *Plant Cell* **11**, 2283-2290.
- Kuroha, T., and Satoh, S.** (2007). Involvement of cytokinins in adventitious and lateral root formation. *Plant Root* **1**, 27-33.
- Kwak, J.M., Mäser, P., and Schroeder, J.I.** (2009). The clickable guard cell, version II: Interactive model of guard cell signal transduction mechanisms and pathways. In *The Arabidopsis Book* (The American Society of Plant Biologists), pp. 1-17.
- Lam, H.-M., Chiu, J., Hsieh, M.-H., Meisel, L., Oliveira, I.C., Shin, M., and Coruzzi, G.** (1998). Glutamate-receptor genes in plants. *Nature* **396**, 125-126.
- Lam, H.M., Peng, S.S., and Coruzzi, G.M.** (1994). Metabolic regulation of the gene encoding glutamine-dependent asparagine synthetase in *Arabidopsis thaliana*. *Plant Physiol.* **106**, 1347-1357.
- Lam, H.M., Coschigano, K., Schultz, C., Melo-Oliveira, R., Tjaden, G., Oliveira, I., Ngai, N., Hsieh, M.H., and Coruzzi, G.** (1995). Use of *Arabidopsis* mutants and genes to study amide amino acid biosynthesis. *Plant Cell* **7**, 887-898.
- Lariguet, P., Boccacandro, H.E., Alonso, J.M., Ecker, J.R., Chory, J., Casal, J.J., and Fankhauser, C.** (2003). A growth regulatory loop that provides homeostasis to phytochrome A signaling. *Plant Cell* **15**, 2966-2978.
- Lariguet, P., Schepens, I., Hodgson, D., Pedmale, U.V., Trevisan, M., Kami, C., de Carbonnel, M., Alonso, J.M., Ecker, J.R., Liscum, E., and Fankhauser, C.** (2006). PHYTOCHROME KINASE SUBSTRATE 1 is a phototropin 1 binding protein required for phototropism. *Proc. Natl. Acad. Sci. U.S.A.* **103**, 10134-10139.
- Larkin, M.A., Blackshields, G., Brown, N.P., Chenna, R., McGettigan, P.A., McWilliam, H., Valentin, F., Wallace, I.M., Wilm, A., Lopez, R., Thompson,**

- J.D., Gibson, T.J., and Higgins, D.G.** (2007). Clustal W and Clustal X version 2.0. *Bioinformatics* **23**, 2947-2948.
- Last, R.L., Bissinger, P.H., Mahoney, D.J., Radwanski, E.R., and Fink, G.R.** (1991). Tryptophan mutants in *Arabidopsis*: The consequences of duplicated tryptophan synthase β genes. *Plant Cell* **3**, 345-358.
- Lea, P.J., and Mifflin, B.J.** (1980). Transport and metabolism of asparagine and other nitrogen compounds within the plant. In *Amino Acids and Derivatives*, B.J. Mifflin, ed (New York: Academic Press, Inc.), pp. 569-607.
- Lea, P.J., Sodek, L., Parry, M.A.J., Shewry, P.R., and Halford, N.G.** (2007). Asparagine in plants. *Ann. Appl. Biol.* **150**, 1-26.
- Leasure, C.D., Tong, H., Yuen, G., Hou, X., Sun, X., and He, Z.-H.** (2009). ROOT UV-B SENSITIVE2 Acts with ROOT UV-B SENSITIVE1 in a root ultraviolet B-sensing pathway. *Plant Physiol.* **150**, 1902-1915.
- Ledwidge, R., and Blanchard, J.S.** (1999). The dual biosynthetic capability of *N*-acetylornithine aminotransferase in arginine and lysine biosynthesis. *Biochemistry* **38**, 3019-3024.
- Lee, M.W., Jelenska, J., and Greenberg, J.T.** (2008a). *Arabidopsis* proteins important for modulating defense responses to *Pseudomonas syringae* that secrete HopW1-1. *Plant J.* **54**, 452-465.
- Lee, Y., Lee, H.-S., Lee, J.-S., Kim, S.-K., and Kim, S.-H.** (2008b). Hormone- and light-regulated nucleocytoplasmic transport in plants: current status. *J. Exp. Bot.* **59**, 3229-3245.
- Li, J., Zhu, S., Song, X., Shen, Y., Chen, H., Yu, J., Yi, K., Liu, Y., Karplus, V.J., Wu, P., and Deng, X.W.** (2006). A rice glutamate receptor-like gene is critical for the division and survival of individual cells in the root apical meristem. *Plant Cell* **18**, 340-349.
- Liepmann, A., and Olsen, L.** (2004). Genomic analysis of aminotransferases in *Arabidopsis thaliana*. *Crit. Rev. Plant Sci.* **23**, 73-89.
- Lin, C.** (2000). Plant blue-light receptors. *Trends Plant Sci.* **5**, 337-342.
- Lin, C.** (2002). Blue light receptors and signal transduction. *Plant Cell* **14 Suppl**, S207-225.
- Lin, C., and Shalitin, D.** (2003). Cryptochrome structure and signal transduction. *Annu. Rev. Plant Biol.* **54**, 469-496.
- Lin, C., Ahmad, M., Chan, J., and Cashmore, A.** (1996). *CRY2*: A second member of the *Arabidopsis* cryptochrome gene family. *Plant Physiol.* **110**, 1047-1048.
- Liscum, E., Hodgson, D.W., and Campbell, T.J.** (2003). Blue light signaling through the cryptochromes and phototropins. So that's what the blues is all about. *Plant Physiol.* **133**, 1429-1436.
- Llácer, J.L., Fita, I., and Rubio, V.** (2008). Arginine and nitrogen storage. *Curr. Opin. Struc. Biol.* **18**, 673-681.
- López-Bucio, J., Cruz-Ramírez, A., and Herrera-Estrella, L.** (2003). The role of nutrient availability in regulating root architecture. *Curr. Opin. Plant Biol.* **6**, 280-287.
- Malamy, J.E., and Benfey, P.N.** (1997). Organization and cell differentiation in lateral roots of *Arabidopsis thaliana*. *Development* **124**, 33-44.
- Mandoli, D.F., Ford, G.A., Waldron, L.J., Nemson, J.A., and Briggs, W.R.** (1990). Some spectral properties of several soil types: implications for photomorphogenesis. *Plant Cell Environ.* **13**, 287-294.
- Mansour, M.M.F.** (2000). Nitrogen containing compounds and adaptation of plants to salinity stress. *Biol. Plantarum* **43**, 491-500.

- McKay, G., and Shargool, P.D.** (1981). Purification and characterization of *N*-acetylglutamate 5-phosphotransferase from pea (*Pisum sativum*) cotyledons. *Biochem J* **195**, 71-81.
- Meinke, D.W.** (1991). Embryonic mutants of *Arabidopsis thaliana*. *Dev. Genet.* **12**, 382-392.
- Micallef, B.J., and Shelp, B.J.** (1989). Arginine metabolism in developing soybean cotyledons : I. Relationship to nitrogen nutrition. *Plant Physiol.* **90**, 624-630.
- Miesak, B.H., and Coruzzi, G.M.** (2002). Molecular and physiological analysis of *Arabidopsis* mutants defective in cytosolic or chloroplastic aspartate aminotransferase. *Plant Physiol.* **129**, 650-660.
- Miyashita, Y., Dolferus, R., Ismond, K.P., and Good, A.G.** (2007). Alanine aminotransferase catalyses the breakdown of alanine after hypoxia in *Arabidopsis thaliana*. *Plant J.* **49**, 1108-1121.
- Mo, X., Zhu, Q., Li, X., Li, J., Zeng, Q., Rong, H., Zhang, H., and Wu, P.** (2006). The *hpa1* mutant of *Arabidopsis* reveals a crucial role of histidine homeostasis in root meristem maintenance. *Plant Physiol.* **141**, 1425-1435.
- Mobley, E.M., Kunkel, B.N., and Keith, B.** (1999). Identification, characterization and comparative analysis of a novel chorismate mutase gene in *Arabidopsis thaliana*. *Gene* **240**, 115-123.
- Mollá-Morales, A., Sarmiento-Mañús, R., Robles, P., Quesada, V., Pérez-Pérez, J.M., González-Bayón, R., Hannah, M.A., Willmitzer, L., Ponce, M.R., and Micol, J.L.** (2011). Analysis of *ven3* and *ven6* reticulate mutants reveals the importance of arginine biosynthesis in *Arabidopsis* leaf development. *Plant J.* **65**, 335-345.
- Monshausen, G.B., and Gilroy, S.** (2009). The exploring root - root growth responses to local environmental conditions. *Curr. Opin. Plant Biol.* **12**, 766-772.
- Monshausen, G.B., Bibikova, T.N., Weisenseel, M.H., and Gilroy, S.** (2009). Ca²⁺ regulates reactive oxygen species production and pH during mechanosensing in *Arabidopsis* roots. *Plant Cell* **21**, 2341-2356.
- Moreno, N., Bougourd, S., Haseloff, J., and Feijó, J.A.** (2006). Imaging plant cells. In *Handbook of Biological Confocal Microscopy*, J.B. Pawley, ed (New York: SpringerScience+Business Media), pp. 769-787.
- Mozo, T., Fischer, S., Shizuya, H., and Altmann, T.** (1998). Construction and characterization of the IGF *Arabidopsis* BAC library. *Mol. Gen. Genet.* **258**, 562-570.
- Müller, A., Hillebrand, H., and Weiler, E.W.** (1998). Indole-3-acetic acid is synthesized from L-tryptophan in roots of *Arabidopsis thaliana*. *Planta* **206**, 362-369.
- Müller, R., Bleckmann, A., and Simon, R.** (2008). The receptor kinase CORYNE of *Arabidopsis* transmits the stem cell-limiting signal CLAVATA3 independently of CLAVATA1. *Plant Cell* **20**, 934-946.
- Mumberg, D., Mailer, R., and Funk, M.** (1995). Yeast vectors for the controlled expression of heterologous proteins in different genetic backgrounds. *Gene* **156**, 119-122.
- Muralla, R., Sweeney, C., Stepansky, A., Leustek, T., and Meinke, D.** (2007). Genetic dissection of histidine biosynthesis in *Arabidopsis*. *Plant Physiol.* **144**, 890-903.
- Nagatani, A.** (2004). Light-regulated nuclear localization of phytochromes. *Curr. Opin. Plant Biol.* **7**, 708-711.
- Nagatani, A., Reed, J.W., and Chory, J.** (1993). Isolation and initial characterization of *Arabidopsis* mutants that are deficient in Phytochrome A. *Plant Physiol.* **102**, 269-277.
- Nakai, K., and Horton, P.** (1999). PSORT: a program for detecting sorting signals in proteins and predicting their subcellular localization. *Trends Biochem Sci* **24**, 34-36.

- Nakajima, K., and Benfey, P.N.** (2002). Signaling in and out: control of cell division and differentiation in the shoot and root. *Plant Cell* **14 Suppl**, S265-276.
- Naqvi, S., Farré, G., Sanahuja, G., Capell, T., Zhu, C., and Christou, P.** (2010). When more is better: multigene engineering in plants. *Trends Plant Sci.* **15**, 48-56.
- Nemhauser, J., and Chory, J.** (2002). Photomorphogenesis. In *The Arabidopsis Book* (The American Society of Plant Biologists), pp. 1-12.
- Noctor, G., Novitskaya, L., Lea, P.J., and Foyer, C.H.** (2002). Co-ordination of leaf minor amino acid contents in crop species: significance and interpretation. *J. Exp. Bot.* **53**, 939-945.
- Noutoshi, Y., Ito, T., and Shinozaki, K.** (2005). *ALBINO AND PALE GREEN 10* encodes BBMII isomerase involved in histidine biosynthesis in *Arabidopsis thaliana*. *Plant Cell Physiol.* **46**, 1165-1172.
- Ohta, D., Fujimori, K., Mizutani, M., Nakayama, Y., Kunpaisal-Hashimoto, R., Münzer, S., and Kozaki, A.** (2000). Molecular cloning and characterization of ATP-phosphoribosyl transferase from *Arabidopsis*, a key enzyme in the histidine biosynthetic pathway. *Plant Physiol.* **122**, 907-914.
- Oyama, T., Shimura, Y., and Okada, K.** (1997). The *Arabidopsis HY5* gene encodes a bZIP protein that regulates stimulus-induced development of root and hypocotyl. *Genes Dev.* **11**, 2983-2995.
- Patil, S.S., Tama, L.Q., and Sakai, W.S.** (1972). Mode of action of the toxin from *Pseudomonas phaseolicola*. *Plant Physiol.* **49**, 803-807.
- Pauwels, K., Abadjieva, A., Hilven, P., Stankiewicz, A., and Crabeel, M.** (2003). The N-acetylglutamate synthase/N-acetylglutamate kinase metabolon of *Saccharomyces cerevisiae* allows co-ordinated feedback regulation of the first two steps in arginine biosynthesis. *Eur. J. Biochem.* **270**, 1014-1024.
- Pepper, A., Delaney, T., Washburn, T., Poole, D., and Chory, J.** (1994). *DET1*, a negative regulator of light-mediated development and gene expression in *Arabidopsis*, encodes a novel nuclear-localized protein. *Cell* **78**, 109-116.
- Percudani, R., and Peracchi, A.** (2003). A genomic overview of pyridoxal-phosphate-dependent enzymes. *EMBO Rep.* **4**, 850 - 854.
- Peterhansel, C., Horst, I., Niessen, M., Blume, C., Kebeish, R., Kürkcüoğlu, S., and Kreuzaler, a.F.** (2010). Photorespiration. In *The Arabidopsis Book* (The American Society of Plant Biologists), pp. 1-24.
- Petersen, L.N., Marineo, S., Mandalà, S., Davids, F., Sewell, B.T., and Ingle, R.A.** (2010). The missing link in plant histidine biosynthesis: *Arabidopsis myoinositol monophosphatase-like2* encodes a functional histidinol-phosphate phosphatase. *Plant Physiol.* **152**, 1186-1196.
- Pokorny, R., Klar, T., Hennecke, U., Carell, T., Batschauer, A., and Essen, L.-O.** (2008). Recognition and repair of UV lesions in loop structures of duplex DNA by DASH-type cryptochrome. *Proc. Natl. Acad. Sci. U.S.A.* **105**, 21023-21027.
- Potel, F., Valadier, M.-H., Ferrario-Méry, S., Grandjean, O., Morin, H., Gaufichon, L., Boutet-Mercey, S., Lothier, J., Rothstein, S.J., Hirose, N., and Suzuki, a.A.** (2009). Assimilation of excess ammonium into amino acids and nitrogen translocation in *Arabidopsis thaliana* – roles of glutamate synthases and carbamoylphosphate synthetase in leaves. *FEBS J.* **276** 4061-4076.
- Pratelli, R., and Pilot, G.** (2007). Altered amino acid metabolism in *glutamine dumper1* plants. *Plant Signal. Behav.* **2**, 182-184.
- Quail, P.H.** (2002). Photosensory perception and signalling in plant cells: new paradigms? *Curr. Opin. Cell Biol.* **14**, 180-188.

- Quesada, V., Ponce, M.R., and Micol, J.L.** (1999). *OTC* and *AUL1*, two convergent and overlapping genes in the nuclear genome of *Arabidopsis thaliana*. *FEBS Lett.* **461**, 101-106.
- Radwanski, E.R., and Last, R.L.** (1995). Tryptophan biosynthesis and metabolism: biochemical and molecular genetics. *Plant Cell* **7**, 921-934.
- Radwanski, E.R., Barczak, A.J., and Last, R.L.** (1996). Characterization of tryptophan synthase alpha subunit mutants of *Arabidopsis thaliana*. *Mol. Gen. Genet.* **253**, 353-361.
- Raghava, G.P.S.** (2002). APSSP2 : A combination method for protein secondary structure prediction based on neural network and example based learning. *CASP5*, A-132.
- Rate, D.N., and Greenberg, J.T.** (2001). The *Arabidopsis aberrant growth and death2* mutant shows resistance to *Pseudomonas syringae* and reveals a role for NPR1 in suppressing hypersensitive cell death. *Plant J.* **27**, 203-211.
- Reed, J.W., Nagpal, P., Poole, D.S., Furuya, M., and Chory, J.** (1993). Mutations in the gene for the red/far-red light receptor phytochrome B alter cell elongation and physiological responses throughout *Arabidopsis* development. *Plant Cell* **5**, 147-157.
- Reed, J.W., Nagatani, A., Elich, T.D., Fagan, M., and Chory, J.** (1994). Phytochrome A and phytochrome B have overlapping but distinct functions in *Arabidopsis* development. *Plant Physiol.* **104**, 1139-1149.
- Reisbacher, S.** (2009). Functional analysis of cryptochrome 3 from *Arabidopsis thaliana* (Marburg: Philips Universität Marburg).
- Remacle, C., Cline, S., Boutaffala, L., Gabilly, S., Larosa, V., Barbieri, M.R., Coosemans, N., and Hamel, P.P.** (2009). The *ARG9* gene encodes the plastid-resident *N*-acetyl ornithine aminotransferase in the green alga *Chlamydomonas reinhardtii*. *Eukaryot. Cell* **8**, 1460-1463.
- Replogle, A., Wang, J., Bleckmann, A., Hussey, R.S., Baum, T.J., Sawa, S., Davis, E.L., Wang, X., Simon, R., and Mitchum, M.G.** (2011). Nematode CLE signaling in *Arabidopsis* requires CLAVATA2 and CORYNE. *Plant J.* **65**, 430-440.
- Rhee, S.Y., Zhang, P., Foerster, H., and Tissier, C.** (2006). AraCyc: Overview of an *Arabidopsis* metabolism database and its applications for plant research. In *Plant Metabolomics*, K. Saito, R.A. Dixon, and L. Willmitzer, eds (Springer Berlin Heidelberg), pp. 141-154.
- Riefler, M.** (2001). Identifizierung und Charakterisierung der *tumor prone* Mutanten von *Arabidopsis thaliana* und *Atckx*-Mutanten. PhD thesis (Eberhard-Karls-Universität Tübingen).
- Rockwell, N.C., Su, Y.-S., and Lagarias, J.C.** (2006). Phytochrome structure and signaling mechanisms. *Annu. Rev. Plant Biol.* **57**, 837-858.
- Roosens, N.H., Thu, T.T., Iskandar, H.M., and Jacobs, M.** (1998). Isolation of the ornithine-delta-aminotransferase cDNA and effect of salt stress on its expression in *Arabidopsis thaliana*. *Plant Physiol.* **117**, 263-271.
- Rose, A.B., and Last, R.L.** (1994). Molecular genetics of amino acid, nucleotide, and vitamin biosynthesis. In *Arabidopsis*, E.M. Meyerowitz and C.R. Somerville, eds (Cold Spring Harbor Laboratory Press), pp. 835-879.
- Rosen, E., Chen, R., and Masson, P.H.** (1999). Root gravitropism: a complex response to a simple stimulus? *Trends Plant Sci.* **4**, 407-412.
- Rotman, B., and Papermaster, B.W.** (1966). Membrane properties of living mammalian cells as studied by enzymatic hydrolysis of fluorogenic esters. *Proc. Natl. Acad. Sci. U.S.A.* **55**, 134-141.
- Ruppel, N.J., Hangarter, R.P., and Kiss, J.Z.** (2001). Red-light-induced positive phototropism in *Arabidopsis* roots. *Planta* **212**, 424-430.

- Sabatini, S., Beis, D., Wolkenfelt, H., Murfett, J., Guilfoyle, T., Malamy, J., Benfey, P., Leyser, O., Bechtold, N., Weisbeek, P., and Scheres, B.** (1999). An auxin-dependent distal organizer of pattern and polarity in the *Arabidopsis* root. *Cell* **99**, 463-472.
- Sablowski, R.** (2007). The dynamic plant stem cell niches. *Curr. Opin. Plant Biol.* **10**, 639-644.
- Saito, K.** (1999). Biosynthesis of cysteine. In *Plant Amino Acids*, B.K. Singh, ed (New York: Marcel Dekker, Inc.), pp. 267-291.
- Sakai, T., Kagawa, T., Kasahara, M., Swartz, T.E., Christie, J.M., Briggs, W.R., Wada, M., and Okada, K.** (2001). *Arabidopsis* nph1 and npl1: Blue light receptors that mediate both phototropism and chloroplast relocation. *Proc. Natl. Acad. Sci. U.S.A.* **98**, 6969-6974.
- Sakamoto, K., and Briggs, W.R.** (2002). Cellular and subcellular localization of phototropin 1. *Plant Cell* **14**, 1723-1735.
- Sambrook, J., and Russel, D.** (2001). *Molecular Cloning. A Laboratory Manual.* (Cold Spring Harbor, New York.: Cold Spring Harbor Laboratory Press).
- Sánchez-Calderón, L., López-Bucio, J., Chacón-López, A., Cruz-Ramírez, A., Nieto-Jacobo, F., Dubrovsky, J.G., and Herrera-Estrella, L.** (2005). Phosphate starvation induces a determinate developmental program in the roots of *Arabidopsis thaliana*. *Plant Cell Physiol.* **46**, 174-184.
- Sanders, A., Collier, R., Trethewy, A., Gould, G., Sieker, R., and Tegeder, M.** (2009). AAP1 regulates import of amino acids into developing *Arabidopsis* embryos. *Plant J.* **59**, 540-552.
- Sarrobert, C., Thibaud, M.-C., Contard-David, P., Gineste, S., Bechtold, N., Robaglia, C., and Nussaume, L.** (2000). Identification of an *Arabidopsis thaliana* mutant accumulating threonine resulting from mutation in a new dihydrodipicolinate synthase gene. *Plant J.* **24**, 357-367.
- Scheres, B., Benfey, P., and Dolan, L.** (2002). Root development. In *The Arabidopsis Book* (The American Society of Plant Biologists), pp. 1-18.
- Schultz, C.J., Hsu, M., Miesak, B., and Coruzzi, G.M.** (1998). *Arabidopsis* mutants define an *in vivo* role for isoenzymes of aspartate aminotransferase in plant nitrogen assimilation. *Genetics* **149**, 491-499.
- Schwacke, R., Schneider, A., van der Graaff, E., Fischer, K., Catoni, E., Desimone, M., Frommer, W.B., Flugge, U.-I., and Kunze, R.** (2003). ARAMEMNON, a novel database for *Arabidopsis* integral membrane proteins. *Plant Physiol.* **131**, 16-26.
- Shargool, P.D., Jain, J.C., and McKay, G.** (1988). Ornithine biosynthesis, and arginine biosynthesis and degradation in plant cells. *Phytochemistry* **27** 1571-1574.
- Siehl, D.L., and Conn, E.E.** (1988). Kinetic and regulatory properties of arogenate dehydratase in seedlings of *Sorghum bicolor* (L.) moench. *Arch. Biochem. Biophys.* **260**, 822-829.
- Singh, B.K.** (1999). Biosynthesis of valine, leucine and isoleucine. In *Plant Amino Acids*, B.K. Singh, ed (New York: Marcel Dekker, Inc.), pp. 227-247.
- Singh, B.K., and Matthews, B.F.** (1994). Molecular regulation of amino acid biosynthesis in plants. *Amino Acids* **7**, 165-174.
- Skoog, F., and Miller, C.O.** (1957). Chemical regulation of growth and organ formation in plant tissues cultured *in vitro*. *Symp Soc Exp Biol* **11**, 118-131.
- Slocum, R.D.** (2005). Genes, enzymes and regulation of arginine biosynthesis in plants. *Plant Physiol. Bioch.* **43** 729-745.
- Slocum, R.D., Nichols, H.F., III, and Williamson, C.L.** (2000). Purification and characterization of *Arabidopsis* ornithine transcarbamoylase (OTCase), a member of a

- distinct and evolutionarily-conserved group of plant OTCases. *Plant Physiol. Bioch.* **38**, 279-288.
- Somerville, C.R., and Ogren, W.L.** (1980). Photorespiration mutants of *Arabidopsis thaliana* deficient in serine-glyoxylate aminotransferase activity. *Proc. Natl. Acad. Sci. U.S.A.* **77**, 2684-2687.
- Somerville, C.R., and Ogren, W.L.** (1982). Mutants of the cruciferous plant *Arabidopsis thaliana* lacking glycine decarboxylase activity. *Biochem. J.* **202**, 373-380.
- Song, J.T., Lu, H., and Greenberg, J.T.** (2004). Divergent roles in *Arabidopsis thaliana* development and defense of two homologous genes, *ABERRANT GROWTH AND DEATH2* and *AGD2-LIKE DEFENSE RESPONSE PROTEIN1*, encoding novel aminotransferases. *Plant Cell* **16**, 353-366.
- Spalding, E.P., and Folta, K.M.** (2005). Illuminating topics in plant photobiology. *Plant Cell Environ.* **28**, 39-53.
- Splittstoesser, W.E.** (1969). Metabolism of arginine by aging and 7 day old pumpkin seedlings. *Plant Physiol.* **44**, 361-366.
- Stepansky, A., and Leustek, T.** (2006). Histidine biosynthesis in plants. *Amino Acids* **30**, 127-142.
- Suesslin, C., and Frohnmeyer, H.** (2003). An *Arabidopsis* mutant defective in UV-B light-mediated responses. *Plant J.* **33**, 591-601.
- Sugimoto, K., Jiao, Y., and Meyerowitz, E.M.** (2010). *Arabidopsis* regeneration from multiple tissues occurs via a root development pathway. *Dev. Cell* **18**, 463-471.
- Sullivan, J.A., and Deng, X.W.** (2003). From seed to seed: the role of photoreceptors in *Arabidopsis* development. *Dev Biol* **260**, 289-297.
- Sun, Q., Yoda, K., and Suzuki, H.** (2005). Internal axial light conduction in the stems and roots of herbaceous plants. *J. Exp. Bot.* **56**, 191-203.
- Szabados, L., and Saviouré, A.** (2010). Proline: a multifunctional amino acid. *Trends Plant Sci.* **15**, 89-97.
- Székely, G., Ábrahám, E., Cséplő, Á., Rigó, G., Zsigmond, L., Csiszár, J., Ayaydin, F., Strizhov, N., Jásik, J., Schmelzer, E., Koncz, C., and Szabados, L.** (2008). Duplicated *P5CS* genes of *Arabidopsis* play distinct roles in stress regulation and developmental control of proline biosynthesis. *Plant J.* **53**, 11-28.
- Taiz, L., and Zeiger, E.** (2002). *Plant Physiology*. (Sunderland, Massachusetts: Sinauer Associates, Inc.).
- Taylor, A.A., and Stewart, G.R.** (1981). Tissue and subcellular localization of enzymes of arginine metabolism in *Pisum sativum*. *Biochem. Biophys. Res. Co.* **101**, 1281-1289.
- Thimm, O., Bläsing, O., Gibon, Y., Nagel, A., Meyer, S., Krüger, P., Selbig, J., Müller, L.A., Rhee, S.Y., and Stitt, M.** (2004). MAPMAN: a user-driven tool to display genomics data sets onto diagrams of metabolic pathways and other biological processes. *Plant J.* **37**, 914-939.
- Thompson, J.F.** (1980). Arginine synthesis, proline synthesis, and related processes. In *Amino Acids and Derivatives*, B.J. Mifflin, ed (New York: Academic Press, Inc.), pp. 375-402.
- Tian, B.-j., Wang, Y., Zhu, Y.-r., Lü, X.-y., Huang, K., Shao, N., and Beck, C.F.** (2006). Synthesis of the photorespiratory key enzyme serine:glyoxylate aminotransferase in *C. reinhardtii* is modulated by the light regime and cytokinin. *Physiol. Plantarum* **127**, 571-582.
- Titiz, O., Tambasco-Studart, M., Warzych, E., Apel, K., Amrhein, N., Laloi, C., and Fitzpatrick, T.B.** (2006). PDX1 is essential for vitamin B6 biosynthesis, development and stress tolerance in *Arabidopsis*. *Plant J.* **48**, 933-946.

- Tong, H., Leasure, C.D., Hou, X., Yuen, G., Briggs, W., and He, Z.-H.** (2008). Role of root UV-B sensing in *Arabidopsis* early seedling development. *Proc. Natl. Acad. Sci. U.S.A.* **105**, 21039-21044.
- Tóth, R., Kevei, É., Hall, A., Millar, A.J., Nagy, F., and Kozma-Bognár, L.** (2001). Circadian clock-regulated expression of phytochrome and cryptochrome genes in *Arabidopsis*. *Plant Physiol.* **127**, 1607-1616.
- Tucker, M.R., and Laux, T.** (2007). Connecting the paths in plant stem cell regulation. *Trends Cell Biol.* **17**, 403-410.
- van den Berg, C., Willemsen, V., Hage, W., Weisbeek, P., and Scheres, B.** (1995). Cell fate in the *Arabidopsis* root meristem determined by directional signalling. *Nature* **378**, 62-65.
- van den Berg, C., Willemsen, V., Hendriks, G., Weisbeek, P., and Scheres, B.** (1997). Short-range control of cell differentiation in the *Arabidopsis* root meristem. *Nature* **390**, 287-289.
- VanEtten, C.H., Miller, R.W., I.A.Wolff, and Jones, Q.** (1963). Amino acid composition of seeds from 200 angiospermous plant species. *J. Agr. Food Chem.* **11**, 399-410.
- Verbruggen, N., and Hermans, C.** (2008). Proline accumulation in plants: a review. *Amino Acids* **35**, 753-759.
- Verma, D.P.S., and Zhang, C.-S.** (1999). Regulation of proline and arginine biosynthesis in plants. In *Plant Amino Acids*, B.K. Singh, ed (New York: Marcel Dekker, Inc.), pp. 249-265.
- Vernoux, T., Wilson, R.C., Seeley, K.A., Reichheld, J.P., Muroy, S., Brown, S., Maughan, S.C., Cobbett, C.S., Van Montagu, M., Inze, D., May, M.J., and Sung, Z.R.** (2000). The *ROOT MERISTEMLESS1/CADMIUM SENSITIVE2* gene defines a glutathione-dependent pathway involved in initiation and maintenance of cell division during postembryonic root development. *Plant Cell* **12**, 97-109.
- Vogel, H.J.** (1953). Path of ornithine synthesis in *Escherichia coli*. *Proc. Natl. Acad. Sci. U.S.A.* **39**, 578-583.
- Voll, L.M., Allaire, E.E., Fiene, G., and Weber, A.P.** (2004). The *Arabidopsis phenylalanine insensitive growth* mutant exhibits a deregulated amino acid metabolism. *Plant Physiol.* **136**, 3058-3069.
- Walch-Liu, P., Liu, L.-H., Remans, T., Tester, M., and Forde, B.G.** (2006). Evidence that L-glutamate can act as an exogenous signal to modulate root growth and branching in *Arabidopsis thaliana*. *Plant Cell Physiol.* **47**, 1045-1057.
- Wang, G., and Fiers, M.** (2010). CLE peptide signaling during plant development. *Protoplasma* **240**, 33-43.
- Ward, E., and Ohta, D.** (1999). Histidine biosynthesis. In *Plant Amino Acids*, B.K. Singh, ed (New York: Marcel Dekker, Inc.), pp. 293-303.
- Ward, J.T., Lahner, B., Yakubova, E., Salt, D.E., and Raghothama, K.G.** (2008). The effect of iron on the primary root elongation of *Arabidopsis* during phosphate deficiency. *Plant Physiol.* **147**, 1181-1191.
- Waters, B.M., Chu, H.-H., DiDonato, R.J., Roberts, L.A., Eisley, R.B., Lahner, B., Salt, D.E., and Walker, E.L.** (2006). Mutations in *Arabidopsis Yellow Stripe-Like1* and *Yellow Stripe-Like3* reveal their roles in metal ion homeostasis and loading of metal ions in seeds. *Plant Physiol.* **141**, 1446-1458.
- Weigel, D., and Glazebrook, J.** (2002). *Arabidopsis: A laboratory manual*. (Cold Spring Harbor, New York: Cold Spring Harbor Laboratory Press).
- Werner, T., and Schmülling, T.** (2009). Cytokinin action in plant development. *Curr. Opin. Plant Biol.* **12**, 527-538.

- Wildwater, M., Campilho, A., Perez-Perez, J.M., Heidstra, R., Blilou, I., Korthout, H., Chatterjee, J., Mariconti, L., Gruissem, W., and Scheres, B. (2005). The *RETINOBLASTOMA-RELATED* gene regulates stem cell maintenance in *Arabidopsis* roots. *Cell* **123**, 1337-1349.
- Winter, D., Vinegar, B., Nahal, H., Ammar, R., Wilson, G., and Provart, N.J. (2007). An “electronic Fluorescent Pictograph” browser for exploring and analyzing large-scale biological data sets. *PLoS ONE* **2**, e718.
- Wishart, D.S., Knox, C., Guo, A.C., Eisner, R., Young, N., Gautam, B., Hau, D.D., Psychogios, N., Dong, E., Bouatra, S., Mandal, R., Sinelnikov, I., Xia, J., Jia, L., Cruz, J.A., Lim, E., Sobsey, C.A., Shrivastava, S., Huang, P., Liu, P., Fang, L., Peng, J., Fradette, R., Cheng, D., Tzur, D., Clements, M., Lewis, A., De Souza, A., Zuniga, A., Dawe, M., Xiong, Y., Clive, D., Greiner, R., Nazyrova, A., Shaykhutdinov, R., Li, L., Vogel, H.J., and Forsythe, I. (2009). HMDB: a knowledgebase for the human metabolome. *Nucleic Acids Res.* **37**, D603-610.
- Xiang, C., Han, P., Lutziger, I., Wang, K., and Oliver, D.J. (1999). A mini binary vector series for plant transformation. *Plant Mol. Biol.* **40**, 711–717.
- Yadegari, R., Paiva, G.R.d., Laux, T., Koltunow, A.M., Apuya, N., Zimmerman, J.L., Fischer, R.L., Harada, J.J., and Goldberg, R.B. (1994). Cell differentiation and morphogenesis are uncoupled in *Arabidopsis* raspberry embryos. *Plant Cell* **6**, 1713-1729.
- Yamada, K., Lim, J., Dale, J.M., Chen, H., Shinn, P., Palm, C.J., Southwick, A.M., Wu, H.C., Kim, C., Nguyen, M., Pham, P., Cheuk, R., Karlin-Newmann, G., Liu, S.X., Lam, B., Sakano, H., Wu, T., Yu, G., Miranda, M., Quach, H.L., Tripp, M., Chang, C.H., Lee, J.M., Toriumi, M., Chan, M.M.H., Tang, C.C., Onodera, C.S., Deng, J.M., Akiyama, K., Ansari, Y., Arakawa, T., Banh, J., Banno, F., Bowser, L., Brooks, S., Carninci, P., Chao, Q., Choy, N., Enju, A., Goldsmith, A.D., Gurjal, M., Hansen, N.F., Hayashizaki, Y., Johnson-Hopson, C., Hsuan, V.W., Iida, K., Karnes, M., Khan, S., Koesema, E., Ishida, J., Jiang, P.X., Jones, T., Kawai, J., Kamiya, A., Meyers, C., Nakajima, M., Narusaka, M., Seki, M., Sakurai, T., Satou, M., Tamse, R., Vaysberg, M., Wallender, E.K., Wong, C., Yamamura, Y., Yuan, S., Shinozaki, K., Davis, R.W., Theologis, A., and Ecker, J.R. (2003). Empirical analysis of transcriptional activity in the *Arabidopsis* genome. *Science* **302**, 842-846.
- Yang, J., Zhang, J., Liu, K., Wang, Z., and Liu, L. (2007). Involvement of polyamines in the drought resistance of rice. *J. Exp. Bot.* **58**, 1545-1555.
- Yu, X., Klejnot, J., Zhao, X., Shalitin, D., Maymon, M., Yang, H., Lee, J., Liu, X., Lopez, J., and Lin, C. (2007). *Arabidopsis* cryptochrome 2 completes its post-translational life cycle in the nucleus. *Plant Cell* **19**, 3146-3156.
- Zhang, Y.X., and Patil, S.S. (1997). The *phtE* locus in the phaseolotoxin gene cluster has ORFs with homologies to genes encoding amino acid transferases, the AraC family of transcriptional factors, and fatty acid desaturases. *Mol. Plant Microbe In.* **10**, 947-960.
- Zhao, J., Williams, C.C., and Last, R.L. (1998). Induction of *Arabidopsis* tryptophan pathway enzymes and camalexin by amino acid starvation, oxidative stress, and an abiotic elicitor. *Plant Cell* **10**, 359-370.
- Zirak, P., Penzkofer, A., Moldt, J., Pokorny, R., Batschauer, A., and Essen, L.O. (2009). Photocycle dynamics of the E149A mutant of cryptochrome 3 from *Arabidopsis thaliana*. *J. Photochem. Photobiol. B, Biol.* **97**, 94-108.
- Zonia, L.E., Stebbins, N.E., and Polacco, J.C. (1995). Essential role of urease in germination of nitrogen-limited *Arabidopsis thaliana* seeds. *Plant Physiol.* **107**, 1097-1103.

Zrenner, R., Stitt, M., Sonnewald, U., and Boldt, R. (2006). Pyrimidine and purine biosynthesis and degradation in plants. *Annu. Rev. Plant Biol.* **57**, 805–836.

8 Acknowledgments / Danksagungen

Ich danke Prof. Dr. Thomas Schmülling für die Überlassung dieses spannenden Promotionsthemas, seine guten Ideen, seine Geduld in einer schwierigen Phase, sein Mutmachen und für seine unglaubliche Unterstützung.

Prof. Dr. Wolfgang Schuster möchte ich für die Übernahme der Korrektur dieser Arbeit, für anregende Gespräche und Gedanken, für sein schnelles Protoplastenprotokoll, die Hilfe bei Computerproblemen und seine aufmunternden Worte danken.

Dr. Michael Riefler möchte ich herzlich für all das danken, was ich von ihm gelernt habe, für seinen kompetenten Rat, seine kreativen Lösungsansätze und seine positive, motivierende Betreuung (auch besonders in einer schwierigen Phase).

Dr. Rainer Höfgen, Dr. Stephan Krüger, Dr. Hans-Michael Hubberten und Dr. Mariusz Bromke (MPI für Molekulare Pflanzenphysiologie, Golm) danke ich für die Möglichkeit, in der Arbeitsgruppe HPLC-Proben zu analysieren, außerdem danke ich für die Einarbeitung und die große Hilfe bei der Proben-Untersuchung.

Prof. Dr. Grimm und PD Dr. Christina Kühn (Institut für Biologie, Humboldt Universität zu Berlin) möchte ich für die Möglichkeit zur Nutzung des konfokalen Mikroskops und die Einführung in dessen Benutzung danken.

Danke an Prof. Dr. Winslow Briggs (Stanford University, USA) für die freundliche Überlassung der *phot1-5* Mutante.

Euroscarf (Frankfurt) danke ich für die Überlassung der Hefemutante Y37711.

Ich möchte mich bei der Deutschen Forschungsgemeinschaft, der Kommission zur Vergabe von NaFöG-Promotionsstipendien und der Dahlem Research School für die Finanzierung bedanken.

Dr. Andrea Stolz danke ich sehr für die wertvollen Klonierungstips und für die Herstellung des komplementierenden BAC-Subklons!

Vielen Dank an Dr. Wolfram Brenner für seine Hilfe in vielen Computer- und qRT-Fragen.

PD Dr. Alexander Heyl danke ich für die Beratung und gute Protokoll-Abwandlungen zu Hefe- und Gatewayfragen und für seine super Art zu lachen (die „d. L.“).

Danke schön auch an Dr. Eva Krupková für kritische und anregende Diskussionen, das Anlernen am konfokalen Mikroskop und die guten Tips in Laborfragen.

Ulrike Deppe möchte ich für die Vorarbeiten und die Einführung zu *tup5-1* danken, Dr. Erika Nehnevajova für sehr gute Hinweise zu Excel, Miriam Baradari für Hilfe bei proble-

matischen Word-Angelegenheiten, Dr. Tomáš Werner für die häufige und schnelle Wiederherstellung des (übrigens nicht von mir) geschundenen Mikroskops, wenn es gerade dringend war, Sabine Thiel für die freundliche und engagierte Erledigung der Formalien, und allen GärtnerInnen möchte ich für die gute Pflege der *Arabidopsen* danken.

Dem gesamten Labor 104 danke ich für die schöne Zeit, die Unterstützung und die angenehme Arbeitsatmosphäre!

Außerdem möchte ich natürlich allen Institutsmitgliedern für Ihre Hilfe, interessante Diskussionen und die moralische Unterstützung bedanken.

Wärmster Dank gilt auch allen Freunden, Bekannten und allen Personen in meinem Umfeld, die mich immer wieder abgelenkt und seelisch und moralisch unterstützt haben!

Mein ganz besonderer Dank gilt meinen Eltern und Großeltern für ihr Mutmachen und ihre Unterstützung. Ohne ihre Hilfe wäre diese Arbeit nicht möglich gewesen.

9 Supplemental data

9.1 Gene search

Table 9-1: Analysed T-DNA insertion lines of genes in the *tup5* mapping interval.

Data shown in the columns: Gene number; 5'- and 3'-coordinates on the BAC clone; Name of the gene product, Clone number of the analysed T-DNA insertion line; Insertion site within the gene: e. g. exon / intron / 5' or 3' UTR). 300-5' or 300-3': The insertion is located within 300 bp of 5' or 3' UTR; 1000-Promoter: The insertion is located within 1000 bp of the promoter region.

Gene number	5'-coordinate	3'-coordinate	Predicted gene product (from http://www.tigr.org)	analysed SALK line	Site of the insertion
Locus on BAC T21F11:					
At1g80550	31926	33684	Pentatricopeptide (PPR) repeat-containing protein	SALK_016702	300-3'
At1g80560	30840	28333	3-isopropylmalate dehydrogenase, chloroplast, putative	-	-
At1g80570	28305	26210	F-box protein family (FBL14)	-	-
At1g80580	25072	24302	Ethylene-responsive element binding protein family (EREBP)	SALK_102940	300-5'
At1g80590	21474	22420	WRKY family transcription factor	-	-
At1g80600	18077	20112	Acetylornithine aminotransferase, mitochondrial, putative	SALK_122547	1000-Promoter
At1g80610	14597	17897	Expressed protein	SALK_069585	300-3'
At1g80620	13266	11214	Ribosomal protein S15 family protein	-	-
At1g80630	7974	9934	Leucine-rich repeat family protein	-	-
At1g80640	6963	4255	Protein kinase family protein	-	-
At1g80650	4052	2811	Double-stranded RNA-binding domain-containing protein	-	-
Locus on BAC F23A5:					
At1g80660	3931	210	ATPase 9, plasma membrane-type, putative	SALK_127945 SALK_076800	Intron Intron
At1g80670	7731	4559	Transducin family protein / WD-40 repeat family protein	-	-
At1g80680	7991	12741	Nucleoporin family protein	SALK_109957 SALK_051954 SALK_051955 SALK_051963 SALK_030479	Exon 300-3' 300-3' 300-3' 300-3'
At1g80690	14786	13052	Expressed protein	SALK_016370 SALK_016376 SALK_022740 SALK_095839 SALK_070697	300-3' 300-3' 300-3' Intron 300-5'
At1g80700	15910	17378	Expressed protein	SALK_002149 SALK_002147	Intron Intron
At1g80710	19854	17406	Transducin family protein / WD-40 repeat family protein	-	-

Table 9-2: Continuation of Table 9-1.

Gene number	5'-coordinate	3'-coordinate	Predicted gene product (from http://www.tigr.org)	analysed SALK line	Site of the insertion
At1g80720	20121	21541	Mitochondrial glycoprotein family / MAM33 family	-	-
At1g80730	24230	23306	Zinc finger (C2H2 type) family protein (ZFP1)	-	-
At1g80740	26377	31031	Chromomethylase 1 (CMT1)	SALK_047414	Exon
				SALK_047398	Exon
				SALK_013851	Intron
				SALK_138685	Intron
At1g80750	32806	34547	60S ribosomal protein L7 (RPL7A)	SALK_097969	300-3'
At1g80760	36191	34522	Major intrinsic family protein / MIP family protein		300-3'
At1g80770	39233	41947	Expressed protein	SALK_062867	300-5'
				SALK_099309	300-5'
				SALK_099501	300-5'
				SALK_052666	300-5'
				SALK_048569	Exon
At1g80780	42098	43356	CCR4-NOT transcription complex protein, putative	SALK_142773	300-5'
				SALK_059854	Exon
				SALK_051460	Exon
				SALK_145876	300-3'
				SALK_125692	300-3'
				SALK_033898	300-3'
				SALK_033977	300-3'
				SALK_125691	300-3'
				SALK_145884	300-3'
SALK_055434	300-3'				
At1g80790	43706	46839	XH/XS domain-containing protein / zinc finger family protein	SALK_052192	300-5'
				SALK_133912	300-5'
				SALK_126388	300-5'
				SALK_081362	Intron
				SALK_026822	300-3'
At1g80800	47996	48293	Pseudogene, 40S ribosomal protein S12 (RPS12B)	-	-
At1g80810	49165	52881	Expressed protein	SALK_010025	Intron
At1g80820	54556	56653	Cinnamoyl-CoA reductase, putative	-	-
At1g80830	59679	56862	NRAMP metal ion transporter 1 (NRAMP1)	SALK_040356	Exon
				SALK_053226	Exon
				SALK_125551	Exon
				SALK_079306	Exon

Table 9-3: Primers used for sequencing and gene identification during BAC complementation.

Name of primer	Sequence	Name of primer	Sequence
At1g80550_1708r	agcaaccacatcgagtttcatc	AtZFP1 f (At1g80730)	ttagtattgtactacatggact
At1g80550_806f	tttggcccataaatggtattc	AtZFP1 r (At1g80730)	acgaccacatcagttcacatc
At1g80550_2425r	cagtgttttctcctcggtttg	NF_At1g80740a	gcaacgccttcatcttttacttgc
At1g80550_1503f	atctgattctctcggtgggtgc	NF_At1g80740b	aggatgggtctacaacatggac
NF_At1g80570a	gcgtttgacatggcaatc	NF_At1g80740c	tatgaaccgtttgggttttgc
NF_At1g80570b	catctcattcgatgcctaaacg	NF_At1g80740d	cagcaccagacttgcctcatc
NF_At1g80570c	tcctcagcttgatcaaatcacc	NF_At1g80740e	aacattgtgcaggtgagaaac g
NF_At1g80570d	Gaagagttcattccaacaacaaatg	NF_At1g80740f	atgtgttgggaggggataagg
At1g80580fw	Tctccaacagacaaaaacaaag	NF_At1g80740g	gctccctcagcttagaacagg
At1g80580rv	tctcatcgaaatgacagcagatc	NF_At1g80740h	acgatttcatccccaaagtc
At1g80590fw	cagattaacctgaattatcctaaacag	NF_At1g80740i	ttcgagcaaagttgaaatctgg
At1g80590rv	caaaacatgaacatgaaaagaaatg	NF_At1g80740j	gcaactgaattacgcaaaatcg
NF_At1g80630a	caagcccagtttgaaatitg	At1g80750-F1	ggtctggtggcaagttgtt
NF_At1g80630b	gttaaacgccgaagaacatcc	At1g80750-F2	ccattcgttttactgcctcaa
NF_At1g80630c	tcggattcgttttgtctgatg	At1g80750-R	gccagaggaagatgaagcac
NF_At1g80630d	gtgattgctattgccttggg	NF_At1g807160a (At1g80760)	tgtaagaggctaaaaccaac c
At1g80640a	ccaaacttactaactgtctctcg	NF_At1g807160b (At1g80760)	gtttgtggacattgatcctg
At1g80640b	tatcttcacgagcattgccatc	NF_At1g807160c (At1g80760)	tcatgtggttctctcagtaacatc c
At1g80640c	caagaagatcctcagaagccttg	NF_At1g807160d (At1g80760)	cacgaccatttctcataaagat agc
At1g80640d	atggcttatttggcttgg	At1g80770-f	tgatgacgcggaaatcatta
At1g80640e	tggttcttctcacaagaatc	At1g80770-r	ggttagggtttcaggggaagg
At1g80640f	aaatctgttagctttacgtataaaagg	NF_At1g80780fw	cagaacaagaaaactgtgg agaac
NF_At1g80650_fw	gcaagagagaatgcaacaaaacc	NF_At1g80780rev	tggagtataagtgtctgatgatg c
NF_At1g80650_rev	ttgcttaaatggaaccgagagac	NF_At1g80790a	attgcaatcagcgttttagttg
(NF_At1g80650intfw)	tggttcaagcttccctcgttag	NF_At1g80790b	cgcagcccctaactctatattc
NF_At1g80660a	aagaagaagccacatccactgc	NF_At1g80790c	gtctcaggcagttgtggatgac
NF_At1g80660b	ggcgttctctggcacttac	NF_At1g80790d	tccttcagctctgaatctcc
NF_At1g80660c	tcatgcgatttccactgatag	NF_At1g80790e	ttgcgtttaaagattccaacattc
NF_At1g80660d	ttgtgacagaggacttctgttc	NF_At1g80790f	ttgtgtaccaagatcaatgaga agac
NF_At1g80660e	gcctgattgtctgcactgtc	At1g80800-f	ttgctgttgaagcgtatgag
NF_At1g80660f	tcaagttgggtgacattgttcc	At1g80800-r	tggtcccgccttattaatcg
NF_At1g80660g	tcaacaagatgagcagctttgc	Promoterprimer - At1g80820 5'end	attgtggcacagagagcttcg
NF_At1g80660h	tccttttgttcttctgttgc	At1g80820_a	gccctttcataacctgtaaacc
NF_At1g80670a	tttgctccgacagtaacaatg	At1g80820_b	tggatactccgggaagaatttg
NF_At1g80670b	tccagatcctatctaaatcaca	At1g80820_c	ctaaatccggttttggttctcg
NF_At1g80670c	cttaccgggtggaattcagag	At1g80820_d	cggataataaaaccattgcttcc
NF_At1g80670d	ggtgttgggaaatatcccgtag	At1g80840-f	gtggaggatcagtcctgtt
NF_At1g80670e	gcatcagattcaaaggcaaaag	At1g80840-r	cgaaagccgagttgataagc
NF_At1g80670f	aaccgaattccttccaataaag	At1g80870-f	tcctccactgcttccagatt
NF_At1g80690_1234 f	gccccaaatgtaagaatgagg	At1g80870-r	tcgctgcacgttcaagttac
NF_At1g80690_1440 r	ttggtccttggaaagtcagagcc	At1g80890-f	ggagaagaagcacggtttgg
NF_At1g80690_441f	tgattgctactgaccgagaatttg	At1g80890-r	ttgtgtgagaacgatgctttg
NF_At1g80690_2230 r	ggcatcggaaatctcaaaagac	At1g80920-f	taccacacaattgcttctc
NF_At1g80700_2521 r	Cacagctggaggacaagtctatg (caution: Also binds to direct strand)	At1g80920-r	catgccaagtaccaacaacct
NF_At1g80700_810f	tgatcgaaccaataaccctagacc		

Table 9-4: Sequencing results of predicted genes in the *tup5* mapping interval.

Nr.	Locus	5' coordinate	3' coordinate	Gene product name	Sequencing result
1	At1g80650	4052	2811	double-stranded RNA-binding domain-containing protein	Gene sequence was incomplete.
2	At1g80640	6963	4255	protein kinase family protein	No difference found in the coding sequence
3	At1g80630	7974y	9934	leucine-rich repeat family protein	No difference found in the coding sequence
4	At1g80620	13266	11214	ribosomal protein S15 family protein	Not sequenced
5	At1g80610	14597	17897	expressed protein	Not sequenced
6	At1g80600	18077	20112	acetylornithine aminotransferase, mitochondrial, putative	See chapter 5.2.6
7	At1g80590	21474	22420	WRKY family transcription factor	No difference found in the coding sequence
8	At1g80580	25072	24302	ethylene-responsive element binding protein family (EREBP)	No difference found in the coding sequence
9	At1g80570	28305	26210	F-box protein family (FBL14)	No difference found in the coding sequence
10	At1g80560	30840	28333	3-isopropylmalate dehydrogenase, chloroplast, putative	Not sequenced
11	At1g80550	31926	33684	pentatricopeptide (PPR) repeat-containing protein	Gene sequence was incomplete.
	Locus F23A5	5' coordinate	3' coordinate	Gene product name	Sequencing result
12	At1g80660	3931	210	ATPase 9, plasma membrane-type, putative	No difference found in the coding sequence
13	At1g80670	7731	4559	transducin family protein / WD-40 repeat family protein	Gene sequence was incomplete.
14	At1g80680	7991	12741	nucleoporin family protein	Not sequenced
15	At1g80690	14786	13052	expressed protein	No difference found in the coding sequence
16	At1g80700	15910	17378	expressed protein	A few bases are slightly ambiguous, but the gene seems to have no differences in the coding sequence
17	At1g80710	19854	17406	transducin family protein / WD-40 repeat family protein	Not sequenced
18	At1g80720	20121	21541	mitochondrial glycoprotein family / MAM33 family	Not sequenced
19	At1g80730	24230	23306	zinc finger (C2H2 type) family protein (ZFP1)	No difference found in the coding sequence
20	At1g80740	26377	31031	chromomethylase 1 (CMT1)	No difference found in the coding sequence
21	At1g80750	32806	34547	60S ribosomal protein L7 (RPL7A)	No difference found in the coding sequence
22	At1g80760	36191	34522	major intrinsic family protein / MIP family protein	No difference found in the coding sequence
23	At1g80770	39233	41947	expressed protein	Not sequenced
24	At1g80780	42098	43356	CCR4-NOT transcription complex protein, putative	A few bases are slightly ambiguous, but the gene seems to have no differences in the coding sequence
25	At1g80790	43706	46839	XH/XS domain-containing protein / zinc finger family protein	Gene sequence was incomplete.
26	At1g80800	47996	48293	pseudogene, 40S ribosomal protein S12 (RPS12B)	Not sequenced
27	At1g80810	49165	52881	expressed protein	Not sequenced
28	At1g80820	54556	56653	cinnamoyl-CoA reductase, putative	Difference in sequence found in the second exon. Complementation assay: see chapter 5.2.4
29	At1g80830	59679	56862	NRAMP metal ion transporter 1 (NRAMP1)	Not sequenced

TUP5 genomic DNA sequence

attttgtcttaacgactctttattgtcccgcacacgaaa**ATG**GCGTCTCTTAGCCAAATCACCCCTGCCACG
 CGCGCCGTCGTCGGAGATTGGCCCTCTTACGCCGTCGATTGGAGCGGCCGATCATCAGAACCCGGATCGGATT
 CAACGGCCGGATTGCGAGCGTATTGACTAACGCAGGGGACCAAGCGGTGTCCGTA AAAAGCGAGTGTGAGCCA
 GAAGGTGATTGAAGAGGAAGCCAAAGTTATTGTGGGTACCTACGCGGAGCTCCAGTGGTTCTCTCGAGTGG
 GAAAGTTGTA AATTTGTTTCGACCCTGAAGGAAAAGAGTATCTGGATTGTGCATCTGGAATCGCTGTGAATGC
 TCTTGGTCATGGAGATCCTGATTGGCTTCGAGCTGTCACTGAGCAAGCTGGTGTCTTGGCCATGTCAGCAA
 TGTTTATTACACGATCCCTCAG**gtatttattcgttactgtat**ttttg**cattactgattctg**ttgatggctga
 cgaaagcttaaaactttt**gtt**gtttttatcctctgtgtgattgagctatggcctatggaacatgctagggga
 atgttggattagtccttctacttataatagcgagattattctatgacaagta**cttgc**actttgaaat**ttcatc**
 aaat**tg**gattgtttctacgccttccctatagaaat**ttttat**gagaagtatctgac**ctcattg**taaactctta
 gtgtacatatgctcctcaatgccc**aattcctc**gaaaaaagga**acctttatg**ctcatatctacttcatatggg
 ttgttaaa**actg**aaat**gtt**gaact**ctctg**cag**ATAGAGCTCG**AAAACGCTTGGTGGCGAGTTCTTTTG
 CAGACCGTGTAT**CTTTT**GTAACTCGGGAACGGAAGCCAATGAAGCAGCCATTAAGTTTTC AAGAAAATTC
 AGAGATTCACCCATCCAGAAGACAAAGAAGTCGCGACAGGTTTCATCGCCTTTACAAACAGCTTCCATGGAA
 GAACCTTAGGAGCTCTTGCC**TTGACAAGCAAAGAACAATACAGAACTC**TTTTCGAACCCATCATGCCTGGTG
 TAACCTTCTTAGAATATGGTAACATTCAAGCAGCCACAGACCTTATCCGCTCAGGTAAAATAGCTGCAGTTT
 TTGTGGAACCAATTC AAGGAGAAGGCGGGATTTACTCTGCTACAAAAGAGTTTCTGCAATCTCTGCGCTCTG
 CTTGTGATGCCGCTGGATCTCTTCTCGTCTTCGATGAG**g**taata**ta**ctctacc**gtcc**atccaaa**at**tttatt
 ttctttcttt**gtt**ctgttttt**gatt**gg**cttgc**ctcaactggg**ttcattgt**cccag**GTTCAATGTGGTTT**
 GGGTCGAACGGGTCTCATGTGGGCTTATGAAGCCTTCGGTGTGACTCCTGACATAATGACGGTTGCAAAGCC
 TTTAGCTGGTGGTTTACCTATTGGAGCGGTGCTGGT**GACTGAAAAGGTTGCAGAGACCATAAACTACGGAGA**
 TCATGGAAGTACATTTGCAGGCAGCCCTCTTGTGTGCAGTGCAGCCATTGCAGTTATGGATAAAGTATCGAA
 ACCCTCTTCTTGTCCAGTGTCTCAAATAAAGGTCGATACTTTAGAGACCTGTTGGTGA AAAAACTTGGAGG
 AAAC**TCGCACGTGAAGGAAGTGAGAGGGCAAGGGCTTATCATAGGAGTGGAGCTCGATGTGCCGGCAAGCTC**
 ACTGGTTGATGCTTGCCGAGATTCGGGTCTTCTGATCTTGACAGCG**G**GGAAAGGAAATGTCGTCAGGATTGT
 TCCTCCGTTGGTTATATCAGAGGAGGAAATCGAACGTGCGGTTGAGATCATGTCTCAA**AATTTGACTGCGCT**
 TGAT**TGA**agttctt**gga**agagaaatgatgtggtgttgaagaagagcta**atg**ttttatattcgatctt**gtc**tt
 aaattagcctcaagtg**tacc**gta**agatg**ctctgcacaattgaaaagaaataaaat**ttg**acacaaaact**tg**
 atgaactaattgttcaatctaa**actt**gtataat**ttcc**

Figure 9-1: Genomic DNA sequence of At1g80600.

Red letters: UTRs; yellow capital letters: exon; blue letters: intron; start and stop codons are highlighted in blue; the mutated base in *tup5-1* is highlighted in red (modified from TAIR).

9.2 Vectors and gene constructs

Table 9-5: Vectors used for cloning.

Vector	Antibiotic resistance and other selection marker	Use of the vector in this work, description and references
pCB302	kanamycin in bacteria, PPT in plants	Subcloning for pooled complementation with BAC subclones (Xiang <i>et al.</i> , 1999).
pCB308	kanamycin in bacteria, PPT in plants	<i>pTUP5::GUS</i> fusion construct for expression analysis (Xiang <i>et al.</i> , 1999).
pROKII	kanamycin in bacteria and plants	Overexpression construct <i>p35S::Cinnamoyl CoA reductase</i> (At1g80820) for complementation test with <i>tup5-1</i> (Baulcombe <i>et al.</i> , 1986).
pB2GW7	spectinomycin in bacteria, PPT in plants	Overexpression construct <i>p35S::TUP5</i> . pB2GW7 is Gateway compatible (Karimi <i>et al.</i> , 2005).
pDONR™22 1	chloramphenicol before and kanamycin after recombination.	Donor vector for Gateway® cloning of the GFP construct (Gateway®).
pB7FWG2	Spectinomycin in bacteria, PPT in plants	<i>p35S::TUP5-GFP</i> fusion construct for subcellular localisation analysis: Vector pB7FWG2 for carboxyl-terminal end GFP fusion (Gateway compatible) (Karimi <i>et al.</i> , 2005).
p423TEF	histidine auxotrophy and ampicillin resistance	Yeast vector which contains the strong constitutive promoter of <i>translation elongation factor 1a</i> (TEF) for the expression of a gene of interest in yeast (Mumberg <i>et al.</i> , 1995). It was used in this work for heterologous complementation of the arginine-deficient yeast ACOAT mutant strain Y37711.

Table 9-6 Gene constructs received from other sources used for the analysis of *TUP5*.

Name	Description and References	Source
U15579	Contains cDNA of At1g80600. Made by Stanford – SSP Consortium in the vector pENTR/SD/D-TOPO (GenBank Accession: BT002584), approximate size: 4 kb. Kanamycin resistance (Yamada <i>et al.</i> , 2003).	<i>Arabidopsis</i> Biological Resource Center (ABRC)
T21F11	BAC clone containing the genes At1g80410 to At1g80650, chloramphenicol resistance (Choi <i>et al.</i> , 1995).	<i>Arabidopsis</i> Biological Resource Center (ABRC)
F23A5	BAC clone containing the genes At1g80660 to At1g80990, kanamycin resistance (Mozo <i>et al.</i> , 1998).	<i>Arabidopsis</i> Biological Resource Center (ABRC)

Table 9-7: Gene constructs generated during this work for the analysis of *TUP5*.

Working name (on tubes or seed batches) (English translation or exact construct name)	Description	Cloning method
<i>cinnam. compl. 1</i> (pAt1g80820 (~2kb)+ At1g80820)	Cinnamoyl CoA reductase (At1g80820) was cloned into pCB302 with its own promoter (approx. 2 kb) for complementation test of <i>tup5-1</i> .	Classical cloning. Enzymes used: <i>Bam</i> HI (5'-end) and <i>Eco</i> RI (3'-end).
35S:: <i>cinnam.</i> (35S::At1g80820)	Cinnamoyl CoA reductase (At1g80820) was cloned into pROKII downstream of 35S promoter for complementation test of <i>tup5-1</i> .	Classical cloning. Enzymes used: <i>Xba</i> I (5'-end) and <i>Sac</i> I (3'-end).
cDNA 80600 in pB2GW7 (35S:: At1g80600)	cDNA of <i>TUP5</i> (in clone U15579) was cloned into pB2GW7 downstream of the constitutive CaMV 35S promoter (35S:: <i>TUP5</i>) for analysis of <i>TUP5</i> overexpression.	LR reaction with Gateway® system
pAt1g80600:: <i>GUS</i> (2kb) (pAt1g80600 2 kb :: <i>GUS</i>)	The promoter (about 2 kb: starting 1962 bp upstream with a 2 bp gap to Start codon) of <i>TUP5</i> was cloned into pCB308 upstream of <i>GUS</i> gene for expression analysis.	Classical cloning. Enzymes used: <i>Bam</i> HI (5'-end) and <i>Sma</i> I / <i>Cfr</i> 9I (3'-end).
p80600- <i>GUS</i> 2,5 kb (pAt1g80600 2,5kb :: <i>GUS</i>)	The promoter of <i>TUP5</i> (about 2,5 kb: starting 2439 bp upstream with a 2 bp gap to Start codon) was cloned into pCB308 upstream of <i>GUS</i> gene for expression analysis.	
p80600- <i>GUS</i> 3 kb (pAt1g80600 3kb :: <i>GUS</i>)	The promoter of <i>TUP5</i> (about 3 kb: starting 2973 bp upstream with a 2 bp gap to Start codon) was cloned into pCB308 upstream of <i>GUS</i> gene for expression analysis.	
p80600:: <i>GUS</i> 3,2 kb nur Promoter (pAt1g80600 3,2 kb :: <i>GUS</i>)	The promoter of <i>TUP5</i> (3269 bp upstream, exactly ending before start ATG) was cloned into pCB308 upstream of <i>GUS</i> gene for expression analysis.	
p80600:: <i>GUS</i> 3,2 kb + 1. Exon (pAt1g80600 3,2kb+Ex1 :: <i>GUS</i>)	The promoter of <i>TUP5</i> (3269 bp upstream) with 360 bp (= 120 amino acids) of the first exon of <i>TUP5</i> was cloned (in frame) upstream of <i>GUS</i> gene into pCB308 for expression analysis.	
p80600:: <i>GUS</i> 3,2 kb + Anf. 2. Exon (pAt1g80600 3,2kb+ Beginn. Ex2 :: <i>GUS</i>)	The promoter of <i>TUP5</i> (3269 bp upstream) with the first exon, the first intron and 72 bp (= 24 amino acids) of the second exon of <i>TUP5</i> (insertion ends 859 bp after start codon) were cloned (in frame) upstream of <i>GUS</i> gene into pCB308 for expression analysis.	
p80600:: <i>GUS</i> 3,2 kb + ganzes Gen (pAt1g80600 3,2kb+ <i>TUP5</i> :: <i>GUS</i>)	The promoter of <i>TUP5</i> (3269 bp upstream) with whole coding sequence of <i>TUP5</i> (except stop codon) was cloned into pCB308 upstream of <i>GUS</i> gene for <i>GUS</i> expression analysis.	
cDNA 80600 ohne Stop in pDONR™221 (cDNA <i>TUP5</i> without stop codon in pDONR™221)	The cDNA of <i>TUP5</i> from start codon but without stop codon was cloned into pDONR™221 to create an entry clone (for further use in GFP fusion).	PCR product inserted into donor vector by BP reaction with Gateway® system.
cDNA 80600 ohne Stop in pB7FWG2 (cDNA <i>TUP5</i> without stop codon in pB7FWG2)	The cDNA of <i>TUP5</i> was fused to <i>GFP</i> under the control of the constitutive CaMV 35S promoter (35S:: <i>TUP5</i> :: <i>GFP</i>) in the vector pB7FWG2 for subcellular localisation of <i>TUP5</i> .	The entry clone "cDNA 80600 ohne Stop in pDONR™221" was used for LR reaction with pB7FWG2 with Gateway® system
cDNA At1g80600 (WT) in p423TEF	The cDNA of <i>TUP5</i> , the genomic DNA of <i>TUP5</i> and the genomic DNA of <i>TUP5</i> in the mutated version of <i>tup5-1</i> were cloned into p423TEF downstream of the TEF yeast promoter for heterologous complementation experiments in the arginine-deficient yeast mutant Y37711 (YOL140W mutated).	Classical cloning. Enzyme used: <i>Bam</i> HI (5'-end) and <i>Sa</i> II (3'-end).
At1g80600 genomisch (WT) in p423TEF (<i>TUP5</i> genomic (WT) in p423TEF)		
At1g80600 genomisch (Mutation <i>tup5-1</i>) in p423TEF (<i>TUP5</i> genomic (with the mutation <i>tup5-1</i>) in p423TEF)		

9.3 Primers

Table 9-8: Primers used in this work, except for the sequencing of candidate genes (those primers are listed in Table 9-3).

Use of primers	Name of primer	Sequence	Description / comments	Sequence length in bp	Restriction enzyme
Primers used for mapping	F19K16 f	ctttatgggtttgcctccaa	SSLP marker	Col 181 / Ler 162	-
	F19K16 r	gacgtgcccgatgatacaata			
	F18B13 f	gctgcaggagtcagatatcca	SSLP marker	Col 291 / Ler 361	-
	F18B13 r	cttccggttctgtcggatcat			
	F5I6-B (-38) f	tcagccctttcatcgttca	SSLP marker	Col 149 / Ler 129	-
	F5I6-B (-38) r	tttgcattggcattgttgagt			
	F5I6-72 f	ttcgtgataatgaaacatttagtcg	SSLP marker	Col 150 / Ler 132	-
	F5I6-72 r	tcaattcgtcaaccacgtct			
	F5I6-100 f	ggaaggacgaccaattgaga	SSLP marker	Col 123 / Ler 107	-
	F5I6-100 r	ccgagatcgaagaagacgaa			
	F5I6 (-114) f	cagaagcccgaacggagtaag	SSLP marker	Col 279 / Ler 254	-
	F5I6 (-114) r	tcacctctggatggctcaat			
	F5I6-124 f	agtcacgcctcaatacacactct	SSLP marker	Col 111 / Ler 102	-
	F5I6-124 r	Aaacctctccgcaccaaaag			
	F23A5-9 f	agattggactcgcgaaaga	CAPS marker	Col 665 + 498 Ler: 1063	<i>XmnI</i>
	F23A5-9 r	aaacctccggtttcgcactt			
	F23A5-22 f	cccacatggccaaatatcat	CAPS marker	Col 636 Ler 309 + 325	<i>HinfI</i>
	F23A5-22 r	ttgccactagattgtcacc			
	F23A5-28 f	cacatgggaaccttactctgg	SSLP marker	Col 134 / Ler 157	-
	F23A5-28 r	cccattctatcacgtactcctca			
	F23A5-41 f	tgcttactcgtcgtcgtcta	CAPS marker	Col: 57 + 96 + 268 Ler: 57 + 364	<i>BseGI</i>
	F23A5-41 r	agaccaattattcggcaaaa			
	F23A5 (-58) f	aagttccggttatcgtcgcag	CAPS marker	Col 435 + 326. Ler 435 + 171 + 155	<i>HinfI</i>
	F23A5 (-58) r	tgttatgggtcgttgctgaa			
	F23A5-95 f	tctatgtgaactatttcctcgcgat	SSLP marker	Col 164 / Ler 143	-
	F23A5-95 r	caacaatgctcgcgatcaaaa			

Table 9-8: Continued.

Use of primers	Name of primer	Sequence	Description / comments	Sequence length in bp	Restriction enzyme
TUP5 sequencing	T21F11_CDS6_a	ggtgcgaccaatgcataca	-	-	-
	T21F11_CDS6_b	ctctggaagatgtattacatcgac	-	-	-
	T21F11_CDS6_c	ttgaagaggaagccaaagtt	-	-	-
	T21F11_CDS6_d	acatatgctcctcaatgcc	-	-	-
Identification of T-DNA insertions	LB1 SAIL	gcctttcagaaatggataaatagccttgcttc	Used with T21F11_CDS6_d (see above) for the proof of T-DNA insertions (PCR product is synthesised only in case of insertion).	Approx. 1000-1200 bp	-
	80600 gfp entry r	atcaagcgcagtgcaaat	Used with T21F11_CDS6_d (see above) for the proof of alleles lacking the T-DNA insertion (amplifies a part of the intact gene).	1131 bp	-
Primers used for cloning	Cinnam compl1 f	cggatccaaattcagagggtgagag	Cinnamoyl CoA reductase (At1g80820) with its own promoter (approx. 2 kb) for complementation test of <i>tup5-1</i> .	4310 bp	<i>Bam</i> HI and <i>Eco</i> RI
	Cinnam compl1 r	ggaattc ttaaccagatctctgtagg			
	cinnam 35S f	gctctagatacaaatcactaacgacacatc	Cinnamoyl CoA reductase (At1g80820) cloning behind 35S promoter for complementation test of <i>tup5-1</i> .	2447 bp	<i>Xba</i> I and <i>Sac</i> I
	cinnam 35S r	cgagctctctgtaggaaacaaacttct			
	p80600-GUS bam f	cgggatccgacaagtgtgtgtggaga	Promoter of <i>TUP5</i> (about 2 kb) in pCB308 for <i>GUS</i> expression	1960 bp	<i>Bam</i> HI (5'-end); <i>Sma</i> I / <i>Cfr</i> 9I (3'-end)
	p80600-GUS sma r	accccggtcgtgtgtcgggacaataaa			
	p80600-GUS 2,5 kb sma f	acccggggaccctgtcaccagggttagc	Promoter of <i>TUP5</i> (about 2,5 kb) in pCB308 for <i>GUS</i> expression. (Primer used with "p80600-GUS sma r")	2437 bp	<i>Sma</i> I / <i>Cfr</i> 9I (5' and 3'-end) (nondirectional cloning)
	p80600-GUS 3 kb sma f	acccgggggtgtgtgtgggctgatct	Promoter (about 3 kb) of <i>TUP5</i> in pCB308 for <i>GUS</i> expression. (Primer used with "p80600-GUS sma r")	2971 bp	<i>Sma</i> I / <i>Cfr</i> 9I (5' and 3'-end) (nondirectional cloning)
	p80600 3,2 kb upstream sma f (renamed, previously: p80600 3,2 kb+Gen sma f)	acccggggccacaccgcttctctggagc	Promoter (3,2 kb) of <i>TUP5</i> with whole coding sequence of <i>TUP5</i> in pCB308 for <i>GUS</i> expression.	5105 bp	<i>Sma</i> I / <i>Cfr</i> 9I (5' and 3'-end) (nondirectional cloning)
	p80600 3,2kb+Gen real sma r	acccgggatcaagcgcagtgcaaat			
	p80600 3,2 kb upstream sma r (renamed, previously: p80600 3,2 kb+Gen sma r)	acccgggttctgtgtcgggacaata	Promoter (3,2 kb) of <i>TUP5</i> in pCB308 for <i>GUS</i> expression (used with p80600 3,2 kb upstream sma f).	3269 bp	<i>Sma</i> I / <i>Cfr</i> 9I (5' and 3'-end) (nondirectional cloning)
p80600 3,2 kb + 1.Ex sma r	acccgggagtgacagctcgaagccaat	Promoter (3,2 kb) of <i>TUP5</i> with part of the 1st exon (360 bp) of <i>TUP5</i> in pCB308 for <i>GUS</i> expression (used with p80600 3,2 kb upstream sma f).	3629 bp	<i>Sma</i> I / <i>Cfr</i> 9I (5' and 3'-end) (nondirectional cloning)	

Table 9-8: Continued.

Use of primers	Name of primer	Sequence	Description / comments	Sequence length in bp	Restriction enzyme
Primers used for cloning	p80600 3,2kb + Anf2.Ex	accccggttccgttcccaggttataaaa	Promoter (3,2 kb) of <i>TUP5</i> with beginning of the 2nd exon (72 bp) of <i>TUP5</i> in pCB308 for <i>GUS</i> expression (used with p80600 3,2 kb upstream sma f)	4128 bp	<i>SmaI</i> / <i>Cfr9I</i> (5' and 3'-end) (nondirectional cloning)
	AttB1 80600 gfp neu	aaaaagcaggctatggcgtctcttagccaaatc	Amplification of <i>TUP5</i> cDNA from start codon but without stop codon with half of attB sites.	1396 bp	-
	AttB2 80600 gfp neu	agaaagctgggtcatcaagcgcagtcaaat			
	attB1-GW-5's	Ggggacaagttgtacaaaaaagcaggct	Addition of the rest of attB to the PCR product of the primers "AttB1 and 2 80600 gfp neu" (see above) sites for BP reaction for insertion into pDONR™221.	1430 bp	-
	attB2-GW-3'a	Ggggaccactttgtacaagaaagctgggt			
	At1g80600 from Start Bam f	cgggatccatggcgtctcttagccaaatc	At1g80600 (<i>TUP5</i>) in p423TEF for heterologous complementation in the arginine-deficient yeast mutant Y37711 (YOL140W mutated).	1857 bp genomic, 1393 bp cDNA	<i>Bam</i> HI and <i>Sal</i> I
At1g80600 to Stop Sal r	acgcgctgactcaatcaagcgcagtcaaat				
Primers used for semi-quantitative RT-PCR and real-time PCR	Actin2/7 f (At5g09810)	tacaacgagctctcgtgttc	Housekeeping gene as control for semi-quantitative RT-PCR	851 bp genomic; 765 bp cDNA	-
	Actin2/7 r (At5g09810)	gattgatcctccgatccaga			
	RT-PCR cinnam f	ggctaaagccaaggctcaagc	Semi-quantitative RT-PCR of At1g80820 for T-DNA insertion line control (N809694)	Without insertion: 520 bp genomic; 386 bp cDNA. With insertion: no PCR product.	-
	RT-PCR cinnam r	aggggtcctcgttagaccaga			
	RT-Primer 80600 f	aggtctgtggctgcttgaat	Semi-quantitative RT-PCR of <i>TUP5</i>	967 bp genomic; 594 bp cDNA	-
	RT-Primer 80600 r	tcgagcgtattgactaacg			
	Oligo dT	tttttttttttttttttttttt	cDNA synthesis	-	-
	N9 random primer	nnnnnnnnn	cDNA synthesis	-	-
	UBC10 qPCR fw (At5g53300)	ccatgggctaaatggaaa	Housekeeping gene as control for real-time PCR	134 bp	-
	UBC10 qPCR rv (At5g53300)	ttcatttggtctgtcttcag			
	At3g25800 qPCR fw	ccattagatctgtctctctgct	Housekeeping gene as control for real-time PCR	100 bp	-
	At3g25800 qPCR rv	gacaaaaccgtaccgag			
AOAT qRT 3.exon f	tcggtgtgactcctgacat	Real-time PCR on <i>TUP5</i> expression	149 bp	-	
AOAT qRT 3.exon r	actgcacacaagagggt				
Primers used for other purposes	At1g80600 from Start Bam f (see above)	cgggatccatggcgtctcttagccaaatc	CAPS marker for identification of the <i>tup5-1</i> mutation	Genomic: WT: 1197+536+106 bp; <i>tup5-1</i> : 1197+642 bp cDNA: WT: 824+444+106 bp <i>tup5-1</i> : 824+550 bp	<i>Msp</i> A1I
	At1g80600 to Stop Sal r (see above)	acgcgctgactcaatcaagcgcagtcaaat			

9.4 TUP5::GUS reporter gene constructs

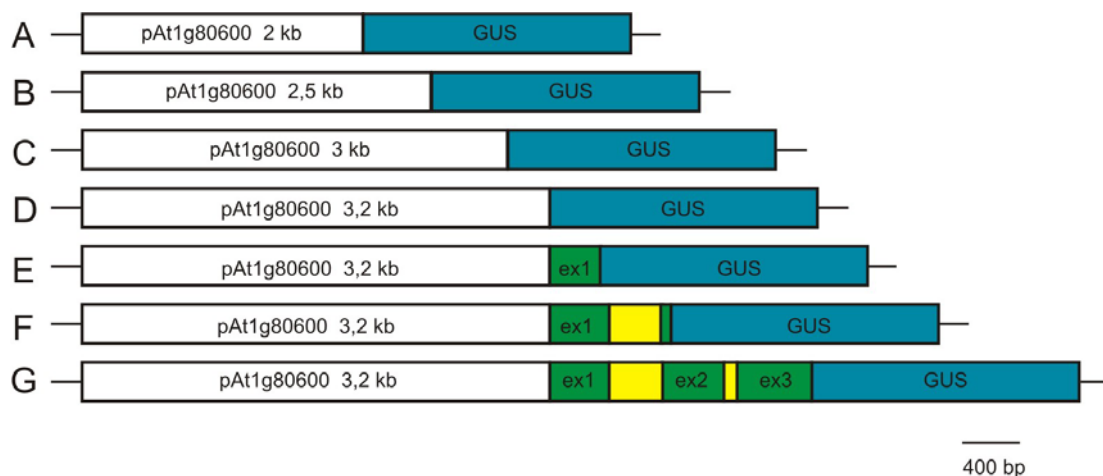


Figure 9-3: Reporter gene constructs used for expression analysis of *TUP5*.

Promoter sequences of *TUP5* of various lengths were cloned upstream of the *GUS* gene (β -glucuronidase) into the vector pCB308 (Xiang *et al.*, 1999). In the case of the constructs E-G parts of the ORF of *TUP5* (E and F) or the whole gene (G) were fused to *GUS* to produce hybrid proteins (*GUS* in frame with *TUP5*). For exact sequence coordinates see Table 9-7 and Table 9-8. White boxes: promoter region of *TUP5* (pAt1g80600) with sequence lengths in kb; blue boxes: *GUS* gene; green boxes: exons of *TUP5* (ex 1-3); yellow boxes: introns of *TUP5*.

9.5 Free amino acid content of WT and *tup5-1*

Table 9-9: Free amino acid content of WT and *tup5-1* plants (7 d old) grown under standard conditions (first experiment).

The concentration of each amino acid in WT and *tup5-1* is listed as nmol /g FW and in percent referring to the values measured in WT set as 100% respectively. Mean \pm SD of three samples. n.a.: not analysed (usually when values were too low).

Amino acid	WT [nmol /g FW]	WT [%]	SD of WT [nmol /g FW]	SD of WT [%]	<i>tup5-1</i> [nmol /g FW]	<i>tup5-1</i> [%]	SD of <i>tup5-1</i> [nmol /g FW]	SD of <i>tup5-1</i> [%]
asp	112,6	100	\pm 2,0	\pm 1,8	137,6	122,2	\pm 4,9	\pm 4,3
glu	77,8	100	\pm 0,5	\pm 0,7	97,6	125,4	\pm 8,9	\pm 11,5
asn	364,9	100	\pm 17,6	\pm 4,8	615,1	168,5	\pm 67,4	\pm 18,5
ser	410,9	100	\pm 77,8	\pm 18,9	1232,0	299,8	\pm 326,4	\pm 79,4
gln	11431,3	100	\pm 952,0	\pm 8,3	16171,2	141,5	\pm 597,0	\pm 5,2
gly	n.a.		n.a.		6376,9	-	\pm 1598,2	-
thr	57,4	100	\pm 5,3	\pm 9,2	227,5	396,2	\pm 54,8	\pm 95,5
his	328,4	100	\pm 25,1	\pm 7,7	337,3	102,7	\pm 17,8	\pm 5,4
ala	334,6	100	\pm 18,5	\pm 5,5	494,4	147,7	\pm 29,3	\pm 8,8
arg	1097,1	100	\pm 61,5	\pm 5,6	163,1	14,9	\pm 28,3	\pm 2,6
met	7,3	100	\pm 1,3	\pm 17,5	12,2	167,3	\pm 0,5	\pm 6,7
val	43,4	100	\pm 1,4	\pm 3,3	120,9	279,0	\pm 11,8	\pm 27,2
phe	25,2	100	\pm 0,1	\pm 0,5	44,4	176,0	\pm 1,1	\pm 4,4
ile	18,6	100	\pm 2,3	\pm 12,4	24,1	129,9	\pm 0,4	\pm 2,2
leu	28,4	100	\pm 3,9	\pm 13,9	20,0	70,4	\pm 0,8	\pm 2,6
lys	37,7	100	\pm 1,6	\pm 4,1	16,2	43,1	\pm 1,9	\pm 5,0

9. SUPPLEMENTAL DATA

Table 9-10 Free amino acid content of WT and *tup5-1* plants (7 d old) grown under standard conditions (second experiment).

The concentration of each amino acid in WT and *tup5-1* is listed as nmol /g FW and in percent referring to the values measured in WT set as 100% respectively. Mean \pm SD of six samples.

Amino acid	WT [nmol /g FW]	WT [%]	SD of WT [nmol /g FW]	SD of WT [%]	<i>tup5-1</i> [nmol /g FW]	<i>tup5-1</i> [%]	SD of <i>tup5-1</i> [nmol /g FW]	SD of <i>tup5-1</i> [%]
asp	358,0	100	\pm 83,2	\pm 23,2	516,1	144,1	\pm 100,9	\pm 28,2
glu	1318,6	100	\pm 273,9	\pm 20,8	1563,6	118,6	\pm 322,9	\pm 24,5
asn	1905,1	100	\pm 259,7	\pm 13,6	3184,4	167,2	\pm 552,3	\pm 29,0
ser	1597,1	100	\pm 292,1	\pm 18,3	3088,3	193,4	\pm 637,7	\pm 39,9
gln	20327,8	100	\pm 4582,0	\pm 22,5	31263,2	153,8	\pm 6270,0	\pm 30,8
gly	945,6	100	\pm 201,7	\pm 21,3	4563,0	482,5	\pm 1694,9	\pm 179,2
thr	263,6	100	\pm 67,4	\pm 25,6	423,3	160,6	\pm 117,7	\pm 44,6
his	170,3	100	\pm 34,1	\pm 20,0	165,9	97,4	\pm 37,9	\pm 22,2
ala	798,1	100	\pm 71,2	\pm 8,9	1113,1	139,5	\pm 235,9	\pm 29,6
arg	2823,4	100	\pm 384,7	\pm 13,6	883,9	31,3	\pm 171,3	\pm 6,1
tyr	30,1	100	\pm 2,3	\pm 7,6	31,8	105,4	\pm 1,7	\pm 5,6
met	22,9	100	\pm 7,9	\pm 34,4	37,8	165,1	\pm 18,9	\pm 82,4
val	51,0	100	\pm 12,8	\pm 25,0	132,6	260,0	\pm 34,6	\pm 67,9
trp	176,2	100	\pm 153,5	\pm 87,1	157,2	89,2	\pm 97,9	\pm 55,5
phe	100,8	100	\pm 98,4	\pm 97,6	139,9	138,8	\pm 96,5	\pm 95,7
ile	76,1	100	\pm 36,5	\pm 48,0	89,9	118,2	\pm 44,7	\pm 58,8
leu	119,1	100	\pm 17,2	\pm 14,4	70,4	59,1	\pm 9,6	\pm 8,1
lys	243,2	100	\pm 21,0	\pm 8,6	186,7	76,8	\pm 39,1	\pm 16,1

Table 9-11 Free amino acid content of WT shoot, WT root and *tup5-1* shoot (11 d old) grown under standard conditions.

The concentration of each amino acid is listed as nmol /g FW and in percent referring to the values measured in WT shoot set as 100% respectively. Mean of WT shoot n=4; WT root n=3; *tup5-1* shoot n=4 respectively, SD in extra columns respectively.

Amino acid	WT shoot [nmol /g FW]	WT shoot [%]	SD of WT shoot [nmol /g FW]	SD of WT shoot [%]	WT root [nmol /g FW]	WT root [%]	SD of WT root [nmol /g FW]	SD of WT root [%]	<i>tup5-1</i> shoot [nmol /g FW]	<i>tup5-1</i> shoot [%]	SD of <i>tup5-1</i> shoot [nmol /g FW]	SD of <i>tup5-1</i> shoot [%]
asp	643	100	\pm 126	\pm 19,6	524	81,4	\pm 48	\pm 7,4	1039	161,5	\pm 21	\pm 33,8
glu	2831	100	\pm 227	\pm 8,0	1696	59,9	\pm 140	\pm 5,0	2907	102,7	\pm 676	\pm 23,9
asn	2395	100	\pm 298	\pm 12,5	3759	156,9	\pm 269	\pm 11,2	6741	281,4	\pm 372	\pm 15,5
ser	3218	100	\pm 510	\pm 15,9	1936	60,2	\pm 202	\pm 6,3	3977	123,6	\pm 583	\pm 18,1
gln	9273	100	\pm 1860	\pm 20,1	20891	225,3	\pm 2225	\pm 24,0	41866	451,5	\pm 1446	\pm 15,6
gly	845	100	\pm 396	\pm 46,9	929	109,9	\pm 76	\pm 8,9	6663	788,1	\pm 1896	\pm 224,3
thr	314	100	\pm 50	\pm 16,1	660	210,2	\pm 52	\pm 16,5	668	212,8	\pm 88	\pm 28,1
his	84	100	\pm 19	\pm 23,0	176	209,7	\pm 24	\pm 29,1	101	120,1	\pm 7	\pm 8,7
ala	489	100	\pm 101	\pm 20,7	1108	226,4	\pm 84	\pm 17,2	939	192,0	\pm 210	\pm 43,0
arg	3084	100	\pm 673	\pm 21,8	61	2,0	\pm 11	\pm 0,4	1214	39,4	\pm 252	\pm 8,2
tyr	50	100	\pm 5	\pm 9,5	142	286,5	\pm 13	\pm 27,2	103	207,7	\pm 8	\pm 15,5
met	21	100	\pm 2	\pm 10,1	21	97,0	\pm 3	\pm 13,1	31	147,4	\pm 1	\pm 4,9
val	62	100	\pm 15	\pm 23,7	150	243,1	\pm 37	\pm 60,5	159	258,5	\pm 17	\pm 27,5
trp	41	100	\pm 15	\pm 37,5	11	26,5	\pm 2	\pm 4,3	115	279,9	\pm 21	\pm 51,2
phe	61	100	\pm 14	\pm 23,6	85	137,9	\pm 11	\pm 17,4	188	306,8	\pm 23	\pm 38,0
ile	51	100	\pm 8	\pm 16,7	127	249,4	\pm 18	\pm 34,8	92	179,4	\pm 6	\pm 12,4
leu	99	100	\pm 18	\pm 18,4	157	158,5	\pm 36	\pm 36,6	123	124,5	\pm 5	\pm 5,5
lys	532	100	\pm 43	\pm 8,1	223	41,9	\pm 49	\pm 9,1	791	148,8	\pm 100	\pm 18,8

Table 9-12: Free amino acid content of *tup5-1* compared to WT plants (17 d old) grown under standard conditions.

The concentration of each amino acid in WT and *tup5-1* is listed as [nmol /g FW] and in percent referring to the values measured in WT set as 100% respectively. Mean \pm SD of five samples for WT and two samples for *tup5-1*.

Amino acid	WT (17 d) [nmol /g FW]	WT (17 d) [%]	WT SD [nmol /g FW]	WT SD [%]	<i>tup5-1</i> (17 d) [nmol /g FW]	<i>tup5-1</i> (17 d) [%]	<i>tup5-1</i> SD [nmol /g FW]	<i>tup5-1</i> SD [%]
asp	1359,4	100	477,0	35,1	1301,5	95,7	45,2	3,3
glu	4647,9	100	829,5	17,8	4036,5	86,8	50,2	1,1
asn	3676,9	100	667,1	18,1	11100,3	301,9	791,5	21,5
ser	3213,9	100	432,5	13,5	3340,4	103,9	33,2	1,0
gln	9418,7	100	703,8	7,5	67475,9	716,4	4740,8	50,3
gly	325,5	100	70,5	21,7	n.a.	n.a.	n.a.	n.a.
thr	730,4	100	83,8	11,5	903,8	123,7	97,1	13,3
his	120,9	100	21,3	17,6	221,7	183,4	58,1	48,1
ala	920,2	100	279,5	30,4	829,8	90,2	55,3	6,0
arg	2098,5	100	655,0	31,2	509,1	24,3	40,5	1,9
tyr	173,3	100	36,8	21,3	175,3	101,2	25,9	15,0
met	27,0	100	3,1	11,4	57,3	212,0	12,2	45,1
val	342,1	100	86,5	25,3	357,1	104,4	80,6	23,6
trp	152,9	100	34,7	22,7	317,1	207,4	102,8	67,2
phe	265,0	100	46,5	17,6	207,9	78,4	18,7	7,0
ile	276,0	100	56,4	20,4	225,9	81,9	49,7	18,0
leu	381,9	100	86,7	22,7	296,9	77,7	53,1	13,9
lys	711,8	100	296,2	41,6	1698,3	238,6	598,0	84,0

9.6 T-DNA insertion lines of TUP5

In line *TUP5* - IS2 (TIS2) the germination rate was 79%. (46 from 58 seeds germinated). This might give a hint to a 1:3 segregating lethality, which would need to be verified with a bigger seed population. It is not clear whether in TIS2 an insertion has taken place in At1g80600 because the verification of the T-DNA insertion by PCR failed.

9.7 Amino acid content of overexpression lines

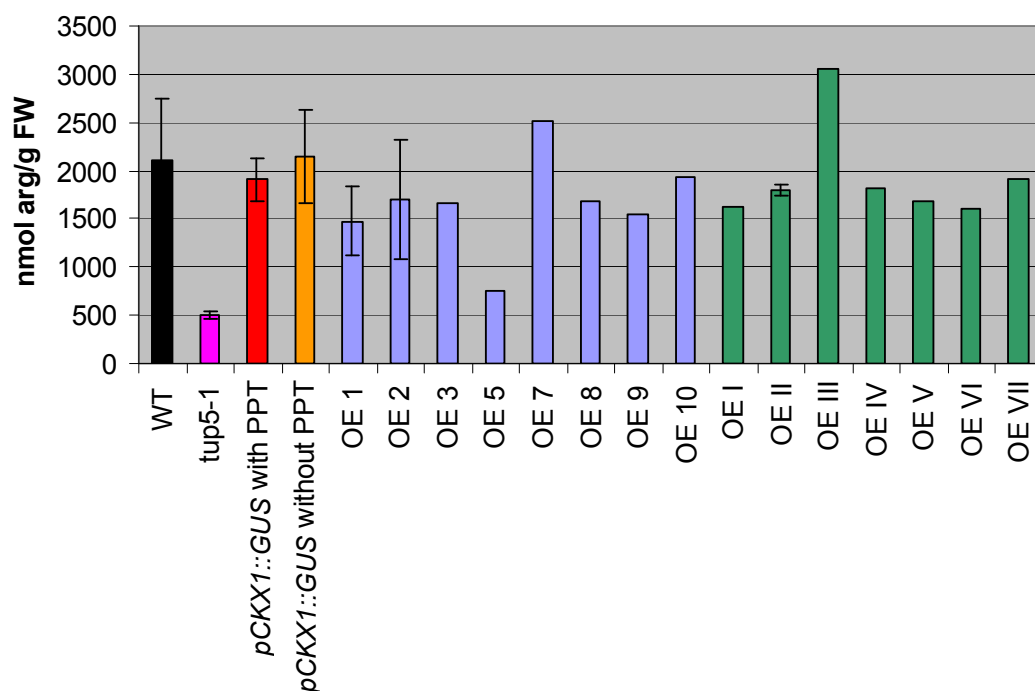


Figure 9-4: Free arginine content in *TUP5* overexpressing lines.

Plants (17 d) were grown *in vitro*: WT, *tup5-1* and *pCKX1::GUS* as controls were grown on MS medium without PPT, transgenic plants: *TUP5* overexpressing lines and *pCKX1::GUS* were grown on MS medium containing PPT. OE 1 to 10: *TUP5* overexpressing lines in WT background. OE I - VII: *TUP5* overexpressing lines in *tup5-1* background. (WT: n = 5; *tup5-1*: n = 2; *pCKX1::GUS* with PPT: n = 4; *pCKX1::GUS* without PPT: n = 3; *TUP5* overexpressing lines: n = 1, except for OE 1, OE 2 and OE II: n = 2.)

Table 9-13: Free arginine concentration in *TUP5* overexpressing lines.

Plants (17 d) were grown *in vitro*: WT, *tup5-1* and *pCKX1::GUS* as controls were grown on MS medium without PPT, transgenic plants: *TUP5* overexpressing lines and *pCKX1::GUS* were grown on MS medium containing PPT. OE 1 to 10: *TUP5* overexpressing lines in WT background. OE I - VII: *TUP5* overexpressing lines in *tup5-1* background. (WT: n = 5; *tup5-1*: n = 2; *pCKX1::GUS* with PPT: n = 4; *pCKX1::GUS* without PPT: n = 3; *TUP5* overexpressing lines: n = 1, except for OE 1, OE 2 and OE II: n = 2.) Arginine concentrations are given in nmol per g fresh weight (nmol arg / g FW); SD: standard deviation.

Sample	Arginine mean conc. [nmol arg / g FW]	Arg. SD [nmol arg / g FW]	Sample	Arginine mean conc. [nmol arg / g FW]	Arg. SD [nmol arg / g FW]
WT	2099	655	OE 9	1538	-
<i>tup5-1</i>	509	40	OE 10	1939	-
<i>pCKX1::GUS</i> with PPT	1908	220	OE I	1618	-
<i>pCKX1::GUS</i> without PPT	2142	485	OE II	1797	60
OE 1	1475	355	OE III	3054	-
OE 2	1702	622	OE IV	1820	-
OE 3	1654	-	OE V	1690	-
OE 5	751	-	OE VI	1599	-
OE 7	2506	-	OE VII	1907	-
OE 8	1679	-			

Table 9-14: Free asparagine concentration in *TUP5* overexpressing lines.

Plants (17 d) were grown *in vitro*: WT, *tup5-1* and *pCKX1::GUS* as controls were grown on MS medium without PPT, transgenic plants: *TUP5* overexpressing lines and *pCKX1::GUS* were grown on MS medium containing PPT. OE 1 to 10: *TUP5* overexpressing lines in WT background. OE I - VII: *TUP5* overexpressing lines in *tup5-1* background. (WT: n = 5; *tup5-1*: n = 2; *pCKX1::GUS* with PPT: n = 4; *pCKX1::GUS* without PPT: n = 3; *TUP5* overexpressing lines: n = 1, except for OE 1, OE 2 and OE II: n = 2.) Asparagine concentrations are given in nmol per g fresh weight (nmol asn /g FW); SD: standard deviation.

Sample	Asparagine mean conc. [nmol asn/g FW]	Asn. SD [nmol asn / g FW]	Sample	Asparagine mean conc. [nmol asn /g FW]	Asn. SD [nmol asn / g FW]
WT	3677	667	OE 9	4005	-
<i>tup5-1</i>	11100	791	OE 10	3484	-
<i>pCKX1::GUS</i> without PPT	3330	487	OE I	3597	-
<i>pCKX1::GUS</i> with PPT	4530	409	OE II	4037	262
OE 1	3873	1489	OE III	4819	-
OE 2	4107	749	OE IV	3431	-
OE 3	3420	-	OE V	3764	-
OE 5	4201	-	OE VI	4187	-
OE 7	4424	-	OE VII	3754	-
OE 8	4174	-		-	-

Table 9-15: Free glutamine concentration in *TUP5* overexpressing lines.

Plants (17 d) were grown *in vitro*: WT, *tup5-1* and *pCKX1::GUS* as controls were grown on MS medium without PPT, transgenic plants: *TUP5* overexpressing lines and *pCKX1::GUS* were grown on MS medium containing PPT. OE 1 to 10: *TUP5* overexpressing lines in WT background. OE I - VII: *TUP5* overexpressing lines in *tup5-1* background. (WT: n = 5; *tup5-1*: n = 2; *pCKX1::GUS* with PPT: n = 4; *pCKX1::GUS* without PPT: n = 3; *TUP5* overexpressing lines: n = 1, except for OE 1, OE 2 and OE II: n = 2.) Glutamine concentrations are given in nmol per g fresh weight (nmol gln /g FW); SD: standard deviation.

Sample	Glutamine mean conc. [nmol gln /g FW]	Gln. SD [nmol gln / g FW]	Sample	Glutamine mean conc. [nmol gln /g FW]	Gln. SD [nmol gln / g FW]
WT	9419	704	OE 9	15118	-
<i>tup5-1</i>	67476	4741	OE 10	12912	-
<i>pCKX1::GUS</i> without PPT	10338	1335	OE I	17168	-
<i>pCKX1::GUS</i> with PPT	19603	1711	OE II	13163	3353
OE 1	16128	7745	OE III	17279	-
OE 2	15021	680	OE IV	13393	-
OE 3	11087	-	OE V	15178	-
OE 5	19706	-	OE VI	18848	-
OE 7	16998	-	OE VII	13564	-
OE 8	15477	-		-	-

Table 9-16: Free tryptophan concentration in *TUP5* overexpressing lines.

Plants (17 d) were grown *in vitro*: WT, *tup5-1* and *pCKX1::GUS* as controls were grown on MS medium without PPT, transgenic plants: *TUP5* overexpressing lines and *pCKX1::GUS* were grown on MS medium containing PPT. OE 1 to 10: *TUP5* overexpressing lines in WT background. OE I - VII: *TUP5* overexpressing lines in *tup5-1* background. (WT: n = 5; *tup5-1*: n = 2; *pCKX1::GUS* with PPT: n = 4; *pCKX1::GUS* without PPT: n = 3; *TUP5* overexpressing lines: n = 1, except for OE 1, OE 2 and OE II: n = 2.) Tryptophan concentrations are given in nmol per g fresh weight (nmol trp / g FW); SD: standard deviation.

Sample	Tryptophan mean conc. [nmol trp / g FW]	Trp SD [nmol trp / g FW]	Sample	Tryptophan mean conc. [nmol trp / g FW]	Trp SD [nmol trp / g FW]
WT	153	35	OE 9	118	-
<i>tup5-1</i>	317	103	OE 10	31	-
<i>pCKX1::GUS</i> without PPT	148	71	OE I	120	-
<i>pCKX1::GUS</i> with PPT	155	47	OE II	67	14
OE 1	51	19	OE III	112	-
OE 2	82	29	OE IV	55	-
OE 3	73	-	OE V	61	-
OE 5	38	-	OE VI	78	-
OE 7	107	-	OE VII	120	-
OE 8	69	-		-	-

Table 9-17: Free lysine concentration in *TUP5* overexpressing lines.

Plants (17 d) were grown *in vitro*: WT, *tup5-1* and *pCKX1::GUS* as controls were grown on MS medium without PPT, transgenic plants: *TUP5* overexpressing lines and *pCKX1::GUS* were grown on MS medium containing PPT. OE 1 to 10: *TUP5* overexpressing lines in WT background. OE I - VII: *TUP5* overexpressing lines in *tup5-1* background. (WT: n = 5; *tup5-1*: n = 2; *pCKX1::GUS* with PPT: n = 4; *pCKX1::GUS* without PPT: n = 3; *TUP5* overexpressing lines: n = 1, except for OE 1, OE 2 and OE II: n = 2.) Lysine concentrations are given in nmol per g fresh weight (nmol lys / g FW); SD: standard deviation.

Sample	Lysine mean conc. [nmol lys / g FW]	Lys SD [nmol lys / g FW]	Sample	Lysine mean conc. [nmol lys / g FW]	Lys SD [nmol lys / g FW]
WT	712	296	OE 9	238	-
<i>tup5-1</i>	1698	598	OE 10	184	-
<i>pCKX1::GUS</i> without PPT	515	245	OE I	77	-
<i>pCKX1::GUS</i> with PPT	553	126	OE II	265	26
OE 1	235	10	OE III	306	-
OE 2	96	48	OE IV	232	-
OE 3	574	-	OE V	476	-
OE 5	155	-	OE VI	233	-
OE 7	181	-	OE VII	681	-
OE 8	258	-		-	-

Table 9-18: Free glycine concentration in *TUP5* overexpressing lines.

Plants (17 d) were grown *in vitro*: WT, *tup5-1* and *pCKX1::GUS* as controls were grown on MS medium without PPT, transgenic plants: *TUP5* overexpressing lines and *pCKX1::GUS* were grown on MS medium containing PPT. OE 1 to 10: *TUP5* overexpressing lines in WT background. OE I - VII : *TUP5* overexpressing lines in *tup5-1* background. (WT: n = 5; *tup5-1*: n = 2; *pCKX1::GUS* with PPT: n = 4; *pCKX1::GUS* without PPT: n = 3; *TUP5* overexpressing lines: n = 1, except for OE 1, OE 2 and OE II: n = 2.) Glycine concentrations are given in nmol per g fresh weight (nmol gly /g FW); SD: standard deviation. n.d.: not determined.

Sample	Glycine mean conc. [nmol gly /g FW]	Gly SD [nmol gly / g FW]	Sample	Glycine mean conc. [nmol gly /g FW]	Gly SD [nmol gly / g FW]
WT	325	71	OE 9	363	-
<i>tup5-1</i>	n.d.	-	OE 10	463	-
<i>pCKX1::GUS</i> without PPT	282	123	OE I	795	-
<i>pCKX1::GUS</i> with PPT	n.d.	-	OE II	521	141
OE 1	905	681	OE III	927	-
OE 2	550	57	OE IV	516	-
OE 3	405	-	OE V	577	-
OE 5	897	-	OE VI	797	-
OE 7	731	-	OE VII	440	-
OE 8	422	-		-	-

Eidesstattliche Erklärung

Ich versichere hiermit, die vorliegende Arbeit selbständig angefertigt und keine anderen als die angegebenen Quellen und Hilfsmittel verwendet zu haben. Ich versichere, daß diese Arbeit an keiner anderen Hochschule als der Freien Universität Berlin eingereicht wurde.

Berlin, den 8. Februar 2011

Nathalie Frémont